Programa de Doctorado en Biomedicina y Biotecnología

Investigación en Biología Molecular, Celular y Genética

Extracellular vesicles in the human maternal-embryo crosstalk during the preconception period

Vesículas extracelulares en la comunicación materno-embrionaria humana durante el periodo preconcepcional

David Bolumar Recuero

Igenomix foundation

Directors:

Carlos Simón Vallés, MD, PhD

Felipe Vilella Mitjana, PhD

Valencia, June 2020

El Dr. Carlos Simón Vallés, catedrático de Pediatría, Obstetricia y Ginecología de la Universidad de Valencia y Head of the Scientific Advisory Board of Igenomix y el Dr. Felipe Vilella Mitjana, director del departamento de investigación de Igenomix Foundation e investigador Miguel Servet del INCLIVA.

CERTIFICAN:

Que el trabajo de investigación titulado: "Extracellular vesicles in the human maternal-embryo crosstalk during the preconception period" ha sido realizado íntegramente por David Bolumar Recuero bajo su dirección. Dicha memoria está concluida y reúne todos los requisitos para su presentación y defensa como TESIS DOCTORAL ante un tribunal.

Y para que así conste a los efectos oportunos, firman la presente certificación en Valencia a 16 de Junio de 2020.

Fdo. Dr. Carlos Simón Valles Fdo. Dr. Felipe Vilella Mitjana

ACKNOWLEDGEMENTS

En primer lugar, querría agradecer a mis directores de tesis, así como a la Fundación Igenomix la posibilidad de realizar este doctorado, y no menos importante al programa de ayudas para la formación de profesorado universitario por cerrar el círculo que permite la subsistencia del becario durante el desarrollo inherente de su actividad investigadora, así como de sus restantes dos e incluso tres horas de asueto personal semanal.

Mas allá de formalismos, me llevo conmigo una gran experiencia personal y profesional que, con sus momentos buenos y malos, hacen que un titulo doctor signifique algo más allá de un PhD escrito sobre un trozo de papel.

En cuanto a mis directores, gracias por haberme permitido ir más allá del plano profesional y habernos podido conocer y compartir algunos momentos extramuros del laboratorio.

A todos los compañeros que he tenido a lo largo de la tesis, desde los que terminaron cuando yo empezaba a los recién llegados, a los que encomiendo suerte, paciencia y una cierta resistencia a la alopecia y al envejecimiento facial prematuro (creedme sobre todo que debéis temerle a este último). Con todos he disfrutado mucho trabajando y de todos he aprendido mucho. Y por supuesto, más importantemente, por los momentos más allá de la tesis, sentados a la bancada del laboratorio biotecnológico más grande del mundo y fletado de los productos con mayor trascendencia y legado que los biotecnólogos a lo largo de la historia se han esforzado en desarrollar, ese centro de estudio en el que nacen las teorías más importantes (y posiblemente se olvidan) y que sin embargo es conocido por el simple pero sugerente nombre de “bar”.

Creo que, aun sin dar nombre, le debo un par de líneas a una de estas personas, a la cual conocí en el laboratorio y que desde entonces no he querido sacar de mi vida. Y no, no es amor lo que ha surgido de ahí, sino el convencimiento mutuo de recorrernos el mundo buscando cada escenario donde pongan buena música, buena compañía y ganas de disfrutar de la vida (amén de otras actividades lúdico-festivas).

Por supuesto agradecer el apoyo de mi familia, que como siempre y de manera incondicional ha estado ahí. Siempre es más fácil recorrer el camino sabiendo que por muy alta que sea la posición de la que caigas, nunca llegarás al suelo.

Finalmente, sin duda la persona que más se merece estas palabras, es la que estando más cerca o más lejos siempre me ha acompañado en el camino. Soportando el mal humor, la ausencia de tiempo libre y la verborrea monotemática que en algún que otro momento el trabajo de doctorando suele producir. Por ella y por todo lo vivido juntos, sigamos caminando.

Ya casi lo tienes…

RESUMEN

1. INTRODUCCIÓN

La comunicación intercelular es un mecanismo esencial para coordinar las diferentes funciones biológicas en organismos multicelulares, ya sea mediante contacto directo célula-célula, mediante la secreción de intermediarios químicos como hormonas o citocinas, o a través de la secreción de estructuras de membrana conocidas como vesículas extracelulares (VEs). Dichas VEs son secretadas por las células en respuesta a diferentes estímulos, en condiciones fisiológicas o patológicas, y pueden encontrarse en los diferentes fluidos biológicos (1). Diferentes VEs están asociadas a contenido específico, pueden ejercer su acción por interacción con receptores de membrana o transferencia de su contenido y muestran tropismo por sus células diana (2-4).

Las VEs pueden ser clasificadas en tres tipos principales en función de su mecanismo de biogénesis: cuerpos apoptóticos (CAPs), microvesículas (MVs) y exosomas (EXOs) (**Figura 1**). Los CAPs se forman por fragmentación celular durante el proceso de muerte celular programada y suelen presentar tamaños entre 50 nm y 5µm (5, 6). Entre sus funciones, se les atribuye la transferencia de DNA entre células, donde el DNA llega a integrarse en el núcleo de la célula diana y es funcional (7). Esto es de especial importancia en cáncer, donde se ha visto que la transferencia de DNA en CAPs aumenta el potencial tumorigénico in vivo (8). Las MVs se generan por gemación a nivel de la membrana plasmática (9) y presentan tamaños típicamente entre 100 y 1000 nm de diámetro (10). Se les atribuyen funciones en evolución de cánceres (11, 12), modulación del sistema inmune (13) y, reseñablemente, en comunicación materno-embrionaria (14) y regulación paracrina del embrión (15). Los EXOs comienzan su formación por gemación interna de endosomas tardíos, para dar lugar a vesículas intraluminales (VIL) en cuerpos multivesiculares (CMVs).

Posteriormente, los CMVs se fusionan con la membrana plasmática para liberar las VIL, ahora llamadas EXOs, al medio extracelular (16). Suelen presentar tamaños entre 30 y 150 nm y se han visto implicados en gran variedad de funciones biológicas (17), incluyendo la comunicación materno-embrionaria y biología de la reproducción (18-20).

Hasta la fecha se han desarrollado diferentes métodos de aislamiento de VEs basados en diferentes principios (tamaño, forma, densidad, marcadores moleculares, agregación), los cuales se diferencian en qué poblaciones son capaces de aislar y su relación entre pureza y rendimiento del aislamiento (**Tabla 1**). El método más extendido es la centrifugación diferencial seriada, basado en el aislamiento sucesivo de poblaciones vesiculares de tamaño/densidad decreciente mediante aumento de la fuerza centrífuga (6). Con el fin de mejorar la pureza del aislamiento, pueden intercalarse diferentes pasos como gradientes de densidad (2) o filtrados entre ciclos de centrifugación (21). La alternativa más popular a la ultracentrifugación es la cromatografía de exclusión por tamaños, la cual permite el aislamiento de vesículas de tamaños decrecientes en sucesivas fracciones de elución. Permite una mejor purificación de las VEs respecto a proteínas libres, pero suele dar menores rendimientos (22). Otros métodos de aislamiento con aplicaciones más específicas son la purificación por inmunoafinidad (23), la precipitación polimérica (24) o la utilización de dispositivos de microfluídica.

Una vez aisladas, se han desarrollado diferentes métodos para el análisis de las poblaciones de VEs, en función de la característica que se desee estudiar (**Tabla 2**). Entre las técnicas de análisis morfológico, destacan las basadas en microscopía electrónica, ya que son las únicas que permiten la visualización directa de las VEs, debido a su pequeño tamaño. Diferentes variantes de la técnica permiten el análisis de la morfología externa, interna y marcadores moleculares de las VEs (25-27). Del mismo modo, se han desarrollado diferentes técnicas para el análisis del tamaño de las VEs, desde las técnicas de “dynamic light scattering” (DLS) (28) o “nanoparticle

tracking análisis" (NTA) (29) que permiten la medida de las vesículas gracias a su movimiento browniano, hasta técnicas más sensibles como "tunable resistive pulse sensing" basada en cambios de propiedades eléctricas causados por las VEs y que amplían el rango de tamaños y concentraciones medibles (30). Finalmente, las técnicas de análisis de marcadores moleculares han avanzado desde los clásicos western blots hasta técnicas más sensibles, con menores requerimientos de muestra de partida y que permiten de forma simultánea una cuantificación relativa de las VEs, como ExoScreen (31), µMNR (32) o nPLEX (33).

El contenido de las VEs presenta variaciones en función del origen celular, de la subpoblación vesicular y de las condiciones fisiológicas, lo que permite el estudio de sus funciones biológicas y utilidad como biomarcadores. No obstante, dicho contenido también se ve influenciado por las técnicas de aislamiento (3). Se ha demostrado la presencia de contenido específico en VEs para diferentes biomoléculas, incluyendo proteínas, lípidos y RNA (17, 34, 35). El contenido en DNA de las VEs es todavía un campo en desarrollo. Se ha visto que contienen DNA de simple y doble cadena (36), cuyo perfil varía dependiendo de la célula de origen y la población vesicular (37), y que son capaces de transportarlo hasta las células diana (38), donde el DNA se internaliza en el núcleo y es funcional (39). La transferencia de DNA en VEs se ha involucrado especialmente en la inducción del fenotipo canceroso, donde el transporte de fragmentos grandes de DNA genómico se asocia principalmente con los CAPs (40), mientras que MVs y EXOs se asocian con la transferencia de DNA mitocondrial (DNAmt) (41). Entre otras funciones, el envío de DNA en VEs también se ha propuesto como un nuevo mecanismo para la transferencia de material genético entre especies con implicaciones evolutivas (42).

Se ha demostrado la existencia de VEs en los diferentes fluidos reproductivos, incluyendo el líquido folicular (43), oviductal (44) y el endometrial (LE) (19), así como en los tejidos de origen (45). Durante el periodo pre-implantatorio, la producción de VEs se detecta en diferentes tejidos y estas se asocian con funciones específicas (VEs

del fluido folicular, oviductosomas, VEs de la cavidad uterina) (**Tabla 3**). Tras la implantación, la placenta se convierte en el principal sitio de producción de VEs, donde las vesículas generadas por el sincitiotrofoblasto desempeñan funciones importantes en la inmunomodulación de la madre (46).

En el líquido folicular se ha identificado la presencia de VEs con un perfil proteico y de miRNAs específico, y diferente al encontrado libre en el mismo líquido. Se ha demostrado la internalización de dichas VEs y su contenido en miRNA en células de la granulosa, lo cual producía variaciones en el contenido de miRNAs y mRNA de las células receptoras, con algunos de los genes afectados involucrados en desarrollo folicular (47, 48). De hecho, se descubrió un perfil de miRNAs diferencial entre folículos pequeños y grandes, donde el primero estaba relacionado con la promoción de la división celular y el segundo con la respuesta inflamatoria (49). Se observó además que el perfil de miRNAs de las VEs variaba con la edad (50) y con el grado de crecimiento de los ovocitos en los folículos (47). Finalmente, las VEs del fluido folicular se han visto implicadas en la promoción de la expansión de las células del cúmulo (51). En cuanto a los oviductosomas, además de sus funciones en la promoción de la capacidad fecundativa de los espermatozoides (44), se han propuesto como soporte durante el desarrollo embrionario temprano (52).

Tras la llegada del embrión al útero se establece una comunicación entre este y la madre a través de moléculas liberadas a las secreciones uterinas, que en conjunto conforman el LE (53). La secreción de dichas moléculas varia a lo largo del ciclo menstrual (54) y la composición del LE se ve afectada por la exposición ambiental materna, teniendo esto efectos a corto y largo plazo sobre el embrión (55). Se ha descrito la presencia de VEs de origen tanto materno como embrionario en el LE y se les ha atribuido funciones desde la promoción del desarrollo embrionario, capacidad migratoria del trofoblasto e implantación, hasta la regulación de la angiogénesis endometrial (**Tabla 3**) (1).

En cuanto a las VEs producidas por el endometrio, en primera instancia se observó que contenían un perfil de miRNAs diferente al de las células de origen, cuyos genes diana tienen funciones en implantación embrionaria (56) y, del mismo modo, en oveja, se observaron diferencias en el contenido en proteínas y RNAs en vesículas secretadas al fluido luminal de animales gestantes y no gestantes (57). Además, se describió a las VEs como el mecanismo de transporte de los genes *env* del retrovirus ovino Jaagsiekte endógeno desde el endometrio al embrión, donde este tiene un papel crucial en el desarrollo del trofectodermo (57) y promovía la secreción de interferón tau, el cual a su vez anuncia al útero la presencia del embrión pre-implantatorio (58). En humanos, nuestro grupo observó la presencia de EXOs en el LE. Dichos EXOs contenían hsa-miRNA-30d, y eran capaces de transferirlo desde el epitelio endometrial al embrión, donde este era internalizado y modificaba la transcriptómica embrionaria aumentando la expresión de moléculas de adhesión (19). Se propuso la ribonucleoproteína nuclear heterogénea C1 como el transportador del miR-30d al contenido exosomal (59) y se observó que la carencia de miR-30d en embriones estaba asociada a una reducción de los ratios de implantación (60). Reseñablemente, el proteoma de los EXOs producidos por el epitelio endometrial se ha visto variar con los cambios en las proporciones de hormonas esteroides del ciclo menstrual, y que EXOs producidos por células en condiciones hormonales de la fase receptiva incrementaban significativamente la capacidad adhesiva de líneas trofoblásticas en cultivo (18).

Se ha descrito la producción de VEs por parte del embrión, mostrando que la comunicación materno-embrionaria es recíproca y específica, donde las vesículas embrionarias eran internalizadas por el epitelio endometrial pero no por otros tejidos maternos (61). Se ha observado que VEs producidas por el trofectodermo eran capaces de estimular la proliferación de células endoteliales in vitro (62) y la migración de células de músculo liso vascular (63), situando a las VEs como posibles reguladoras de la angiogénesis endometrial y la remodelación de las arterias espirales uterinas. Por otra parte, se ha observado una regulación paracrina del

embrión, donde MVs producidas por la masa celular interna eran capaces de llegar al trofectodermo para estimular su capacidad migratoria y eficiencia implantatoria (15).

Finalmente, es importante remarcar la utilidad de las VEs como biomarcadores en biología reproductiva. Se han propuesto las VEs en plasma materno como biomarcadores de parto pretérmino a través de su firma proteómica (64) y de miRNAs, en el último caso relacionándose con condiciones de tensión de oxígeno bajas (65). Del mismo modo, las VEs en plasma se han propuesto como biomarcadores de pre-eclampsia a través de su contenido proteico en TIMP1 y PAI1 (66), óxido nítrico sintasa endotelial (67) y en los miRNAs miR-486-1-5p y miR-486-2-5p (68). Como marcador de cardiomiopatía periparto, se ha propuesto el contenido en miR-146a en EXOs en suero materno y producidos por células endoteliales de vena umbilical humana (69). También se han propuesto las VEs placentarias como indicadoras de enfermedades infecciosas durante el embarazo (70).

2. HIPÓTESIS

La comunicación entre el endometrio materno y el embrión preimplantatorio mediante VEs es clave para entender la implantación embrionaria y el desarrollo fetal posterior.

Hipotetizamos que el endometrio materno secreta diferentes tipos de VEs con contenido específico durante el ciclo menstrual. Estas adquieren relevancia durante la ventana de implantación, cuando son internalizadas por el embrión modificando su firma genética/transcriptómica y realizan funciones específicas en el proceso de implantación.

3. OBJETIVOS

- Identificar y analizar la morfología, tamaño y marcadores moleculares de las diferentes VEs secretadas por el endometrio humano a la cavidad endometrial durante el ciclo menstrual e investigar su contenido en DNA.
- Investigar si las VEs pueden transportar su contenido en DNA desde el endometrio materno al embrión, así como el impacto metabólico sobre el embrión.

4. MATERIALES Y MÉTODOS

4.1. Obtención de muestras de líquido endometrial

Las muestras de LE se obtuvieron de mujeres sanas siguiendo los criterios de inclusión del estudio en clínica IVI Valencia (CEIC: 1603-IGX-017-FV), mediante succión con un catéter de transferencia de embriones a nivel de la superficie del fundus uterino, y se clasificaron en función de la fase del ciclo menstrual en fase I (días 1-8), fase II (días 9-14), fase III (días 15-18), fase IV (días 19-24) y fase 5 (días 25-30).

4.2. Obtención de embriones murinos y cultivo

Se utilizaron hembras B6C3F1/Crl de 6-8 semanas bajo la autorización del protocolo 2015/VSC/PEA/00048. Las hembras se estimularon con 10 UI Foligon/PMSG seguido 48 horas después de 10 UI de Ovitrelle 250 µg/0.5 mL y cruce con machos de la misma cepa. Las hembras se sacrificaron tras la observación de tapón vaginal y los embriones se obtuvieron de los oviductos mediante "flushing" con PBS. Los embriones obtenidos se lavaron y cultivaron hasta día E3.5 en medio G-2 plus oxigenado.

4.3. Aislamiento de vesículas

Las muestras de LE resuspendidas en PBS se procesaron por centrifugación diferencial seriada para el aislamiento de VEs siguiendo el siguiente esquema: 300 x g, 10 min (x2, eliminación de restos celulares) → 2.000 x g, 10 min (CAPs) → Filtrado 0,8 µm + 10.000 x g, 30 min (MVs) → Filtrado 0,22 µm + 120.000 x g, 70 min (EXOs + sobrenadante) (**Figura 3**).

4.4. Caracterización fenotípica de las VEs

La caracterización de las poblaciones vesiculares presentes en el LE humano se realizó mediante diferentes técnicas:

Microscopía electrónica: las diferentes poblaciones vesiculares se fijaron en solución de Karnovsky y se procesaron por deposición o inclusión en resina LR-white y cortes ultrafinos. En ambos casos se realizó tinción positiva y se realizó visualización en un JEM-1010 a 80 kV.

Western blotting: calnexina, calretiulina, VDAC1, ARF6, CD63, CD9 y TSG-101 se analizaron en las diferentes poblaciones de VEs del LE, el sobrenadante del aislamiento y un lisado células Ishikawa (control positivo).

Análisis del tamaño/concentración de las VEs: los rangos de tamaño de las VEs en muestras únicas de LE humano se analizaron mediante ZetaSizer Nano y NanoSight300. NanoSight300 se utilizó también para calcular concentraciones de vesículas y para analizar la variación en rangos de tamaño y concentración de MVs y EXOs del LE a lo largo del ciclo menstrual. Para ello se utilizaron 6 muestras en fase I, 7 en fase II, 7 en fase III, 6 en fase IV y 6 en fase V del ciclo. La existencia de diferencias en concentración se comprobó mediante test de Kruskal-Wallis. Como control negativo se utilizó PBS. Para mejorar la precisión de las medidas, se calibró el NanoSight con estándares de nanoesferas de sílice.

4.5. Secuenciación del DNA de las VEs

El análisis del contenido de DNA de las VEs del LE se realizó a dos niveles, para secuencias codificantes y sitios de unión para factores de transcripción (SUFT). (1º) Análisis de diferencias para cada tipo de vesícula en pre-receptividad frente a la ventana de implantación. Para ello se utilizaron 4 muestras de LE en fase II y 4 en fase IV. (2º) Análisis de contenido específico del tipo de vesícula durante el periodo receptivo. Para ello se utilizaron las muestras en fase IV y se incrementó el tamaño muestral a 10. Las vesículas aisladas se trataron con DNasa para eliminar el DNA externo, se extrajo el DNA con QIAamp DNA Mini Kit y se concentró mediante SpeedVac. Las librerías se construyeron con el kit Nextera XT DNA Library Prep Kit y se secuenciaron en un NextSeq500 usando un cartucho 300 cycles NextSeq 500 High Output v2 Kit (**Figura 7**). Adicionalmente, se comprobó la necesidad de tratamiento con DNasa para evitar enmascaramiento por DNA externo en un experimento previo. Para este, se utilizó un pool de 6 muestras de LE. Tras el aislamiento de vesículas, cada población se separó en tres fracciones las cuales se trataron, con una (DNasaI), dos (DNasaI y Exonucleasa T5) o ninguna DNasa para comparar el efecto del tratamiento. El resto del protocolo de secuenciación se realizó como en los experimentos previos. Para el análisis bioinformático, se utilizó bcl2fastq para generar los ficheros FASTQ y se normalizó mediante el método TMM del paquete egdeR en R (71). El alineamiento de las lecturas se realizó mediante BWA (72), se filtraron las lecturas con calidad de mapeo >90% mediante Samtools (73) y se eliminaron los duplicados con PICARD. Se obtuvo la cobertura de las diferentes regiones genómicas (secuencias codificantes y SUFTs) mediante Bedtools utilizando las anotaciones hg19 de ENSEMBL (74). El análisis de enriquecimiento diferencial se realizó mediante edgeR (75, 76). Se utilizó una fórmula aditiva incluyendo grupo (tipo de vesícula + fase) y paciente para eliminar las diferencias debidas al paciente. Se utilizó el método de Bonferroni para ajustar el P-valor. Finalmente, para calcular la proporción de DNAmt en las VEs, se calculó el número de reads mapeadas en cada cromosoma con samtools idxstats y se obtuvo la proporción lecturas DNAmt /

lecturas en resto de cromosomas. Para las comparativas entre tipos de VEs y fase del ciclo se utilizó test de Kruskal-Wallis.

4.6. Estudio de la transferencia de DNA de las VEs a embriones murinos

Se utilizaron células Ishikawa para generar VEs con DNA marcado que pudiera ser posteriormente diferenciado del genómico del embrión. Para ello, se cultivaron en presencia de 5-ethinil-2'-desoxiuridina (EdU), el cual se inserta en las cadenas de DNA durante la replicación celular. Posteriormente, las VEs se aislaron del medio condicionado (CAPs, MVs, EXOs + SN) y se incubaron con embriones en hatching en día E3.5 de desarrollo. Como control negativo, se co-incubaron embriones con una mezcla de los distintos tipos de VEs sin EdU. Al día siguiente, se lavaron los embriones y se marcó el DNA vesicular mediante reacción de Click-it (Click-iT™ EdU Alexa Fluor™ 488 Imaging Kit), los núcleos con DAPI y las membranas celulares y zona pelúcida con Wheat Germ Agglutinin, Texas Red™-X Conjugate. Finalmente, se analizó la internalización de DNA vesicular en un microscopio confocal Olympus FV1000 (**Figura 9**).

4.7. Análisis del efecto de las VEs sobre la bioenergética del embrión

Análisis del contenido en ATP: se aislaron las poblaciones vesiculares de un pool de 5 muestras de LE en fase IV del ciclo menstrual y se co-incubaron durante la noche con embriones en día E3.5 de desarrollo en las siguientes combinaciones: CAPs, MVs, EXOs, mezcla de todas las poblaciones y sin vesículas. Al día siguiente, se lavó los embriones y se midió su contenido en ATP utilizando el kit FLASC (Sigma-Aldrich) (**Figura 10**). Se seleccionaron embriones de buena calidad en grupos de 10, consiguiendo 6 replicados para CAPs y MVs, 5 replicados para EXOs y la combinación de VEs, y 3 replicados para la condición sin vesículas. Para analizar diferencias entre condiciones se utilizó test ANOVA (77, 78) y test de Tukey para el análisis post-hoc. El contenido en ATP en las muestras se obtuvo mediante regresión lineal a partir de

la curva de estándares y se muestra como la media de replicados conteniendo 10 embriones ± desviación estándar (**Figura 45**).

Análisis del potencial de membrana mitocondrial: se estudió potencial de membrana como una medida de la actividad mitocondrial. Se obtuvieron las diferentes poblaciones de VEs del medio condicionado de células Ishikawa y se incubaron durante la noche con embriones murinos siguiendo el esquema del experimento previo. Tras la incubación, se analizaron diferencias en potencial de membrana utilizando el sistema de JC-1 (79). Como control de mitocondria despolarizada, una parte de los embriones incubados en ausencia de vesículas se trató con valinomicina (80). El análisis de fluorescencia se realizó en microscopio confocal Olympus FV1000 (**Figura 11**). Finalmente, se utilizó ImageJ para calcular la intensidad media de fluorescencia para los diferentes canales y se calculó para cada condición la proporción agregados / monómeros.

5. RESULTADOS Y DISCUSIÓN

5.1. Caracterización fenotípica de las VEs del liquido endometrial humano

Las imágenes de microscopía electrónica de transmisión (MET) mostraron a los CAPs diferenciados por su gran tamaño entre 1.5 µm y 8 µm, aunque también se observó una población más pequeña de CAPs con tamaños entre los 50 y los 700 nm (**Figura 12**). Su patrón de marcadores moleculares destacó por la presencia de calreticulina y VDAC1. Calreticulina se observó en los mismos niveles en CAPs y MVs, hecho que ya había sido reportado (81, 82). VDAC1 fue más específico de CAPs, aunque se encontró una señal menor en MVs (**Figura 15**). Esto podría explicarse por la incapacidad de las técnicas de aislamiento para separar poblaciones únicas de VEs (6, 83). Los CAPs se describieron como una población multimodal con dos centros de tamaño bajo DLS. La población principal tenía un tamaño medio aproximado de 2 µm y representaba el 61,1% del total de partículas. La segundo mostró un tamaño

medio de 274.7 nm, correspondiente al 38.4% del contenido total de partículas (**Figura 18**). Esta segunda población podría haber surgido después del aislamiento inicial de CAPs (de lo contrario, se habría aislado junto a la fracción de MVs) y concuerda con nuestras observaciones MET que indican una población de CAP de menor tamaño (**Figura 12**). Un posible origen de estos CAPs de pequeño tamaño puede ser la fragmentación de la membrana del retículo endoplásmico (RE) durante la apoptosis, dando lugar a vesículas más pequeñas que los CAPs canónicos (84, 85) las cuales se liberarían durante su procesamiento. Esto además podría relacionarse con la presencia de calnexina y calreticulina, dos proteínas conocidas del RE, en MV, una fracción que muestra un rango de tamaño superpuesto al de los CAPs pequeños (**Figura 16**).

Mediante MET, las MVs se observaron mucho más abundantes, presentaban tamaños de 200 a 700 nm y un contenido electrón-denso de elevada heterogeneidad (**Figura 13**). ARF6, un marcador propuesto para esta población (9, 86), también se encontró en EXOs, aunque con un patrón de banda diferente: EXO mostraban dos bandas en comparación con una banda única para MVs. Esto se confirmó al observar el patrón de los CAPs, donde ambas bandas estaban presentes, con la banda específica para EXO en niveles relativamente más bajos (**Figura 16**). Las MVs presentaban tamaños en su rango canónico de 100 – 1000 nm, en una sola población con un tamaño medio de 290.8 nm, observado por DLS (**Figura 18**). Un análisis más detallado por NTA delimitó la mayoría de estas vesículas entre los 150 – 550 nm, con un tamaño modal de 267,2 nm, y 83,49% del total de partículas mayores de 200 nm (**Figura 20**). El tamaño de las MVs se observó similar en las diferentes fases del ciclo menstrual. Su concentración fue comparable a la de los EXOs, especialmente durante fase I y se apreció una tendencia decreciente no significativa con la progresión del ciclo ($p > 0.05$) (**Figura 21**).

Los EXOs mostraron aspectos y abundancia similares a las MVs por MET, con tamaños entre 40 – 160 nm y estructuras aparentemente más homogéneas en

comparación con otras poblaciones de VEs (**Figura 14**). Las tetraspaninas CD9 y CD63, así como TSG101, seleccionados como marcadores clásicos de EXOs (3), se observaron en las tres poblaciones de VEs (**Figura 17**), descartando su uso como marcadores específicos de EXOs. Del mismo modo, se confirmó señal negativa de calnexina para los EXOs (87, 88) y se observó un patrón de distribución en VEs similar al de la calreticulina, lo que es consistente ya que ambas proteínas proceden del retículo endoplásmico (88, 89) (**Figura 15**). Los EXO mostraron una población de un solo tamaño, parcialmente solapante al de las MVs, con un tamaño medio en DLS de 143,2 nm (**Figura 18**). Bajo detalle de NTA se delimitaron al intervalo de 70 a 400 nm, aunque los tamaños >200 nm mostraron un error estándar aumentado, indicando inestabilidad y la probable presencia de agregados. El tamaño modal de los EXOs fue de 155.5 nm, y el 62.68% de las partículas totales fueron <200 nm. Los perfiles de tamaño de EXOs se mantuvieron constantes a lo largo del ciclo y tampoco se apreciaron diferencias en concentración (**Figura 21**).

En conjunto, nuestros datos sugieren una contribución similar de MVs y EXOs en el LE en términos de número total de vesículas, con un perfil de tamaño que muestra la prevalencia de EXOs en la porción más alta de su intervalo canónico y MVs de tamaños pequeños dentro de su rango de tamaño clásico (1). Finalmente, el sobrenadante del proceso de aislamiento de vesículas mostró una cantidad reducida de partículas de pequeño tamaño en DLS y NTA, posiblemente correspondientes a agregados proteicos. El PBS, utilizado para la resuspensión de las VEs tras la extracción no mostró un número de partículas medible (**Figura 20**).

5.2. Contenido en DNA de las VEs del LE en función del momento del ciclo y del tipo de vesícula (secuencias codificantes y SUFT)

Previamente a analizar el contenido específico en DNA de las VEs del LE, se evaluó la necesidad de tratamiento con DNasa para eliminar el DNA que pudiera quedar pegado externamente y enmascarar el contenido real de las vesículas. Los resultados

de secuenciación mostraron enriquecimiento tanto en secuencias codificantes como en SUFT sobre el DNA genómico total en las poblaciones vesiculares sólo tras el tratamiento con DNasa (**Figura 23**), indicando que existía un patrón específico de transmisión de DNA que sería enmascarado si no se eliminara el DNA externo previo a la extracción del DNA vesicular.

Las secuencias génicas se estudiaron bajo la hipótesis de que pudieran llegar al embrión en VEs, al menos al trofectodermo, donde podrían expresarse para aumentar la producción de ciertos RNAs. Los SUFT se exploraron por su capacidad de unión a factores de transcripción (FT), proteínas reguladoras de la estructura del DNA para la modulación de la expresión génica. Se planteó que una vez dentro del embrión podrían unir FTs para promover la expresión de ciertos genes o, por el contrario, secuestrarlos para disminuir la expresión génica. Se hipotetizó que el DNA podría alcanzar los núcleos embrionarios y sobrevivir cierto tiempo como un elemento satélite transcripcionalmente funcional para apoyar la implantación.

Tras definir las condiciones experimentales, se llevó a cabo un análisis para identificar diferencias en el contenido en DNA de cada tipo de vesícula en el momento de receptividad (fase IV) frente a la fase proliferativa del endometrio (fase II). El análisis de secuenciación no evidenció diferencias en SUFT entre fases del ciclo, pero sí se descubrió un pequeño número de secuencias génicas diferencialmente secretadas en todas las poblaciones vesiculares tanto en fase proliferativa como receptiva (**Figura 25**, **Tabla 5**). Entre las secuencias enriquecidas en fase IV, cabe destacar el gen para la enzima glutatión S-transferasa theta 1 (*GSTT1*), para el cual se descubrió un enriquecimiento de entre 326 y 423 veces en las distintas VEs. GSTT1 es una enzima con importantes funciones en detoxificación de especies reactivas del oxígeno (ERO) (90) y cuya pérdida de función se asocia con mayores riesgos de parto pretérmino ligados a incremento del estrés oxidativo (91), pre-eclampsia (92) y pérdida del embarazo (93). Además, la transmisión de *GSTT1* durante la ventana de implantación podría constituir un mecanismo materno para la sobreexpresión

embrionaria de esta enzima para combatir el incremento de ERO producidas por el embrión en desarrollo (y tejidos circundantes) y que limitan su capacidad implantatoria (94). Entre las secuencias enriquecidas en fase proliferativa, *UGT2B17* fue la más específica con valores de fold-change entre 14,15 y 17,4 en las diferentes VEs. Su producto codificado tiene funciones en la eliminación de hormonas esteroides, como los estrógenos, de células en proliferación. No existen actualmente evidencias de las funciones de UGT2B17 durante la etapa de restauración endometrial, pero se ha visto involucrado en cáncer de endometrio, donde su eliminación conduce a la inhibición del crecimiento celular y a la apoptosis de las células cancerosas (95).

En vista de las escasas diferencias observadas entre fases, se decidió aumentar el tamaño muestral en fase receptiva para evaluar un posible papel diferencial de las VEs del LE sobre el embrión peri-implantatorio. El análisis de secuencias génicas reveló a las MVs como la única población con contenido diferencial en DNA, destacando un enriquecimiento de 11.12 ± 0.53 fold-change en los 13 genes mitocondriales conocidos al comparar con EXOs (**Tabla 6**). Dichos genes codifican para subunidades proteicas de la cadena de transporte de electrones (96, 97). En cuanto al análisis de SUFT, se observó una gran variedad y enriquecimiento de nuevo sólo en MVs al compararlas con el resto de las poblaciones. Concretamente, se observó enriquecimiento en 28 SUFT en la comparativa con CAPs (fold-change entre 7,1 y 26,7) y en 192 SUFT al comparar con EXOs (fold-change entre 8.61 y 22.35), la mayoría de los cuales procedían del genoma mitocondrial (**Tabla 7, Figura 29**). Para facilitar la interpretación de resultados, se clasificaron los SUFT por el FT que son capaces de unir, algunos de los cuales tienen funciones conocidas en desarrollo embrionario (**Tabla 8**).

En conjunto, el análisis de las secuencias génicas mostró a las MVs como potenciales vehículos para aumentar las copias de los genes del DNAmt en las mitocondrias embrionarias. En cuanto a los SUFT, observamos que, aunque la mayoría tenían

origen mitocondrial, los FTs relacionados tienen función a nivel nuclear, pudiendo esto constituir un vínculo entre el control genético compartido nuclear y mitocondrial de la fisiología mitocondrial (98). Particularmente, TRF4 resulta interesante por su función en la protección contra el estrés oxidativo (99), lo que podría estar en línea con la transmisión de GSTT1 durante la ventana de implantación (90, 94). También cabe destacar la transmisión de SUFT para GABP, FT con funciones sobre la biogénesis y función mitocondrial (100, 101), que además fueron el segundo grupo de SUFT con mayor enriquecimiento (**Figura 29**). Estos resultados demostraron por primera vez que el endometrio libera DNAmt en VEs, especialmente MVs, al líquido endometrial como un posible mecanismo de regulación de la bioenergética del embrión en el momento de la implantación. El análisis de la proporción de DNAmt frente a DNA nuclear en VEs del LE reveló una tendencia positiva en receptividad frente a la fase proliferativa del ciclo, aunque no significativa. Sin embargo, si se observó un aumento significativo para esta proporción en MVs en comparación con CAPs y EXOs independientemente de la fase del ciclo (**Figura 34**).

5.3. Capacidad de las VEs endometriales para transportar DNA al embrión en cocultivo

Se demostró la transmisión de DNA a través de CAPs tanto a nivel citoplasmático como nuclear y se observó una gran cantidad de DNA transmitido que tendía a acumularse en grandes depósitos en zonas discretas del embrión, principalmente a nivel citoplasmático (**Figura 35**). Las MVs también se observaron capaces de transportar DNA al citoplasma y núcleos embrionarios. En este caso, la transmisión siguió un patrón de pequeños puntos situados principalmente a nivel perinuclear (**Figura 36**). En cuanto a los EXOs, aunque se observó potencial para la transferencia de DNA, este fue más residual (**Figura 37**). Estos resultados sugieren reconsiderar la utilidad de los EXOs en la transmisión de DNA, al menos a nivel del LE. Por el contrario, se han descrito como un vehículo clave para la transmisión de RNAs

pequeños (19, 56). Finalmente, el sobrenadante del proceso de aislamiento, el cual contendría principalmente DNA libre y potencialmente una cantidad residual de VEs de pequeño tamaño, no mostró señal de transmisión de DNA (**Figura 38**), de lo que se concluyó que la transmisión de DNA a nivel del LE se produciría principalmente a través de VEs y no en forma de DNA libre. Remarcablemente, independientemente de la población, la transferencia de DNA se observó sólo en zonas del embrión que ya se habían liberado de la zona pelúcida, donde el contacto intermembrana es posible, y al menos a nivel del trofoblasto.

5.4. Papel potencial de las VEs del LE en la modulación de la bioenergética embrionaria

Para evaluar si el cargo de las VEs del LE en DNAmt y su habilidad para transportar el DNA al embrión se correlacionaban con una modulación de la actividad energética del mismo, se llevaron a cabo dos experimentos. En el primero, se midió la cantidad de ATP en embriones murinos tras la exposición a los diferentes tipos de VEs del LE. No se observaron diferencias significativas en embriones co-incubados con CAPs o MVs frente a embriones cultivados sin el estímulo de VEs del LE. En cambio, al co-incubar los embriones con EXOs y, en menor medida, con una combinación de los tres tipos de vesículas, se apreció una reducción significativa del ATP embrionario (**Figura 45**). Para intentar averiguar el origen de la reducción en ATP producida por los EXOs, se llevó a cabo un segundo experimento donde se analizó el potencial de membrana mitocondrial utilizando las condiciones del experimento previo y el sistema de marcaje de JC-1. Mediante este sistema, una mayor proporción de agregados frente a monómeros de JC-1 se relacionaría con un mayor potencial de membrana y, por tanto, con mitocondrias más activas en la producción de ATP. Se introdujo una condición tratada con valinomicina, un desacoplante de la fosforilación oxidativa, como control de embriones con mitocondrias no cargadas. La lectura de fluorescencia demostró que los embriones estimulados con EXOs, aislados o en combinación con el resto de VEs, presentaban niveles de JC-1 más bajos

tanto en forma monomérica como en agregados en comparación con el resto de condiciones. Por el contrario, los estímulos de CAPs y MVs mantuvieron la señal JC-1 al mismo nivel que embriones sin VEs (**Figura 46**). Sin embargo, no se observaron diferencias en la relación agregados/monómeros entre las diferentes condiciones (0.74 ± 0.05, 0.66 ± 0.13, 0.74 ± 0.06, 0.69 ± 0.12, 0.64 ± 0.15 para CAPs, MVs, EXOs, combinación de VEs y sin VEs, respectivamente), y en todos los casos fue superior a la del control con valinomicina (0.35 ± 0.08). Por ello se concluyó que la incubación de los embriones con EXOs no conducía a una reducción de su potencial de membrana mitocondrial y, por tanto, de su producción de ATP. Sin embargo, la reducción en el contenido de monómeros de JC-1, y en consecuencia de agregados, también se ha relacionado con una reducción de la masa mitocondrial total, sin afectar a la proporción monómeros/agregados (102-104). Por ello, este trabajo propone que la reducción en ATP en embriones incubados en presencia de EXO podría deberse a una reducción en el contenido mitocondrial en lugar de a una afectación de su funcionalidad.

Tomando todos los resultados en conjunto, nuestra hipótesis es que las VEs del LE desempeñarían un papel cooperativo para regular la funcionalidad mitocondrial. Por una parte, las MVs transportan DNAmt que puede interactuar con las mitocondrias y FTs nucleares en el trofoblasto para regular la producción de ATP mientras protegen las células del aumento del consumo de oxígeno y producción de ERO a medida que se acerca el momento de la implantación (94, 105). Además, los SUFT transportados podrían tener un papel para el posterior desarrollo de tejidos embrionarios especializados, lo está respaldado por recientes estudios que posicionan a las mitocondrias como orgánulos que integran señales celulares y se comunican con el núcleo y otros orgánulos celulares para desencadenar cascadas de señalización con impacto desde la división celular hasta la especialización de linajes celulares, y cuya pérdida de función afecta al desarrollo embrionario post-implantatorio (98, 106). Por otra parte, los EXOs tendrían el papel de controlar la población mitocondrial hacia una reducción de la masa total. Esto podría vincularse

con los embriones de buena calidad en ciclos de reproducción asistida, que carecen de los estímulos de las VEs del LE durante el cultivo in vitro, muestran un contenido elevado de DNAmt y están asociados con tasas de implantación más bajas (107, 108). También podría plantearse la hipótesis de que una reducción en la masa mitocondrial total podría responder a un incremento en la demanda de energía rápida cuando el embrión se acerca al momento de la implantación, pasando a utilizar la glicólisis para saciar dicha demanda. Se ha observado que el embrión elige la glicólisis para generar energía tras alcanzar el estadío de blastocisto y acercarse el momento de implantación. Además, se produce una reducción de la concentración de oxígeno en la transición entre las trompas de Falopio y el útero, lo que reduce la eficiencia del ciclo de los ácidos tricarboxílicos para producir energía (efecto Warburg). Además, en el estadío de blastocisto, el piruvato se convierte en el sustrato energético más importante (109, 110). Una reducción en la eficiencia del ciclo de Krebs y la promoción de la glicólisis, podría también hacer innecesario el mantenimiento de parte de la población mitocondrial, por lo que su eliminación podría favorecer la eficiencia energética del embrión. Las mitocondrias reducidas en número por acción de los EXOs podrían ser sobrecargadas con elementos de la cadena de transporte de electrones por acción de las MVs a nivel mitocondrial y nuclear. Esto podría incrementar y concentrar la producción de ATP, el cual sería rápidamente consumido por las crecientes necesidades energéticas del embrión peri-implantatorio. Consecuentemente, se haría necesario fortalecer las barreras contra los estreses oxidativo e ionizante producidos por una cadena de transporte de electrones hiperactivada, a través de la sobreexpresión de intermediarios como GSTT1 (90) o TR4 (99, 111).

6. CONCLUSIONES

- El líquido endometrial humano contiene diferentes poblaciones de vesículas extracelulares que pueden ser clasificadas como cuerpos apoptóticos, microvesículas y exosomas. Estas poblaciones presentan morfología, marcadores moleculares y perfiles de tamaño específicos.

- La concentración de microvesículas y exosomas es similar en el líquido endometrial, y no se aprecian diferencias significativas en tamaño ni en concentración a lo largo del ciclo menstrual.

- Los distintos tipos de vesículas extracelulares endometriales contienen DNA que representa todos los cromosomas y el DNA mitocondrial, observándose un enriquecimiento específico en secuencias génicas y SUFT dependiendo de la fase del ciclo menstrual y del tipo de vesícula.

- Durante la fase de receptividad endometrial, las vesículas extracelulares endometriales están enriquecidas en la secuencia del gen *GSTT1*, cuyo producto tiene funciones importantes en la protección frente al estrés oxidativo. Además, se identificó un enriquecimiento en DNA mitocondrial en las MVs, incluyendo todas las proteínas codificadas en el genoma mitocondrial para complejos de la cadena de transporte de electrones, y SUFT relacionados con factores de transcripción implicados en la fisiología mitocondrial y modulación epigenética.

- Las vesículas extracelulares endometriales transfieren su contenido en DNA al embrión, que lo internaliza en las células del trofectodermo que han hecho hatching. Esta transmisión aparece especialmente acentuada para CAPs y MVs, mientras que la transmisión de DNA mediante EXOs es menor, y no se observa transmisión en la fracción libre de vesículas, sugiriendo que esta es llevada a cabo principalmente por las VEs.

- Los EXOs aislados del endometrio receptivo provocan una reducción de los niveles de ATP en los embriones en cocultivo posiblemente relacionada con una reducción en la masa mitocondrial total.

TABLE OF CONTENT

LIST OF FIGURES

LIST OF TABLES

TABLE OF ABBREVIATIONS

ABBREVIATION	MEANING
λ	Wavelength
µNMR	Micro nuclear magnetic resonance
ABs	Apoptotic Bodies
ACVR1	Activin A receptor type 1
AFM	Atomic force microscopy
ALIX	Apoptosis-Linked Gene 2-Interacting Protein X
ams	Approximate mean size
ANOVA	Analysis of variance
ARF6	ADP-ribosylation factor 6
BMP	Bone morphogenetic protein
BSA	Bovine serum albumin
BWA	Burrows-Wheeler Aligner
CAD	Coronary arterial disease
Chr	Chromosome
CPM	Count per million
Cryo-EM	Cryo-electron microscopy
CTCF	CCCTC-Binding Factor
DC	Dendritic cell
DiO	3,3'-Dioctadecyloxacarbocyanine Perchlorate
DLS	Dynamic light scattering
DMD	Differentially methylated domain
dsDNA	Double stranded DNA
EdU	5-Ethynyl-2'-deoxyuridine
EE	Early endosome
EF	Endometrial fluid
ELISA	Enzyme-Linked ImmunoSorbent Assay
EMCT	Embryo-maternal crosstalk
enJSRV	endogenous Jaagsiekte sheep retrovirus
ER	Endoplasmic reticulum
ESCRT	Endosomal Sorting Complex Required for Transport
EVs	Extracellular Vesicles
EXOs	Exosomes
ExV	Exocytic Vesicle
FAK	Focal adhesion kinase
FBS	Foetal Bovine Serum
FC	Fold Change
FOXO3	Forkhead Box O3
FSH	Follicle stimulating hormone
FWER	Family-Wise Error Rate
GABP	GA Binding Protein
GATA1	GATA Binding Protein 1
GATA2	GATA Binding Protein 2
H19	H19 Imprinted Maternally Expressed Transcript
HBSS	Hanks' Balanced Salt solution
HIV	Human Immunodeficiency virus
HRT	Hormone replacement therapy
HSC70	Heat shock cognate 71 kDa protein

ABBREVIATION	MEANING
HSPA8	Heat Shock Protein Family A (Hsp70) Member 8
HUVEC	Human umbilical vein endothelial cells
ICM	Ischemic cardiomyopathy
ID2	Inhibitor of DNA Binding 2
IFNT	Interferon tau
IGV	Integrative Genomic Viewer
IL	Interleukine
ILVs	Intraluminal Vesicles
JC-1	5,5',6,6'-tetrachloro-1,1',3,3'-tetraethylbenzimidazolylcarbocyanine iodide
JNK	c-Jun N-terminal kinase
LE	Late endosome
LH	Luteinizing hormone
lncRNA	Long non-coding RNA
LOT	Low-oxygen tension
miRNA	MicroRNA
mRNA	Messenger RNA
MT	Mitochondrion
mtDNA	Mitochondrial DNA
MVBs	Multivesicular Bodies
MVs	Microvesicles
N	Number of samples
NF-κB	Nuclear factor kappa-light-chain-enhancer of activated B cells
NK	Natural Killer
nPLEX	Nano-plasmonic exosome assay
NR2C1	Nuclear Receptor Subfamily 2 Group C Member 1
NR2C2	Nuclear Receptor Subfamily 2 Group C member 2
NRF2	Nuclear Respiratory Factor 2
NS300	NanoSight 300 (NTA)
NTA	Nanoparticle tracking analysis
O/N	Overnight
OVGP	Oviduct Specific Glycoprotein
OXPHOS	Oxidative Phosphorylation
PAGE	Polyacrylamide gel electrophoresis
PAI1	Plasminogen activator inhibitor type 1
PAX5	Paired Box 5
PBS	Phosphate buffered saline
PBS-T	PBS-Tween-20 (1%)
PC (in PCAs)	Principal component
PCA	Principal Component Analysis
PE	Pre-eclampsia
piRNA	Piwi-interacting RNA
PLAP	Placental Alkaline Phosphatase
PlGF	Placental growth factor
PMCA4	Plasma membrane calcium ATPase 4
PMSG	Pregnant mare serum gonadotropin
PPCM	Peripartum cardiomyopathy
PR	Progesterone receptor
PS	Phosphatidylserine
PVDF	Polyvinylidene fluoride
RI	Refractive index

ABBREVIATION	MEANING
RIPA	Radioimmunoprecipitation assay buffer
ROS	Reactive oxygen species
rRNA	Ribosomal RNA
RT	Room temperature
SDS	Sodium Dodecyl Sulfate
SEM	Scanning Electron Microscopy
siRNA	Small interference RNA
SN	Supernatant
snoRNA	Small nucleolar RNA
SPAM1	Sperm Adhesion Molecule 1
SPB	Spontaneous premature births
SPZ	Sperm
SRE	Serum response element
SRF	Serum Response Factor
ssDNA	Single stranded DNA
STB	Syncytiotrophoblast
STBM	Syncytiotrophoblast microvillous membrane vesicles
TCL	Tissue cell lysate
TEM	Transmission Electron Microscopy
TF	Transcription factor
TFBS	Transcription Factor Binding Site
TGF-β1	Transforming growth factor-β1
TIMP1	Tissue Inhibitor Of Metalloproteinase 1
TLR	Toll-like receptor
TMM (normalization method)	Trimmed Mean of M-values
TNFα	Tumor necrosis factor α
TR2	Testicular Receptor 2
TR4	Testicular Receptor 4
tRNA	Transfer RNA
TRPS	Tunable resisting pulse sensing
TSG101	Tumor Susceptibility Gene 101
VDAC1	Voltage-dependent anion-selective channel 1
WOI	Window of implantation

INTRODUCTION

HYPOTHESIS
OBJECTIVES
MATERIALS AND METHODS
RESULTS AND DISCUSSION
CONCLUSIONS
REFERENCES

1. INTRODUCTION

Intercellular communication is an essential process both for multicellular organism's physiology and for the relationship of unicellular organisms with the environment and hosts (17). Classically, communication has been defined as direct via cell-to-cell contact or indirect as endocrine, paracrine and autocrine by the secretion, release, and uptake of chemical moieties such as cytokines, hormones, growth factors or neurotransmitters (112, 113). According to The Human Protein Atlas, nearly 39% of the human protein-coding genes are annotated to give rise to membrane (28%) and secreted (15%) forms of signaling protein variants, some of them producing both isoforms.

In the last decades, a new mechanism has been in the spotlight for cellular communication, which is the releasing/uptaking of extracellular vesicles (EVs). EVs broadly designate a group of membrane-enclosed structures that are released by cells in response to different stimuli, either in physiological or pathological conditions. They have been found in different body fluids such as, semen (114), saliva (115), plasma (116), breast milk (117), urine (118) and amniotic fluid (119), among others (2), and are produced by both specialized and non-specialized cells. There is evidence of EVs conservation throughout evolution, as these structures are involved in the physiology of living beings from bacteria to humans (120). They have been associated to a rich molecular cargo, which can be transported from one cell or tissue to another, protected from extracellular degradation or modification. EVs exert their biological roles by either direct interaction with cell surface receptors or by transmission of their contents by endocytosis, phagocytosis or fusion with the membrane of the target cells. Recipient cell specificity appears to be driven by specific receptors between target cells and EVs (2-4). All these features have placed EVs secretion as an important mechanism for intercellular communication.

1.1 Extracellular vesicles: Types, Isolation, Characterization, and main cargo

1.1.1 Types of EVs

EVs can be classified in different populations based on different criteria, such as, cellular origin, biophysical (density and size) and biochemical (biological markers) features, composition, or biological function. Nevertheless, the most common system for EVs definition is based on their biogenetic pathway and gives rise to three major categories: apoptotic bodies (ABs), microvesicles (MVs) and exosomes (EXOs) (3, 121, 122) (**Figure 1**).

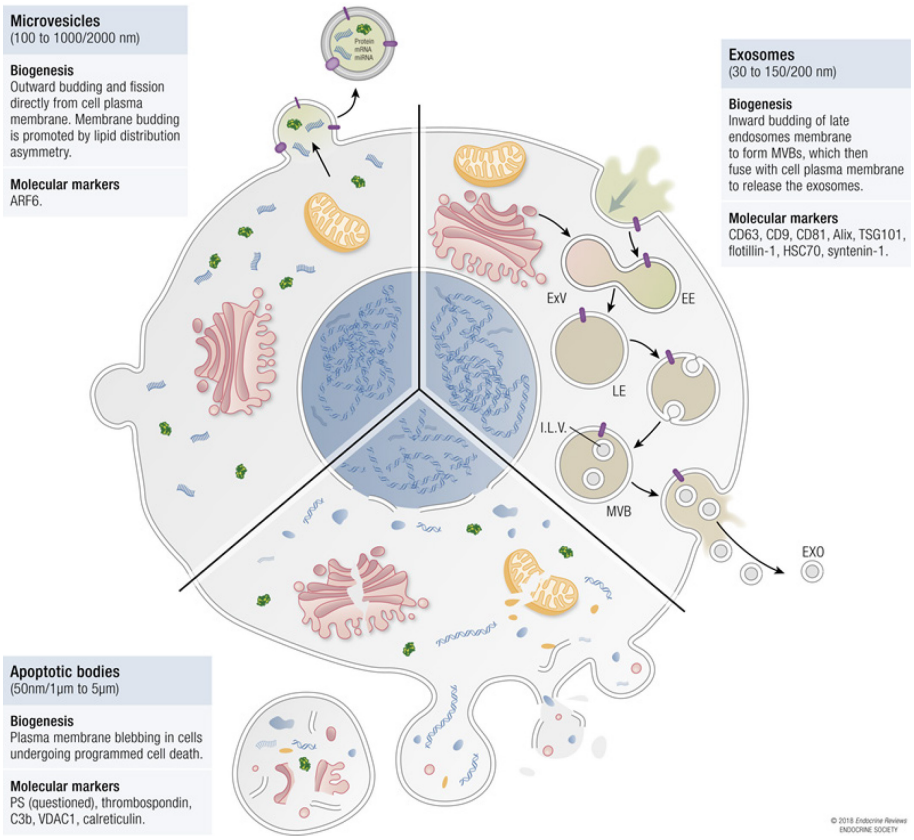

Figure 1. Main types of EVs present in body fluids and culture media. EVs are classified in three groups according to their biogenetic pathways. EXOs are produced in the endosomal pathway by invagination of the membrane of late endosomes to form intraluminal vesicles (ILVs) enclosed in multivesicular bodies (MVBs). MVBs can then fuse with lysosomes and degrade their content, or fuse with cell plasma membrane to release ILVs, now regarded as EXOs. MVs are produced directly from the cell plasma membrane by outward budding. ABs are generated as blebs in cells undergoing programmed cell death. EE, early endosome; ExV, exocytic vesicle; LE, late endosome (Simon C. *et al*, Extracellular Vesicles in Human Reproduction in Health and Disease, Endocr Rev, 2018;39(3):292-332, by permission of the Endocrine Society. License number 4735010508282).

1.1.1.1 Apoptotic bodies

ABs are EVs produced by blebbing of plasma membrane in cells undergoing programmed cell death. This term was coined by Kerr and colleagues who defined them as 'small, roughly spherical or ovoid cytoplasmatic fragments, some of which contain pyknotic remnants of nuclei' (123). Indeed, one of the events that characterize ABs is the fragmentation and packaging of cellular organelles such as the nucleus, endoplasmic reticulum or Golgi apparatus into these vesicles (124, 125).

ABs have widely been described to be 1 - 5 µm in diameter, thus overlapping with the size range of platelets (5, 126). Nevertheless, some groups extend the lower range to 50 nm (6, 82, 127). Their buoyant density in a sucrose gradient is in the range of 1.16 to 1.28 g/mL (128, 129).

This vesicle population is characterized by cytoskeletal and membrane alterations, including the translocation of phosphatidylserine (PS) from the inner to the outer leaflet of the lipid bilayer (130). In this way, PS serves as an 'eat me' signal for phagocytes to target and clear apoptotic debris (131, 132). Moreover, PS can naturally be recognized by annexin V, which turns out a useful marker of ABs (133, 134). Another specific feature of ABs is the oxidation of surface molecules, what creates sites that can be recognized by specific molecules such as thrombospondin (135) or C3b complement protein (136), which are also useful as ABs markers.

Different functions have been attributed to ABs. DNA can be horizontally transmitted by ABs between somatic cells, with possible integration of this DNA within the receptor cell where it can be functional (7). These vesicles are also a vehicle for the horizontal transfer of oncogenes, which are internalized by target cells and consequently increase their tumorigenic potential in vivo (8, 137). ABs have also been related to the immune response where they are associated with an under-activation of the immune system (138), and with antigen presentation with special regard to the self-tolerance (139-141).

1.1.1.2 Microvesicles

MVs constitute an EVs population that is formed and released directly from the cell plasma membrane by outward budding and fission (9, 142, 143). Plasma membrane blebbing is triggered by different mechanisms. These are accompanied by the remodelling of membrane proteins and lipids distribution, what has the ability of modulating membrane rigidity and curvature (86). All this changes within the periphery of the plasma membrane have been associated with cargo sorting in MVs (144). MVs population was detected for the first time by the group of Chargaff (145) as a factor that could be precipitated at high centrifugal forces (31,000 x g) but never at weaker fields (5,000 x g).

The size range of MVs has been classically established between 100 and 1000 nm (10), thus overlapping with that of bacteria (121). Other groups extend this range up to 1500 nm (146) or even 2000 nm (147). The buoyant density of MVs is not as clear as that from other vesicles populations. Nonetheless, it has been established around 1.16 g/mL in sucrose gradient (148) although another groups state 1.04-1.07 g/mL (149). The flotation density in iodixanol gradient is placed between 1.18-1.19 g/mL (150).

Among the functions related to MVs, they have been observed to play pivotal roles in cancer cell invasiveness (11, 151), transformation potential (12), progression (142, 152, 153) and drug resistance (154). MVs have also been involved in autoimmune diseases (155-157), immune system modulation and coagulation (10, 13, 158), embryo-maternal cross-talk (14) and embryo self-regulation (15).

1.1.1.3 Exosomes

EXOs constitute an EVs population that arise from the endosomal pathway. Their biogenesis initiates with the inward budding of the limiting membrane of late endosomes, giving place to intraluminal vesicles (ILVs) that remain enclosed inside a bigger membrane compartment regarded now as multivesicular body (MVB). The MVBs can then fuse with lysosomes to degrade their content or with the plasma membrane to release the ILVs, now EXOs (16). There are several molecular mechanisms, either canonical or alternative, implicated in the formation (endosomal sorting complex required for transport (ESCRT), tetraspanins, other membrane proteins and lipids), release (Rab GTPase family members) and extracellular fate of EXOs, which likely vary in different tissues and cell types depending on metabolic needs (3). The first description of EXOs comes from 1981, when they were described as a second population of vesicles that appeared in the preparations of MVs and the term exosome was coined (159). Nevertheless, it was two years later when their biogenetic pathway was formally described by transmission electron microscopy when analysing trafficking of transferrin molecules (160).

Most studies place EXOs in a size range of 30 to 150 nm (3, 161) or even 200 nm (162), thus overlapping with that of virus (122). The buoyant density of EXOs in sucrose gradients has been set in a wide range of 1.10 to 1.21 g/mL (127, 163), and 1.10 to 1.12 g/mL in iodixanol gradients (164).

The enormous effort devoted to the study of the role of EXOs in different biological processes, both in normal or pathological conditions, has prompted an important growth of the field of EXOs in the last years and they have been implicated in many functions (17, 165). EXOs have been involved in cancer physiology, participating in tumour progression and maintenance, resistance, immune modulation and angiogenesis (166). Their function in immune regulation has also been well studied in antigen presentation modulation, immune activation and suppression (167, 168). Finally, the role of EXOs in embryo-maternal cross-talk and reproductive biology has been extensively analysed (18-20).

1.1.2 Methods for EVs isolation

Many different methods have been developed for the isolation of the different populations of EVs from biological samples. These are based in different principles including physical properties (size, shape, density, surface charge), specific surface molecules or aggregation to increase weight. Nevertheless, all of them face the same problem: being able to isolate the desired EV fraction avoiding contamination with other fractions while ensuring enough yield for downstream applications. For this reason, an appropriate choice of the isolation technique is mandatory depending on the population or subpopulation of interest and an evaluation of the impact of potential contaminations with other EVs fractions or free-floating biomolecules should be considered. The main current isolation techniques are described next and their features are summarized in **Table 1**.

Table 1. Main methods for EVs isolation. Advantages and limitations.

METHOD	TECHNIQUE (principle)	ADVANTAGES	LIMITATIONS
Centrifugation	Serial differential centrifugation (Sedimentation velocity)	- Versatile. - Standardization. - Ease of use. - Reproducibility. - Yield.	- Affected by density, tube length, viscosity, concentration, EVs aggregation.
	Density gradient (Buoyant density)	- EVs purity. - Preserves EVs functionalities. - Clinically applicable. - EVs homogeneity.	- Lower yield. - Low reproducibility. - Trained user. - Time-consuming.
Size-exclusion	Filtration (Size/Shape)	- Easy to use. - Improved separation by size. - Reproducibility	- Yield loss. - EVs damage risk.
	Ultrafiltration (Size)	- Easy to use. - Quick. - Reproducibility.	- Yield loss. - EVs damage risk.
	Chromatography (Size/Charge)	- Improved EVs purification from proteins and lipid particles. - Reduced aggregation - Less affected by viscosity. - Preserves EVs functionalities. - Shorter isolation.	- Coupled centrifugation usually needed. - Volume / elution buffer limitations.
Immunoaffinity	(Presence of specific surface markers)	- Selectivity (surface markers). - Resolution. - Quickness.	- Coupled centrifugation / filtration needed. - EVs markers not always available. - Cost. - Yield.
Polymeric precipitation	(Weight increase + low-speed centrifugation)	- Quickness. - Simple procedure.	- Co-isolation of impurities. - Only for small (60 to 180 nm) EVs.
Microfluidics	(Presence of specific surface molecules / size)	- Reduced sample volume. - Reduced times and costs. - High sensitivity. - Downstream processing within the system.	- Usually coupled to centrifugation needed. - Unable to differentiate EVs. - Still under development.

1.1.2.1 Serial differential centrifugation

Differential centrifugation is the most common and well-known method for EVs isolation. It was initially described for the isolation of EXOs from the supernatant of cell cultures and different biological fluids (169) and lately was adapted for the isolation of the rest of EVs by the introduction of serial steps of centrifugations at increasing centrifugal forces (6, 170). Although different modification in times and centrifugal speeds have been introduced to meet samples specific needs, the backbone protocol generally is composed of four centrifugation/ultracentrifugation steps consisting in 300 x g/10 min, 2,000 x g/10 min, 10,000-20,000 x g/30 min and 100,000-200,000 x g/70 min to sequentially pellet cells and big debris (discarded fraction), ABs, MVs and EXOs. After each step supernatants are transferred to new tubes for the isolation of the subsequent vesicle population and pellets, containing the different populations, are washed by resuspension in PBS and centrifugation under the same conditions.

Centrifugation alone cannot achieve pure separations due to various reasons: sedimentation of particles in the supernatant depends on density, distance of the particles from the bottom of the tube and vesicles/particles aggregation, apart from vesicles size itself (171). In order to achieve an improvement of EVs populations purity, a gradient step can be added to the centrifugation protocol. This system is intended to avoid contamination of EVs pellets with large protein/protein-RNA aggregates and proteins non-specifically bound to EVs (2). To do so, generally the technique consists in resuspending the pellet from previous serial differential centrifugation in PBS, to subsequently load it onto the top of a sucrose cushion (169, 172) or a sucrose gradient (173, 174). Next, different-in-length/speed ultracentrifugation processes are undergone, and vesicles are recovered from the bottom of the tube for cushions and from a specific fraction of the gradient, depending on their buoyant density. More recently, iodixanol, a non-ionic density gradient medium, is used as a substitute of sucrose and offers advantages such as

better separation of viral particles from EVs, low toxicity towards biological material, clinical applicability, and ability to form isosmotic solutions which are respectful with the size and shape of EVs in a wide range of densities (175, 176).

1.1.2.2 Size exclusion methods: filtration and chromatography.

Filtration is usually used in combination with ultracentrifugation to improve the separation of populations based on size. Filtration steps using 0.8, 0.2 or even 0.1 µm filters can be inserted between the centrifugation steps depending on the size of the desired population (21, 169, 177). Alternatively, ultrafiltration uses of filtration units of different molecular weight cut-offs prepared for centrifugation at moderate centrifugal forces. They allow the concentration of vesicles in the interface of the filters, from where they can be recovered washing (89, 178). The main problem of these methods is that applying pressure to the samples may lead to EVs deformation or breaking into smaller vesicles, which further may get stuck to the filter membrane, leading to a yield loss. Filtration by gravity may circumvent these problems (21) but, in contrast, increases processing times and filters get obstructed more easily.

Size exclusion chromatography is the technique of choice, alternatively to ultracentrifugation, for EVs isolation. The method consists in loading the media for vesicles recovery into the chromatography device, generally a gel size exclusion column, letting it equilibrate into the column and eluting it with PBS, recovering fractions of different volumes (22, 179). The technique is usually coupled to previous low-speed centrifugation to remove big debris and to subsequent ultracentrifugation to wash and concentrate the vesicles in the different chromatography fractions (180, 181). The separation of vesicles is based on their size: bigger particles go across the column more easily and are recovered previously to the ones of smaller size, what is a consequence of the ability of the different particles to penetrate the stationary phase. It has several advantages such as enhanced separation of EVs from proteins and high density lipoproteins, prevention

of protein and vesicles aggregates formation, reduced sensitive to the viscosity of the vesicles media and preservation of the biological properties, structure and functionalities of the isolated vesicles (22). Moreover, it offers shorter isolation times and relatively low cost although it normally shows lower recovery yields compared to other techniques (182, 183).

1.1.2.3 Other methods

Apart from the aforementioned, other methods have been developed that allow the isolation of particular vesicles populations/subpopulations for specific purposes.

Immunoaffinity isolation. Uses microbeads, normally magnetic, coated with specific antibodies that recognize EVs with specific surface markers (23, 184). It can be coupled to initial centrifugation/filtration to remove big debris (164, 185). Limitations include the need of markers specific of the desired population and beads working surface that may limit access to big-sized EVs (186).

Polymeric precipitation. Consists of the incubation of EXOs-containing media with commercial reagents to form a polymeric complex that captures EXOs overnight for a subsequent recovery by low-speed centrifugation. It offers quickness and simplicity compared to other systems and has been proven to provide elevated yields and purity in the recovery of exosomal RNAs (24, 187). Nevertheless, the method may drag impurities, such as lipoproteins, along with isolated EVs and is only useful for the isolation of EXOs, ideally in the size range of 60 to 180 nm (171).

Microfluidic devices. Isolation is based in different principles depending on the chip platform. A first approach included coating of the chip surface with antibodies for recognition and capture of the EXOs. The first prototype used anti-CD63 antibodies for capture and allowed direct scanning electron microscopy (SEM) imaging and lysis of EVs for RNA isolation (188). Later on, DiO-staining of EXOs was implemented for simultaneous quantitation (189). A different platform used anti-CD41 antibodies to

specifically separate CD41-bearing-MVs, but the technique had to be coupled to centrifugation to discard smaller-in-size EVs, thus reflecting the inability of the method to differentiate between EVs populations (190). A second microfluidic approach was based in physical properties, such as size, for EVs isolation. A first prototype combined microfluidics with porous polymer monoliths of adjustable pore size for the isolation of EVs under certain nanometric diameter (191). Recently, a new system has been proposed that combines microfluidic channels conformation with adjusted acoustic pressure to isolate EXOs with highly controlled size and purity even from whole blood or conditioned media from cell cultures (192). Although still under development, all these systems promise reduction of needed sample volumes, processing times and costs, maintaining a high sensitivity.

1.1.3 Methods for EVs characterization

The interest on the study of EVs has led to the adaptation of classical molecular biology techniques for the study and differentiation of vesicles subpopulations within the same sample, samples from different tissues or samples in different physiological and pathological conditions. The possibility of defining different EVs populations turns out interesting as they arise as potential biological markers of the cellular status. A summary of the main methods of characterization is offered in **Table 2**.

Table 2. Main methods for EVs characterization. Principle and main features.

TECHNIQUE		PRINCIPLE	MAIN FEATURES
MICROSCOPY	TEM	Negative staining of EVs with heavy metals.	✓ Direct imaging of EVs morphology / size. ✓ Immunogold labelling. × Dehydrating (fixation).
	SEM	Microgold particles covering and electron reflexion scanning.	✓ 3D imaging of EVs structures.
	Cryo-EM	Freezing in liquid ethane / nitrogen instead of fixation.	✓ No fixation / contrasting steps. ✓ Structures closer to their native states. × Highly trained user.
	AFM	Cantilever with a free end that touches the surface to obtain topographical information.	✓ Sub-nanometric resolution. ✓ Combinable with microfluidic devices. ✓ Quantitative. × It does not provide direct imaging of EVs. × Needs homogeneous EVs purification.
SIZE DISTRIBUTION ANALYSIS	**DLS**	Sensor measure of time dependent fluctuations in the scattered light of laser irradiated particles (Brownian motion).	✓ Wide size range (1 - 6000 nm). ✓ Samples can be recovered. × Mainly qualitative. × Limited by polydispersity and big EVs.
	NTA	Particles are challenged with a laser and scattered light is real-time captured by a microscope (Brownian motion).	✓ Precise size distribution and concentration. ✓ Low sample usage. ✓ Able to study EVs markers (fluorescence). ✓ Standardization is possible. × Reduced size range (50 - 1000 nm). × Concentration range (10^6 - 10^9 part/mL).
	TRPS	Alteration of membrane electrophoretic flow by EVs crossing through pores, and translation into size data.	✓ Qualitative and quantitative. ✓ Size range (70 nm - 10 µm). ✓ Concentration range (10^5 - 10^{12} part/mL). ✓ Measures single EVs.
	Flow cytometry	EVs laser-scattered light is used to get information about size and molecular markers by forward and side scatters.	✓ New cytometers: 100 nm detection limit. ✓ Quantitative. ✓ Versatile for EVs markers analysis. ✓ Use of beads for small EVs markers study. × Rely on EVs markers or fluorescent labels.
MOLECULAR MARKERS CHARACTERIZATION	**Western blotting / ELISA**	Proteins are attached to a support (membrane or plate) and challenged with tagged antibodies.	✓ Easy to perform. ✓ Cheap and available. ✓ Relatively quick. ✓ Quantitative (ELISA)
	ExoScreen	ELISA sandwich-like system. When all the components are close enough (within the same vesicle), a laser stimulus can be transferred between them and detected at the end.	✓ Reduced time consumption. ✓ Increased sensitivity. ✓ Qualitative and quantitative. ✓ No need of EVs isolation. ✓ Little sample volume requirement.
	µNMR	Labelling of EVs surface markers with antibodies coupled to magnetic nanoparticles and detection by microfluidic µNMR.	✓ Greatly higher sensitivity. ✓ Qualitative and quantitative.
	nPLEX	Joining of EVs to antibodies in a gold film with nanoholes causes plasmon intensity changes that are proportional to the amount of joined EVs.	✓ Qualitative and quantitative. ✓ Label-free. ✓ Easy to miniaturize. ✓ Scalable for higher throughput detection. ✓ A magnitude order sensitivity over µNMR

1.1.3.1 Microscopy: morphology and size assessment

Electron microscopy are the only current techniques that allow direct visualization of EVs due to their reduced size, and further offer different information. Transmission EM (TEM) is based on the staining of EVs with heavy metals such as lead citrate, uranyl acetate and osmium tetroxide, that attach to different cell structures, such as EVs lipid bilayer, providing electron-density. Electron-dense regions repel the electrons emitted by the microscope and appear as dark regions over a white background. This technique allowed the initial description of EXOs as cup-shaped vesicles by the group of Raposo (25). By TEM, EVs can be fixed, stained and directly observed as whole structures or can be embedded in resin for ultrathin cuts to analyse their content. This second approach allows immunogold staining of specific markers that are observed as electron-dense spots (26, 193). Cryo-EM uses freezing of EVs to avoid fixation and contrasting, making possible to observe EVs as close as possible to their native state. Indeed, this technique revealed that classical cup shape attributed to EXOs was an artefact of the fixation process (112) and a great variety of EVs morphologies has been uncovered (27). Finally, Scanning-EM (SEM) offers three-dimensional imaging of the EVs for a further morphological description (19, 194).

Alternatively, atomic force microscopy (AFM) permits the analysis of size distribution, at the subnanometric level, and quantity of EVs within a sample. The system is based on the scanning of the sample by a mechanical probe, a cantilever with a tip in the free end, which physically touches the sample to get topographical information through a piezoelectric system. In offers the possibility to measure EVs in aqueous media thus further preserving their biological properties and structure (195, 196).

1.1.3.2 Size distribution analysis techniques

Dynamic Light Scattering (DLS) allows measuring of EVs size distribution in the range of 1 to 6000 nm. It uses a laser for irradiating particles in the samples which, thanks to their Brownian motion and refractive index (RI), produce a light dispersion pattern that is captured by a sensor. This pattern is constituted by time dependent fluctuations in the scattered light intensity that are mathematically converted into particle size data (28). It has limited ability for measuring polydisperse samples, which is the normal situation for a biological sample. This means that a population composed of particles of varied sizes although with different relative abundances, would appear fused into a big Gaussian distribution peak assuming a single mean. Also, the technique is limited for measuring samples containing big EVs, since the bigger particles scatter more light and mask the smaller ones. Finally, if calculating particle concentrations is possible, these are mathematically calculated from the intensity plots so only a relative concentration calculation is possible for controlled monodisperse samples (197). On the other hand, samples can be recovered for further use after the analysis.

Nanoparticle tracking analysis (NTA) is also a light-scattering technique based in measurement of particles Brownian motion. In this case, scattered light is captured by a microscope camera and the NTA software tracks the movement of each single particle in a time lapse. Tracking information, along with medium viscosity and temperature, is used to calculate EVs diameter (29, 198). This allows precise size distributions and to calculate interval and total particles concentration. For further standardization of measurements, the use of silica nanospheres has been proposed as their refraction index (RI = 1.46) is more similar to that observed for most of EVs (IR around 1.39) than the RI of classically employed polystyrene beads (RI = 1.59), even when this factor may change between vesicles of different origin (29, 199). As a limitation from the previous system, its measuring range is limited to 50 to 1000 nm.

Tunable resistive pulse sensing (TRPS) uses a polyurethane membrane of nanopores of controlled size in which an electrophoretic flow is stablished. When EVs cross the nanopores cause a raise in resistance that is translated into size information per single particle. Its working range is 70 nm to 10 µm and 10^5 to 10^{12} particles/mL and permits the study of multimodal populations thanks to the measurement at the single particle level. Pores can be adjusted to a single morphology for the analysis of particular vesicles populations/sizes, or different sizes and morphologies can be combined to widen the size range and increase the analyzable sample volume (30, 200).

Finally, flow cytometry can also be used for the analysis of size distribution, concentration, and qualitative features of EVs. Classical light scatter flow cytometers only allowed the analysis of particles from 300-500 nm and were not able to resolve particles that differed in less than 200 nm in size (201, 202). This limited the power of flow cytometry for the study of small EVs. The introduction of innovative flow cytometry technology (high-power 488 lasers, reduced wide-angle forward scatter measurements, sensitive forward scatter detector) and the use of fluorescent labelling of EVs, allowed to reduce the limit of detection to approx. 100 nm, being possible to discriminate between vesicles 100 to 200 nm in size (203, 204). In order to achieve similar thresholds with more simple flow cytometer designs, the current trend points at using 405 nm lasers instead of the classical 488 nm for the side scatter (205). Finally, EVs can be coupled to latex beads of higher size for surface markers analysis. In this way, even the smaller EVs can be analysed, but no quantification or differentiation between vesicles populations is possible (56, 206).

1.1.3.3 Molecular markers characterization

The most common techniques for the analysis of EVs markers are Western Blotting and ELISA, the last being adaptable for EVs quantitation (207, 208). A recent evolution, ExoScreen, offers both EVs detection and quantitation, improving time consumption and sensitivity. Moreover, no previous isolation step and little sample volumes are required. Shortly, samples are co-incubated with biotinylated EVs specific antibodies, donor beads coated with streptavidin and acceptor beads conjugated to a second antibody that has its epitope in the EVs. When EVs targeted are present in the sample, both beads remain close one to the other (~200 nm), donor beads can be excited and subsequently excite acceptor beads, which emit light at a precise wavelength (31).

Micro nuclear magnetic resonance (μNMR), combined with microfluidics, has been adapted for EVs characterization and quantitation, through the labelling of EVs surface markers with antibodies coupled to magnetic nanoparticles. Magnetism gain of EVs is related to a faster decay of the NMR signal in a manner that the decay rate is proportional to the number of magnetic particles coupled to the EVs and, thus, to the amount of target EVs and their protein expression. Detection sensitivity level greatly surpasses ELISA or flow cytometry (32).

Nano-plasmonic exosome assay (nPLEX), based in transmission surface plasmon resonance, consists of a gold film patterned with series of nanoholes arrays coated with specific monoclonal antibodies for recognition of exosomal proteins. Light illumination causes excitement of the electromagnetic field (surface plasmons) producing transmission spectral peaks. When exosomes join the antibodies, spectral peaks suffer a red shift and intensity changes occur which correlate to the amount of targeted protein and, thus, to the amount of joined EXOs. The system is label-free, easier to miniaturize, scalable for higher throughput detection and guarantees a magnitude order lower detection sensitivity than μNMR (33, 209).

1.1.4 EVs main cargo

EVs content is complex and some minor components may be masked by the most abundant ones. In addition, due to the technically limited methods of isolation, differentiating populations of vesicles, in order to assess their content, remains far from possible (6, 83). This fact limits analysis to fractions enriched in a vesicle population more than pure isolations, and last trends point at combining different isolation techniques for the study of specific subpopulations (120). Nevertheless, thanks to the implementation of high-throughput techniques, such as mass spectrometry and sequencing, it has been possible to develop databases gathering information about protein, lipid and RNA content of extracellular vesicles from different sources: ExoCarta (210), EVpedia (211) and Vesiclepedia (212).

Regarding proteins, EVs proteome has been thoroughly studied since the emergence of mass spectrometry techniques (87). Apart from the components of EVs biogenetic machinery, these are enriched in proteins from cytoskeleton, cytosol, plasma membrane and heat-shock proteins, while proteins from cellular organelles are less abundant (17). Different EVs contain common proteins but also specific cargo depending on the cell of origin and vesicle type. Importantly, the method of isolation further influences final protein composition (3). Finally, EVs number, protein content and protein concentration are also modified by the stimuli for vesiculation, even in the same subpopulation of vesicles (213). Cytokines are of great interest among EVs protein cargo. EVs secretion has been proposed as an alternative mechanism of exocytosis for proteins lacking leader signal peptide such as IL-1β (214). IL-1α has been reported to be selectively transported by ABs but no by smaller EVs (<1μm) in endothelial cells (215), what reinforces the concept of cargo sorting in different EVs populations. Of interest, EVs levels of TGF-β1 and IL-10 were observed increased in pregnant vs nonpregnant women. This was coupled to an enhanced induction of caspase-3 activity in cytotoxic NK cells, what promotes an immunosuppressive response through the apoptosis in these cells. This constitutes a mechanism by which

EVs may contribute to maternal tolerance of the fetus (216). Other examples of cytokines reported to be released into EVs are IL-18 (217), IL-32 (218), TNFα (219) and IL-6 (220).

Lipid distribution has been shown to differ in EVs from that of parent cells. EVs have higher levels of sphingomyelin, cholesterol, phosphatidylserine (34, 221), ceramide and its derivates and, in general, saturated fatty acids (222). Their lipids-to-proteins ratio is also higher than in parent cells. Contrarily, phosphatidylinositols, phosphatidyglycerols, phosphatidylcholine and phosphatidylethanolamines are more represented in parent cells (34). A pivotal feature of EVs lipids is their asymmetrical distribution in membranes forming domains called lipid rafts (223) mainly maintained by cholesterol (224). Lipid rafts have been attributed functions in EVs formation and sorting of specific proteins (225), again with participation of cholesterol through the maintenance of lipid rafts structure and, so, regulation of membrane fluidity (226). Lipid rafts may also be important for EVs stability in the extracellular medium (227).

Valadi's group was the first to describe RNA, particularly mRNA and miRNA, content in EXOs, as well as their ability to transport it into other cells, where the RNA was functional (228). Posteriorly, new sequencing studies demonstrated that exosomes contain various classes of small non-coding-RNAs in addition to mRNA: miRNA, small interference RNA (siRNA), small nucleolar RNA (snoRNA), Y-RNA, vault RNA, rRNA, tRNA, long non-coding RNA (lncRNA), piwi-interacting RNA (piRNA) (19, 35, 229, 230). Further, different RNA profile and thus sorting, was observed for EVs compared to originating cells (56). A capital problem in EVs RNA analysis is the existence of free-floating RNA that sticks to EVs outer wall and, in this way, is isolated along with internal RNA. RNaseA treatment before extraction is advisable to cope with the problem (231). Despite this measure, still extra-EVs RNA coupled to proteins, such as argonauts, may resist the RNaseA treatment (232, 233), so combined treatment with proteinase K has been proposed for dissociation of RNA-protein complexes

(234). Nevertheless, care should be taken as proteases may provoke vesicle lysis and subsequent yield loss.

1.1.4.1 EVs as DNA transporters

Knowledge on DNA transmission in EVs is still a field in early development. An initial study observed that both single (ssDNA) and double stranded DNA (dsDNA) were present intra- and extravesicularly, and that dsDNA was the most abundant form. Likewise RNA, this study reflected the importance of DNase treatment previously to EVs DNA extraction to avoid bias with external DNA (36). A previous study on tumor cells observed that EVs DNA was more abundant and mainly ssDNA in MVs from tumor cells compared to normal cells (235). Other works pointed at specific sorting of DNA molecules depending on the cell of origin and EVs subpopulation (37) and at the ability of EVs to convey DNA into target cells (38), where this DNA could get to the nucleus and be actively transcribed (39). Current reports point at EVs as vehicles for DNA horizonal transfer with potential functions in cancer development promotion, with special regard to a possible mechanism involving retrotransposons (42) and highlighting the ability of the different EVs to cross the blood-brain barrier (236). ABs have been attributed key roles in DNA horizontal transfer, which then integrates into receptor cells and remain functional (7). ABs have been reported to form DNA molecule hybrids or hybrid chromosomes (137, 237) and to transfer oncogenes that can be internalized and increase the tumorigenic potential of target cells in vivo (8, 137). Recently, large fragment of chromosomal DNA from prostate cancer plasma, was found in large EVs rather than in EXOs or in its free form, while similar amount of proteins were found in both EVs populations. Large EVs-DNA reflected cancer genetic aberrations and status (40). On the other hand, EXOs were observed as transporters of mitochondrial DNA (mtDNA) as a possible mechanism to transmit altered mtDNA or associated pathologies (238), but also for the restoring of proper mtDNA (239). Cancer fibroblast-derived EXOs have been observed to transfer

mtDNA to breast cancer cells, fusing with recipient mitochondria and promoting mitochondrial activation and a hormonal therapy-resistant phenotype in previous hormonal therapy-sensitive and hormonal therapy-quiescent cells (41). Recent research showed that T-cell-derived EXOs delivered upon antigen-dependent contact with dendritic cells (DCs) were able to unidirectionally transfer genomic and mtDNA to the DCs triggering DCs resistance for subsequent viral infections (240). Interestingly, exposure of first trimester placenta to antiphospholipid antibodies, a known risk factor of pre-eclampsia, was observed to increase the levels of mtDNA in secreted MVs and EXOs, and to subsequently enhance activation of endothelial cells response (241). As a further function, EVs-DNA horizontal transfer has been proposed as a new mechanism for the transfer of genetic material across species with potential impact in genome evolution (42).

1.2 EVs as messengers in female reproductive physiology

Normal reproductive processes are highly dynamic, with transient nature and well characterized stages. The possibility of biologically defining the different events that lead the progression to subsequent stages has prompted the study of EVs in the different processes from pre-conception to birth in different fluids such as follicular fluid (43, 242), oviductal fluid (44, 243), cervical mucus (244), endometrial fluid (19, 56), amniotic fluid (174, 245), breast milk (246) and the originating tissues (reviewed in (45)).

EVs key roles have been discovered in different reproductive functions including follicle and ovum development and maturation, early embryo development, crosstalk with the endometrium and implantation, preparation of endometrial vascular net and even communication between in vitro cocultured embryos for quorum improved development (247). During pre-conception, EVs are widely produced by different organs and show specific functions (follicular fluid EVs,

oviductosomes, uterine cavity EVs). After implantation, EVs generation continues throughout pregnancy being the placenta the main producing organ. During early pregnancy, EVs are released by the extravillous trophoblast. Afterwards, the syncytiotrophoblast (STB) is formed, establishes contact with maternal blood-flow and constitutes the main site of EVs (STBMs) generation. STBMs get access to the maternal systemic vasculature and participate in important roles in immune modulation (46). EVs are also found in amniotic fluid, where they are attributed inflammatory and pro-coagulant activities (248); and in maternal breast milk, where they have been involved in bone formation, immune modulation and gene expression regulation, with special emphasis for long non-coding RNAs (246, 249).

Embryo implantation is a process that progresses with a tight communicative component between the mother and the embryo. This embryo-maternal crosstalk (EMCT) is established by direct contact between the hatched trophectoderm and the endometrial epithelial lining, what triggers a series of biological events that end up with trophoblast invasion of the maternal decidua (250, 251). In parallel, EMCT is also established by the delivery of molecules into the uterine secretions, which constitute the endometrial fluid (EF): a viscous liquid secreted into the endometrial cavity composed by serum transudates, residual products of womb cells apoptosis, products secreted by the endometrial epithelial cells (mainly glands) and, in the case of fertilization, by those substances released by the developing embryo (53). Moreover, the secretion of molecules into the fluid varies depending on the phase of the menstrual cycle under steroid hormones stimuli (54). The study of EF provides an accurate perspective of the environment where the embryo develops and implants (252), and is proposed to reflect maternal exposures and eating habits, with an impact in embryo quality, expression and epigenetic long-term regulation (55).

EVs have been found in the EF with both endometrial and embryo origin/target that have been attributed roles in different reproductive-related processes, such as promotion of embryo development (57, 58, 61) and implantation (18, 19, 56),

enhancement of trophoblast migratory ability (15) and regulation of endometrial angiogenesis (62, 63). The main reproductive roles described for EVs in the different female reproductive tract compartments are summarised in **Table 3**.

Table 3. Main roles of EVs in female reproductive physiology. Origin, targets and main functions.

EV TYPE	TARGET	FUNCTIONS	
Follicular EVs	**Cumulus-oocyte complex**	Follicle development and oocyte growth (specific miRNA cargo, ACVR1, ID2)	
		Follicle maturation: proliferation of small follicles and inflammatory response of large developed follicles (specific miRNA signatures).	
		Cumulus-oocyte complex expansion and related genes upregulation.	
Oviductal EVs	**SPZ**	Regulation of SPZ storage and promotion of capacitation, acrosome reaction and hypermotility (PMCA4a).	
		Regulation of molecule delivery into SPZ (Integrins α5β1 and αvβ3).	
	Embryo	Enhancement of embryo quality and early development.	
Uterine EVs	**Endometrium**	**Endometrial origin**	Promotion of embryo implantation (specific miRNA cargo)
		Embryo origin	Regulation of endometrial angiogenesis (specific miRNA and protein cargo) and uterine spiral arteries remodelling.
	Embryo	**Endometrial origin**	Embryo development (enJSRV *env* gene RNA) and subsequent priming of the endometrium for embryo harbouring.
			Promotion of embryo implantation (miR-30d, specific protein cargo, influenced by uterine hormones – functional with trophectoderm).
		Embryo origin	Enhancing of trophoblast cells migratory ability and implantation efficiency (laminin, fibronectin).
	SPZ	Sperm maturation (SPAM1)	
		Capacitation, acrosome reaction and motility promotion (PMCA4).	

1.2.1 Female reproductive physiology: menstrual cycle and receptivity

Oocyte development starts in the fetal period until these become arrested in prophase I of meiosis in their primordial follicles until female reproductive maturity. From this moment, cohorts of oocytes cyclically restart growth, forming the zona pellucida while granulosa cells proliferate to form the cumulus, which will support posterior egg fertilization. Concomitantly, meiosis is reinitiated, extruding the first polar body and arresting again at metaphase II prior to ovulation (253). Resumption of meiosis is stimulated by the luteinizing hormone (LH) surge, which is triggered by

a great increase in oestradiol-17β levels by granulosa cells from preovulatory follicles and ends up in ovulation 36 hours later (10 - 12 hours after LH peak) (254). After ovulation, cumulus cells extracellular matrix adheres to the oviduct and eggs travel until the ampulla to wait for fertilization (255).

After conception, embryo develops throughout the fallopian tubes, reaching the uterus at day 4 after ovulation. At this point, the embryo in blastocyst stage finishes its maturation in the maternal EF and implantation can only occur during a short period of the luteal phase of the menstrual cycle, known as window of implantation (WOI) that typically extends from days 5.5 and 9.5 after ovulation in healthy normal cycling women (256, 257). Different factors orchestrate embryo implantation: embryo quality, endometrial receptivity and embryo-endometrial crosstalk (251), where EVs stand as important potential mediators.

A regular menstrual cycle has a median duration of 28 days (most cycles between 25 and 30 days) and is divided it three main stages that progress thanks to the hormonal stimuli from the hypothalamus, pituitary and ovaries: menses, follicular/proliferative phase and secretory/luteal phase. Follicular phase is considered from the first day of menses until ovulation. It is characterized by the development of ovarian follicles and restoration of the endometrial lining after menses and is mainly driven by oestradio-17β, whose levels rise along with follicle size and number of granulosa cells. Rising levels of estradiol stimulate an increase of LH secretion from mid-follicular phase. A dramatic rise in estradiol produced by the preovulatory follicle leads to the LH surge and subsequent ovulation 10-12 hours after the LH peak, triggering the entrance in luteal phase of the cycle. LH surge promotes secretion of progesterone by granulosa cells, stimulates resumption of meiosis and release of the first polar body by the oocyte. Prior to LH peak, estradiol levels fall dramatically. After ovulation, follicle becomes the corpus luteum and produces progesterone for endometrium preparation for embryo harboring. Eight-to-nine days after ovulation, coinciding with the receptive moment, the corpus luteum achieves its maximum

vascularization and peak serum levels of estradiol and progesterone are achieved. From here on, corpus luteum is maintained while LH support is continued until the end of the luteal phase unless pregnancy occurs and chorionic gonadotropin is produced (254). A schematic view of menstrual cycle stages and associated hormonal levels variations is offered in **Figure 2**.

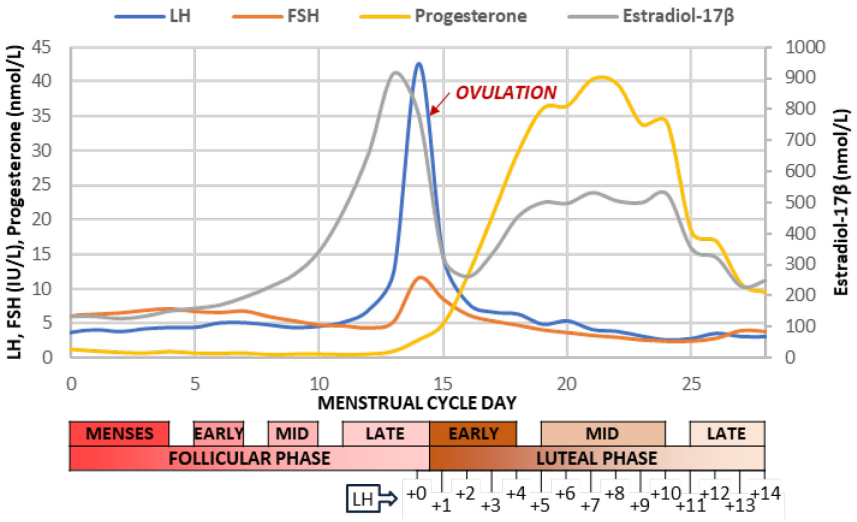

Figure 2. Schematic overview of the phases of the menstrual cycle and their associated hormonal profile. Reference values for hormonal levels by day in normal cycling women were obtained from (258).

1.2.2 EVs roles throughout the female reproductive tract and during the process of implantation

1.2.2.1 Follicular fluid EVs

Follicular fluid offers an accurate view of early oocyte and follicle maturation and its composition reflects fertility status (259). This fact together with its easy availability during oocyte retrieval makes follicular fluid appealing in the search of biomarkers for oocyte quality (260).

The existence of EXOs/MVs-like vesicles in follicular fluid was demonstrated in mares. Follicular EVs were observed to be uptaken by granulosa cells and were associated to protein and miRNA cargo. EVs miRNAs were found in the surrounding granulosa and cumulus cells, suggesting EVs as vehicles for biomolecule transfer within the ovary. Interestingly, the miRNA signature of follicular EVs varied with the age of the female and was proposed as an indicative of age-related decline in oocyte quality (50). A subsequent study confirmed the existence of small RNAs in human follicular fluid EVs and discovered four miRNA differentially expressed between young and old women follicular fluid. These were predicted to affect several pathways related to fertility but were not demonstrated to be directly carried by EVs (261).

Bovine follicular fluid EXOs showed a different miRNA profile from that found free in the fluid, and could be internalised by granulosa cells in vitro, leading to an increase in their miRNA content and variations in mRNA profiles, with some of the affected genes involved in follicle development. Moreover, EXOs miRNAs may have roles in oocyte growth as a different profile was found in follicles containing growing and fully-grown oocytes (47). Posteriorly, variations in bovine follicular fluid EVs number, protein markers and miRNA content were associated to the developmental stage of follicles. EVs miRNAs from small follicles preferentially promoted cell proliferation pathways while those from large follicles were related to inflammatory response pathways (49). Back into the mare, exposure of granulosa cells to follicular fluid EXOs revealed a possible role of these EVs in follicle development and growth through the TGFβ/BMP axis ACVR1 and ID2 regulators by direct delivery of ACVR1 and ID2 regulatory miRNAs within EXOs (48).

Cumulus-oocyte complex expansion is a critical process for ovulation, and the LH peak that induces ovulation also increases the expression of a set of genes that stimulate cumulus growth. In this context, in vitro coculture of bovine follicular fluid EXOs and cumulus-oocyte complexes from mouse and bovine revealed that follicular

EVs are uptaken by cumulus cells, promoting both cumulus expansion and related genes expression (51).

1.2.2.2 Oviductal EVs (Oviductosomes)

The oviduct is the place where fertilization takes place. After capacitation, sperm (SPZ) acrosome reaction and motility are regulated by high intracellular Ca^{2+} levels. The major murine Ca^{2+} efflux pump PMCA4a has been found mainly expressed in oviductal fluid and completely associated with EVs. PMCA4a carrying vesicles showed exosomal features, constituting the first study to report the presence of EXOs in the oviducts. EXOs were uptaken by SPZ, where the efflux pump was functionally relocated to their membranes (243). Posteriorly, integrins α5β1 and αvβ3, found in both oviduct EVs and SPZ, were involved in EVs to SPZ fusion for cargo delivery. Interestingly, EXOs appeared to be more efficient in fusing with SPZ than MVs (44).

On the other hand, bovine oviductal EVs, produced by in vitro cell line culture, have been reported to promote quality and development of in vitro cocultured embryos, thus suggesting a functional communication between the oviduct and the embryo to support it during early stages of development (52). However, oviductal EVs produced in vitro have been observed to carry a differential cargo and, therefore, different potential compared with in vivo produced EVs. This is the case of OVGP and HSPA8 (also known as HSC70), a couple of oviductal proteins known to be important in the fertilization process and early pregnancy. While HSPA8 was found in both in vitro and in vivo EXOs, OVGP was absent in EXOs of in vitro origin (262).

1.2.2.3 Uterine microenvironment EVs

To date, the existence of EVs has been reported throughout the menstrual/estrous cycle in the EF of different species, including humans (19, 56) and sheep (57, 58, 61, 263), and also released by endometrial epithelial cells in culture (18, 19, 56, 62).

The group of Ng released the first work describing the production of EVs by endometrial epithelial cells in primary culture. They observed that EVs from these cells contained a specific subset of miRNAs, different from that of parent cells, with target genes involved in the process of embryo implantation. They also verified the presence of EVs in uterine fluid and associated mucus (56). A year after, Burns and colleagues, working in sheep, isolated a comparable population of EVs from uterine luminal fluid. They observed that these vesicles were enriched in proteins from the endometrial epithelia and conceptus trophectoderm, and even that a specific cargo pattern was appreciable for pregnancy/non-pregnancy. RNA in EVs was mainly constituted by molecules of less than 200 bp, in contrast to larger RNAs in parent cells. Among these RNAs, *gag* and *env* RNAs from endogenous Jaagsiekte sheep retrovirus (enJSRV) were found inside EVs and were demonstrated to be transmissible to surrounding cells. This indicated uterine fluid EVs as the mechanism of transport for *env* genes from the endometrium to the conceptus, a capital event where these genes play crucial roles in embryo trophectoderm development (57). Posteriorly, the same group demonstrated in vivo, in the same animal model, the establishment of a bidirectional crosstalk, where EVs produced by the endometrial epithelium and present in uterine fluid were uptaken by both the embryo and the epithelium itself, and conceptus derived EVs were uptaken by the endometrial epithelium. No other tissue of the female reproductive tract showed uptake of these EVs. Moreover, protein and RNA cargo of embryo derived EVs was uncovered (61). Continuing the line of research in the ewe, uterine fluid EXOs were observed to contain mRNA for interleukins, interferon regulatory factors and enJSRV-*env* genes, appreciating a decrease in the mRNA levels for enJSRV-*env* genes as pregnancy

progressed from day 10/12 (pre-implantation) to 16 (moment of attachment). Co-incubation of uterine fluid EXOs with trophectoderm cell lines in vitro revealed that enJSRV-*env* genes promoted trophectoderm cells proliferation along with the secretion of interferon tau (IFNT) in an exosome dose-dependent manner, likely via TLR signaling. Importantly, IFNT acts as the pregnancy recognition signal, which announces the presence of the embryo to the uterus around the day 10-12 of pregnancy for its attachment on day 16 (58).

In humans, our group was pioneer demonstrating the effective communication of the mother with the peri-implantation embryo through EVs. First, the presence of EVs in the human endometrial fluid, previously appreciated by Ng's group, was reasserted. Subsequently, EXOs containing hsa-miR-30d were described to be actively transferred from endometrial epithelial cells to the embryo trophoblast cells, where the miRNA was internalized. Finally, murine embryos treated with a synthetic analogue of human miR-30d displayed an altered expression pattern, showing a greater expression of genes coding for molecules involved in embryo adhesion, thus highlighting the importance of miR-30d transference inside EXOs (19). Posteriorly, heterogeneous nuclear ribonucleoprotein C1 (hnRNPC1) was uncovered as a likely transporter involved in the biogenesis and sorting of miR-30d into the EXOs (59). The relevance of these findings was tested in vivo in the murine model, where miR-30d deficiency in embryos limited their implantation rates while the same deficiency in mothers reduced size of implantation sites, increased rates of embryo resorption and impaired fetal growth (60).

Of importance, Greening et al. demonstrated in human endometrial epithelial cells cultured in vitro that the proteome of EXOs is regulated by steroid hormones, and thus varies with the progression of the menstrual cycle. Under follicular phase hormonal conditions (estrogen-dominant) the EXOs proteome was enriched in proteins related to cytoskeletal reorganization and signaling cascades, coinciding with the phase of endometrial restoration. After ovulation, under receptive phase

hormonal conditions (estrogen plus progesterone), the proteome shifted towards enrichment in extracellular matrix reorganization and embryo implantation. EXOs protein profiles were shown distinct from parental cells. Importantly, endometrial EXOs were demonstrated to be internalized by human trophoblastic cells (HTR-8), enhancing their adhesive capacity, partially through the focal adhesion kinase (FAK) cascade, what was significantly increased with EXOs derived from cells under receptive phase hormonal conditions (18).

EVs have also been reported to be produced by the embryo and to participate both in the crosstalk with the endometrium (61) and in the self-paracrine regulation (15).

A recent study showed that murine embryonic stem cells from the inner cell mass generated MVs that were able to reach the trophoblast layer, either as isolated cells or in the whole embryo, and enhance their migration ability. This effect was carried out thanks to the laminin and fibronectin cargo of the inner cell mass MVs, which were able to attach to integrins in the trophoblast cells surface and stimulate JNK and FAK kinases cascades, which ended up in increased trophoblast migration. Further, they observed that the injection of these MVs directly inside the cavity of 3.5-day blastocysts increased their implantation efficiency (15).

Interestingly, EVs from a pig trophectoderm cell line were discovered to stimulate proliferation of porcine endothelial cells in vitro, thus becoming potential regulators of maternal endometrial angiogenesis. In fact, EVs communication was established bidirectionally and embryonic EVs contained a miRNA and protein cargo including species with annotated functions in the angiogenesis process. Nonetheless, care should be taken with these results as they were retrieved from cell line models cultured in vitro and pig is a species with epitheliochorial placentation, so important differences are likely present in human physiology (62). In line with these results, a previous study on the roles of extravillous trophoblast cells (HTR-8/SVneo and Jeg3)-derived EXOs showed that these vesicles promoted vascular smooth muscle cells

migration, a process involved during human uterine spiral arteries remodeling in successful pregnancies (63). However, different trophoblast cell lines produced differential migration results, raising the situation that cell origin, content and bioactivity of the EXOs may suppose an important factor for their pro-migratory activity and, thus, results cannot be directly extrapolated in vivo.

Finally, EVs in the uterine cavity have also been attributed roles in sperm maturation, where they have been reported to reach the SPZ and effectively transfer their cargo. One of the molecules tested to be transferred to the SPZ was SPAM1, a hyaluronidase known to play important roles in fertilization and sperm maturation, which is also conveyed by EV at the epidydimal level (264). A recent study reasserted that EVs derived from epithelial endometrial cells fuse with SPZ and prompt their fertilizing capability. Particularly, co-incubation of SPZ with either endometrial epithelial cells conditioned medium or derived EVs stimulated SPZ capacitation, supporting the hypothesis that this process may initiate at the uterine level and end in the oviducts (265). This idea is in line with previous reports where conditioned medium produced by endometrial cells was able to induce sperm capacitation, even when EVs where not considered at that moment (266). Finally, uterine EVs, along with EVs from vagina and mainly oviducts, have been observed to deliver PMCA4a to the SPZ, what has important functional impact on SPZ motility, capacitation, acrosome reaction and fertility in general. Interestingly, it was reported that PMCA4a was only found associated to EVs but never as a soluble form (243).

1.3 EVs as biomarkers in reproductive biology

EVs potential as indicators of reproductive outcome is currently under evaluation. Placenta releases EVs from the sixth week of pregnancy and its secretion increases as pregnancy proceeds, peaking at term (267). This secretion is modulated by a series

of factors that arise from placental physiology and, so, postulates EVs as potential mirrors of placental/foetal health and evolution (268). Placental Alkaline Phosphatase (PLAP) has been proposed as a marker to differentiate placental EVs from those of maternal origin (269, 270), what is of especial importance when working in blood.

Alterations in both levels and cargo of placental-derived EVs during pregnancy is associated with different pregnancy complications. A signature of 62 proteins able to differentiate spontaneous premature births (SPB) from normal term births was found in microparticles from plasma of women in the 10-12 gestation week. Functional analyses showed enrichment in processes related with preterm birth such as inflammation, fibrinolysis, immune modulation, coagulation cascade or steroid metabolism. This potential early diagnosis of SPB stands as an alternative to the classical measurement of cervical length by ultrasounds (64). Posteriorly, a specific miRNA signature in plasma placental EXOs was found for SPB and pre-eclampsia (PE) prior to the 18th week of pregnancy. Interestingly, a common variation in over 45% of the miRNA profile was discovered between SPB and low-oxygen tension (LOT) conditions. LOT-EXOs decreased endothelial cell migration potential and increased TNF-α production, what was proposed to compromise spiral arteries remodeling during placentation. In this sense, placental EVs composition may be altered under circumstances that favour pro-inflammatory environment or reduction of oxygen tension, such as advanced gestational age, this compromising spiral arteries remodeling and leading to the development of pathologies such as PE or SPB (65). Finally, both total and placental-derived EVs have been found increased in women delivering low-birthweight babies compared to those with normal-birthweight deliveries (70).

Regarding EVs as PE biomarkers, an immunoadsorption system was initially developed to purify EVs based either in GM1 ganglioside or phosphatidylserine markers. It was possible to find specific protein signatures for PE vs healthy pregnant

controls using plasma from approx. 32-week pregnant women, for both markers independently (271). The main limitation of the study is that plasma was directly used for immunoadsorption without previous steps to remove debris and no experiments were conducted to verify the isolation of vesicles, so proposed protein profiles cannot be directly attributed EVs. Nevertheless, a subsequent study by the same group, confirmed that usefulness of classical PE biomarkers, such as plasma PlGF, can be reinforced with the combined predictive value of TIMP1 and PAI1 EVs biomarkers, isolated by their immunoadsorption system in a large cohort of low-risk PE plasma samples (66). A recent study confirmed an increase in total and placental($PLAP^+$)-derived EXOs in maternal plasma in PE vs healthy pregnant women, the later showing a trend towards an increase with the gestational age. Further, miR-486-1-5p and miR-486-2-5p, were upregulated in PE conditions and were functionally related to migration, placental development and angiogenesis (68). Finally, reduced EV-associated endothelial nitric oxide synthase expression and activity, a common feature of PE, was observed in EVs (especially EXOs) coming from PE placentas ($PLAP^+$), either in serum or placental perfusates, compared with healthy controls (67).

EVs have also been proposed as biomarkers of peripartum cardiomyopathy (PPCM), an idiopathic disorder which usually appears by the end of pregnancy or in the next few months and is only diagnosed by exclusion of other heart failure causes (272). An initial study reported increased levels of blood-derived activated, but not apoptotic, endothelial microparticles in PPCM compared to healthy post-partum, pregnant and non-pregnant controls but also with patients of ischemic cardiomyopathy (ICM) and stable coronary arterial disease (CAD). Similar results were obtained for platelet-derived and monocyte microparticles. Treatment with bromocriptine, a therapy proved to work in animal models and human patients, significantly reduced endothelial and platelet-derived microparticles in PPCM compared to patients treated with standard undirected heart failure therapy (273). Posteriorly, EXOs miR-146a was proposed as a PPCM biomarker. 16-kDa N-terminal

prolactin fragment, the main molecule involved in the triggering of PPCM, stimulated the release of miR-146a into HUVECs EXOs, which then were able to reach cardiomyocytes and trigger PPCM. miR-146a was enriched in plasma from PPCM patients but not in dilated cardiomyopathy or in healthy post-partum controls, and treatment with bromocriptine reduced miR-146a back to healthy control levels (69).

Also, placental EVs have been suggested as biomarkers of infectious diseases during pregnancy. Total and placental-derived EVs were increased in plasma from HIV-positive pregnant women compared with non-infected controls. In contrast, no differences were found in the level of plasma EVs for malaria infection, but miR-517c was increased in microparticles from plasma of women with active placental malaria compared with non-infected controls (70).

INTRODUCTION

HYPOTHESIS

OBJECTIVES

MATERIALS AND METHODS

RESULTS AND DISCUSSION

CONCLUSIONS

REFERENCES

2. HYPOTHESIS

Communication between the maternal endometrium and the preimplantation embryo by EVs is key to understand embryo implantation and subsequent fetal development.

We hypothesize that maternal endometrium secretes different types of EVs with specific cargo during the menstrual cycle. These become relevant during the window of implantation when they are uptaken by the embryo modifying its genetic/transcriptomic signature and act in specific functions in the implantation process.

OBJECTIVES

3. OBJECTIVES

- To identify and analyze the morphology, size and molecular markers of the different EVs secreted by the human endometrium to the endometrial cavity throughout the menstrual cycle and to assess their DNA cargo.
- To investigate whether endometrial EVs are able to transport their DNA content from the maternal endometrium to the embryo, as well as their metabolic impact over it.

INTRODUCTION
HYPOTHESIS
OBJECTIVES

MATERIALS AND METHODS

RESULTS AND DISCUSSION
CONCLUSIONS
REFERENCES

4. MATERIALS AND METHODS

4.1. Patients

Healthy, naturally cycling women aged 18–35 years were enrolled in the study (n = 61) if they met the following criteria: normal karyotype; body mass index of 18–30 kg/m^2; regular menstrual formula (3-4/28-30-day cycle); absence of contraceptive devices in the past 3 months and hormonal treatments in the past 2 months; negative for bacterial/viral infectious diseases; and negative for polycystic ovary syndrome and uterine or adnexal pathologies. All the samples were collected in IVI Valencia, the subjects provided signed informed consent, and the project was approved by the *Comité Ético de Investigación Clínica* at IVI Valencia, Spain (1603-IGX-017-FV).

4.2 EF sampling

Single EF samples were collected from each donor and were classified according to stage of the menstrual cycle, divided into five phases: phase I (days 0–8; n = 6), representing menses phase; phase II (days 9–14; n = 9), representing follicular phase; phase III (days 15–18; n = 7), representing early luteal phase; phase IV (days 19–24; n = 12), representing mid-luteal phase; and phase V (days 25–30; n = 6), representing late luteal phase. Phase IV represents the moment when the endometrium becomes receptive for an incoming embryo.

After cleaning the vaginal channel, EF samples were obtained from the uterine fundus by introducing an embryo transfer catheter (Wallace, Smiths Medical International, Minneapolis, MN, USA) 6 cm into the uterine cavity and applying gradual suction using a 10-mL syringe. Suction was stopped before transversing the

internal os to prevent contamination with cervical mucus. EF samples were stored at –80ºC until processing.

4.3 EVs isolation from EF

Each EF sample was resuspended in 1 mL of cold (4ºC) Dulbecco's PBS without Ca^{2+}/Mg^{2+} (L0615-500; Biowest, Barcelona, Spain) to prevent salt precipitates. Resuspensions were homogenized by extensive pipetting and vortexing. Samples were treated with 50 U/mL DNase I and incubated at RT for 30 min in gently agitation (D4513; Sigma-Aldrich, Madrid, Spain) to further disaggregate mucus.

For EVs isolation, each resuspended EF sample volume was increased up to 4 mL with PBS, and samples underwent a series of differential centrifugations and filtrations. Samples were first centrifuged twice at 300 x g for 10 min to pellet residual cells and debris. Resulting supernatants were centrifuged at 2,000 x g for 10 min, passed through 0.8 µm-diameter filters (GE Healthcare, Life Sciences, Whatman, UK), centrifuged at 10,000 x g for 30 min, passed through 0.22 µm-diameter filters (Acrodisc syringe filters, Pall Corp., Newquay Cornwall, UK), and ultracentrifuged at 120,000 x g for 70 min using a P50AT4 rotor (Hitachi Koki Co. Ltd., Tokyo, Japan). Resulting pellets from previous centrifugation steps were washed in 1 mL PBS and centrifuged again under the same conditions to obtain fractions subsequently enriched in ABs (2,000 x g for 15 min), MVs (10,000 x g for 40 min), and EXOs (120,000 x g for 70 min, using a Hitachi P50A3 rotor). Resulting supernatants were kept as EVs negative controls for further analysis. All centrifugations were conducted at 4ºC. The whole process of EVs isolation from human EF samples is depicted in **Figure 3**.

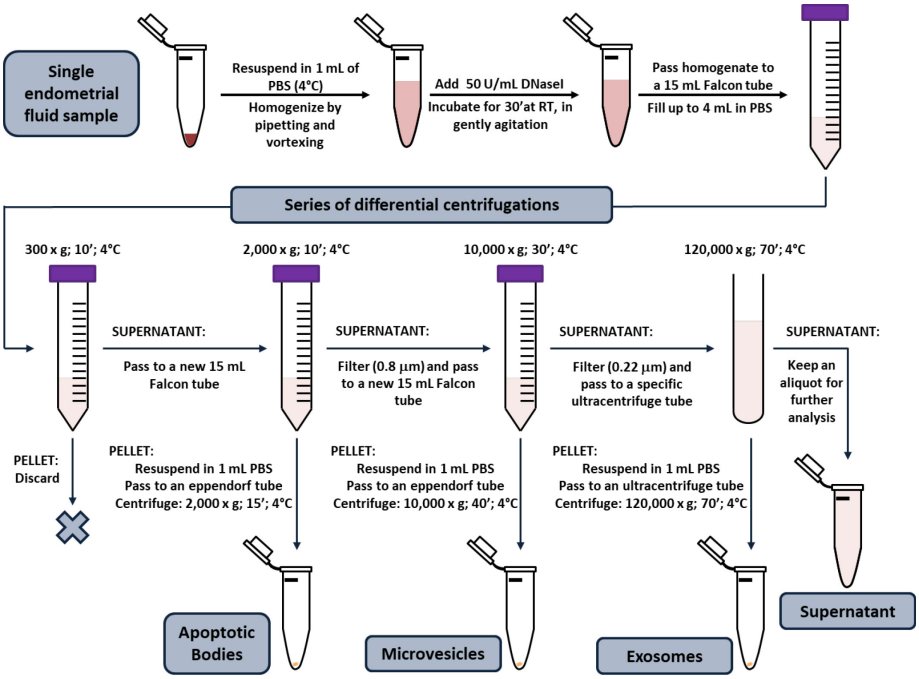

Figure 3. Isolation process of the extracellular vesicles from human endometrial fluid samples.

4.4 Transmission electron microscopy

Pellets from serial differential centrifugations of single EF samples (n = 3) were analysed by two transmission electron microscopy (TEM) techniques. *Deposition and positive staining (to evaluate external aspects and preliminary size):* Pellets were resuspended in 50 µL of Karnovsky's fixative solution (2.5% glutaraldehyde/2% formaldehyde in 0.1 M phosphate buffer, pH = 7.4), and a drop of the resulting mix was laid onto a 300-mesh grid. Samples were incubated for 10 min and were subsequently contrasted with 2% uranyl acetate for 10 min. Grids were then washed twice in distilled water for 1 min, incubated in Reynold's lead citrate solution (80 mM lead nitrate, 120 mM sodium citrate dihydrate, 100 mM NaOH in distilled water) for 10 min, washed again 5 times in distilled water, and air-dried for imaging. *Inclusion in LR-white resin and ultrathin cuts (to evaluate EV internal structures and general*

contents): Isolated pellets were carefully fixed in 50 µL of Karnovsky's solution without disturbing the pellet. Fixed pellets were washed 5 times in PBS for 5 min each and stained in a 2% osmium tetroxide/0.2 M PBS solution for 2 h. Samples were then dehydrated using the following sequence: 3 washes in distilled water at 4°C for 5 min each, wash in 30% ethanol for 5 min, wash in 50% ethanol for 5–10 min, 2 washes in 70% ethanol for 10 min each, 2 washes in 2:1 90% ethanol:LR-white for 45 min each, wash in 2:1 100% ethanol:LR-white for 45 min, and overnight wash in 1:2 100% ethanol:LR-white with continuous shaking. Ethanol was allowed to evaporate, and wash media was changed to 100% LR-white with continuous shaking for 30 min. Finally, samples were put in a mold to polymerize for 1 day at 60°C, protected from the air by gelatin encapsulation. Resin-embedded samples were ultrasectioned in 60-nm slices, incubated for 1 h on Formvar carbon-coated copper grids, and contrasted with uranyl acetate. The entire process was conducted in a flow hood. Ultrathin cuts were made on a UC6 Leica (Leica, Wetzlar, Germany) equipped with an Ultra 45° diamond blade (Diatome, Hatfield, PA, USA). For both procedures, prepared samples were observed using a JEM-1010 TEM (Jeol Korea Ltd., Seoul, South Korea) coupled to a digital camera MegaView III at 80 kV. Imaging was done at *Servei Central de Suport a la Investigació Experimental* (SCSIE, Burjassot, Valencia, Spain).

4.5 Western blotting

EVs populations isolated from human EF (n = 3) were resuspended in 50 µL of RIPA buffer (150 mM NaCl, 1% IGEPAL CA 630, 0.5% Na-DOC, 0.1% SDS, 0.5 M EDTA, 50 mM Tris-HCl, pH 8) prepared with protease inhibitors [89% RIPA, 1% 0.1 M PMSF (Sigma-Aldrich, Madrid, Spain), 10% Roche Mini Complete (Roche, Madrid, Spain)] and incubated overnight at –80°C to lyse vesicles. Samples, including vesicles kept in RIPA buffer, residual supernatants from EVs isolation, and a tissue cell lysate were quantified by Bio-Rad Protein Assay (Bio-Rad Laboratories, Hercules, CA, USA). Cell lysate was generated as a western blot positive control from the human endometrial

epithelium Ishikawa cell line (Sigma-Aldrich, Madrid, Spain), as in previous work (19). Protein concentration was equalized among samples, and proteins were denatured at 95°C for 5 min. Samples were electrophoresed by SDS-PAGE before electro-transfer to PVDF membranes (Bio-Rad Laboratories).

Membranes were blocked in 5% skim milk in 1% Tween-20 in PBS (PBS-T) for 1 h at room temperature with continuous shaking. Blocked membranes were incubated overnight at 4°C with continuous shaking with specific primary antibodies in 3% skim milk in PBS-T: rabbit anti-calnexin (1:1,000; ADI-SPA-865; Enzo Life Sciences, Farmingdale, NY, USA), mouse anti-calreticulin (1:1,000; ab22683; Abcam, Cambridge, UK), rabbit anti-VDAC1 (1:1,000; ab154856; Abcam), rabbit anti-ARF6 (1:1,000; ab77581; Abcam), mouse anti-CD63 (1:1,000; ab59479; Abcam), rabbit anti-CD9 (1:1,000; ab92726; Abcam), and rabbit anti-TSG101 (1:1,000; 125011; Abcam). The following day, membranes were washed 3 times with PBS-T and incubated with secondary antibodies: goat anti-mouse (1:10,000; sc-2005; Santa Cruz Biotechnology, Dallas, TX, USA) or goat anti-rabbit (1:20,000; EXOAB-KIT-1; System Biosciences, Palo Alto, CA, USA). Antibody dilutions were adjusted to manufacturer's datasheet specifications. Finally, target proteins were detected using SuperSignal West Femto Chemiluminiscent kit (Thermo Fisher Scientific, Waltham, MA, USA) and a LAS-3000 imaging system (Fujifilm, Japan).

4.6 Dynamic Light Scattering

ZetaSizer Nano (Malvern Instruments Corp., Malvern, UK), a device based in dynamic light scattering (DLS) technology, was used to generate general size distribution patterns of the different EVs fractions in a wide size rage (1–6,000 nm), including that of ABs, on the basis of their light refraction properties. For analysis, pellets from serial differential centrifugation steps were resuspended in 1 mL of PBS without Ca^{2+}/Mg^{2+}, transferred to 4 mL polystyrene cuvettes, and analyzed on a Malvern ZetaSizer Nano-ZS 90.

ZetaSizer measurement provides a value for the size of each possible subpopulation within EVs fractions and their relative contribution to the total of particles as a percentage on the basis of intensity of light scattered by particles, which is the primary and most robust result generated by the equipment. Although absolute quantification is possible, it is mathematically calculated from the previous information, so we did not use this technique to measure concentration. Finally, accuracy and validity of the measurements were controlled by checking fitting of the size model to the correlogram, cumulant fit, and distribution fit curves, with results meeting quality criteria for all measures. Correlogram informs about mean size of the sample, and its decay line shape allows evaluation of accuracy of the measure in the size range. Cumulant fit and distribution fit graphs show fit of the data points to the model from which sizes and intensities were calculated (**Figure 4**).

Adjusted reading parameters: water as dispersant; 4°C; general purpose algorithm of measurement; 3 measurements per sample; rest of parameters set automatically.

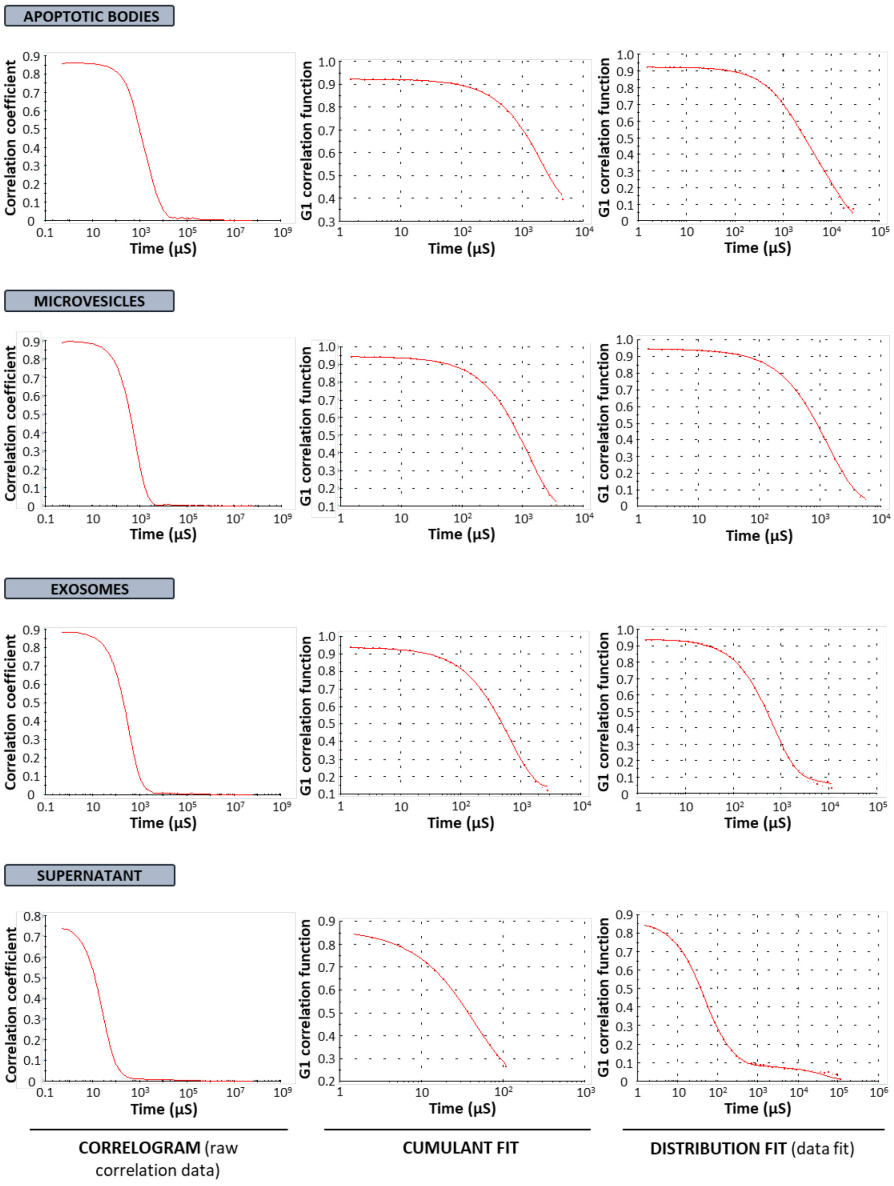

Figure 4. Quality control of DLS results. Correlogram, cumulant fit, and distribution fit graphs for size distribution measures of apoptotic bodies, microvesicles, exosomes and supernatant from a single human EF sample.

4.7 Nanoparticle Tracking Analysis

NanoSight 300 (Malvern Instruments Corp.), a technology based in nanoparticle tracking analysis (NTA), was used for fine EVs size distributions acquisition as well as concentrations from EF samples throughout the menstrual cycle. Due to its more limited size working range (up to 1,000 nm), ABs could not be analyzed.

In order to normalize concentration measurements, EF volumes were measured prior to EVs isolation so that we could refer to EVs concentration per mL. Pellets containing isolated vesicles were resuspended in 1 mL PBS without Ca^{2+}/Mg^{2+} and introduced into the NanoSight 300. PBS alone also was measured as a negative control to account for natural occurring particles that could bias results.

To improve accuracy and calibrate the equipment, known dilutions of silica nanosphere standards (Polysciences Inc., Hirschberg an der Bergstrasse, Germany) were measured using the same conditions. Different size standards were used depending on the size range: 167/170 nm for EXOs, supernatant, and PBS; and 300/310 nm for MVs. Mode of standards distribution was accepted as the nominal size of nanospheres and was used to calculate a factor to correct size measures in unknown samples. Similarly, concentration measures were used to calculate a calibration factor for this parameter based on known standards dilutions.

To measure EVs concentration variations throughout the menstrual cycle, MVs and EXOs were isolated from EF samples from different phases of the menstrual cycle for NTA analysis as previously described. In detail, we analysed 6 samples from phase I, 7 samples from phase II, 7 samples from phase III, 6 samples from phase IV, and 6 samples from phase V of the menstrual cycle. Due to the elevated number of samples and because the technique is time consuming, samples were measured on different days. Therefore, standards were read at various times each day, using a batch-

specific average to cope with possible batch effects and with possible deviations over the batch progression (**Figure 6**).

Standards profiles and calibration factors are included in **Figure 5** and **6**, for the analysis of single EF in combination with DLS and for the analysis of EVs variation throughout the menstrual cycle, respectively.

Adjusted reading parameters: sCMOS camera type; static flow conditions; 5 consecutive measures of 1 min each, changing the field between readings; 25°C; manual focusing; rest of parameters set automatically.

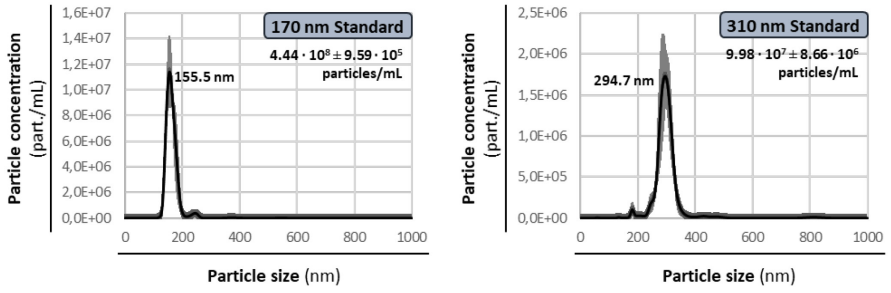

Standard size (nm)	Known particle concentration (part./mL)	Measured mode (nm)	Calibration factor for size	Measured EVs concentration (part./mL)	Calibration factor for concentration
170	2.14E+08	155.50	**1.09**	4.44E+08	**0.48**
310	3.40E+07	294.70	**1.05**	8.40E+07	**0.41**

Figure 5. Calibration standards and factors for NTA measures of EVs found within a single human EF sample. NTA graphs of EVs concentrations within one EF sample, with black line representing mean concentration of particles in 1-nm intervals. Gray area represents standard error. Figures show particle concentrations (particles/mL) and modes (nm) of standards size distributions.

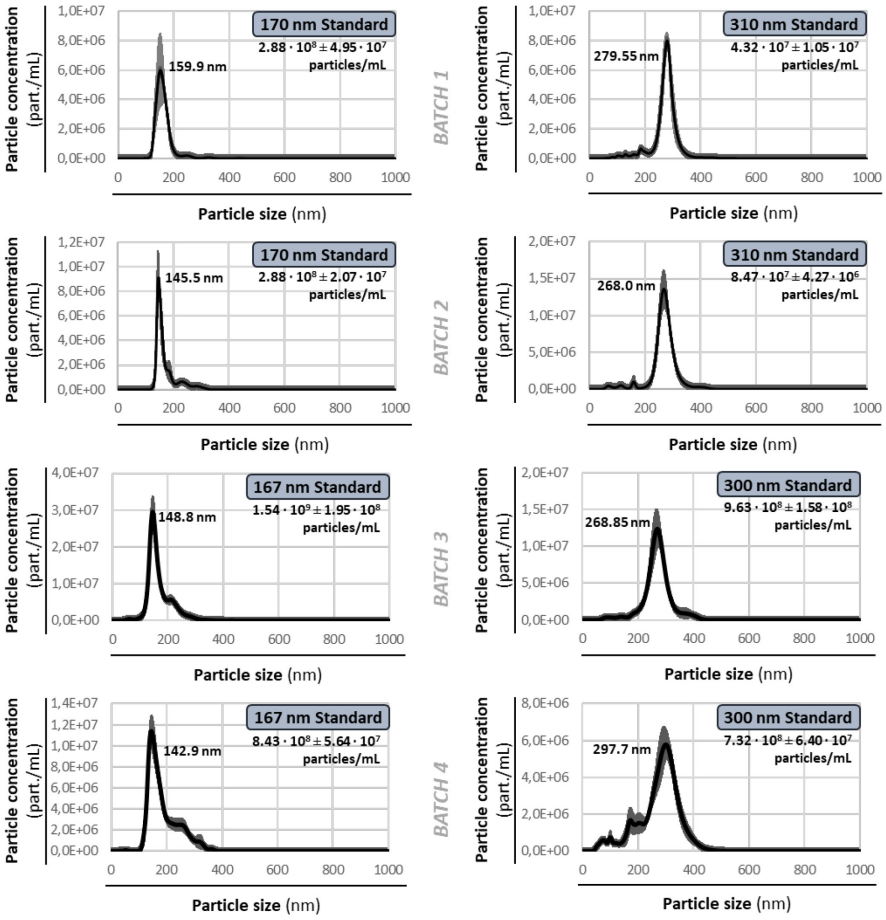

Measuring batch	Standard size (nm)	Known particle concentration (part./mL)	Measured mode (nm)	Calibration factor for size	Measured EVs concentration (part./mL)	Calibration factor for concentration
1	170	2.14E+08	159.90	**1.06**	2.88E+08	**0.74**
	310	3.40E+07	279.55	**1.11**	4.32E+07	**0.79**
2	170	2.14E+08	145.50	**1.17**	2.88E+08	**0.74**
	310	3.40E+07	268.00	**1.16**	8.47E+07	**0.40**
3	167	2.14E+09	148.80	**1.12**	1.54E+09	**1.39**
	300	1.23E+09	268.85	**1.12**	9.63E+08	**1.28**
4	167	1.07E+09	142.90	**1.17**	8.43E+08	**1.27**
	300	9.21E+08	297.70	**1.01**	7.32E+08	**1.26**

Figure 6. Calibration standards and factors for NTA measures of EVs in EF samples throughout the menstrual cycle. NTA graphs of EVs concentrations throughout the menstrual cycle. Black line represents mean concentration of particles in 1-nm intervals. Gray area represents standard error. Figures show particle concentrations (particles/mL) and modes (nm) of standard size distributions.

4.8 High throughput sequencing of human endometrial fluid EVs DNA cargo

After the initial description and characterization of the EVs populations found in human endometrial fluid, a series of sequencing experiments were set up to analyze differences in the DNA cargo of these vesicles due to the phase of the menstrual cycle and to the type of vesicle. To do so, EVs were isolated from single EF samples in phase II (n=4) and phase IV (n=10) of the menstrual cycle as described above. From these, 4 samples in phase II and 4 samples in phase IV were initially used to evaluate differences due to the moment of the menstrual cycle and, specifically, receptive state specific DNA cargo (phase IV). Posteriorly, the number of samples in phase IV was increased up to 10 to analyse differences between EVs populations DNA cargo during the receptive phase.

Pellets containing isolated vesicles were resuspended in nuclease-free water and treated with 50 U/mL DNaseI (Sigma-Aldrich, ref. D4513) in order to cleave DNA that could be externally stuck to the vesicles. The digestion reaction was implemented with Tris-HCl (Thermo Fisher Scientific, ref. 15567027), $MgCl_2$ (Thermo Fisher Scientific, ref. AM9530G) and $CaCl_2$ (Sigma-Aldrich, ref. 21115-100ML) to a final concentration of 20 mM, 10 mM and 1 mM, respectively, and was incubated at 37°C for 30 min while gently shaking. After digestion, DNaseI was heat-inactivated by incubation at 75°C during 10 min in 2:30 v:v of 0.5M EDTA (Thermo Fisher Scientific, ref. 15575020). Next, DNA contained in EVs was extracted using QIAamp DNA Mini Kit protocol for cultured cells (Qiagen, ref. 51306), implemented with 100 mg/mL RNaseA (Qiagen, ref. 19101). Final elution was done in 30 µL of nuclease-free water. Eluted samples were then concentrated using an SpeedVac system up to 9 µL. From this volume, 3 µL were used for quantification by Qubit dsDNA HS Assay Kit (Thermo Fisher Scientific, ref. Q32854) and 5 µL were reserved for DNA libraries construction. Only those samples that accomplished a minimum of 0.03 ng/µL of DNA in all the vesicles populations from the same EF were chosen for libraries construction. We chose this lower threshold in the basis of our previous experience. Samples over 0.2

ng/µL were adjusted to this concentration with nuclease-free water. Finally, libraries were constructed by Nextera XT DNA Library Prep Kit (Illumina, ref. FC-131-1024) following the protocol provided by the product. As variable parameters, libraries AMPure XP (Beckman Coulter, ref. 082A63881) purification was done 1X, bead-based normalization was chosen and, following Illumina instructions, a 4 µL volume was chosen for serial dilution in 996 µL and 750 µL/750 µL in HT1. Libraries were sequenced by an Illumina NextSeq 500 (Illumina) using a 300 cycles NextSeq 500 High Output v2 Kit cartridge (Illumina, ref. FC-404-2004). The complete workflow for the analysis of DNA cargo in human EF EVs is shown in **Figure 7**.

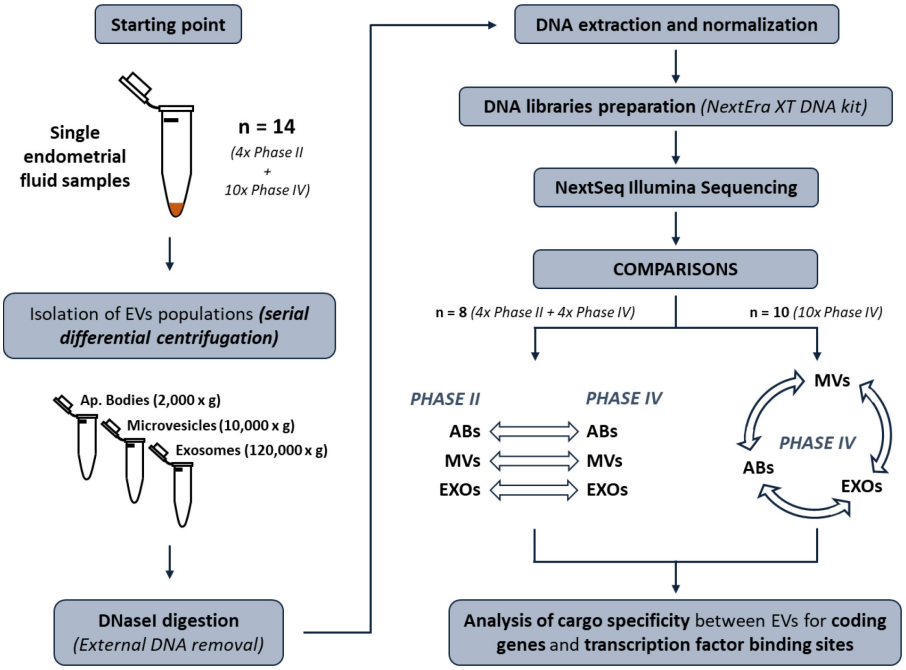

Figure 7. DNA sequencing workflow for the analysis of human endometrial fluid EVs specific DNA cargo.

The need of DNase treatment for avoiding masking of results was verified in a previous experiment. In that, 6 EF samples dated in different random points of the menstrual cycle were pooled for EVs isolation following the previous method. Pellets

containing the three EVs populations were resuspended in 50 µL of nuclease-free water and separated into three equal fractions, which were subsequently treated with DNaseI, DNaseI + T5 exonuclease (New England Biolabs, ref. M0363S) or H_2O, respectively. T5 exonuclease was chosen to complement DNaseI endonuclease activity. Digestion, inactivation, DNA extraction, concentration and quantitation were carried out as described above. Figures showing DNA concentrations, measured by Qubit dsDNA HS Assay, are shown in **Table 4**.

Table 4. Starting DNA from DNase set up experiment. Qubit DNA quantification after extraction and concentration of the 3 conditions from the DNase set up experiment.

Qubit DNA quantitation after DNase digestion (ng/µL)			
	Apoptotic Bodies	**Microvesicles**	**Exosomes**
Control	7.950	0.228	6.330
DNase I	0.171	0.051	0.170
DNase I + T5	0.207	0.168	0.129

Taking advantage of those samples with DNA excess from the previous assay, i.e. DNase untreated ABs (7.95 ng/µL) and EXOs (6.33 ng/µL), these were used to create serial dilutions in order to analyze the effect of lowering the DNA input amount for libraries construction. The assay was conducted to meet the limitation of those samples with initial suboptimal DNA, mainly DNase treated MVs and EXOs. Dilution series were: 0.3, 0.2, 0.15, 0.1, 0.05 and 0.01 ng/µL. Dilutions for DNase untreated ABs and EXOs along with treated ABs and EXOs, as well as treated and untreated MVs fractions were used for Nextera XT libraries preparation as previously described. Bioanalyzer 2100 HS DNA assay (Affymetrix) libraries profiles are shown in **Figure 8**.

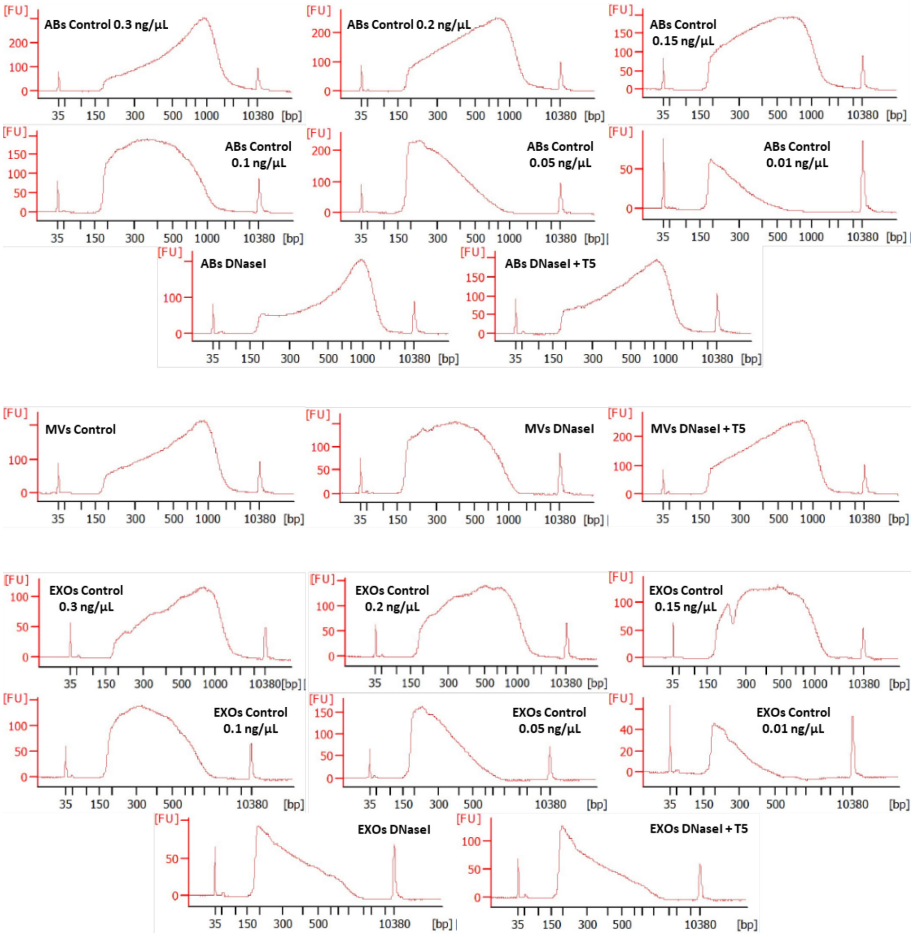

Figure 8. Sequencing libraries from DNase/Concentration set up experiment. Nextera XT sequencing libraries obtained from the DNase treated conditions and untreated ABs/EXOs dilutions.

Resulting libraries from 0.05 ng/µL untreated ABs and EXOs dilutions, as well as those in the ideal concentration point (0.2 ng/µL and 0.15 ng/µL for ABs and EXOs, respectively. Selection was based on libraries bioanalyzer profiles), where chosen to evaluate the effect of reducing DNA input for sequencing, based in the similarity of DNA concentrations and libraries profiles, measured by Bioanalyzer, between 0.05 ng/µL DNA dilutions and initial limiting DNA samples (**Table 4**, **Figure 8**). Along with them, treated ABs and EXOs, as well as MVs conditions, were included in the sequencing run to evaluate the effect of DNase treatment over sequencing output.

4.9 Ishikawa EVs generation for murine embryos co-incubation experiments

The human Ishikawa cell line was used as a model of human endometrial epithelium to harvest EVs. For this purpose, cells were grown in flasks in Modified Eagle's Medium (MEM, Gibco, Thermo Fisher Scientific, ref. 10370021), supplemented with 5% Foetal Bovine Serum (FBS, Biowest, Barcelona, Spain, ref. S181B-500), 1% non-essential aminoacids (Gibco, Thermo Fisher Scientific, ref. 11140035), 1% Glutamax (Gibco, Thermo Fisher Scientific, ref. 35050-038), 0.2% 50 mg/mL gentamicin (Gibco, Thermo Fisher Scientific, ref. 15750-037) and 0.2% 250 µg/mL amphotericin B (Gibco, Thermo Fisher Scientific, ref. 15290026), until 60-70% confluence. Three T175 flasks were cultured for each experiment. At that point, cells were washed in Dulbecco's Phosphate Buffered Saline without Ca^{2+}/Mg^{2} (PBS, Biowest, Barcelona, Spain, ref. L0615-500ml) and added Ishikawa medium with FBS treated to remove EVs (Biowest, ref: S181M-100).

For the generation of EdU DNA-tagged EVs, at the point of 60-70% confluence, Ishikawa growing medium was supplemented with 1 µM 5-ethynyl-2'-deoxyuridine (EdU, Thermo Fisher Scientific) and incubated O/N to allow cell division and incorporation of EdU in the endogenous DNA during this process. The next day, cells were washed twice in PBS and added Ishikawa medium with FBS treated to remove EVs.

Finally, conditioned medium containing EVs was collected after 24h, and the different EVs populations were isolated as previously described.

4.10 Murine embryos obtaining and culture

Murine embryos were obtained from B6C3F1/Crl strain mice (Charles River Laboratories, Saint-Germain-Nuelles, Francia). The project was authorized by the Animal Care and Use Committee of the Valencia University (CEBA) under the

identifier: 2015/VSC/PEA/00048. The process for embryo recovery and culture was adapted from our previous work (19). In short: female mice aged 6-8 weeks were stimulated to ovulate by 10 IU intraperitoneal injection of Foligon/PMSG (MSD Animal Health, Spain) followed by intraperitoneal administration of 10 IU of Ovitrelle 250 µg/0.5 mL (Merck Serono, Germany) 48h later. At that point, females were mated with males of the same strain for 48h, during that period, checking for the presence of vaginal plug. Next, plug positive females were sacrificed by cervical dislocation and embryos were collected from the oviduct by flushing with PBS using a 30-gauge blunt needle. Embryos were then washed four times in O/N oxygenated G-2 plus medium (G-2 PLUS, Vitrolife, Barcelona, Spain) and cultured until hatching for 48 hours in the same medium (day E3.5 of embryo development) in groups of 30-40 embryos per well (ThermoFisher Scientific, ref: 144444). An average of 30-40 embryos per female were obtained, the 60% reaching the hatching state with good quality in E3.5.

4.11 Study of EVs-DNA internalization into murine embryos by confocal imaging

Pellets containing Ishikawa EdU DNA-tagged EVs from the isolation step were resuspended in oxygenated G-2 plus medium. Good quality E3.5 hatching embryos were separated in different conditions in groups of 50 for O/N co-incubation with the different DNA-tagged EVs populations, the supernatant of the isolation process and a negative control. The negative control was constructed with a mixture of EVs populations generated by Ishikawa cells cultured in absence of EdU.

After embryos coculture with EVs, transferred EVs-DNA was stained by click-it chemistry reaction using Click-iT™ EdU Alexa Fluor™ 488 Imaging Kit (Thermo Fisher Scientific, ref: C10337). The protocol was done as recommended by the manufacturers with some modifications. In short: embryos were fixed in PBS/3,7% formaldehyde for 15 min at RT. Next, embryos were washed in HBSS and stained

with Wheat Germ Agglutinin, Texas Red™-X Conjugate (Thermo Fisher Scientific, ref: W21405) for 20 min at 37°C, protecting them from light until the end of the process. Embryos were then washed in PBS/3% BSA for 5 min and permeabilized with PBS/0.5% Triton X-100 for 20 min at RT. After that, embryos were washed in PBS/3% BSA for 5 min, labelled with EdU as indicated in the data sheet and washed again in PBS/3% BSA for 5 min. Finally, embryos were stained in 1:1000 1mg/mL DAPI solution (Thermo Fisher Scientific, ref: 62248), incubated 20 min at 37°C and washed in HBSS. The mounting of embryos was done in IBIDI plates (IBIDI, ref: AI-80826) as it follows: embryos were laid onto the IBIDI plate well surface trying to remove as much washing medium as possible, covered with Aquatex mounting media (Merck-Millipore, ref: 108562) and let air dry in a flow hood.

Finally, imaging of stained embryos was done in a FV1000 Olympus confocal microscope using a 60X oil-immersion lens. The schematic workflow for the analysis of EVs DNA transfer to the embryo is offered in **Figure 9**.

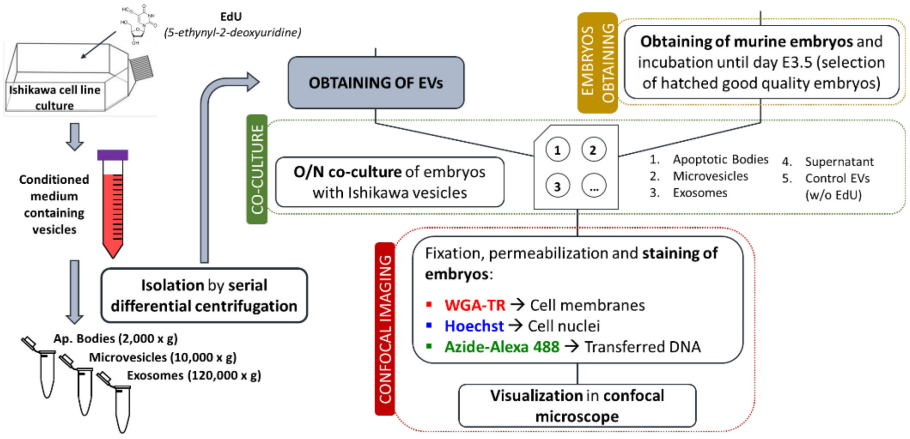

Figure 9. Workflow for the study of the transference of DNA to the embryo through EVs.

4.12 Analysis of embryo ATP levels modulation after co-incubation with human EF EVs

In order to analyze the impact of EVs in embryo bioenergetics modulation, 5 EF samples in phase IV of the menstrual cycle were pooled and their EVs populations isolated as described above and re-suspended in G2-plus oxygenated medium. In parallel, embryos from 10 mice were obtained and incubated until day E3.5. At that point, good quality hatching embryos were separated and O/N co-incubated with previously isolated EF EVs fractions in five conditions: ABs, MVs, EXOs, a fraction combining a third of each of the previous vesicles and G2-plus fresh media, representing an EF EVs-free condition. The following day, embryos were washed four times in PBS, collected in 1µL PBS and passed into 96-well opaque plates (Sigma-Aldrich, ref: CLS3917-100EA) in 50 µL H_2O. Replicates of 10 good-quality embryos were set up, achieving 6 replicates for ABs and MVs, 5 replicates for EXOs and all EVs condition, and 3 replicates for fresh G2 condition. 1 µL PBS was included in duplicate in 50 µL H_2O as a control of the embryo transport vehicle and an ATP standards curve was built up with 15 total ATP points from 5 fmol to 50 pmol in duplicate (including a blank) in 50 µL H_2O. The plate containing the samples and standards was sealed and maintained at -80°C until its analysis within the same day. ATP measurements were done using Adenosine 5'-triphosphate (ATP) bioluminescent somatic cell assay kit (FLASC, Sigma) adapting the protocol from previous works on human/mouse blastomeres and oocytes (77, 78, 274-277). Stock solutions were prepared following manufacturer's instructions. Reaction mix was prepared by diluting FLAAM working solution 1:10 in FLAAB and incubating for 5 min at 28°C in the dark. Samples on the plate were added 100 µL 1X ice-cold FLSAR, incubated for 5' at 4°C and continued processing in a ClarioStar BMG Labtech (BMG Labtech, Germany, Software Version 5.21.R2). The device dispensed 100 µL reaction mix and measured luminescence produced by the luciferase reporter system in consecutive cycles of: 1,8 sec. reaction mix injection, 2 sec. shaking and 2 sec. measurement. Gain was adjusted with the

higher ATP standard. The experimental design set up for embryo ATP measure after EVs stimulation is shown in **Figure 10**.

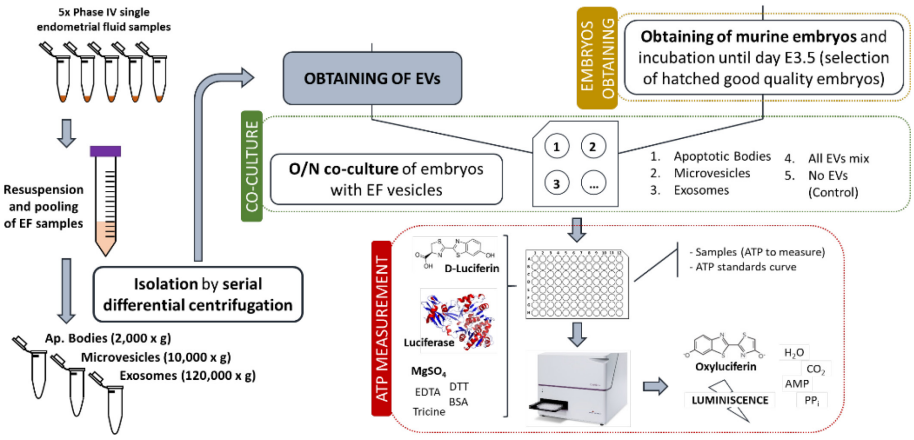

Figure 10. Workflow for the analysis of murine blastocysts ATP content after stimulation with the different populations of endometrial fluid EVs.

4.13 Evaluation of embryo mitochondrial membrane potential modulation by endometrial-derived EVs

In line with the previous experiment, evaluation of embryo mitochondrial membrane potential was proposed as an indicator of the energetic status of mitochondria under the stimuli of the different types of endometrial derived EVs. To do so, Ishikawa cells were cultured as previously described and EVs populations were isolated from conditioned media. Embryos were obtained from 10 mice and those of good quality in hatching state at day E3.5 were separated into five conditions of 35 embryos each for co-incubation with Ishikawa ABs, MVs, EXOs, a fraction combining a third of each of the previous vesicles, and G2-plus fresh media, representing an EVs-free condition, respectively. The following day, embryos membrane potential was assessed by using JC-1 (5,5',6,6'-tetrachloro-1,1',3,3'-tetraethylbenzimidazolylcarbocyanine iodide) cyanine dye. The system is based in

that JC-1 emits maximum fluorescence at λ = 525 nm (here represented as the green channel) as a monomer but maximum fluorescence at λ = 595 nm when it forms aggregates (red channel). JC-1 migrates towards cell compartments of higher membrane potential, such as energized mitochondria, thus reaching high concentrations and aggregating, in this way, offering a view of mitochondrial energetic status. Further, Valinomycin, a potassium ionophore that uncouples mitochondrial electron transport chain and abrogates mitochondrial membrane potential, was introduced for negative control and fluorescence thresholding (80). The protocol for membrane potential assessment was adapted from Troiano and collaborators (79). Briefly, O/N co-incubated embryos were washed in G2-plus oxygenated media. Half of the embryos from the fresh G2 condition were treated with 50 nM valinomycin, incubated at 37°C, 5% CO_2 for 15 min, and washed again in G2-plus medium. From here, all the generated embryo conditions were treated with 2.5 µg/mL JC-1 (original dilution: 1 mg/mL in DMSO), incubated at 37°C, 5% CO_2 for 20-30 min and washed in G2-plus medium. Finally, embryos were imaged in IBIDI plates in a FV1000 Olympus confocal microscope using a 60X oil-immersion lens. A schematic description of the assay methodology is shown in **Figure 11**.

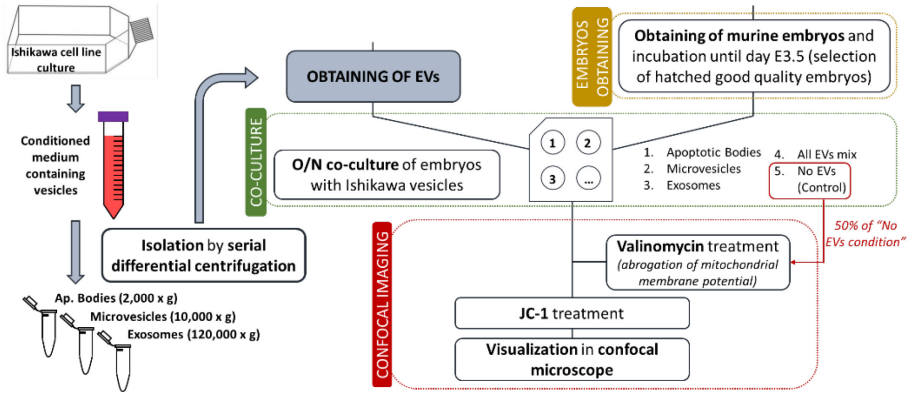

Figure 11. Workflow for the assessment of murine blastocysts mitochondrial membrane potential after stimulation with the different populations of endometrial fluid EVs.

4.14 Data analysis

4.14.1 NTA concentration measurements

NS300 curves corresponding to particle concentrations for different EV populations were obtained as an average value from 5 independent measures of random NTA fields. Standard error for different measures was calculated and represented for each curve as an indicator of evenness of particles across the sample.

To evaluate variation in vesicle concentration throughout the menstrual cycle, concentration data for different samples were uploaded into R software, and the Kruskal-Wallis algorithm was used to detect differences. This test allowed comparison of the five groups at once, because the small sample size prevented assumptions of normality among data.

4.14.2 DNA sequencing data analysis

Raw data from pair-ended Illumina sequencing was converted into FASTQ files using bcl2fastq (version 2.16.0.10). Raw counts were transformed with log2(counts+1). In order to filter out lowly enriched regions, only features with greater than 6-7 reads mapped in at least “X” samples (being “X” half of the mean of groups sizes) were kept for normalization and analyses. Raw counts were normalized using TMM method from edgeR R package (71). Then, each sample was aligned to the reference genome (GRCh37) using BWA (version 0.7.10) (72). Reads with mapping quality >90% were filtered using Samtools (version 1.1) (73) and duplicates were removed with PICARD software. Insert size was retrieved from filtered reads using PICARD software and features coverage, coding genes and TFBS, was obtained with Bedtools (version 2.17.0) (74) using Ensembl Biomart hg19 annotations.

For the following bioinformatics analysis, reads mapping to the chromosome Y and noisy samples were filtered out. Coding genes and TFBS coverage data were treated separately. The approach used for differential DNA enrichment analysis was based on the edgeR methodology (75, 76). PCAs were obtained from log2 normalized CPM using prcomp R function (278) for all samples and comparisons. For the analysis of reducing initial DNA concentration effect, a descriptive and a Pearson's correlation analysis were done.

4.14.2.1 Comparison of each EV type in phase II vs phase IV

Samples from both phases of each EV type were used for a differential enrichment analysis and comparisons between phases from all samples and each EV type were obtained using a generalized linear model approach for paired samples (ABs, MVs and EXOs vesicles from each patient). In order to find differentially enriched genes and TFBSs between phase II and phase IV for each vesicle type, we used an additive model formula with group (vesicle type + phase) and patient factors, so that baseline differences between the patients are subtracted out. Bonferroni p-value adjustment method was used in order to plot candidate features.

4.14.2.2 Comparison of EVs types in phase IV

Phase IV samples were used for the following analyses. Batch effect was discarded graphically with a PCA plot using two descriptive factors: run and vesicle type. Outliers were explored with four methods: visually from alignment statistics, Rlof method (279), Hubbert method (280, 281) with 3 PCA components and Hubbert method with 10 PCA components. Then, an intersection of outlier results was performed with all methods. Samples classified as outliers with Hubert method were removed and descriptive analysis was repeated with clean data.

Differential enrichment analysis of genome features was done using a generalized linear model approach for paired samples (ABs, MVs and EXOs from each patient). In order to find differentially enriched genomic features between vesicles types, an additive model formula was used with vesicle and patient factors, so that baseline differences between patients are subtracted out. Bonferroni p-value adjustment method was used in order to plot candidate features. Features were annotated with ensembl biomart (GRCh37).

TFBS: Human binding motifs regions annotation from ensembl biomart hg19 was used in obtaining coverage with Bedtools. Contig chromosomes were filtered out to remove noise. TFBS annotation was collapsed in order to merge overlapped regions by TF for each chromosome using GenomicRanges R package (282). Then, TFBS coverage was obtained using Bedtools. Summary boxplot of significant results and merged overlapped significant regions were plotted.

Regular/Broad peaks: Peak calling was performed with MACS2 software (2.1.1 version) (283). Samples were used to retrieve peak regions from MACS2 results with DiffBind R package (284). Coverage of peak regions was obtained using Bedtools for each sample. Consensus peaks, that is common overlapping peaks across vesicles between at least "X" samples (being "X" half of the mean of groups sizes), were selected for paired differential enrichment analysis. In order to visualize peaks with UCSC genome browser, bedGraph and bigWig files were generated for each sample using Bedtools, bedGraphToBigWig and bigWigToWig software tools.

4.14.2.3 Calculation of EVs mtDNA vs total DNA proportion

The number of reads mapped on each chromosome for previous samples from phase II and IV of the menstrual cycle was obtained using samtools idxstats. Chromosomes used included 1:22, X and MT. The proportion of MT reads was calculated per sample using: MT reads / genomic reads (chr1:22 + chrX).

Descriptive plots and groups comparisons were done for all samples and those in phase IV separately. Homogeneity of variances was checked with Bartlett Test and a non-parametric test because we could not assume homogeneity of variances. Kruskal-Wallis test and post-hoc comparison of MT proportions was applied to ascertain differences between vesicles groups.

4.14.3 Embryo ATP measurements

To analyze differences in ATP content of hatching murine embryos under the stimuli of EVs, differences in luminescence produced by the luciferase reporter system were analyzed by ANOVA test assuming normal distribution in the study groups (77, 78). When ATP is the limiting reagent, in presence of an excess of the rest, the light emitted is proportional to the ATP present in the sample. P-values under 0.05 were considered significant. Tukey multiple pairwise-comparisons test was used to interpret those conditions showing statistical differences between them. Finally, total ATP content in the samples was calculated by linear regression using the values of a 15-point ATP standards curve. For a higher accuracy, the regression model was calculated with those points of the curve framing the interval of luminescence shown by the samples. Graphs in **Figure 45** show the average ATP content of the 10-embryo replicates for each EV condition ± standard deviation.

ImageJ was used to measure JC-1 fluorescence intensity means for monomers and aggregates wavelengths. These mean values were used to calculate the fluorescence aggregates-to-monomers ratio for the embryos incubated with the different EVs populations and controls.

INTRODUCTION
HYPOTHESIS
OBJECTIVES
MATERIALS AND METHODS

RESULTS AND DISCUSSION

CONCLUSIONS
REFERENCES

5. RESULTS AND DISCUSSION

5.1 Morphological characterization of EVs populations in the human endometrial fluid

A series of TEM experiments allowed us to assess whether the three commonly described EVs populations (i.e.: ABs, MVs and EXOs) were present within human EF and whether it was possible to isolate them from single EF samples by serial differential centrifugation. Regardless of visualization processing, ABs were differentiated by their large size (**Figure 12**), ranging from 1.5 µm (micrograph f) to 8 µm (micrograph d).

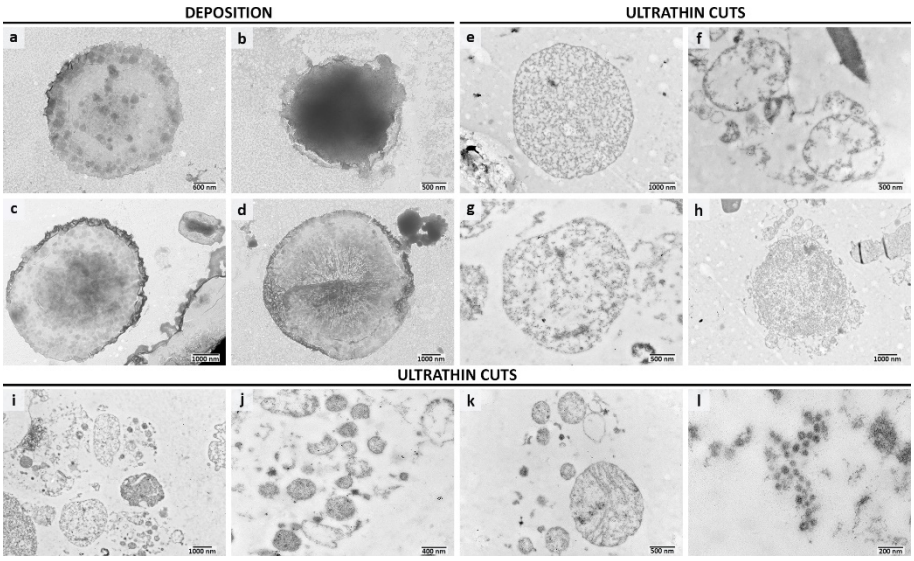

Figure 12. Morphological analysis of human EF ABs by TEM. Images were obtained via two different protocols for either an external (deposition processing) or internal (ultrathin slide processing) view of EVs. Sizes of different vesicles are: (a) 3.66 µm; (b) 2.4 µm; (c) 5.71 µm and 1.82 µm (left to right); (d) 8.12 µm; (e) 5.34 µm; (f) 1.80 µm and 1.50 µm (left to right); (g) 2.47 µm; (h) 4.96 µm. i–l show ultrathin slide micrographs of AB populations with detail of smaller subpopulations, with average sizes of 500 nm (k), 300 nm (i and j), and 50 nm (l). Micrograph j correspond to a higher magnification of micrograph i.

Considering the deposition images, different features were characteristic of ABs, such as edges of the vesicles appearing bent in electron-dense groves, which may reflect folding of ABs walls in deposition due to their large size (micrographs a, c, and d). In some cases, it was possible to appreciate their content, which formed round-shaped aggregates or smaller vesicles (micrographs a and c). Ultrathin slides processing revealed differences in their contents (micrographs e–h). Finally, we found evidence of a smaller-sized ABs population—with vesicles from ~700 nm (micrograph h) and ~500 nm (micrograph k) to ~300 nm (micrographs i and j) or even ~50 nm (micrograph l)—many of them surrounding larger ABs structures and, in some cases, still distinguishable cell organelles, such as mitochondria, arising from degraded cells (micrograph k).

MVs had sizes of between 200 and 700 nm and a considerably higher abundance compared to the previous population, considering different TEM imaging fields (**Figure 13**, micrographs a and b). MVs also had highly varied contents based on electron density (micrographs e, g, and h).

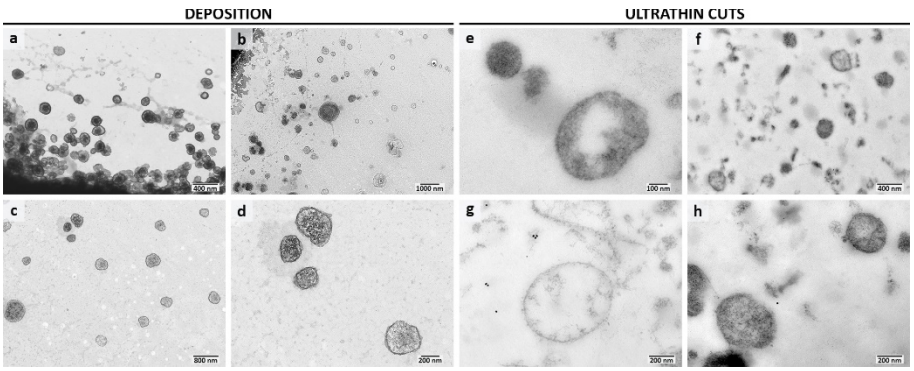

Figure 13. Morphological analysis of human EF MVs by TEM. Sizes of different vesicles are: (a) 200 nm [approximate mean size (ams)]; (b) 400 nm; (c) 330 nm (ams); (d) 340 nm (ams); (e) 190 nm and 540 nm (left to right); (f) 300 nm (ams); (g) 717 nm; (h) 515 nm and 344 nm (left to right). Micrograph d correspond to a higher magnification of micrograph c.

Compared to MVs, EXOs showed similar aspects and abundance (**Figure 14**) and exhibited vesicles with sizes of 40-to-160 nm whose structures got highly compromised after treatment for ultrathin slides (micrographs e-h). EXOs' general contents seemed to be more homogeneous compared to the other EVs populations, which may be due to their small volume.

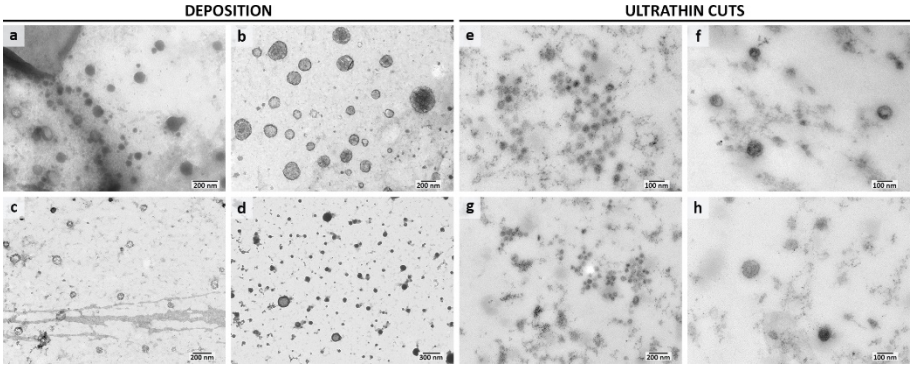

Figure 14. Morphological analysis of human EF EXOs by TEM. Sizes of different vesicles are: (a) 60 nm [approximate mean size (ams)]; (b) 159 nm (ams); (c) 91 nm (ams); (d) bigger vesicles, 186 nm and 147 nm (left to right), and smaller vesicle, 79 nm (ams); (e) 50 nm (ams); (f) 90 nm (ams); (g) 46 nm (ams); and (h) 90 nm (ams).

5.2 Analysis of EVs molecular markers

Once the presence of different-sized EVs populations was confirmed in EF, we characterized their specific molecular signatures. To do so, we investigated known markers described in the bibliography for different EVs populations in EVs isolated from human EF. VDAC1 and Calreticulin were chosen to identify ABs (**Figure 15**).

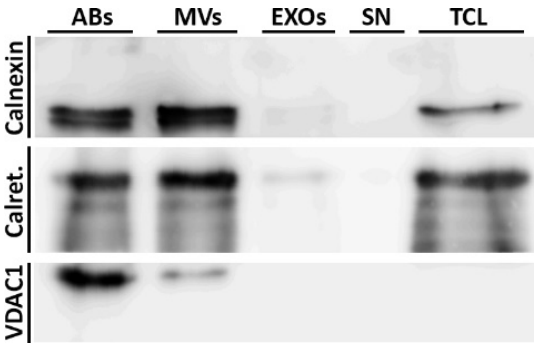

Figure 15. Analysis of specific molecular markers for human EF ABs by western blotting. Studied markers include: calnexin (90–100 kDa), calreticulin (60 kDa) and VDAC1 (31 kDa). Abbreviations: SN, supernatant; TCL, tissue (Ishikawa) cell lysate.

VDAC1, a protein that forms ionic channels in the mitochondrial membrane and has a role in triggering apoptosis, has been described as characteristic of the ABs vesicular fraction (82). Calreticulin, an endoplasmic reticulum (ER) protein, could also function as an ABs marker due to its subcellular location (285), although it has also been observed in the MVs fraction (82). This may be due to apoptosis, during which the ER membrane fragments and forms vesicles smaller than ABs, which would contain calreticulin and sediment at higher centrifugal forces (84, 85). In fact, proteomic studies have related calreticulin with vesicular fractions in the size range of MVs (81) and ABs (286). Phosphatidylserine was not used as a marker for this population because its externalization can also be triggered in non-apoptotic conditions by stimuli such as tissue mechanical disaggregation, enzymatic treatments for detachment of cells, electroporation, chemical transfections or retroviral infections, and PS exposure has also been described in healthy cells (287), during the biogenesis of MVs (288, 289), and exposed on the surface of EXOs (16, 290). Calreticulin was similarly found in ABs and MVs populations, while VDAC1 appeared to be more specific to ABs, although a small signal also was found in MVs (**Figure 15**). Nevertheless, this could be expected because existing isolation

techniques are based in physical principles and do not allow complete separation of vesicle populations, making it necessary to refer to EVs-enriched fractions (6, 83).

ARF6 is a GTP-binding protein that is involved in the regulation of cargo sorting and promotion of budding and release of MVs at the plasma membrane level through the activation of phospholipase D metabolic pathway. For this reason, it was chosen as a differential marker for MVs (**Figure 16**) (9, 86).

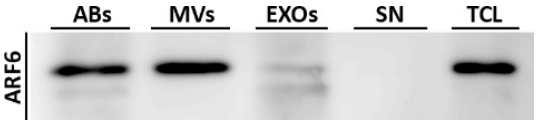

Figure 16. Analysis of specific molecular markers for human EF MVs by western blotting. Studied markers: ARF6 (18 kDa). Abbreviations: SN, supernatant; TCL, tissue (Ishikawa) cell lysate.

When comparing MVs to EXOs, although ARF6 was found in both fractions, a specific difference in the band pattern was evident—EXOs showed two different bands compared to a unique band for MVs. This was confirmed when observing ABs pattern, where both bands were present, with the one specific to EXOs at lower relative levels (**Figure 16**). The fact that ABs showed signals for all markers was not unexpected because during apoptosis, different proteins produced by the cell—including those reported to be specific to different EVs fractions—are likely captured within the ABs lumen.

Classically associated markers of EXOs are molecules mainly involved in their biogenesis, including tetraspanins (CD63, CD9, CD81), Alix, TSG101, and flotillin-1 (3, 163). From these, tetraspanins CD9 and CD63 as well as TSG101 were selected for our study. However, we observed these three markers in all three EVs populations, preventing their use as EXO-specific markers (**Figure 17**).

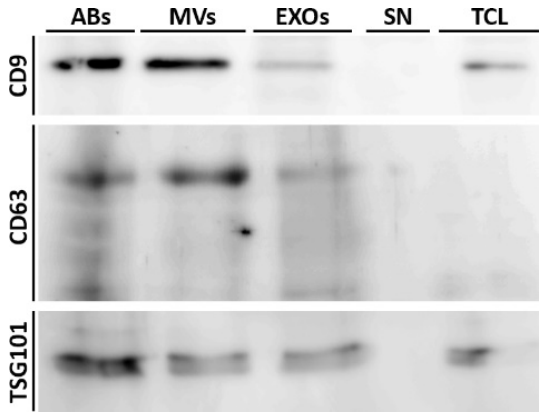

Figure 17. Analysis of specific molecular markers for human EF EXOs by western blotting. Studied markers: CD9 (24 kDa), CD63 (30–60 kDa), and TSG101 (45–50 kDa). Abbreviations: SN, supernatant; TCL, tissue (Ishikawa) cell lysate.

This discrepancy may be because EXOs were the only vesicular fraction considered in initial research. In fact, in recent years, many of the classical markers have been found to be widespread among EVs populations, although with different relative abundances. This is the case for CD9, CD63, HSC70, and flotillin-1 (291). However, some other molecular markers have been ratified as unique to EXOs, including TSG101 and syntenin-1 (82, 291). In our samples, TSG101 was similarly found in the different EVs, thus opposing previous findings, at least for EVs with EF origin. Of note, the absence of CD63 signal in Ishikawa cell lysate (TCL) is likely due to strong sorting of this molecule inside EVs, which makes its relative abundance in cells low when compared to vesicles (292, 293) (**Figure 17**). In cells, CD63 mainly localizes into multivesicular bodies and lysosomes, with low levels in plasma membranes (294, 295). Finally, calnexin was analysed as a negative EXOs marker because it has classically been described to be absent in this fraction (87, 88), which our results confirmed (**Figure 15**). Further, calnexin showed a similar band pattern to that of calreticulin, consistent with the fact that both proteins are located within the ER,

and further indicating little contamination of the EXOs fraction with vesicles from other cell compartments, such as the ER (88, 89).

5.3 Size distribution profiles of endometrial fluid EVs populations

EVs populations from human EF could also be differentiated by their size ranges measured from single EF samples by light scattering techniques. For an initial approach to EVs sizing, we pooled two EF samples from the same phase of the menstrual cycle (phase II) and divided the resulting homogenized pool into two aliquots to achieve technical replicates for DLS and NTA. The idea of measuring the same sample by both techniques was carried out to combine their benefits and fill their methodological gaps. These are, DLS allows to measure EVs in the size range of ABs while NTA offers more accurate size profiles and the possibility of measuring concentrations.

ABs appeared as a multimodal population with two size centres under DLS. The main population had a mean size of approx. 2 µm and accounted for 61.1% of total measured particles. The second population had sizes between 190 and 400 nm with mean size of 274.7 nm and accounted for 38.4% of total particle content (**Figure 18**). This second population is in concordance with our TEM results, where we observed vesicle-like structures inside big ABs in deposition images (**Figure 12**) and also as independent entities indicating a smaller-in-size ABs population from ~50 to ~700 nm (**Figure 12**, micrographs i-l). Although ABs is an EVs population widely described to have sizes of >1 µm, other authors have already indicated the existence of ABs with sizes from 50 nm even when their purification was based on centrifugation at 2,000 x g (6, 82). The origin of these small ABs population is uncertain, as they may be expected to be isolated at higher centrifugal forces with either MVs or EXOs fractions. Thus, it could be argued that they appear after ABs isolation due to further degradation or breakdown of these structures during processing. A possible origin for these small-sized vesicles may lie behind the process of apoptosis, when the ER

membrane is fragmented and forms vesicles smaller than ABs (84, 85). These vesicles may be released during ABs processing and thus are measured by TEM and DLS. Release of ER-derived vesicles from ABs and cells may also link to our results for molecular marker signatures, where we found signals for calnexin and calreticulin, two known ER proteins, in MVs—a fraction that shows an overlapping size range with that of small vesicles in the ABs fraction (**Figure 15**). These results are also in concordance with previous reports (81).

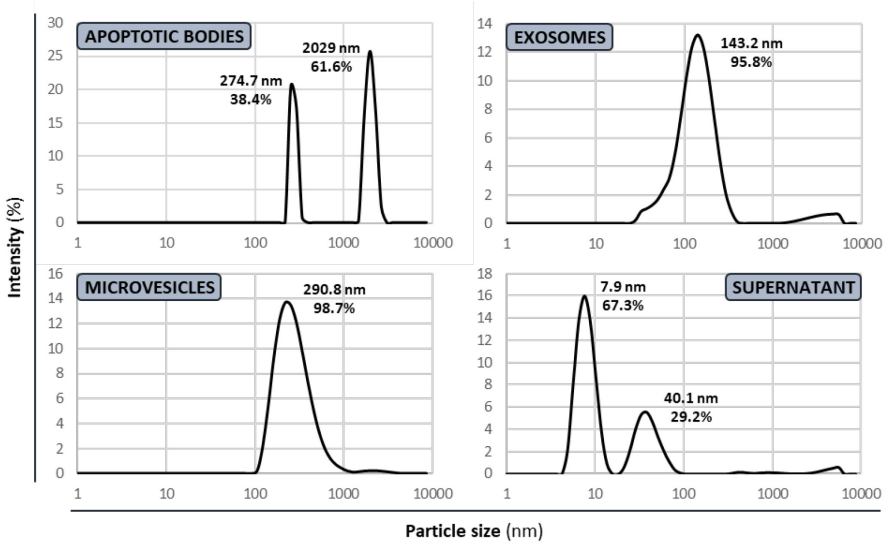

Figure 18. Size distribution ranges for main EVs populations found within a single human EF sample by DLS. Figures show size distribution average and percentage of total particles contained within the different sized populations.

MVs extended in their canonical range of 100–1000 nm, in a single population with a mean size of 290.8 nm. EXOs also showed a single size population, which partially overlapped with that of MVs, and had a mean size of 143.2 nm. Finally, residual supernatant from EVs isolation process showed two different sized populations with mean sizes of 7.9 nm and 40.1 nm, accounting for 67.3% and 29.2%, respectively,

and possibly corresponding to protein aggregates and residual small EXOs (**Figure 18**). All data met quality criteria, supported by correlograms with constant decay slopes that further correlated in time with size output for EVs populations. Further, an appropriate model adjustment was possible from data points both for cumulant and distribution fits, indicating the final sizing outputs were reliable (**Figure 4**).

After a size interval was established for EF EVs, fine size distribution profiles were assessed for MVs and EXOs by NTA (**Figure 19**).

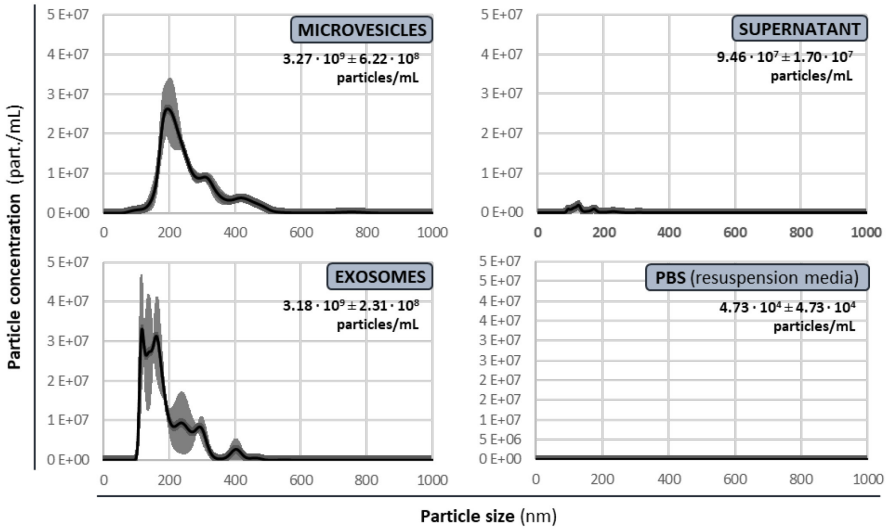

Figure 19. Size distribution ranges for main EVs populations found within a single human EF sample by NTA. Black line represents mean concentration of particles in 1-nm intervals. Grey area represents standard error. EV resuspension media (PBS) was the negative control. Figures show particle concentrations for each EV population.

Normalizing standards profiles showed narrow monodisperse distributions that indicated appropriate disaggregation and homogenization and allowed calculation of calibration factors (**Figure 5**). After corrections, MVs extended from 150 to 500 nm, with modal size of 194.1 nm, and 76.2% of total particles larger than this modal

size. EXOs were contained in the 100-to-300 nm interval, although sizes >200 nm showed augmented standard error, indicating instability and the likely presence of aggregates. EXOs modal size was 117.5 nm, and 67.64% of total particles were <200 nm. Interestingly, both vesicle populations showed similar concentrations. Supernatant from the isolation process showed a low number of small-sized particles, possibly corresponding to protein aggregates, also in concordance with DLS results (**Figure 18**). PBS, the medium where EVs populations pellets were resuspended, did not show a measurable number of particles ($4.73 \times 10^4 \pm 4.73 \times 10^4$ particles/mL; NS300 measuring range: 10^6–10^9 particles/mL), thus discarding potential technical bias of the results. MVs and EXOs showed overlapping size profiles similar to those observed by DLS (**Figure 19**). Altogether, our data suggest a similar contribution of MVs and EXOs in the EF in terms of total vesicle number, with a size profile showing prevalence of EXOs in the higher portion of their canonical interval and MVs of small sizes within their classical size range (1).

5.4 EVs populations variation throughout the human menstrual cycle

NTA was used to analyse EF samples from different phases of the menstrual cycle to identify any trends in MVs and EXOs sizes and/or levels. Standards presented as monodisperse distributions, allowing calculation of specific calibration factors (**Figure 6**). Once corrections were applied, an average size profile was obtained for the samples in the different phases of the menstrual cycle for each EVs population to identify differences in size profiles among menstrual cycle phases and to compare particle concentrations among EVs populations (**Figure 20**).

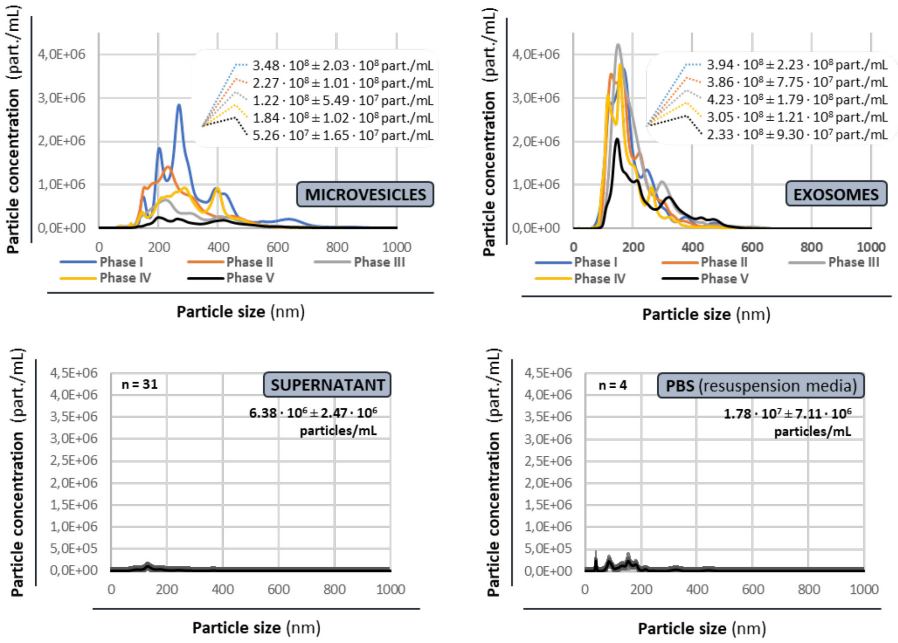

Figure 20. NTA analysis of EF EVs size variation throughout the menstrual cycle. Top graphs show average MVs and EXOs size profiles in the different phases of the cycle. Coloured lines represent mean concentration of particles in 1-nm intervals for the different menstrual cycle phases. Bottom graphs show average concentration and size profiles for supernatant, regardless of the phase of the cycle, and PBS. "n" denotes number of replicates for each comparison. Figures show particle concentrations for each EVs population and phase of the menstrual cycle.

Regarding size distribution, MVs generally extended from approx. 150 to 550 nm, with a modal size of 267.2 nm, and 83.49% of total particles were >200 nm. EXOs extended from approx. 70 to 400 nm, with a modal size of 155.5 nm, and 62.68% of total particles were <200 nm. Larger particles may correspond to EXO aggregates (**Figure 20**). If examining size profiles by phase, while EXO populations remained more constant, the presence of a larger (600–700 nm), low-abundant subpopulation was reported in phase I for MVs, thus coinciding with menses period. As such, these larger particles may be released as a consequence of the degeneration process of the uterine lining. EVs concentrations were similar between both populations,

especially during the first phase of the cycle. Supernatant showed a low number of small-sized particles regardless of the phase of the cycle, and PBS, as the resuspension media, also showed little noise and thus was unlikely to bias EVs measurements (**Figure 20**). Overall, size profiles were similar to those obtained from single EF samples, again indicating overlap between MVs and EXOs populations.

Variation in EVs concentrations over the menstrual cycle was also analyzed for single EF samples (**Figure 21**).

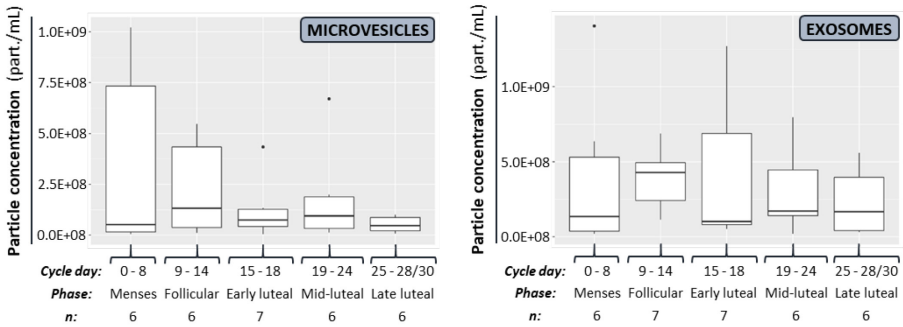

Figure 21. NTA analysis of EF EVs concentration variation throughout the menstrual cycle. Average MVs and EXOs concentration variation throughout the menstrual cycle phases. "n" denotes number of replicates for each comparison.

Neither MVs nor EXOs had a statistically significant difference in vesicle content throughout the menstrual cycle (P-value = 0.83 and 0.76, for MVs and EXOs, respectively), although a decreasing trend with progression of the cycle was apparent, at least for MVs (**Figure 21**). All in all, our results prompted us to postulate that neither MVs nor EXOs showed an appreciable variation in vesicles size pattern or concentration in human EF with the progression of the menstrual cycle. This is an important concept as not only the content but also the total amount of certain molecules may have an impact over the recipient embryo physiology and ability to implant. In fact, changes in EVs levels have been reported in pregnancy disorders

such as pre-eclampsia or preterm birth (1) and have been associated to implantation modulation along with the delivery of altered levels of molecules such as HLA-G (296). Finally, whether these results are a consequence of the nature of our samples or may change with a higher sample size, remains to be studied.

5.5 Endometrial fluid EVs DNA cargo. Influence of the moment of the cycle. Differences in cargo between receptive-stage EVs populations

After the initial description of the different EVs present within human EF, we moved forward into the analysis of their cargo in order to deepen in the mechanism of the mother to assist embryo implantation. We had previously described the role of EXOs for the transmission of miR-30d from the endometrial epithelium to the embryo, and its importance for both embryo implantation and fetal growth (19, 59, 60). In this context, we wondered whether EVs could be a vehicle for the transmission of DNA as a molecule whose functional status remains beyond that of RNA at least into the trophoblast layer.

Previously to deepen in EF EVs DNA cargo, the influence of the menstrual cycle and specific loading depending on the EV type, we dedicated a set of samples to analyse the impact of two factors over sequencing results: *Factor 1*. free-floating DNA in biological fluids is sticky and is isolated along with EVs attached to their external wall (36). For this reason, we used two different combinations of DNases in parallel to a control untreated condition to verify the need of removing the external DNA to avoid bias in analysing EVs real content. *Factor 2*. EF samples are normally scanty with volumes ranging from 1 to 25 µL, in our experience. Therefore, DNA amount after extraction and concentration from EVs populations from single EF samples may be under the optimal input for Nextera XT library kit requirements. For this reason, we analysed whether reducing the starting amount of DNA could lead to altered sequencing output.

After digestion reaction and DNA quantitation, EXOs and ABs untreated conditions were chosen to create dilutions for library construction because they had DNA in excess (**Table 4**). In view of library results (**Figure 8**), 0.05 ng/µL ABs and EXOs control samples were chosen for sequencing to resemble the lower concentration threshold of DNaseI treated MVs (**Table 4**) and the Bioanalyzer profiles of both EXOs treated conditions (**Figure 8**). These would be compared with sequencing results for the samples at optimum concentration (0.2 ng/µL and 0.15 ng/µL for control ABs and EXOs, respectively, based on bioanalyzer profiles). Sequencing results showed a similar distribution of read density in terms of counts per million in the low DNA samples compared to the optimally concentrated ones, as it can be appreciated in violin and correlation plots, both for ABs and EXOs (**Figure 22**).

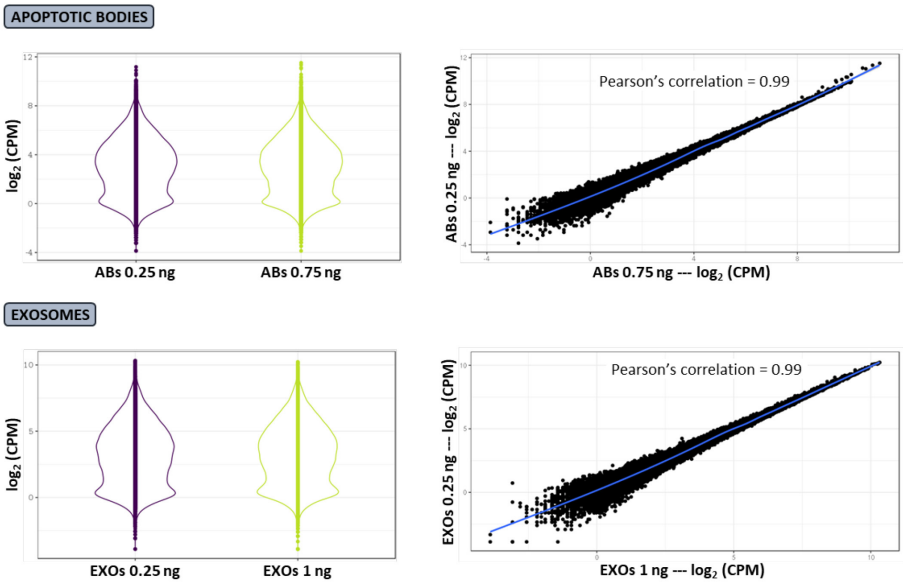

Figure 22. Sequencing impact of reducing DNA input for XT libraries construction. Similarity of DNA sequencing profiles between samples with reduced DNA input (0.25 ng) and samples with optimal starting DNA (0.75 ng and 1 ng for ABs and EXOs respectively) was checked for ABs and EXOs through violin and correlation plots, informing about reads distributions in terms of CPM. DNA amount for each sample is given in terms of total DNA.

These results showed that the sequencing profiles from samples with optimal and limiting DNA input for library construction were indistinguishable and so, it permitted the use of the samples under the ideal concentration for sequencing comparisons with those diluted to the recommended concentration in the DNase effect assay.

Subsequently, sequenced DNase treated and untreated ABs and EXOs samples were compared. Analysis were done both for coding gene sequences and TFBSs to check masking of these two genetic elements by external contaminating DNA (**Figure 23**).

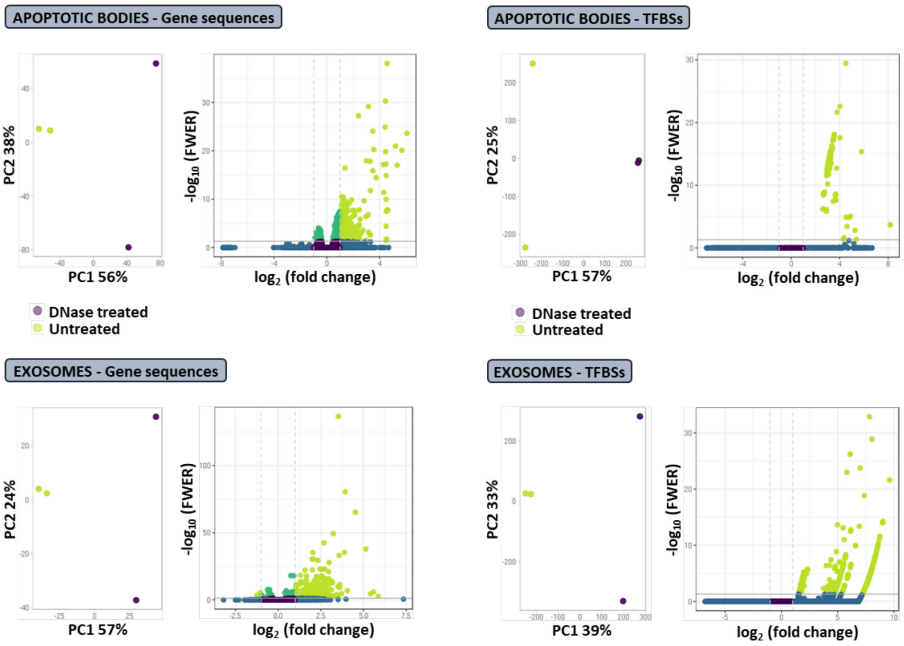

Figure 23. Effects of DNase treatment before DNA sequencing libraries construction. The need of DNase treatment was checked in ABs and EXOs for gene sequences and TFBSs. PCAs inform about samples grouping due to DNase treatment. Volcano plots show enrichment in sequences in DNase treated (right) vs untreated (left) EVs populations.

Principal component analysis showed a clear effect of DNase treatment in the four comparisons, being possible to observe a separation between treated and untreated samples explained in a high percentage by the principal component 1 (56% and 57% for ABs genes and TFBS, and 57% and 39% for EXOs genes and TFBSs, respectively). Volcano plots revealed abundant enrichment in coding and TFBSs sequences over whole genomic DNA for all the comparisons only after DNase treatment (**Figure 23**). These results indicated that external DNA contamination generates a great masking that blocks detection of EVs content over the whole samples, and thus evidenced that DNase treatment is mandatory for the study of specific EVs DNA cargo.

After defining and validating the experimental conditions, a first sequencing analysis was conducted to study those differences in EVs DNA content due to the moment of the menstrual cycle. For an initial approach, the EVs populations from phase II (n = 4) and phase IV (n = 4) EF samples were analysed in a way that the same EV type (i.e.: ABs, MVs and EXOs) was compared between phases (see **Figure 7**).

This analysis would allow to identify those differences in EVs DNA cargo specific to the moment of receptivity compared to the proliferative stage of the cycle. Both coding gene sequences, from the ENSEMBL database, and transcription factor binding sites (TFBSs) were checked in separate for specific enrichment (**Figures 24** and **25**). The interest on gene sequences lied in the possibility that these genetic elements may get to the embryo, at least to the trophectoderm, through EVs, where they could be expressed to increase the production of certain RNAs. TFBSs are sequences that serve as union hot-spots for transcription factors (TFs), proteins whose role is cis/trans regulation of DNA structure for gene expression modulation. They were studied for the possibility that once within the embryo may serve to bind TFs to promote the expression of certain genes or, contrarily, to sequestrate TFs to decrease gene expression. We hypothesized that DNA could reach the embryo nuclei where it could survive during certain time as a transcriptionally functional satellite element to support implantation.

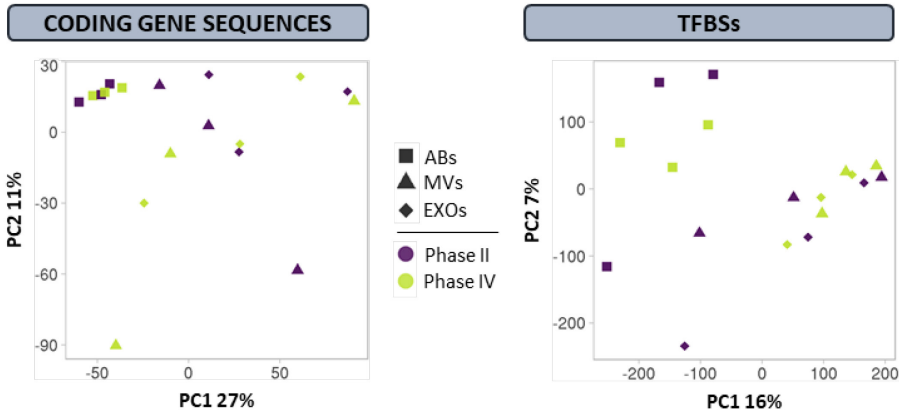

Figure 24. Analysis of differences in DNA cargo of endometrial fluid EVs due to the moment of the menstrual cycle. PCAs show clustering of phase IV (receptive stage) vs phase II (proliferative phase) EF EVs populations based on their DNA cargo.

An initial PCA analysis of all EF EVs did not show a differential clustering of EVs from phase II vs phase IV (**Figure 24**), thus suggesting that no big differences in EVs DNA content existed between vesicles secreted during the endometrial proliferative stage and the window of implantation neither for gene coding sequences nor for TFBSs. Subsequently, DNA cargo variation was analysed for each EV population (**Figure 25**). PCA clustering was neither observed for individual EVs populations. Nevertheless, a small set of gene sequences was discovered differentially secreted during both phases of the menstrual cycle in all three vesicles populations, while no phase specific TFBSs were found. The list of phase specific gene sequences along to their relative enrichment in the different EVs is offered in **Table 5**.

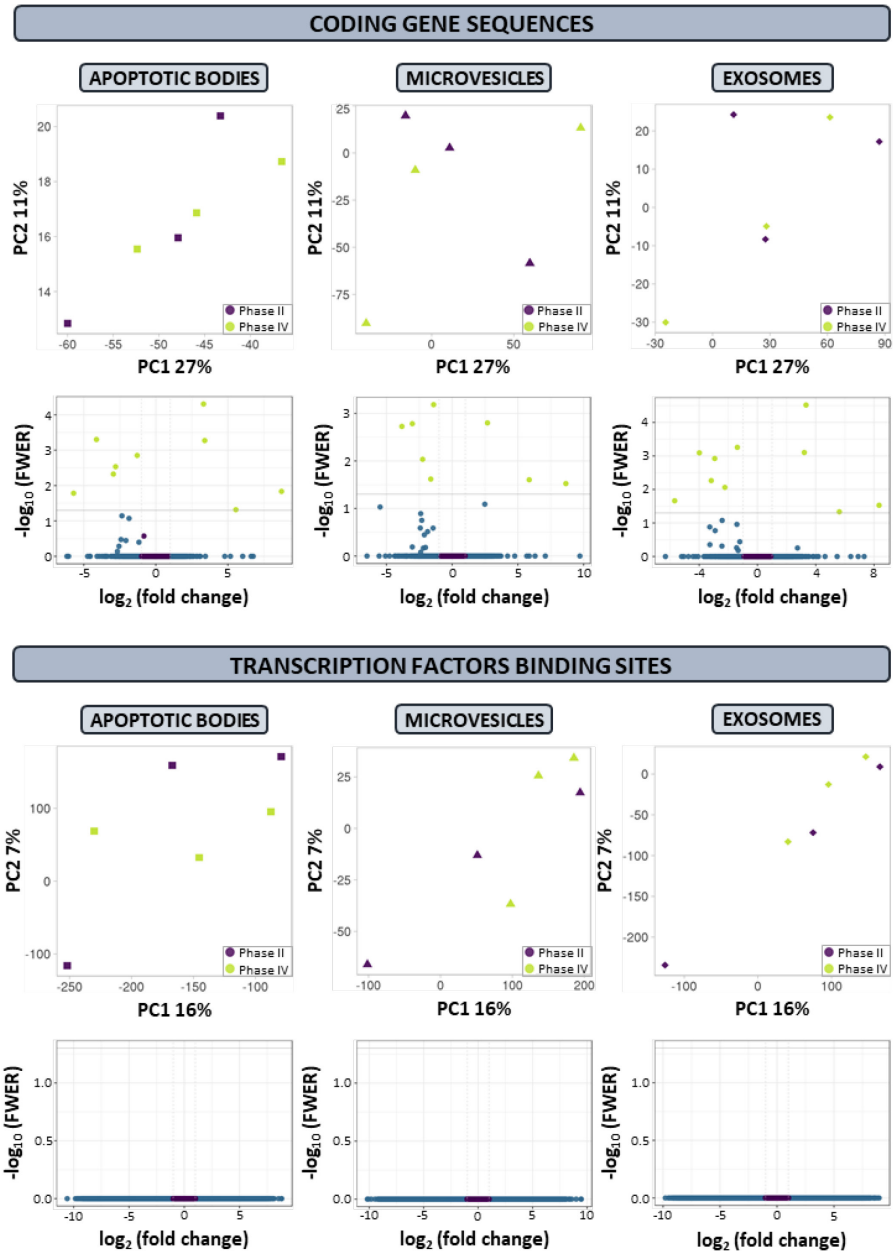

Figure 25. Analysis of differences in isolated EF EVs populations DNA cargo due to the moment of the menstrual cycle. PCAs show clustering of phase IV vs phase II EF EVs populations based on their DNA cargo. Volcano plots show enrichment in DNA regions in phase IV (left side of the plot) vs phase II EVs (right side of the plot). P-value < 0.05 and Fold-Change ≥ 2 (log2FC ≥ 1) were considered for enrichment.

Table 5. Gene sequences differentially enriched in EVs from phase II vs phase IV. Table offers relative enrichment between both phases. Positive FC values indicate enrichment in phase IV vesicles while negative FC values indicate enrichment in phase II.

Gene ID	ABs	MVs	EXOs	Chr	Gene type	Encoded product
	FC	FC	FC			
GSTT1	422.92	402.21	326.01	22	Protein coding	Glutathione S-transferase theta 1
LINC02851	46.97	58.21	49.20	9	lincRNA	Long intergenic non-protein coding RNA 2851
LRRC37A4P	9.93	6.44	10.08	17	Pseudogene	leucine rich repeat containing 37, member A4, pseudogene
ARL17B		-3.09		17	Protein coding	ADP-ribosylation factor-like 17B
NSFP1		-4.74	-4.70	17	Pseudogene	N-ethylmaleimide-sensitive factor pseudogene 1
BMS1P18	-7.70		-9.01	14	lincRNA	BMS1 pseudogene 18
NBPF14	-6.93	-8.16	-7.64	1	Protein coding	neuroblastoma breakpoint family, member 14
UGT2B17	-17.40	-14.15	-15.88	4	Protein coding	UDP glucuronosyltransferase 2 family, polypeptide B17
UGT2B29P	-52.27		-51.38	4	Pseudogene	UDP glucuronosyltransferase 2 family, polypeptide B29 pseudogene

Glutathione S-transferase theta 1 (*GSTT1*) gene was found between 326 and 423-fold enriched in EF EVs populations during the window of implantation compared to the same vesicles secreted during endometrial proliferative stage. *GSTT1* encodes for a cytosolic enzyme with important roles in detoxification of electrophilic compounds and reactive oxygen species (ROS) (90). Along with glutathione S-transferase mu 1 (*GSTM1*), several polymorphisms have been described for these genes, being their complete deletion (i.e: null phenotype) the most common with average 20% prevalence among Caucasians and 47% among Asians (297). Importantly, *GSTT1* and *GSTM1* null phenotypes have been associated to higher risk of pre-term labour along with higher incidence of markers of oxidative stress (91), to higher risk of suffering pre-eclampsia (92) and of early and repeated pregnancy loss (93). All in all, an enhanced transmission of *GSTT1* gene during the window of implantation to the embryo by EVs may constitute a maternal mechanism to promote overexpression of *GSTT1* encoded product to deal with ROS, whose

production by the embryo and surrounding tissues has been reported during its development, limiting the ability of the embryo to implant (94).

On the other hand, among coding gene sequences enriched in proliferative stage vesicles, *UGT2B17* was the most specific with fold change enrichment between 14.15 and 17.4 depending on the vesicle type. UGT2B17 belongs to a protein family with roles in the elimination of endogenous and exogenous steroid hormones, such as estrogens, from proliferating cells by glucuronidation. Interestingly, among other family members, *UGT2B17* expression has been observed to be independent of 17-β estradiol levels. There is still no evidence of *UGT2B17* roles during endometrial restorative stage, but it has been involved in endometrial cancer, where its depletion led to inhibition of cell growth and apoptosis of cancer cells (95). This finding may constitute a clue towards a possible involvement of *UGT2B17* in restoration of the endometrial lining, but this hypothesis requires further investigation that lies beyond the scope of this work. Interestingly, *ARL17B* gene sequence was found to be only enriched in proliferative stage MVs. This may be related to other members of the ADP ribosylation factor family, such as ARF6, with already attributed roles in the process of cell plasma membrane budding to form MVs (9), but no role in endometrial physiology has still been attributed to *ARL17B* gene.

All in all, we found differences in EVs DNA cargo dependent on the moment of the menstrual cycle that accounted for a reduced number of gene sequences, although at a high rate of enrichment, while no differences in TFBSs cargo was observed. The fact that no more varied profiles were observed between menstrual cycle phases may respond to the nature of the endometrial fluid samples included in this study. Complementarily, the sample size of this experiment may suppose a limitation so richer results may arise by increasing the sample population or by comparing the window of implantation to different menstrual cycle phases.

In this context, we focused our efforts in analysing differences in DNA cargo between receptive stage EF EVs populations, in an attempt to define a possible differential

role of the different vesicles towards the peri-implantation embryo. To do so, the number of EF samples dated in the middle of the receptive stage was increased (n = 10), and their EVs populations were isolated and sequenced. Only those EFs meeting the previously defined thresholds and passing quality controls for all the EVs (see section 4.1.14.2) were chosen for sequencing analysis.

A first comparison analysed differences in coding sequences from the ENSEMBL database (**Figure 26**).

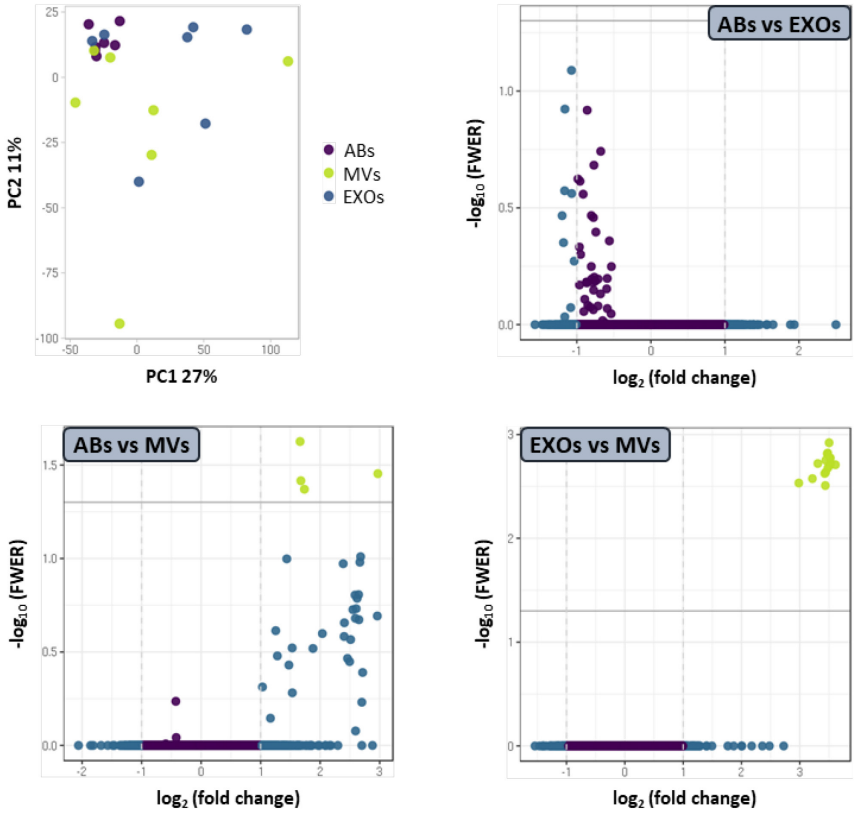

Figure 26. Sequencing comparisons for coding gene sequences cargo of the different phase IV EF EVs populations. PCAs show grouping of the different samples classified by EV type. Volcano plots show enrichment in coding gene sequences. Negative fold change values indicate enrichment in the first population compared (left side of the plot), while positive values indicate enrichment in the second (right side of the plot). P-value < 0.05 and Fold-Change ≥ 2 (log2FC ≥ 1) were considered to accept enrichment.

Principal component analysis of the three vesicles populations showed ABs as the less variable and most differentiated population while MVs and EXOs showed a more dispersed and overlapping distribution. Nevertheless, the different paired comparisons revealed MVs as the only fraction with significantly enriched sequences as shown in volcano plots in terms of FWER ($\alpha < 0.05$) and fold-change over 2, while no significant differences where appreciated between ABs and EXOs population (**Figure 26**). Compared to ABs, MVs showed a great enrichment in a mitochondrial pseudogene from chromosome 1 classified as a lncRNA (*MTND2P28*) and in 3 other protein coding genes in different genomic loci (i.e.: Homo sapiens *CCDC177*, *GAS1* and *MESDC1*). In contrast, a huge enrichment in the 13 known mitochondrial genes was observed when comparing to EXOs. Specifically, MVs showed an average fold change enrichment of 11.12 ± 0.53 in these genomic loci. All of them code for protein subunits that constitute the different complexes of the electron transport chain (96, 97). Additionally, MVs where shown to be enriched in 2 pseudogenes (*MTND2P28* and *MTATP6P1*) and a long intergenic non-coding RNA (*RP5-857K21.4*) from the same region of chromosome 1 (Chr1:536816-659930) (**Table 6**). These results demonstrated for the first time that the endometrium secretes mtDNA into EVs to the endometrial fluid, what might result into a mechanism to increase mtDNA copy number into embryo mitochondria. This finding constitutes a clue towards a possible role of the mother in the regulation of embryo bioenergetics at the peri-implantation moment, to promote mitochondrial oxidative phosphorylation (OXPHOS) activity. In this environment, the coordinated transmission of *GSTT1* could serve to mitigate a likely increase in ROS resulting from an increase in OXPHOS activity.

Table 6. Coding gene sequences differentially enriched in MVs against the rest of populations. MVs enriched sequences are associated to their fold-change, genomic location, type of gene and, when applicable, encoded product.

CODING GENES ENRICHED IN MICROVESICLES					
Comparison	**Gene ID**	**FC**	**Chr**	**Gene type**	**Encoded product**
Exosomes	*MT-ATP8*	12.22	MT	Protein coding	ATP synthase 8
	MT-ND2	11.51			NADH dehydrogenase 2
	MTND2P28	11.49	1	Pseudogene	MT-ND2 pseudogene 28
	MT-CO2	11.47	MT	Protein coding	Cytochrome C oxidase II
	MT-CYB	11.42			Cytochrome B
	MT-ND3	11.34			NADH dehydrogenase 3
	MT-ND6	11.16			NADH dehydrogenase 6
	MT-CO3	11.16			Cytochrome c oxidase III
	MT-ND5	11.08			NADH dehydrogenase 5
	MT-ND4	10.89			NADH dehydrogenase 4
	MT-ND1	10.88			NADH dehydrogenase 1
	MT-ATP6	10.83			ATP synthase 6
	MT-CO1	10.76			Cytochrome c oxidase I
	MT-ND4L	9.91			NADH dehydrogenase 4L
	MTATP6P1	9.29	1	Pseudogene	ATP synthase 6 pseudogene 1
	RP5-857K21.4	7.91		lincRNA	
Apoptotic bodies	*MTND2P28*	7.83	1	Pseudogene	MT-ND2 pseudogene 28
	CCDC177	3.33	14		Homo sapiens CCDC177, mRNA.
	GAS1	3.19	9	Protein coding	Growth arrest-specific 1
	MESDC1	3.17	15		Mesoderm development candidate 1

In a second comparison, TFBSs were checked for specific enrichment. PCA for these genomic loci showed a higher sample dispersion when comparing the three populations at a time. In this case, ABs showed greater intrasample dispersion while MVs samples presented with a more similar pattern although still overlapping with EXOs samples. Volcano plots showed a wide variety and huge enrichment of TFBSs in MVs when compared to the other populations, and specially to EXOs, while no significant differences were observed between ABs and EXOs (**Figure 27**).

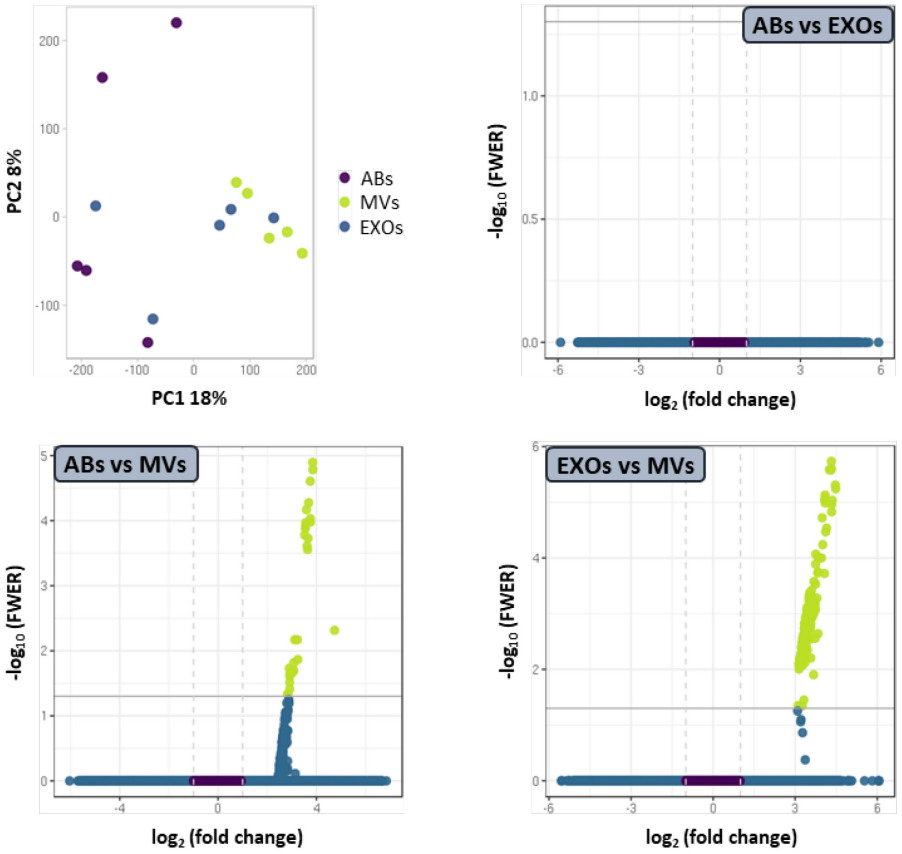

Figure 27. Sequencing comparisons for TFBSs cargo of the different phase IV EF EVs populations. PCA shows grouping of the different samples classified by EV type. Volcano plots show enrichment in TFBSs. Negative fold change values indicate enrichment in the first population compared (left side of the plot), while positive values indicate enrichment in the second (right side of the plot). P-value < 0.05 and Fold-Change ≥ 2 (log2FC ≥ 1) were considered to accept enrichment.

MVs showed enrichment in 28 genomic loci compared to ABs and 192 compared to EXOs. Most of the TFBSs were mapped through the whole length of the mitochondrial genome (**Table 7**). The rest mapped to discrete regions of chromosomes 1 (specific of MVs vs EXOs comparison), 9 (specific of MVs vs ABs comparison) and 17. Particularly, those located in chromosomes 1 (Chr1:565345-

569516, coinciding with the region highlighted in the previous comparison) and 17 (Chr17:22020703-22020811) mapped near or overlapping loci containing nuclear copies of mitochondrial genes and pseudogenes. TFBSs mapping to the chromosome 9 were only composed by 1 event from the ABs vs MVs comparison (**Figure 28**). These events were classified by the TF binding the different TFBSs to facilitate interpretation of results by linking TFBSs to known functionalities (**Table 7** and **8**). The list of TFs and associated genomic events and chromosomic locations are shown in **Table 7**.

Table 7. TFBSs differentially enriched in MVs against the rest of populations. TFBSs were classified by the TF binding them. For each TF, table informs about the chromosomic location and events (hits) of the associated TFBSs throughout the genome for each comparison.

TFBSs ENRICHED IN MICROVESICLES									
TF	vs EXOs		vs ABs		TF	vs EXOs		vs ABs	
	Chr	Hits	Chr	Hits		Chr	Hits	Chr	Hits
Egr1	MT, 17, 1	97	MT, 17	18	HNF4A	MT	2	MT	1
IRF4	MT, 1	11			MEF2A	MT	2		
Srf	MT	10	MT	1	MEF2C	MT	2		
PU1 (SPI1)	MT	8			SRebp1	MT	2		
Gabp	MT, 1	6	MT	4	USF1	MT	2		
ZBTB33	MT, 17	6			Yy1	MT	2		
CTCFL	MT	5			Cfos	MT	1		
E2F4	MT	5			CTCF	MT	1		
Tr4	MT	4	9	1	E2F6	MT	1		
Cjun	MT	3			ETS1	MT	1		
FOXA2	MT	3	MT	2	Gata2	MT	1		
Jund	MT	3			Max	MT	1		
Nrf1	MT, 1	3			Pax5	MT	1		
BHLHE40	MT	2			SP1	MT	1	MT	1
FOSL2	MT	2			SRebp2	MT	1		
FOXA1	MT	2			Tcf12	MT	1		

Figure 28. Genomic locations of the TFBSs enriched in MVs for the comparisons MVs vs ABs and MVs vs EXOs, showed per chromosome. In the whole chromosome view (top view), the red area indicates the chromosomal region were the MVs-enriched TFBSs were mapped for each comparison. In the bottom view, the middle bar expands and indicates the exact portion of the chromosome, in base pairs (bp), within which the different TFBSs mapped, while the specific region where each TFBS mapped is depicted as an orange area edged in gray in the bottom image.

A great enrichment in these TFBSs was observed in the comparisons of MVs with the other populations, with fold changes oscillating between 7.1 and 26.7 in the comparison with ABs, and between 8.61 and 22.35 in the comparison with EXOs. The enrichment distribution of TFBSs classified by TF is shown in **Figure 29**.

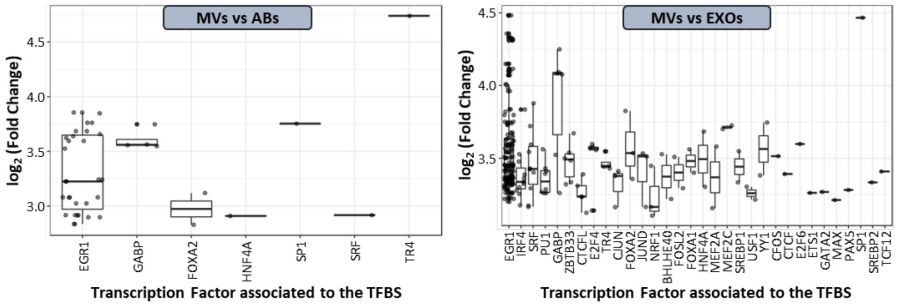

Figure 29. Fold change enrichment of TFBSs in the comparisons of MVs with ABs and EXOs populations. TFBSs were classified by their associated TF and enrichments are shown as box-plots distributions for the fold change of each TFBSs.

Some of these TFs (i.e.: SRF, GABP, E2F4, TR4, FOXA2, FOXA1, CTCF, GATA2 and PAX5) have been involved in in-utero embryonic development, gametogenesis and cell-matrix adhesion (**Table 8**).

Serum Response Factor (SRF) is a transcription factor that binds to the serum response element (SRE) in the promoter region of some target genes. It controls expression of genes that regulate cytoskeleton during development, morphogenesis, cell migration and, importantly, smooth and skeletal muscle development. SRF has been reported to interact with olfactomedin 2 (OLFM2) to promote smooth muscle differentiation by regulating promoters activity at the nuclear level (298). SRF controls the expression of muscle related genes by recruiting a variety of protein intermediates, including members of the myocardin family and, along with myocardin-related transcription factors, controls skeletal muscle growth and maturation from early embryo development (299).

GA Binding Protein (GABP) is a TF constituted by three subunits (α, β1 and β2), also known as Nuclear Respiratory Factor 2 (NRF2). It is involved in activation of cytochrome oxidase expression and nuclear control of mitochondrial function and biogenesis (100, 101).

Testicular Receptor 4 (TR4), also known as Nuclear Receptor Subfamily 2 Group C member 2 (NR2C2), is a ligand-activated TF that belongs to the nuclear hormone receptor family. It is induced by oxidative stress via FOXO3 activation and plays a role in protecting cells from oxidative stress (99) and damage induced by ionizing radiation (111, 300). Plays fundamental roles in early embryonic and postnatal development (301). Together with TR2 (NR2C1) represses embryonic and fetal globin transcription including that of GATA1, thus affecting and regulating erythroid differentiation (302). It is also important for other functions such as cerebellum development (303). Similarly, Paired Box 5 (PAX5) along with other PAX transcriptional factor have been involved in the development of different brain areas and of the cerebellum (304, 305).

CCCTC-Binding Factor (CTCF) is a transcriptional regulator with 11 highly conserved zinc finger domains that can bind different DNA target sequences and proteins. Importantly, CTCF plays an essential role in oocyte and preimplantation embryo development by activating or repressing transcription. Its depletion causes meiotic defects in the oocyte and delayed second mitotic division after fertilization, with subsequent alterations in zygotic genome activation, abnormal nuclear morphology and culminates in apoptotic death prior to the blastocyst stage. Importantly, it was described as a maternal-effect gene, i.e.: a gene whose products, RNA or protein, are produced or deposited in the oocyte or are present in the fertilized egg or embryo before expression of zygotic genome is initiated (306). As such, preimplantation embryos alterations caused by CTCF would be produced by persistent transcriptional defects rather than chromosomal defects (307). A posterior study reasserted the nature of CTCF as a maternal-effect gene and its importance over oocyte and early embryo development, thus highlighting the maternal influence over CTCF phenotype (308). Finally, also the function of CTCF in H19 gene imprinting should be highlighted. CTCF binds to the maternally hypomethylated differentially methylated domain (DMD) and protects this locus from de novo methylation during oocyte growth, what is required for normal preimplantation development (309).

Finally, GATA Binding Protein 2 (GATA2) has been attributed roles in the acquisition of a receptive endometrial status. Initially, GATA2 was observed to be expressed in endometrial epithelium during the pre-implantation stage, in this way coinciding with the expression pattern of progesterone receptor (PR) (310). Posteriorly, a cooperative effect between GATA2 and PR was observed where both TFs bind the same promoter region. In this way, GATA2 promotes both PR expression as well as downstream genes along with PR. Uterine specific *Gata2* knock-out mice were proven to be infertile showing embryo implantation failures (311).

Table 8. TFs associated to the TFBSs enriched in EF MVs with involvement in embryo development.

Main functions in embryo development.

TF	Associated functions during embryo development	References
SRF	- Regulation of cytoskeleton, morphogenesis, cell migration. - Pivotal for smooth and skeletal muscle development.	(298, 299)
GABP (NRF2)	- Activation of cytochrome oxidase expression. - Modulation of mitochondrial function and biogenesis.	(100, 101)
TR4 (NR2C2)	- Protection against oxidative stress and damage induced by ionizing radiation. - Modulation of erythroid differentiation through the repression of TFs such as GATA1. - Cerebellum development.	(99, 111, 300-303)
PAX5	- Brain and cerebellum development.	(304, 305)
CTCF	- Important regulator of transcription in oocyte and early embryo. - Maternal epigenetic influence (maternal effect gene). - Maternal imprinting (H19 gene).	(307-309)
GATA2	- Acquisition of a receptive endometrial status (cooperative action along the progesterone receptor).	(310, 311)

All in all, the analysis of TFBSs returned a message where a possible regulation of the embryo by the mother may arise from the transfer of mitochondrial genetic material. In this case, the functional role of TFBSs may be vectorized through the sequestration of TFs once within the embryo, this possibly having an effect in triggering enhanced activation or, contrarily, repressing those genes regulated by each TF. Importantly, although most TFBSs originated from mitochondrial genome, the associated TFs exert their function at the nuclear level so EVs TFBSs role, if any, may constitute a link between the nuclear and mitochondrial shared genetic control of mitochondrial

physiology. This is a fundamental concept of the endosymbiotic theory which includes the reorganization and mixing of nuclear and mitochondrial genomes over evolution. Interestingly, studies on the field indicate that original proteobacteria and archaea proposed as the first endosymbionts that gave rise to mitochondria, such as the recently described Asgard archaea, already had vesicular trafficking machinery (98). This supports the hypothesis of a mitochondrial and nuclear genomes cross-communication, with involvement at both the structural and functional level.

TRF4, one of the TFs that might be regulated by MVs TFBSs content, becomes interesting for its involvement in protection against oxidative stress (99). This is in line with the previously described transmission by EVs of *GSTT1* gene also during the window of implantation and may be part of a maternal mechanism to deal with ROS produced during early embryo development (90, 94). Also of interest is the transmission of TFBSs that may impact mitochondrial biogenesis and ATP synthesis potential through the regulation of GABP activity (100, 101), which further were the second group of TBFSs with higher fold enrichment (**Figure 29**). The rest of highlighted TFs, prompt maternal mitochondrial TFBSs as possible regulators of embryo specialized tissues development (**Table 8**). Our results showed that both mitochondrial genes for ATP synthesis machinery and mtDNA derived TFBSs were enriched in MVs, although at different relative levels when compared to the other vesicles. Altogether, these results strengthen the hypothesis of a maternal regulation by EVs of embryo energetic potential and mitochondrial physiology while keeping controlled the generation of ROS, regulating gene expression at both nuclear and mitochondrial level.

Back to DNA sequencing analysis, a bioinformatic pipeline (*peak calling analysis*) was designed for a final comparison that allowed to analyse discrete (regular peaks) and large (broad peaks) genomic regions that were differentially represented, in terms of reads, in the different EVs DNA cargo. These regions would appear represented as "peaks" of different area, depending on the number of reads mapped within the

region, over a genomic baseline. It permitted the exploration of regions of the genome not included in previous feature databases but, due to the design of the study, comparisons were only possible for peaks present in at least two populations.

A first comparison was done for those peaks found in the three EVs populations. PCAs for both regular and broad peaks showed great intersample dispersion where ABs and EXOs samples were overlapping. In both cases, MVs was the only population that showed a slightly differential clustering although, over a PC that explained 75% and 77% of the total variability for regular and broad peaks, respectively. This was reflected in volcano plots, which evidenced only one peak enriched in MVs when compared to EXOs both for regular and broad peaks analysis (**Figure 30**). This corresponded to the aforementioned region Chr1:569076-569756, which is found in a genomic locus flanked with mitochondrial pseudogenes and overlapping two of them, *RP5-857K21.4* and *MTATP6P1* (**Figure 31**).

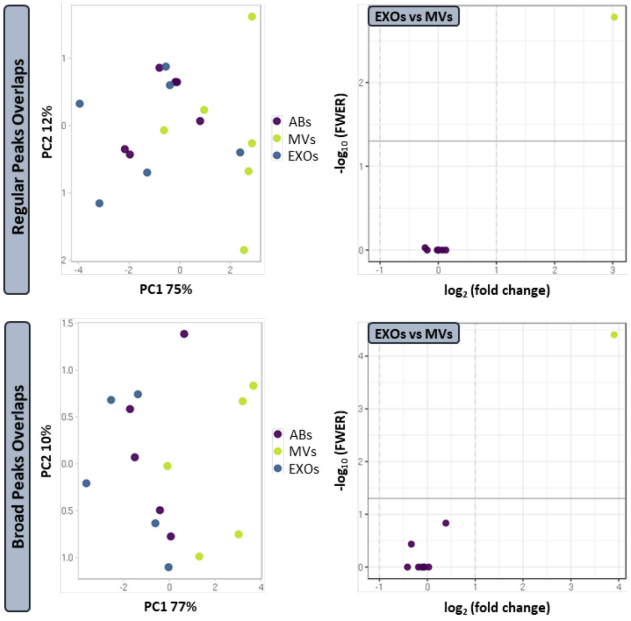

Figure 30. EF EVs DNA peak calling analysis. Differentially enriched peaks among all EVs populations. PCAs show clustering of EVs populations according to their regular and broad peaks profiles. Volcano plots show genomic regions differentially enriched. Negative fold change values indicate enrichment in the first population compared (left side of the plot), while positive values indicate enrichment in the second (right side of the plot). P-value < 0.05 and Fold-Change ≥ 2 (log2FC ≥ 1) were considered to accept enrichment.

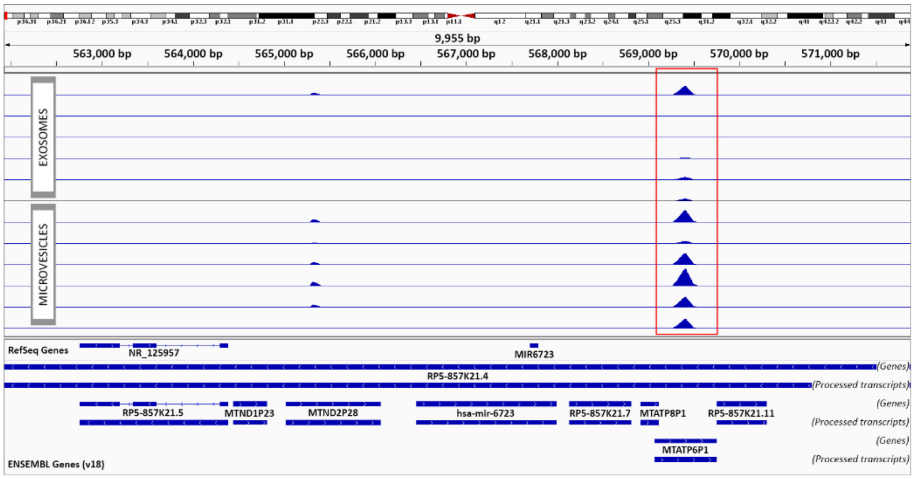

Figure 31. EF EVs DNA peak calling analysis - Chromosome 1 peaks. Integrative Genomic Viewer (IGV) view of the genomic region differentially enriched in MVs in Chr1: 569,076 - 569,756.

Analysis of broad peaks rendered further results for large regions shared between MVs and EXOs. Although PCA showed partial overlap between samples corresponding to both populations, volcano plot revealed two regions specifically enriched in MVs (**Figure 32**), which corresponded to the previous chromosome 1 region (**Figure 31**) and to the whole mitochondrial genome (**Figure 33**).

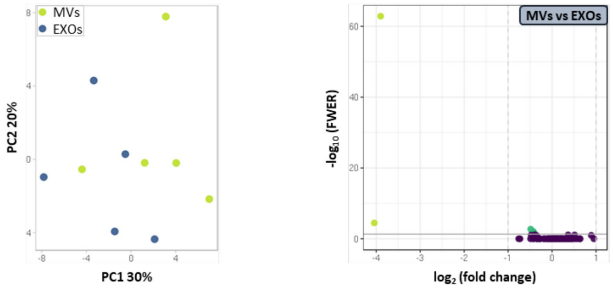

Figure 32. EF EVs DNA peak calling analysis. Differentially enriched broad peaks in MVs and EXOs. PCA show clustering of EVs populations according to their broad peaks profiles. Volcano plots show genomic regions differentially enriched. Negative fold change values indicate enrichment in the first population compared (left side of the plot), while positive values indicate enrichment in the second (right side of the plot). P-value < 0.05 and Fold-Change ≥ 2 (log2FC ≥ 1) were considered to accept enrichment.

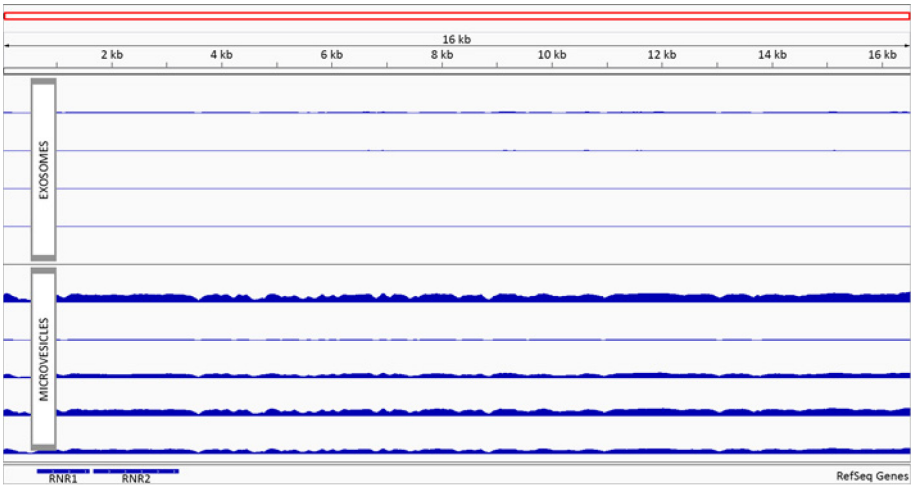

Figure 33. EF EVs DNA peak calling analysis - Mitochondrial chromosome peaks. Integrative Genomic Viewer (IGV) view of the genomic regions differentially enriched in MVs in mitochondrial chromosome.

Summing up, EVs DNA peak calling analysis did not provide any additional result but served to reassert MVs specific cargo in sequences from the mitochondrial genome and from the region Chr1:569076-569756 (**Figure 31**). Transmission of sequences from this chromosome 1 region was observed for all the analysis, including that of genes and TFBSs. Nevertheless, as previously mentioned, this region is rich in mitochondrial pseudogenes which accumulated in chromosome 1 through human evolution, likely by means of transposons. As such, a hypothesis may be stated that sequences mapping to this region was unspecific and a consequence of high similarity with mitochondrial genome. The analysis here conducted do not allow to ascertain this question but, rather, it more strongly points at the sorting of mitochondrial material into human EF MVs.

A gathering of our observations on DNA in human EF EVs reveals that this molecule was present in EVs cargo but also was adhered to EVs external surface possibly arising from apoptotic or necrotic endometrial cells as well as from serum transudates. DNase treatment was necessary to get rid of extravesicular DNA and

uncover EVs DNA cargo (**Figure 23**). Analysis of EVs specific cargo during the window of implantation, compared to the proliferative stage, revealed a great enrichment in *GSTT1* gene sequence (**Table 5**), which encodes for an enzyme with roles in detoxification of ROS and whose depletion has been associated with pregnancy complications related with oxidative stress. In case of conception, the stimuli of *GSTT1* gene transmission would arrive in a moment when the embryo is generating ROS that compromise its implantation ability. We then deepened in the differential cargo of EVs during the receptivity moment. The analysis of coding gene sequences revealed an over 11-fold MVs enrichment in the complete mitochondrial gene set for electron transport chain elements (**Table 6**). This was followed by the observation that MVs were also greatly enriched in TFBSs mainly coming from the mitochondrial genome (**Table 7**, **Figure 29**). Importantly, some of the enriched TFBSs where associated to TFs with known roles in mitochondrial biogenesis and ATP synthesis regulation but also in the protection against oxidative stress and in the development of specialized cell linages during embryo development (**Table 8**). Importantly, whether TFBSs from (maternal) mitochondria may have an impact over nuclear transcriptional regulatory proteins is a line of research still to uncover and would shed light on the mitochondrial and nuclear genomes cross-regulation in mitochondrial physiology. Beyond any hypothesis, what this work showed is that vesicles produced by the mother into the receptive stage endometrial fluid were enriched in mitochondrial genetic material.

Analysis of the proportion of mtDNA vs nuclear DNA into human EF EVs revealed a trend towards an increase in the receptive stage vs the proliferative phase of the menstrual cycle, although this was not statistically significant. However, a significative increase was observed for this proportion in MVs compared to ABs and EXOs (p-values 0.034 and 0.016, respectively) regardless of the phase of the cycle (**Figure 34**). In this context, it would be interesting to test a higher samples size to evaluate whether significant differences in mtDNA content are present between phases of the menstrual cycle, at least for MVs.

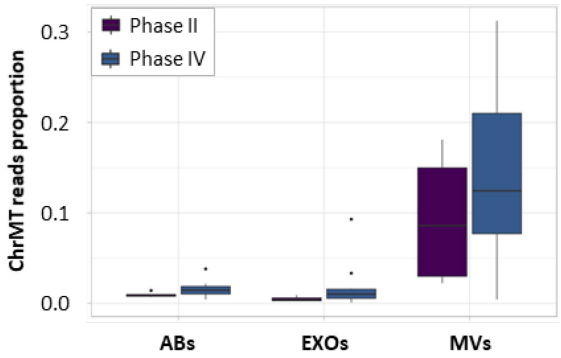

Figure 34. Proportion of mtDNA content in the different EVs from human EF in receptivity vs proliferative stage. Proportion of mtDNA was calculated as reads mapped in the nuclear genome / read mapped to the mitochondrial chromosome.

Summing up, DNA content of human EF EVs suggests a possible role of MVs in the transport of mitochondrial DNA to the embryo with possible implications in embryo mitochondria ATP producing ability and early development regulation while keeping production of ROS controlled.

5.6 DNA transfer from the mother to the pre-implantation embryo through EVs

The next step after EVs specific DNA content uncovering was to analyse whether these populations were biologically able to deliver and internalize their DNA cargo into an embryo in coculture. To do so, we used the Ishikawa cell line to produce EVs whose DNA was tagged with a synthetic molecule that allowed us to distinguish between embryo genomic DNA (stained in blue) and EVs-derived DNA (green) following its internalization by confocal microscopy. We chose this method because the synthetic molecule is included in the DNA sequence during cell replication, so it is reliably differentiated once within embryo cells without risk of contamination. In order to facilitate visualization of the embryo compartments, embryo membranes

and zona pellucida were stained with Wheat Germ Agglutinin (red stain). Both hatching and already hatched embryos were analysed to investigate DNA delivery.

Confocal imaging demonstrated that ABs were able to effectively transport DNA inside the embryo, both reaching the cytoplasm and to a lesser extent the cell nuclei, what can be appreciated by the colocalization of the blue signal from embryo nuclei and the green signal from EVs-DNA. A great amount of transmitted DNA was observed which tended to accumulate in large deposits in discrete zones of the embryo, mainly at the cytoplasmatic level (**Figure 35**, complete embryo in **Figure 39**).

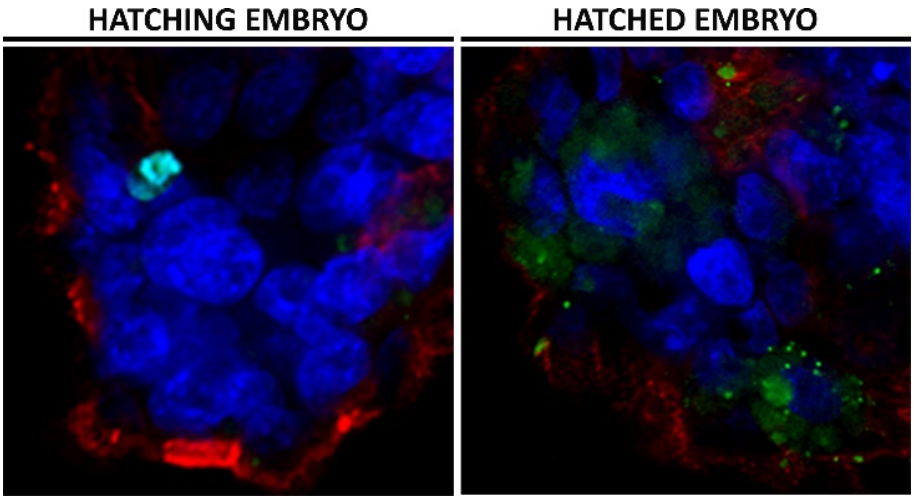

Figure 35. ABs DNA transfer into the murine embryo. Zoom detail of merged images.

MVs were also able to deliver DNA both into cells cytoplasm and nuclei. In this case, DNA transmission pattern into the embryo was observed as abundant spots widespread throughout the embryo, that tended to accumulate preferentially at the perinuclear level (**Figure 36**, complete embryo in **Figure 40**).

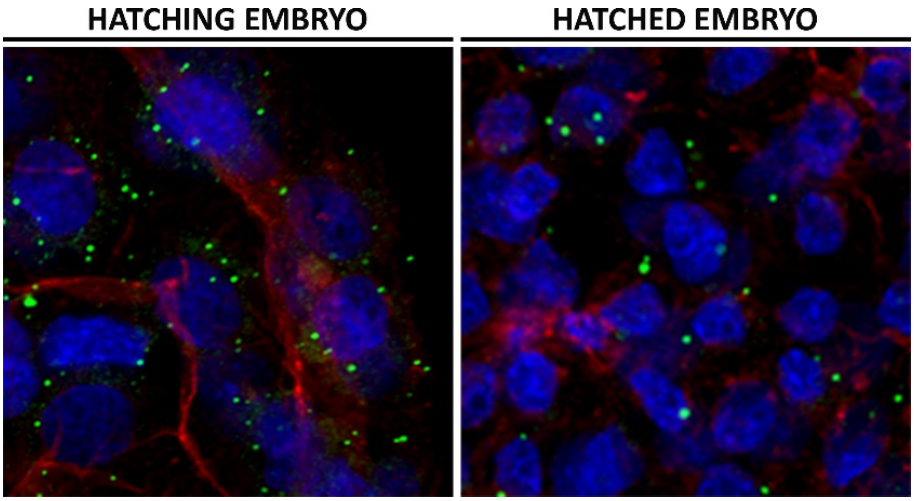

Figure 36. MVs DNA transfer into the murine embryo. Zoom detail of merged images.

Finally, EXOs were also observed to potentially convey DNA into the embryo although at a much lesser extent (**Figure 37**, complete embryo in **Figure 41**).

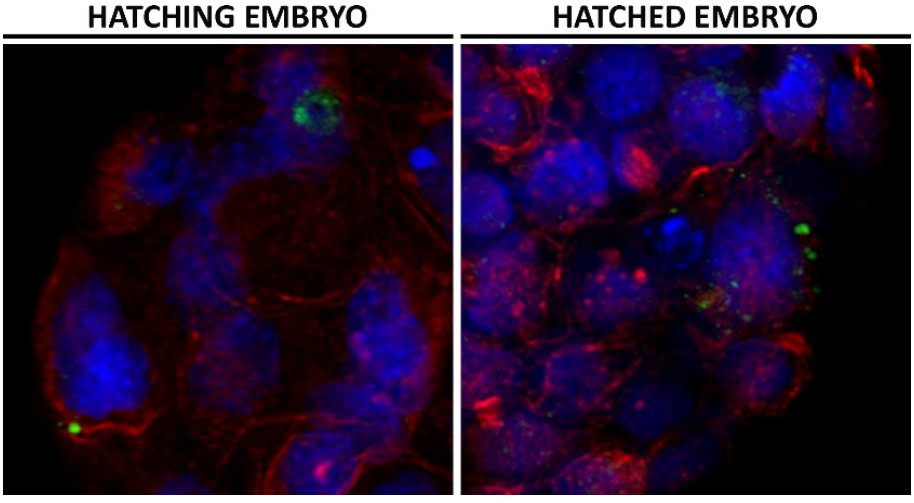

Figure 37. EXOs DNA transfer into the murine embryo. Zoom detail of merged images.

The negative control condition, consisting of embryos incubated with a combination of DNA-non-tagged EVs populations, did not show interferences in EVs-DNA fluorescence wavelength. Finally, the supernatant condition, containing mainly free DNA and potentially a residual amount of small-sized EVs, neither showed an appreciable signal for EdU-tagged-DNA (**Figure 38**).

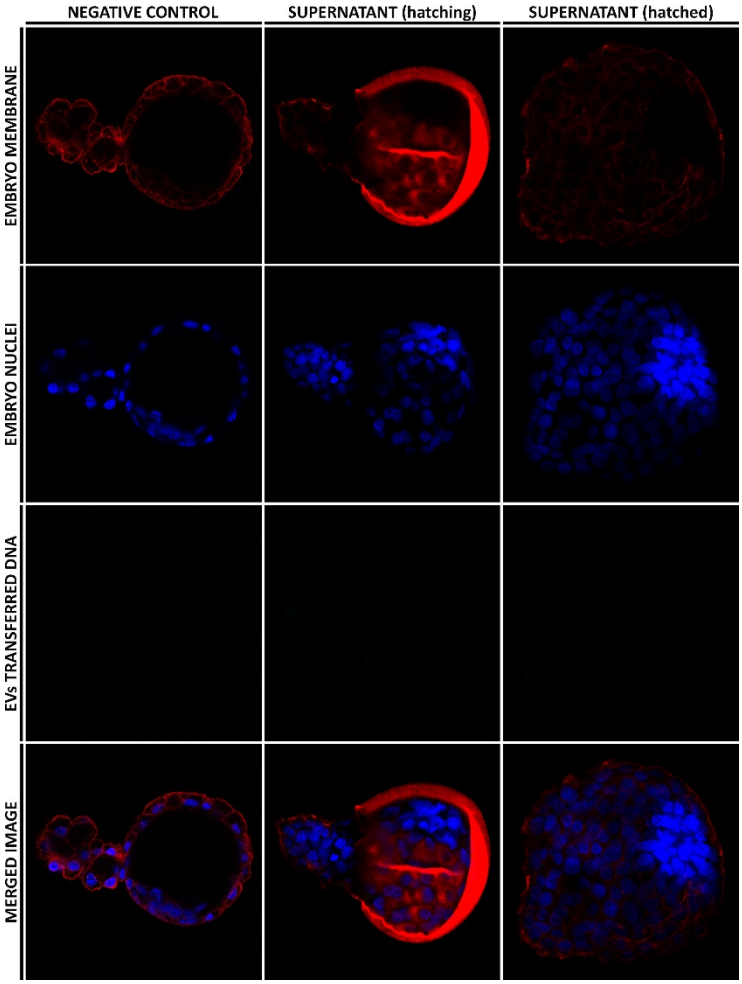

Figure 38. EVs DNA transfer and integration into the murine embryo in coculture. Negative control and supernatant. Confocal images show hatching and already hatched embryos after coculture with EdU-non-tagged EVs (negative control) and with the supernatant from EdU-tagged EVs isolation. Embryo membranes are visualized in red, embryo nuclei in blue and EdU-tagged transferred DNA in green.

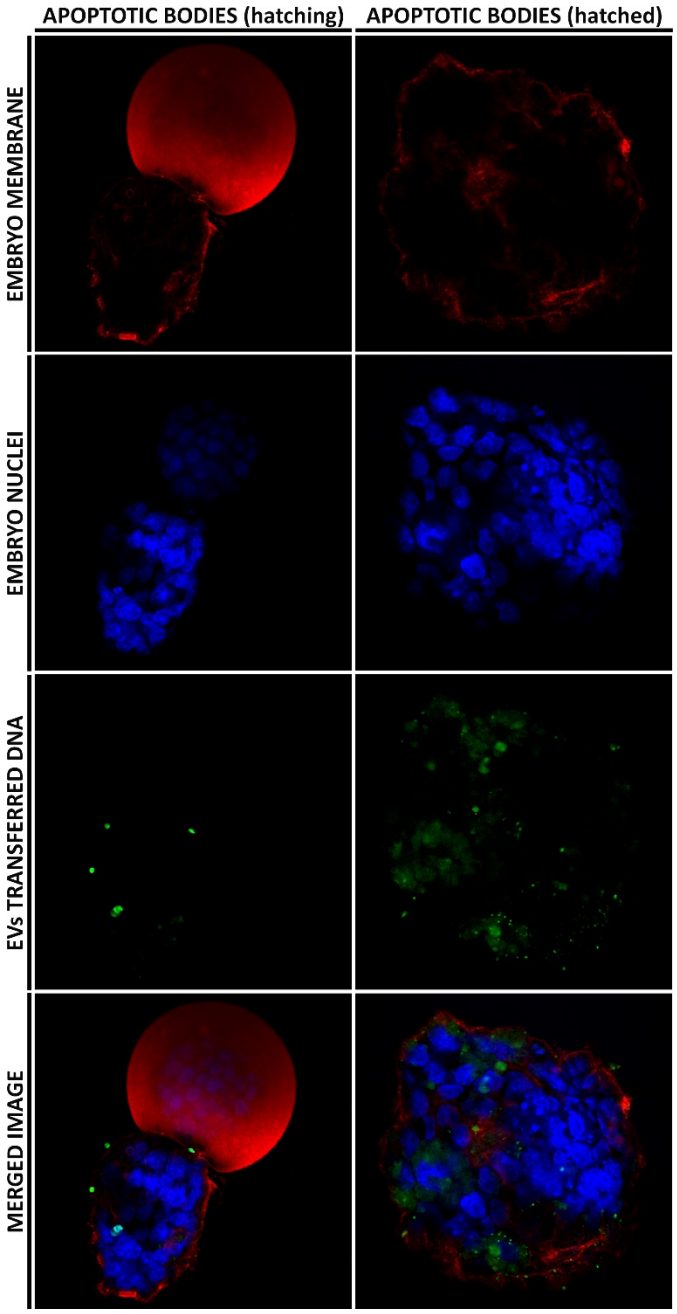

Figure 39. EVs DNA transfer and integration into the murine embryo in coculture. Apoptotic bodies. Confocal images show hatching and already hatched embryos after coculture with EdU-tagged ABs. Embryo membranes are visualized in red, embryo nuclei in blue and EdU-tagged transferred DNA in green.

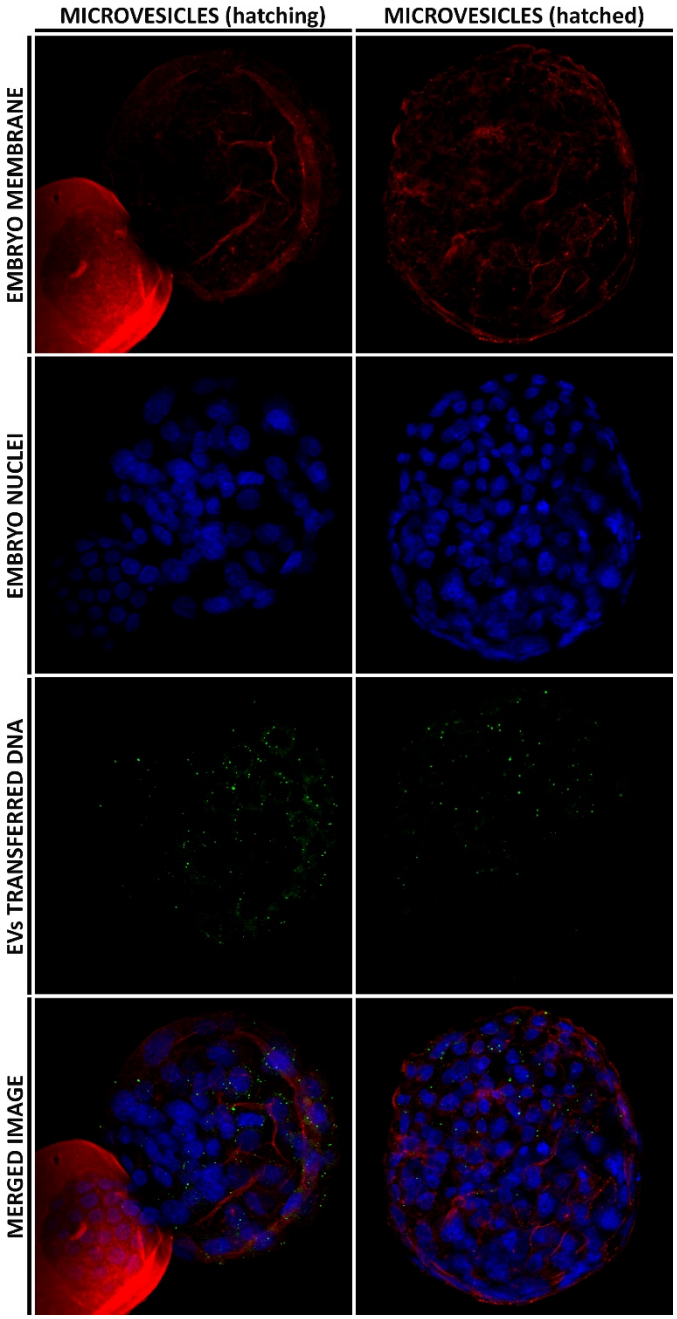

Figure 40. EVs DNA transfer and integration into the murine embryo in coculture. Microvesicles. Confocal images show hatching and already hatched embryos after coculture with EdU-tagged MVs. Embryo membranes are visualized in red, embryo nuclei in blue and EdU-tagged transferred DNA in green.

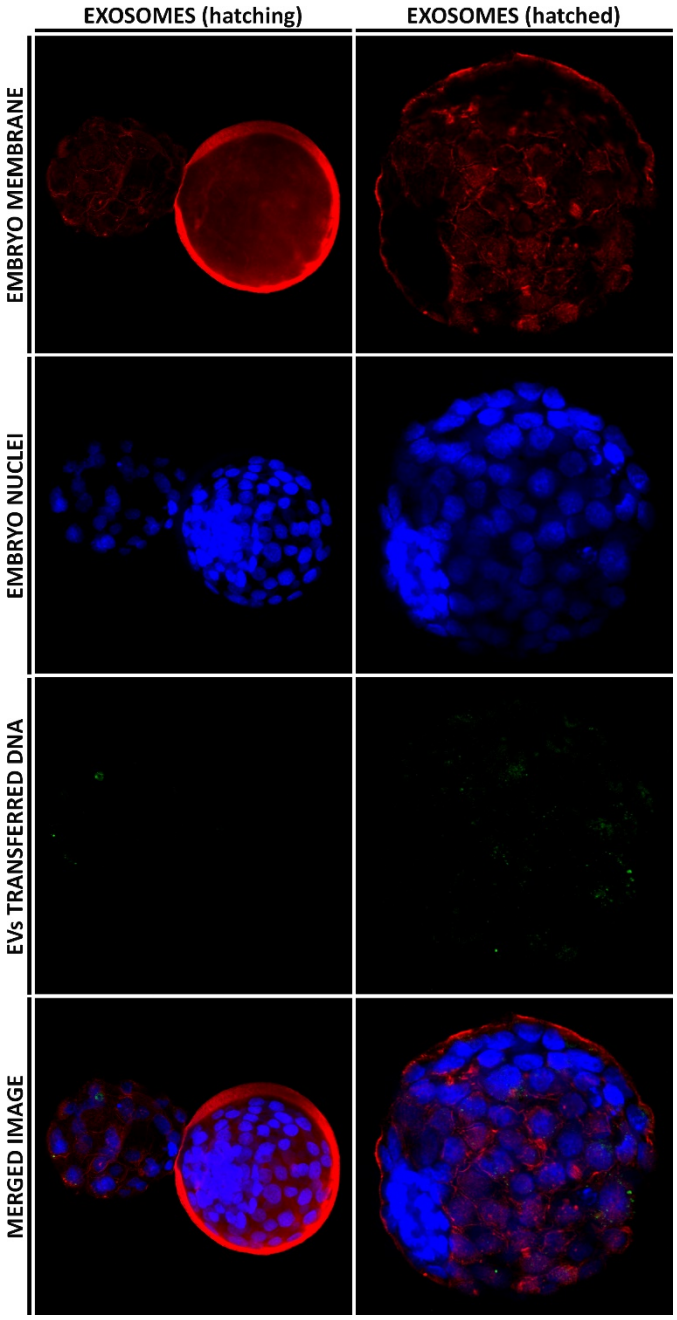

Figure 41. EVs DNA transfer and integration into the murine embryo in coculture. Exosomes. Confocal images show hatching and already hatched embryos after coculture with EdU-tagged EXOs. Embryo membranes are visualized in red, embryo nuclei in blue and EdU-tagged transferred DNA in green.

All in all, analysis of DNA transmission into the embryo revealed potential transporting ability at least for ABs and MVs. In these cases, interesting differences in the pattern of transference and internalization were observed. ABs seemed to deliver large amounts of genetic material that occupied large but discrete regions of the embryo (**Figures 35** and **39**). In contrast, MVs transmission pattern appeared to be widespread throughout the embryo in small spots which, further, were mainly perinuclear (**Figures 36** and **40**). Linking with previous experiments, whether these small spots were somehow interacting with mitochondria, remains to be established. In both, ABs and MVs, although EVs DNA signal was appreciated in the nuclei of cells, this was mainly found in the cytoplasm. EXOs also showed potential for DNA transfer but this was quite reduced compared to the other EVs (**Figures 37** and **41**). Taking together these results and considering their small size, it would not be disparate to reconsider real usefulness of EXOs in DNA transmission, at least for embryo-maternal crosstalk physiological roles. In contrast, they have been largely described to be a key vehicle for the transmission of small RNAs, such as miRNAs (19, 56). Importantly, regardless of the EVs population, EVs-DNA was only seen to reach and be internalized by the embryo in zona pellucida-free regions, where the intermembrane contact is possible, at least into the trophoblast layer. Finally, the absence of epithelial endometrial cells derived DNA signal in the embryos co-incubated with the residual supernatant from EdU-tagged EVs isolation process, prompted the idea that the transport of DNA from the mother to the embryo at the endometrial level may be mainly carried out by EVs and not by DNA in its free form (**Figure 38**).

Z-stack/orthogonal projection images were constructed to further demonstrate EVs DNA internalization for ABs (**Figure 42**), MVs (**Figure 43**) and EXOs (**Figure 44**).

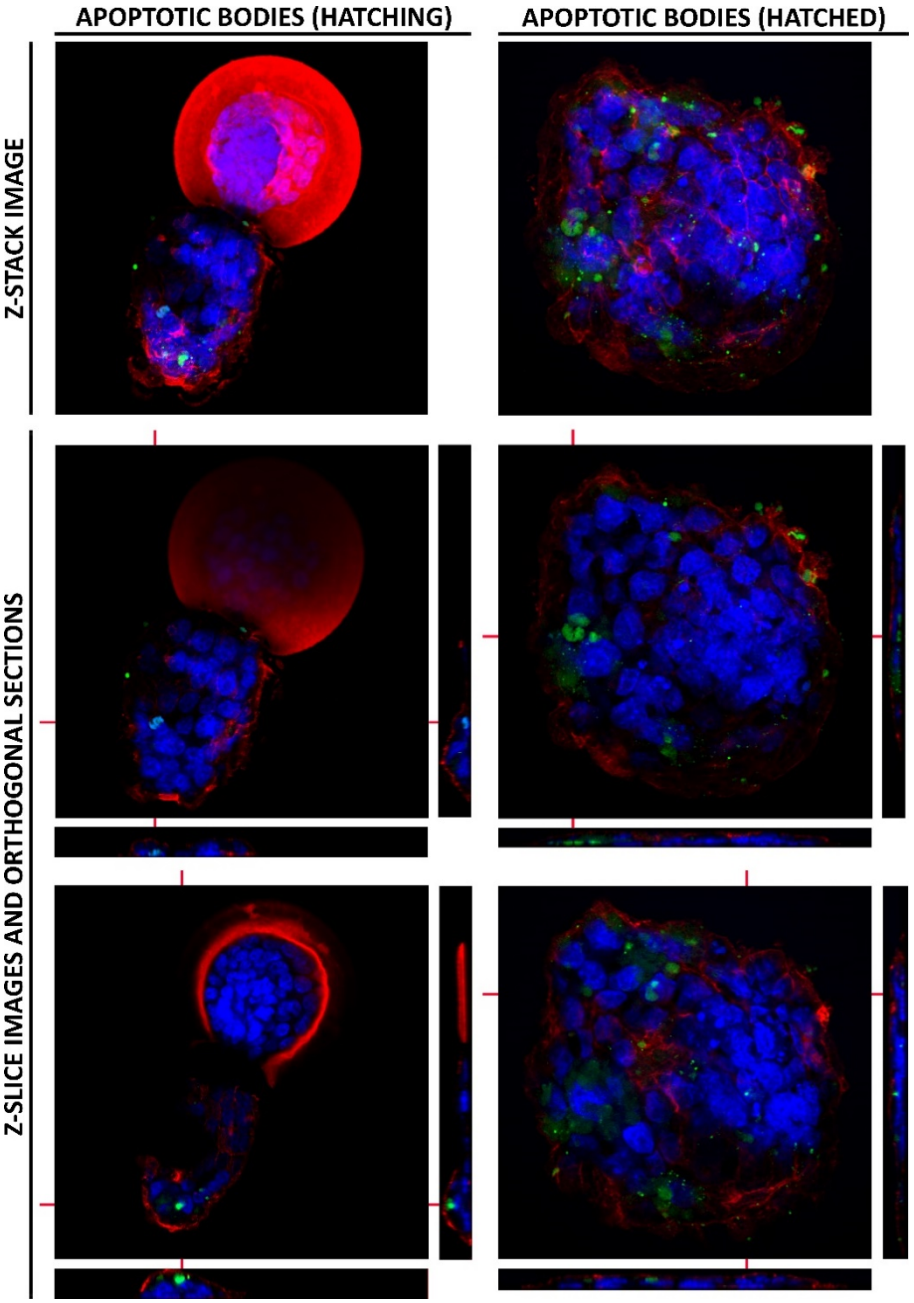

Figure 42. ABs DNA transfer into the murine embryo. Z-stack/orthogonal sections. Images show hatching / hatched embryos after coculture with EdU-tagged ABs. Embryo membranes are visualized in red, embryo nuclei in blue and EdU-tagged transferred DNA in green.

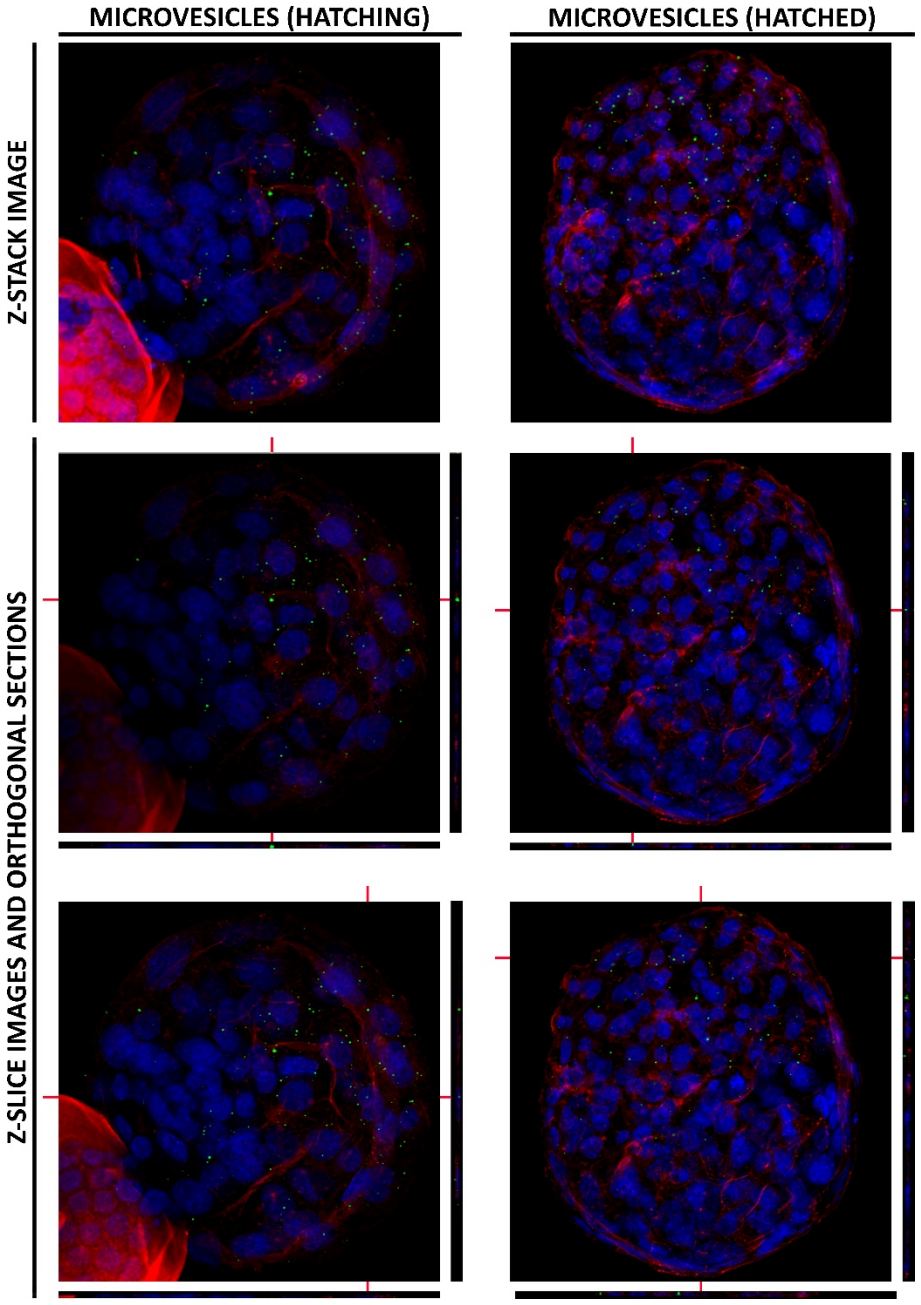

Figure 43. MVs DNA transfer into the murine embryo. Z-stack/orthogonal sections. Images show hatching / hatched embryos after coculture with EdU-tagged MVs. Embryo membranes are visualized in red, embryo nuclei in blue and EdU-tagged transferred DNA in green.

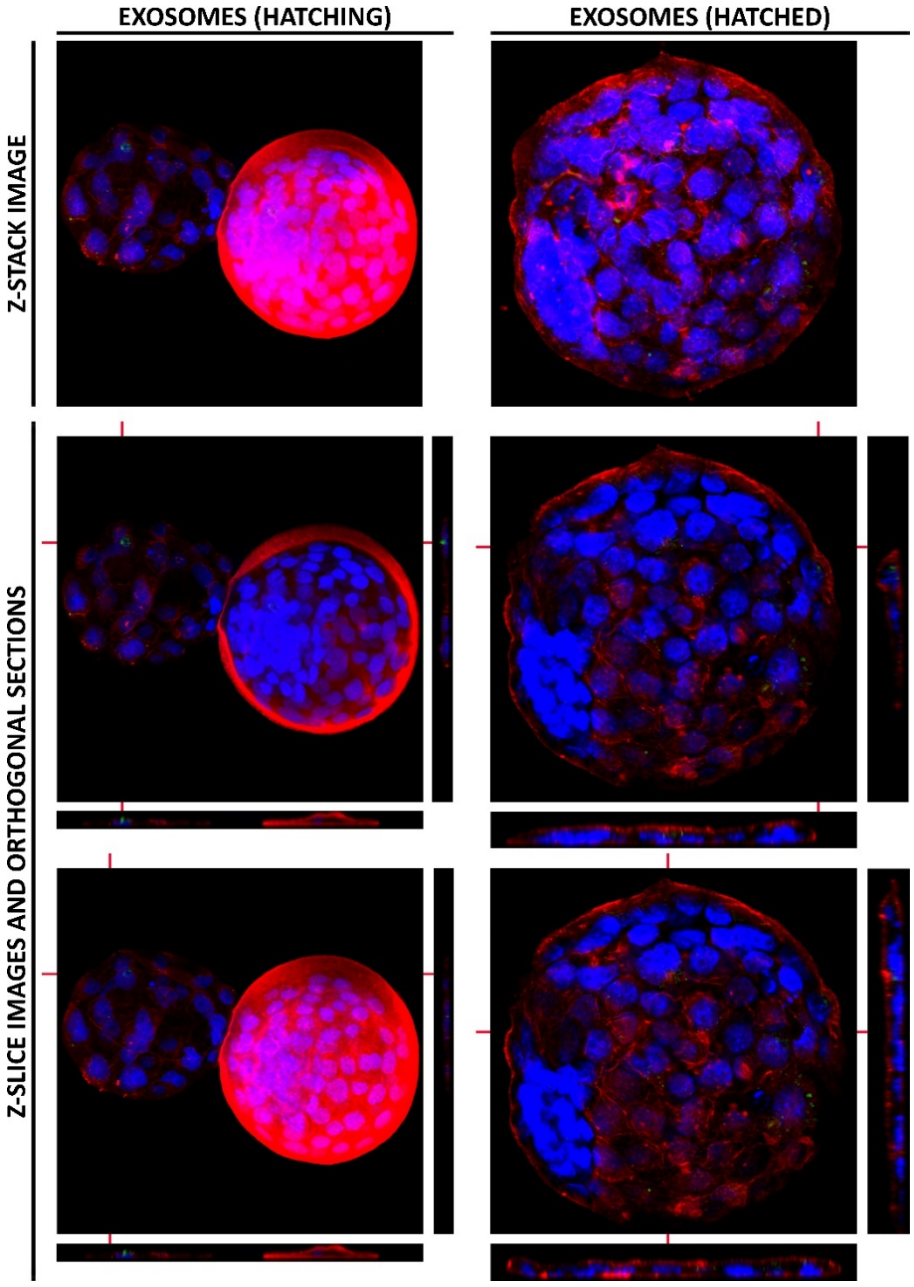

Figure 44. EXOs DNA transfer into the murine embryo. Z-stack/orthogonal sections. Images show hatching / hatched embryos after coculture with EdU-tagged EXOs. Embryo membranes are visualized in red, embryo nuclei in blue and EdU-tagged transferred DNA in green.

5.7 Potential functional role of EF EVs cargo in embryo bioenergetics

DNA sequencing results pointed at EF EVs as carriers of genetic material with potential involvement in pre-implantation embryo development, and specially to MVs as important carriers of mitochondrial DNA sequences. These were composed of gene sequences for the ATP generation machinery as well as of TFBSs sequences, some of whose associated TFs have been involved in pivotal functions for early embryo maturation. Importantly, these TFs (GABP) have also been involved in the regulation of mitochondrial function and biogenesis, while protecting cells from oxidative and ionizing stresses. These observations along with the ability of EVs to transport DNA into embryo cells motivated the idea of assessing a potential functional role of these EVs in embryo bioenergetics.

In order to test the hypothesis, a first experiment was set up to measure embryo differential ATP content after O/N co-incubation with the different EVs populations from human EF. Measurements showed statistical differences only in those embryos co-incubated with EXOs or a condition combining a third of each EF EV population (P value < 0.05) when compared to the control, composed of embryos incubated in absence of EF EVs. Particularly, reduction in ATP levels was observed especially when stimulating embryos with EXOs alone (P value < 0.001) while ATP levels were maintained for MVs and ABs when compared to the control. Reduction in ATP when co-incubating with the three EVs types in combination was observed to a lesser extent, thus suggesting that EXOs might be the EVs fraction negatively affecting ATP cargo. Measurement of PBS, the carrier media used to transport embryos to the plate for measurement, did not show luminescence signal that could bias embryo ATP measurements (**Figure 45**).

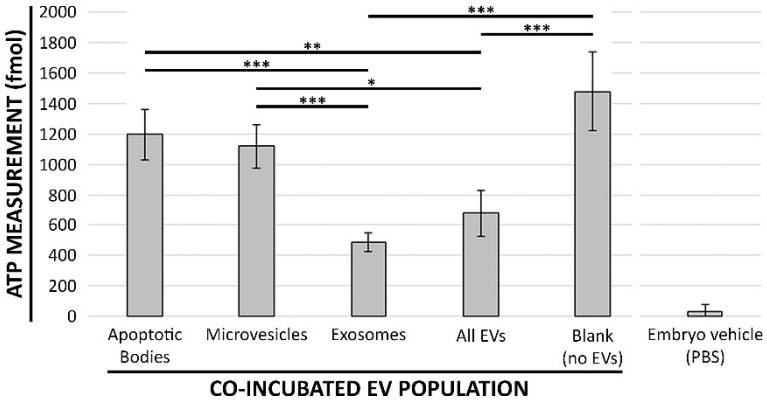

Figure 45. Murine embryos ATP content after O/N co-incubation with the different EVs populations from human EF. Embryos were O/N incubated with the different EF EVs populations in separate, with a combination of the three populations (all EVs) and with none of them (Blank). PBS, the media for transport of embryos to the measurement plate, was also analysed to check the background.

In order to further ascertain EVs impact on embryo energetics, a second experiment was set up to check mitochondrial status under the stimuli of the different EVs through the evaluation of mitochondrial membrane potential. To do so, JC-1, a molecule that migrates to cell regions of higher membrane potential (i.e.: active mitochondria), was used. When mitochondria are actively producing ATP, their membrane potential and thus difference with membrane potential of the rest of cell compartments are increased, establishing an influx of JC-1 from the extracellular environment to the cytosol and from this to the mitochondrial lumen, subsequently. When JC-1 reaches high intracompartment concentrations, aggregates and emits fluorescence in a different wavelength than the monomer. Valinomycin abrogates membrane potential established by potassium channels and so reverts this equilibrium reaction (formation of aggregates), being useful as control for JC-1 function. In line with previous results, confocal visualization of embryos stimulated with EXOs and the condition combining the three EVs types showed reduced levels of JC-1 both in its monomeric and aggregated forms when compared to the other

EVs populations and with the embryos incubated in absence of EVs. Oppositely, ABs and MVs stimuli maintained JC-1 signal to the level of unstimulated embryos for both forms (**Figure 46**).

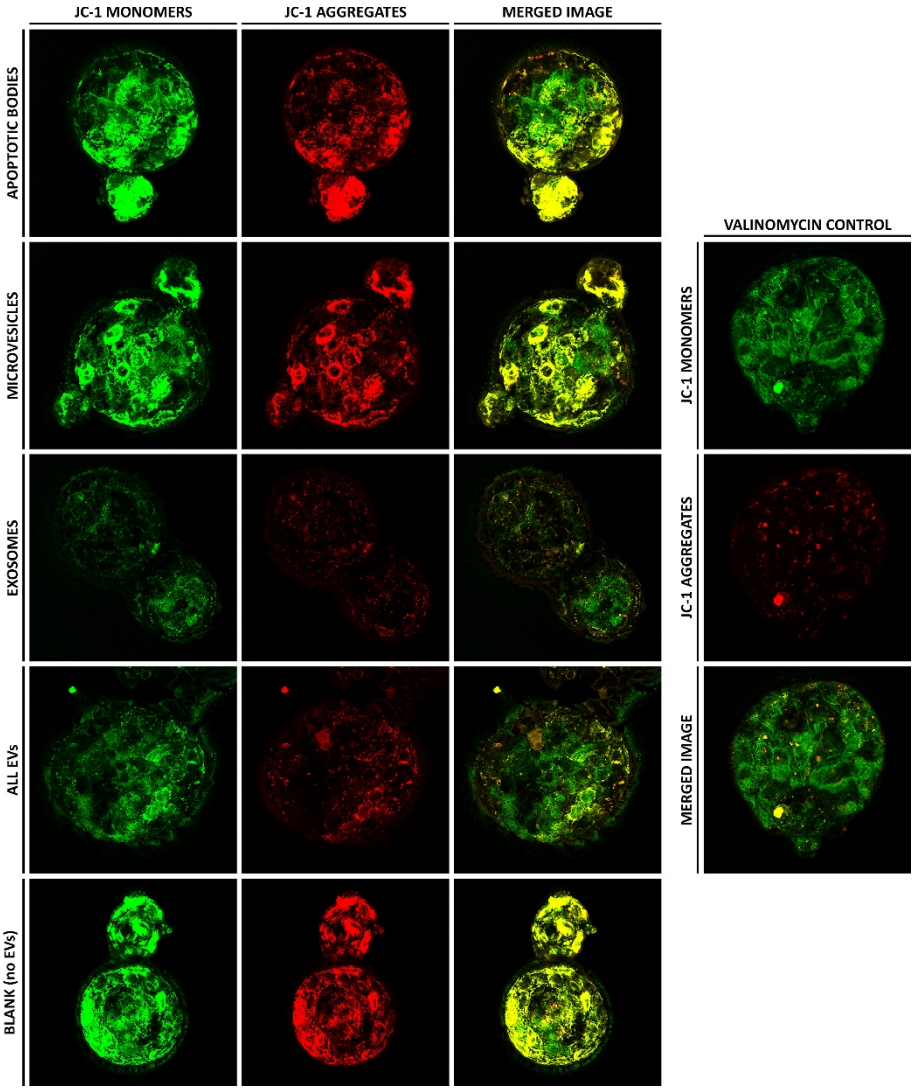

Figure 46. Confocal imaging of murine embryos stained with JC-1 after O/N co-incubation with endometrial-derived EVs. Embryos were O/N incubated with the different endometrial-derived EVs in separate, with a combination of the three populations (all EVs) and with none of them (Blank). Valinomycin treatment was introduced as a control of depolarized mitochondrial membranes.

Valinomycin condition was introduced as a control of depolarised and so non-ATP producing mitochondria for fluorescence thresholding. As expected, this condition showed reduced aggregates-to-monomers ratio, what can be directly related to the abrogation of mitochondrial membrane polarity (**Figure 46**).

If analysing overall signal for JC-1 aggregates, total amount of these structures for EXOs and all vesicles condition was reduced and closer to valinomycin control levels when compared with ABs, MVs and no-EVs conditions. Nevertheless, JC-1 monomers signal was also found decreased under EXOs-containing conditions and no differences were found in the JC-1 aggregates-to-monomers fluorescence ratio among the different conditions (0.74 ± 0.05, 0.66 ± 0.13, 0.74 ± 0.06, 0.69 ± 0.12, 0.64 ± 0.15 for ABs, MVs, EXOs, the condition combining all EVs and the EVs-free condition, respectively), but this was increased for all conditions when compared to the valinomycin control (0.35 ± 0.08). Also of note, green fluorescence of valinomycin treated embryos, which were originally derived from the embryo set incubated in absence of endometrial EVs, showed decreased green intensity compared to valinomycin non-treated embryos (Blank condition).

Reduction in green fluorescence after valinomycin treatment may be directly attributed to the membrane potential uncoupler action. This fact has been previously reported and is a consequence of loss of membrane polarity. Loss of mitochondrial membrane potential leads to the release of JC-1 monomers from mitochondria, displacing the aggregates-to-monomers equilibrium and provoking a sharp reduction of red fluorescence (aggregates) with the decrease of JC-1 concentration. Nevertheless, monomers are less sensitive to potential reduction and are released but not completely from depolarized mitochondria (312). Secondly, a reduction in mitochondrial ATP production activity is clearly defined by the JC-1 system, and validated by the valinomycin control, by the reduction in the ratio of aggregates-to-monomers. Although the total fluorescence intensity was reduced in embryos co-incubated with EXOs, including the condition with the three vesicles

types, this ratio was not changing, thus indicating no change in mitochondrial activity. Nevertheless, a third factor must be considered. JC-1 system has also been used as an indicator of total mitochondrial mass: reduced cell mitochondrial content is related to a decreased JC-1 monomer content, what consequently leads to reduced aggregates but does not directly affect the aggregates-to-monomers proportion (102-104). In this sense, what here is proposed is that reduction in ATP levels observed for embryos co-incubated in the presence of EXOs may be due to a reduction in mitochondrial content rather than to an affectation of their functionality, while MVs and ABs permit maintenance of mitochondrial levels if compared to embryos non stimulated with EVs. This may be in part supported by the enrichment in MVs of TFs such as GABP, which was previously attributed roles in mitochondrial biogenesis (100, 101) and/or by a direct negative effect of EXOs over total mitochondrial mass. Contrarily to valinomycin mechanism, EXOs reduce but not abrogate total JC-1 influx and mitochondrial aggregates-to-monomers ratio is maintained compared to the other EVs, what might explain why total ATP levels are reduced but not fully abrogated (**Figure 45**).

A limitation of previous measurement is that total number of cells may differ for each embryo although they were collected under the same conditions and cultured until the same embryonic day. Measurement of total monomers was done in the whole embryo and not by cell. For this reason, the analysis of a reduction in their concentration was done in a visual basis (see **Figure 46**). Contrarily, calculation of ratios between aggregates and monomers is not affected by embryo size and cell content, thus validating that changes in ATP levels previously observed (**Figure 45**) were not due to a loss of mitochondrial functionality.

Gathering results so far, we observed that: EVs from receptive stage EF were highly enriched in the gene sequence for *GSTT1*, with known important roles in ROS detoxification; Among receptive phase EVs, MVs were highly enriched in mtDNA including the different mitochondrially encoded genes for electron transport chain

elements and even at higher levels TFBSs some of which have been associated to nuclear TFs with roles in mitochondrial biogenesis, ATP synthesis regulation, protection against oxidative stress and development of embryo specialized cell linages; endometrial epithelium derived EVs were able to deliver their DNA content into, at least, embryo trophectoderm cells; finally, among receptive EF EVs, EXOs seemed to promote a decrease of embryo total ATP levels, likely through the reduction of mitochondrial number.

Linking with the current knowledge on embryo bioenergetics, it has been observed that mtDNA copy number per cell decreases from the oocyte, throughout embryo development until blastocyst stage, while the opposite trend was observed for embryo oxygen consumption rate. Importantly, oxygen consumption rise was correlated with an increase in mitochondrial activity, measured by cytochrome c oxidase activity, and this activity was mainly focused at the trophectoderm layer (105). Further, although still under controversy, several studies indicate that elevated embryo mtDNA copy number compared with the total amount of genomic DNA is an indicator of reduced implantation potential (107, 108). A step beyond, a growing core of research is now evolving to show an epigenetic regulatory role of mitochondria towards the pre-implantation embryo with short and long-term effects. Mitochondria have been asserted as signalling organelles that communicate with the nucleus but also with other cell organelles, triggering signalling cascades and having an impact from cell division to linage specification. Mitochondria are evolving as sensors that integrate cell metabolic signals and loss of mitochondrial function and integrity negatively affects post-implantation development (106).

Within this landscape, our hypothesis is that EF EVs may exert a cooperative role to regulate mitochondrial related functionalities. On the one hand, MVs appear to be transporters of mtDNA that may interact with both embryo mitochondria and nuclear TFs within the trophoblast layer to regulate mitochondria ATP producing activity while protecting cells from increasing oxygen consumption and subsequent

ROS production as the implantation moment approaches (94, 105). Further, TFBSs cargo from maternal mitochondria may leave an imprint for posterior development of different embryo specialized tissues (98, 106). On the other hand, the role of EXOs may be that of controlling mitochondrial population towards a reduction in total mitochondrial mass. This may establish a link with those embryos of good quality in assisted reproductive techniques, that lack EF EVs stimuli during in vitro culture, which show elevated mtDNA content and are associated with lower implantation rates (107, 108). Also, a hypothesis could be proposed were a reduction in total mitochondrial mass could respond to an increasing demand of quick energy as the embryo approaches the moment of implantation, favouring the satiation of this demand through glycolysis. This is not a disparate concept, and glycolysis has been observed to be chosen by the embryo to generate energy once it reaches the blastocyst stage and implantation moment approaches. Glycolysis is triggered to cope with embryo elevated energy needs and also with a reduction of oxygen concentration in the transition from fallopian tubes to the uterus, reducing the efficiency of tricarboxylic acids cycle to produce energy (Warburg effect). Further, at the blastocyst stage, pyruvate becomes the most important energy substrate (109, 110). A reduction in Krebs cycle efficiency and promotion of glycolysis, could also indicate that maintaining part of the mitochondrial population becomes unnecessary so its removal would favour the energetic efficiency of the embryo. Reduced-in-number mitochondria by the action of EXOs could be overloaded with electron transport chain elements thanks to the action of MVs at both mitochondrial and nuclear level. This could increase and concentrate the production of ATP which would be rapidly consumed by the increasing energetic needs of the peri-implantation embryo. Consequently, this would make necessary to strengthen the barriers against oxidative and ionizing stresses produced by an overactivated electron transport chain through the overexpression of intermediaries such as GSTT1 (90) or TR4 (99, 111).

All in all, these hypothesis are based on our aforementioned results and the evidence found in the bibliography about mitochondrial physiology in the pre-implantation embryo but, to date, there is no evidence of a direct role of EF EVs and their DNA content in such regulation. Further experiments should be conducted to evaluate the in vivo implications of EF EVs in mitochondrial physiology, but these results open a promising field of research that is still to be explored.

CONCLUSIONS

6. CONCLUSIONS

- Human endometrial fluid contains different populations of extracellular vesicles that can be classified as apoptotic bodies, microvesicles and exosomes. These populations show specific morphology, molecular markers signatures and size profiles.

- Microvesicles and exosomes concentration is similar within endometrial fluid, and no significant differences are appreciated neither in size nor in concentration throughout the menstrual cycle.

- The different types of endometrial extracellular vesicles carry DNA representing all chromosomes and mitochondrial DNA, showing specific enrichment in gene sequences and TFBSs depending on the phase of the menstrual cycle and the type of vesicle.

- The endometrial extracellular vesicles obtained during the phase of endometrial receptivity are enriched in *GSTT1* gene sequence, whose product has important roles in protection from oxidative stress. Furthermore, an enrichment in mitochondrial DNA was identified in MVs, including all mitochondrially encoded proteins for electron transport chain complexes, and TFBSs related to transcription factors involved in mitochondrial physiology and epigenetic modulation.

- Endometrial extracellular vesicles deliver their DNA content into the embryo, this internalizing the DNA in trophectoderm cells in zona pellucida free regions. This is especially evident for ABs and MVs, while EXOs DNA transmission is minor and transfer is not appreciable in the vesicles-free fraction, suggesting that DNA transmission is mainly carried out by EVs.

- EXOs isolated from receptive endometrium promote a reduction in ATP levels of cocultured embryos likely related with a reduction in total mitochondrial mass.

REFERENCES

7. REFERENCES

1. Simon C, Greening DW, Bolumar D, Balaguer N, Salamonsen LA, Vilella F. Extracellular Vesicles in Human Reproduction in Health and Disease. Endocr Rev. 2018;39(3):292-332.

2. Zaborowski MP, Balaj L, Breakefield XO, Lai CP. Extracellular Vesicles: Composition, Biological Relevance, and Methods of Study. Bioscience. 2015;65(8):783-97.

3. Colombo M, Raposo G, Thery C. Biogenesis, secretion, and intercellular interactions of exosomes and other extracellular vesicles. Annu Rev Cell Dev Biol. 2014;30:255-89.

4. S ELA, Mager I, Breakefield XO, Wood MJ. Extracellular vesicles: biology and emerging therapeutic opportunities. Nat Rev Drug Discov. 2013;12(5):347-57.

5. Atkin-Smith GK, Tixeira R, Paone S, Mathivanan S, Collins C, Liem M, et al. A novel mechanism of generating extracellular vesicles during apoptosis via a beads-on-a-string membrane structure. Nat Commun. 2015;6:7439.

6. Szatanek R, Baran J, Siedlar M, Baj-Krzyworzeka M. Isolation of extracellular vesicles: Determining the correct approach (Review). Int J Mol Med. 362015. p. 11-7.

7. Holmgren L, Szeles A, Rajnavolgyi E, Folkman J, Klein G, Ernberg I, et al. Horizontal transfer of DNA by the uptake of apoptotic bodies. Blood. 1999;93(11):3956-63.

8. Ehnfors J, Kost-Alimova M, Persson NL, Bergsmedh A, Castro J, Levchenko-Tegnebratt T, et al. Horizontal transfer of tumor DNA to endothelial cells in vivo. Cell Death Differ. 2009;16(5):749-57.

9. Muralidharan-Chari V, Clancy J, Plou C, Romao M, Chavrier P, Raposo G, et al. ARF6-regulated shedding of tumor cell-derived plasma membrane microvesicles. Curr Biol. 2009;19(22):1875-85.

10. Thery C, Ostrowski M, Segura E. Membrane vesicles as conveyors of immune responses. Nat Rev Immunol. 2009;9(8):581-93.

11. Clancy JW, Sedgwick A, Rosse C, Muralidharan-Chari V, Raposo G, Method M, et al. Regulated delivery of molecular cargo to invasive tumour-derived microvesicles. Nat Commun. 2015;6:6919.

12. Antonyak MA, Li B, Boroughs LK, Johnson JL, Druso JE, Bryant KL, et al. Cancer cell-derived microvesicles induce transformation by transferring tissue transglutaminase and fibronectin to recipient cells. Proc Natl Acad Sci U S A. 2011;108(12):4852-7.

13. Nomura S, Shimizu M. Clinical significance of procoagulant microparticles. J Intensive Care. 2015;3(1):2.

14. Tong M, Chamley LW. Placental extracellular vesicles and feto-maternal communication. Cold Spring Harb Perspect Med. 2015;5(3):a023028.

15. Desrochers LM, Bordeleau F, Reinhart-King CA, Cerione RA, Antonyak MA. Microvesicles provide a mechanism for intercellular communication by embryonic stem cells during embryo implantation. Nat Commun. 2016;7:11958.

16. Thery C, Zitvogel L, Amigorena S. Exosomes: composition, biogenesis and function. Nat Rev Immunol. 2. England2002. p. 569-79.

17. Yanez-Mo M, Siljander PR, Andreu Z, Zavec AB, Borras FE, Buzas EI, et al. Biological properties of extracellular vesicles and their physiological functions. J Extracell Vesicles. 2015;4:27066.

18. Greening DW, Nguyen HP, Elgass K, Simpson RJ, Salamonsen LA. Human Endometrial Exosomes Contain Hormone-Specific Cargo Modulating Trophoblast Adhesive Capacity: Insights into Endometrial-Embryo Interactions. Biol Reprod. 2016;94(2):38.

19. Vilella F, Moreno-Moya JM, Balaguer N, Grasso A, Herrero M, Martinez S, et al. Hsa-miR-30d, secreted by the human endometrium, is taken up by the pre-implantation embryo and might modify its transcriptome. Development. 2015;142(18):3210-21.

20. Saadeldin IM, Oh HJ, Lee BC. Embryonic-maternal cross-talk via exosomes: potential implications. Stem Cells Cloning. 2015;8:103-7.

21. Gyorgy B, Modos K, Pallinger E, Paloczi K, Pasztoi M, Misjak P, et al. Detection and isolation of cell-derived microparticles are compromised by protein complexes resulting from shared biophysical parameters. Blood. 2011;117(4):e39-48.

22. Boing AN, van der Pol E, Grootemaat AE, Coumans FA, Sturk A, Nieuwland R. Single-step isolation of extracellular vesicles by size-exclusion chromatography. J Extracell Vesicles. 2014;3.

23. Hong CS, Muller L, Boyiadzis M, Whiteside TL. Isolation and characterization of CD34+ blast-derived exosomes in acute myeloid leukemia. PLoS One. 2014;9(8):e103310.

24. Taylor DD, Zacharias W, Gercel-Taylor C. Exosome isolation for proteomic analyses and RNA profiling. Methods Mol Biol. 2011;728:235-46.

25. Raposo G, Nijman HW, Stoorvogel W, Liejendekker R, Harding CV, Melief CJ, et al. B lymphocytes secrete antigen-presenting vesicles. J Exp Med. 1996;183(3):1161-72.

26. Melo SA, Luecke LB, Kahlert C, Fernandez AF, Gammon ST, Kaye J, et al. Glypican-1 identifies cancer exosomes and detects early pancreatic cancer. Nature. 2015;523(7559):177-82.

27. Hoog JL, Lotvall J. Diversity of extracellular vesicles in human ejaculates revealed by cryo-electron microscopy. J Extracell Vesicles. 2015;4:28680.

28. Palmieri V. Dynamic light scattering for the characterization and counting of extracellular vesicles: a powerful noninvasive tool. Journal of Nanoparticle Research. 2014;16(9):2583.

29. Gardiner C, Ferreira YJ, Dragovic RA, Redman CW, Sargent IL. Extracellular vesicle sizing and enumeration by nanoparticle tracking analysis. J Extracell Vesicles. 2013;2.

30. van der Pol E, Coumans FA, Grootemaat AE, Gardiner C, Sargent IL, Harrison P, et al. Particle size distribution of exosomes and microvesicles determined by transmission electron microscopy, flow cytometry, nanoparticle tracking analysis, and resistive pulse sensing. J Thromb Haemost. 2014;12(7):1182-92.

31. Yoshioka Y, Kosaka N, Konishi Y, Ohta H, Okamoto H, Sonoda H, et al. Ultra-sensitive liquid biopsy of circulating extracellular vesicles using ExoScreen. Nat Commun. 2014;5:3591.

32. Shao H, Chung J, Balaj L, Charest A, Bigner DD, Carter BS, et al. Protein typing of circulating microvesicles allows real-time monitoring of glioblastoma therapy. Nat Med. 2012;18(12):1835-40.

33. Im H, Shao H, Weissleder R, Castro CM, Lee H. Nano-plasmonic exosome diagnostics. Expert Rev Mol Diagn. 2015;15(6):725-33.

34. Llorente A, Skotland T, Sylvanne T, Kauhanen D, Rog T, Orlowski A, et al. Molecular lipidomics of exosomes released by PC-3 prostate cancer cells. Biochim Biophys Acta. 2013;1831(7):1302-9.

35. Huang X, Yuan T, Tschannen M, Sun Z, Jacob H, Du M, et al. Characterization of human plasma-derived exosomal RNAs by deep sequencing. BMC Genomics. 2013;14:319.

36. Thakur BK, Zhang H, Becker A, Matei I, Huang Y, Costa-Silva B, et al. Double-stranded DNA in exosomes: a novel biomarker in cancer detection. Cell Res. 24. England2014. p. 766-9.

37. Lazaro-Ibanez E, Sanz-Garcia A, Visakorpi T, Escobedo-Lucea C, Siljander P, Ayuso-Sacido A, et al. Different gDNA content in the subpopulations of prostate cancer extracellular vesicles: apoptotic bodies, microvesicles, and exosomes. Prostate. 2014;74(14):1379-90.

38. Waldenstrom A, Genneback N, Hellman U, Ronquist G. Cardiomyocyte microvesicles contain DNA/RNA and convey biological messages to target cells. PLoS One. 2012;7(4):e34653.

39. Cai J, Han Y, Ren H, Chen C, He D, Zhou L, et al. Extracellular vesicle-mediated transfer of donor genomic DNA to recipient cells is a novel mechanism for genetic influence between cells. J Mol Cell Biol. 2013;5(4):227-38.

40. Vagner T, Spinelli C, Minciacchi VR, Balaj L, Zandian M, Conley A, et al. Large extracellular vesicles carry most of the tumour DNA circulating in prostate cancer patient plasma. J Extracell Vesicles. 2018;7(1):1505403.

41. Sansone P, Savini C, Kurelac I, Chang Q, Amato LB, Strillacci A, et al. Packaging and transfer of mitochondrial DNA via exosomes regulate escape from dormancy in hormonal therapy-resistant breast cancer. Proc Natl Acad Sci U S A. 2017;114(43):E9066-e75.

42. Kawamura Y, Yamamoto Y, Sato TA, Ochiya T. Extracellular vesicles as trans-genomic agents: Emerging roles in disease and evolution. Cancer Sci. 2017;108(5):824-30.

43. Franz C, Boing AN, Montag M, Strowitzki T, Markert UR, Mastenbroek S, et al. Extracellular vesicles in human follicular fluid do not promote coagulation. Reprod Biomed Online. 2016;33(5):652-5.

44. Al-Dossary AA, Bathala P, Caplan JL, Martin-DeLeon PA. Oviductosome-Sperm Membrane Interaction in Cargo Delivery: DETECTION OF FUSION AND UNDERLYING MOLECULAR PLAYERS USING THREE-DIMENSIONAL SUPER-RESOLUTION STRUCTURED ILLUMINATION MICROSCOPY (SR-SIM). J Biol Chem. 2015;290(29):17710-23.

45. Foster BP, Balassa T, Benen TD, Dominovic M, Elmadjian GK, Florova V, et al. Extracellular vesicles in blood, milk and body fluids of the female and male urogenital tract and with special regard to reproduction. Crit Rev Clin Lab Sci. 2016;53(6):379-95.

46. Tannetta D, Dragovic R, Alyahyaei Z, Southcombe J. Extracellular vesicles and reproduction-promotion of successful pregnancy. Cell Mol Immunol. 2014;11(6):548-63.

47. Sohel MM, Hoelker M, Noferesti SS, Salilew-Wondim D, Tholen E, Looft C, et al. Exosomal and Non-Exosomal Transport of Extra-Cellular microRNAs in Follicular Fluid: Implications for Bovine Oocyte Developmental Competence. PLoS One. 2013;8(11):e78505.

48. da Silveira JC, Carnevale EM, Winger QA, Bouma GJ. Regulation of ACVR1 and ID2 by cell-secreted exosomes during follicle maturation in the mare. Reprod Biol Endocrinol. 2014;12:44.

49. Navakanitworakul R, Hung WT, Gunewardena S, Davis JS, Chotigeat W, Christenson LK. Characterization and Small RNA Content of Extracellular Vesicles in Follicular Fluid of Developing Bovine Antral Follicles. Sci Rep. 2016;6:25486.

50. da Silveira JC, Veeramachaneni DN, Winger QA, Carnevale EM, Bouma GJ. Cell-secreted vesicles in equine ovarian follicular fluid contain miRNAs and proteins: a possible new form of cell communication within the ovarian follicle. Biol Reprod. 2012;86(3):71.

51. Hung WT, Hong X, Christenson LK, McGinnis LK. Extracellular Vesicles from Bovine Follicular Fluid Support Cumulus Expansion. Biol Reprod. 2015;93(5):117.

52. Lopera-Vasquez R, Hamdi M, Fernandez-Fuertes B, Maillo V, Beltran-Brena P, Calle A, et al. Extracellular Vesicles from BOEC in In Vitro Embryo Development and Quality. PLoS One. 2016;11(2):e0148083.

53. Beier HM. Oviducal and uterine fluids. J Reprod Fertil. 1974;37(1):221-37.

54. Li MQ, Jin LP. Ovarian stimulation for in vitro fertilization alters the protein profile expression in endometrial secretion. Int J Clin Exp Pathol. 2013;6(10):1964-71.

55. Zhang Y, Wang Q, Wang H, Duan E. Uterine Fluid in Pregnancy: A Biological and Clinical Outlook. Trends Mol Med. 2017;23(7):604-14.

56. Ng YH, Rome S, Jalabert A, Forterre A, Singh H, Hincks CL, et al. Endometrial exosomes/microvesicles in the uterine microenvironment: a new paradigm for embryo-endometrial cross talk at implantation. PLoS One. 2013;8(3):e58502.

57. Burns G, Brooks K, Wildung M, Navakanitworakul R, Christenson LK, Spencer TE. Extracellular vesicles in luminal fluid of the ovine uterus. PLoS One. 2014;9(3):e90913.

58. Ruiz-Gonzalez I, Xu J, Wang X, Burghardt RC, Dunlap KA, Bazer FW. Exosomes, endogenous retroviruses and toll-like receptors: pregnancy recognition in ewes. Reproduction. 2015;149(3):281-91.

59. Balaguer N, Moreno I, Herrero M, Gonzalez M, Simon C, Vilella F. Heterogeneous nuclear ribonucleoprotein C1 may control miR-30d levels in endometrial exosomes affecting early embryo implantation. Mol Hum Reprod. 2018;24(8):411-25.

60. Balaguer N, Moreno I, Herrero M, Gonzalez-Monfort M, Vilella F, Simon C. MicroRNA-30d deficiency during preconception affects endometrial receptivity by decreasing implantation rates and impairing fetal growth. Am J Obstet Gynecol. 2019;221(1):46.e1-.e16.

61. Burns GW, Brooks KE, Spencer TE. Extracellular Vesicles Originate from the Conceptus and Uterus During Early Pregnancy in Sheep. Biol Reprod. 2016;94(3):56.

62. Bidarimath M, Khalaj K, Kridli RT, Kan FW, Koti M, Tayade C. Extracellular vesicle mediated intercellular communication at the porcine maternal-fetal interface: A new paradigm for conceptus-endometrial cross-talk. Sci Rep. 2017;7:40476.

63. Salomon C, Yee S, Scholz-Romero K, Kobayashi M, Vaswani K, Kvaskoff D, et al. Extravillous trophoblast cells-derived exosomes promote vascular smooth muscle cell migration. Front Pharmacol. 2014;5:175.

64. Cantonwine DE, Zhang Z, Rosenblatt K, Goudy KS, Doss RC, Ezrin AM, et al. Evaluation of proteomic biomarkers associated with circulating microparticles as an effective means to stratify the risk of spontaneous preterm birth. Am J Obstet Gynecol. 2016;214(5):631.e1-.e11.

65. Truong G, Guanzon D, Kinhal V, Elfeky O, Lai A, Longo S, et al. Oxygen tension regulates the miRNA profile and bioactivity of exosomes released from extravillous trophoblast cells - Liquid biopsies for monitoring complications of pregnancy. PLoS One. 2017;12(3):e0174514.

66. Tan KH, Tan SS, Ng MJ, Tey WS, Sim WK, Allen JC, et al. Extracellular vesicles yield predictive pre-eclampsia biomarkers. J Extracell Vesicles. 2017;6(1):1408390.

67. Motta-Mejia C, Kandzija N, Zhang W, Mhlomi V, Cerdeira AS, Burdujan A, et al. Placental Vesicles Carry Active Endothelial Nitric Oxide Synthase and Their Activity is Reduced in Preeclampsia. Hypertension. 2017;70(2):372-81.

68. Salomon C, Guanzon D, Scholz-Romero K, Longo S, Correa P, Illanes SE, et al. Placental Exosomes as Early Biomarker of Preeclampsia: Potential Role of Exosomal MicroRNAs Across Gestation. J Clin Endocrinol Metab. 2017;102(9):3182-94.

69. Halkein J, Tabruyn SP, Ricke-Hoch M, Haghikia A, Nguyen NQ, Scherr M, et al. MicroRNA-146a is a therapeutic target and biomarker for peripartum cardiomyopathy. J Clin Invest. 2013;123(5):2143-54.

70. Moro L, Bardaji A, Macete E, Barrios D, Morales-Prieto DM, Espana C, et al. Placental Microparticles and MicroRNAs in Pregnant Women with Plasmodium falciparum or HIV Infection. PLoS One. 2016;11(1):e0146361.

71. Robinson MD, McCarthy DJ, Smyth GK. edgeR: a Bioconductor package for differential expression analysis of digital gene expression data. Bioinformatics. 2010;26(1):139-40.

72. Li H, Durbin R. Fast and accurate long-read alignment with Burrows-Wheeler transform. Bioinformatics. 2010;26(5):589-95.

73. Li H. A statistical framework for SNP calling, mutation discovery, association mapping and population genetical parameter estimation from sequencing data. Bioinformatics. 2011;27(21):2987-93.

74. Quinlan AR, Hall IM. BEDTools: a flexible suite of utilities for comparing genomic features. Bioinformatics. 2010;26(6):841-2.

75. McCarthy DJ, Chen Y, Smyth GK. Differential expression analysis of multifactor RNA-Seq experiments with respect to biological variation. Nucleic Acids Res. 402012. p. 4288-97.

76. Nikolayeva O, Robinson MD. edgeR for differential RNA-seq and ChIP-seq analysis: an application to stem cell biology. Methods Mol Biol. 2014;1150:45-79.

77. Van Blerkom J, Davis PW, Lee J. ATP content of human oocytes and developmental potential and outcome after in-vitro fertilization and embryo transfer. Hum Reprod. 1995;10(2):415-24.

78. Stojkovic M, Machado SA, Stojkovic P, Zakhartchenko V, Hutzler P, Goncalves PB, et al. Mitochondrial distribution and adenosine triphosphate content of bovine oocytes before and after in vitro maturation: correlation with morphological criteria and developmental capacity after in vitro fertilization and culture. Biol Reprod. 2001;64(3):904-9.

79. Troiano L, Ferraresi R, Lugli E, Nemes E, Roat E, Nasi M, et al. Multiparametric analysis of cells with different mitochondrial membrane potential during apoptosis by polychromatic flow cytometry. Nat Protoc. 2007;2(11):2719-27.

80. Perelman A, Wachtel C, Cohen M, Haupt S, Shapiro H, Tzur A. JC-1: alternative excitation wavelengths facilitate mitochondrial membrane potential cytometry. Cell Death Dis. 2012;3:e430.

81. Tong M, Kleffmann T, Pradhan S, Johansson CL, DeSousa J, Stone PR, et al. Proteomic characterization of macro-, micro- and nano-extracellular vesicles derived from the same first trimester placenta: relevance for feto-maternal communication. Hum Reprod. 2016;31(4):687-99.

82. Jeppesen DK, Hvam ML, Primdahl-Bengtson B, Boysen AT, Whitehead B, Dyrskjot L, et al. Comparative analysis of discrete exosome fractions obtained by differential centrifugation. J Extracell Vesicles. 2014;3:25011.

83. Lucchetti D, Fattorossi A, Sgambato A. Extracellular Vesicles in Oncology: Progress and Pitfalls in the Methods of Isolation and Analysis. Biotechnol J. 2019;14(1):e1700716.

84. Abas L, Luschnig C. Maximum yields of microsomal-type membranes from small amounts of plant material without requiring ultracentrifugation. Anal Biochem. 2010;401(2):217-27.

85. Lavoie C, Lanoix J, Kan FW, Paiement J. Cell-free assembly of rough and smooth endoplasmic reticulum. J Cell Sci. 1996;109 (Pt 6):1415-25.

86. Tricarico C, Clancy J, D'Souza-Schorey C. Biology and biogenesis of shed microvesicles. Small GTPases. 2017;8(4):220-32.

87. Thery C, Regnault A, Garin J, Wolfers J, Zitvogel L, Ricciardi-Castagnoli P, et al. Molecular characterization of dendritic cell-derived exosomes. Selective accumulation of the heat shock protein hsc73. J Cell Biol. 1999;147(3):599-610.

88. Lasser C, Eldh M, Lotvall J. Isolation and characterization of RNA-containing exosomes. J Vis Exp. 2012(59):e3037.

89. Lobb RJ, Becker M, Wen SW, Wong CS, Wiegmans AP, Leimgruber A, et al. Optimized exosome isolation protocol for cell culture supernatant and human plasma. J Extracell Vesicles. 2015;4:27031.

90. Allocati N, Masulli M, Di Ilio C, Federici L. Glutathione transferases: substrates, inihibitors and pro-drugs in cancer and neurodegenerative diseases. Oncogenesis. 2018;7(1):8.

91. Mustafa MD, Pathak R, Ahmed T, Ahmed RS, Tripathi AK, Guleria K, et al. Association of glutathione S-transferase M1 and T1 gene polymorphisms and oxidative stress markers in preterm labor. Clin Biochem. 2010;43(13-14):1124-8.

92. Akther L, Rahman MM, Bhuiyan MES, Hosen MB, Nesa A, Kabir Y. Association of glutathione S-transferase theta 1 and glutathione S-transferase mu 1 gene polymorphism with the risk of pre-eclampsia during pregnancy in Bangladesh. J Obstet Gynaecol Res. 2019;45(1):113-8.

93. Nair RR, Khanna A, Singh K. Association of GSTT1 and GSTM1 polymorphisms with early pregnancy loss in an Indian population and a meta-analysis. Reprod Biomed Online. 2013;26(4):313-22.

94. Carlomagno G, Minini M, Tilotta M, Unfer V. From Implantation to Birth: Insight into Molecular Melatonin Functions. Int J Mol Sci. 2018;19(9).

95. Hirata H, Hinoda Y, Zaman MS, Chen Y, Ueno K, Majid S, et al. Function of UDP-glucuronosyltransferase 2B17 (UGT2B17) is involved in endometrial cancer. Carcinogenesis. 2010;31(9):1620-6.

96. Chinnery PF, Hudson G. Mitochondrial genetics. Br Med Bull. 2013;106:135-59.

97. Taanman JW. The mitochondrial genome: structure, transcription, translation and replication. Biochim Biophys Acta. 1999;1410(2):103-23.

98. Mehta AP, Supekova L, Chen JH, Pestonjamasp K, Webster P, Ko Y, et al. Engineering yeast endosymbionts as a step toward the evolution of mitochondria. Proc Natl Acad Sci U S A. 2018;115(46):11796-801.

99. Li G, Lee YF, Liu S, Cai Y, Xie S, Liu NC, et al. Oxidative stress stimulates testicular orphan receptor 4 through forkhead transcription factor forkhead box O3a. Endocrinology. 2008;149(7):3490-9.

100. Yang ZF, Drumea K, Mott S, Wang J, Rosmarin AG. GABP transcription factor (nuclear respiratory factor 2) is required for mitochondrial biogenesis. Mol Cell Biol. 2014;34(17):3194-201.

101. Bruni F, Polosa PL, Gadaleta MN, Cantatore P, Roberti M. Nuclear respiratory factor 2 induces the expression of many but not all human proteins acting in mitochondrial DNA transcription and replication. J Biol Chem. 2010;285(6):3939-48.

102. Mancini M, Anderson BO, Caldwell E, Sedghinasab M, Paty PB, Hockenbery DM. Mitochondrial proliferation and paradoxical membrane depolarization during

terminal differentiation and apoptosis in a human colon carcinoma cell line. J Cell Biol. 1997;138(2):449-69.

103. Miettinen TP, Bjorklund M. Cellular Allometry of Mitochondrial Functionality Establishes the Optimal Cell Size. Dev Cell. 2016;39(3):370-82.

104. Negrette-Guzman M, Huerta-Yepez S, Vega MI, Leon-Contreras JC, Hernandez-Pando R, Medina-Campos ON, et al. Sulforaphane induces differential modulation of mitochondrial biogenesis and dynamics in normal cells and tumor cells. Food Chem Toxicol. 2017;100:90-102.

105. Hashimoto S, Morimoto N, Yamanaka M, Matsumoto H, Yamochi T, Goto H, et al. Quantitative and qualitative changes of mitochondria in human preimplantation embryos. J Assist Reprod Genet. 2017;34(5):573-80.

106. Harvey AJ. Mitochondria in early development: linking the microenvironment, metabolism and the epigenome. Reproduction. 2019;157(5):R159-r79.

107. Diez-Juan A, Rubio C, Marin C, Martinez S, Al-Asmar N, Riboldi M, et al. Mitochondrial DNA content as a viability score in human euploid embryos: less is better. Fertil Steril. 2015;104(3):534-41.e1.

108. Fragouli E, McCaffrey C, Ravichandran K, Spath K, Grifo JA, Munne S, et al. Clinical implications of mitochondrial DNA quantification on pregnancy outcomes: a blinded prospective non-selection study. Hum Reprod. 2017;32(11):2340-7.

109. Scott R, 3rd, Zhang M, Seli E. Metabolism of the oocyte and the preimplantation embryo: implications for assisted reproduction. Curr Opin Obstet Gynecol. 2018;30(3):163-70.

110. Redel BK, Brown AN, Spate LD, Whitworth KM, Green JA, Prather RS. Glycolysis in preimplantation development is partially controlled by the Warburg Effect. Mol Reprod Dev. 2012;79(4):262-71.

111. Yan SJ, Lee YF, Ting HJ, Liu NC, Liu S, Lin SJ, et al. Deficiency in TR4 nuclear receptor abrogates Gadd45a expression and increases cytotoxicity induced by ionizing radiation. Cell Mol Biol Lett. 2012;17(2):309-22.

112. Raposo G, Stoorvogel W. Extracellular vesicles: exosomes, microvesicles, and friends. J Cell Biol. 2013;200(4):373-83.

113. Hardie D. Biochemical Messengers: Hormones, Neurotransmitters and Growth Factors. Hall C, editor. London: Chapman & Hall; 1991. 312 p.

114. Ronquist G, Brody I. The prostasome: its secretion and function in man. Biochim Biophys Acta. 1985;822(2):203-18.

115. Ogawa Y, Kanai-Azuma M, Akimoto Y, Kawakami H, Yanoshita R. Exosome-like vesicles with dipeptidyl peptidase IV in human saliva. Biol Pharm Bull. 2008;31(6):1059-62.

116. Caby MP, Lankar D, Vincendeau-Scherrer C, Raposo G, Bonnerot C. Exosomal-like vesicles are present in human blood plasma. Int Immunol. 2005;17(7):879-87.

117. Lasser C, Alikhani VS, Ekstrom K, Eldh M, Paredes PT, Bossios A, et al. Human saliva, plasma and breast milk exosomes contain RNA: uptake by macrophages. J Transl Med. 2011;9:9.

118. Pisitkun T, Shen RF, Knepper MA. Identification and proteomic profiling of exosomes in human urine. Proc Natl Acad Sci U S A. 2004;101(36):13368-73.

119. Asea A, Jean-Pierre C, Kaur P, Rao P, Linhares IM, Skupski D, et al. Heat shock protein-containing exosomes in mid-trimester amniotic fluids. J Reprod Immunol. 2008;79(1):12-7.

120. van Niel G, D'Angelo G, Raposo G. Shedding light on the cell biology of extracellular vesicles. Nat Rev Mol Cell Biol. 2018;19(4):213-28.

121. Akers JC, Gonda D, Kim R, Carter BS, Chen CC. Biogenesis of extracellular vesicles (EV): exosomes, microvesicles, retrovirus-like vesicles, and apoptotic bodies. J Neurooncol. 2013;113(1):1-11.

122. Gyorgy B, Szabo TG, Pasztoi M, Pal Z, Misjak P, Aradi B, et al. Membrane vesicles, current state-of-the-art: emerging role of extracellular vesicles. Cell Mol Life Sci. 2011;68(16):2667-88.

123. Kerr JF, Wyllie AH, Currie AR. Apoptosis: a basic biological phenomenon with wide-ranging implications in tissue kinetics. Br J Cancer. 1972;26(4):239-57.

124. Taylor RC, Cullen SP, Martin SJ. Apoptosis: controlled demolition at the cellular level. Nat Rev Mol Cell Biol. 2008;9(3):231-41.

125. Elmore S. Apoptosis: a review of programmed cell death. Toxicol Pathol. 2007;35(4):495-516.

126. Hristov M, Erl W, Linder S, Weber PC. Apoptotic bodies from endothelial cells enhance the number and initiate the differentiation of human endothelial progenitor cells in vitro. Blood. 2004;104(9):2761-6.

127. Willms E, Johansson HJ, Mager I, Lee Y, Blomberg KE, Sadik M, et al. Cells release subpopulations of exosomes with distinct molecular and biological properties. Sci Rep. 2016;6:22519.

128. Osteikoetxea X, Nemeth A, Sodar BW, Vukman KV, Buzas EI. Extracellular vesicles in cardiovascular disease: are they Jedi or Sith? J Physiol. 2016;594(11):2881-94.

129. van der Pol E, Boing AN, Harrison P, Sturk A, Nieuwland R. Classification, functions, and clinical relevance of extracellular vesicles. Pharmacol Rev. 2012;64(3):676-705.

130. van Engeland M, Kuijpers HJ, Ramaekers FC, Reutelingsperger CP, Schutte B. Plasma membrane alterations and cytoskeletal changes in apoptosis. Exp Cell Res. 1997;235(2):421-30.

131. Hochreiter-Hufford A, Ravichandran KS. Clearing the dead: apoptotic cell sensing, recognition, engulfment, and digestion. Cold Spring Harb Perspect Biol. 2013;5(1):a008748.

132. Wu Y, Tibrewal N, Birge RB. Phosphatidylserine recognition by phagocytes: a view to a kill. Trends Cell Biol. 2006;16(4):189-97.

133. Fadok VA, Bratton DL, Henson PM. Phagocyte receptors for apoptotic cells: recognition, uptake, and consequences. J Clin Invest. 2001;108(7):957-62.

134. Balaji N, Devy AS, Sumathi MK, Vidyalakshmi S, Kumar GS, D'Silva S. Annexin v - affinity assay - apoptosis detection system in granular cell ameloblastoma. J Int Oral Health. 2013;5(6):25-30.

135. Friedl P, Vischer P, Freyberg MA. The role of thrombospondin-1 in apoptosis. Cell Mol Life Sci. 2002;59(8):1347-57.

136. Takizawa F, Tsuji S, Nagasawa S. Enhancement of macrophage phagocytosis upon iC3b deposition on apoptotic cells. FEBS Lett. 1996;397(2-3):269-72.

137. Bergsmedh A, Szeles A, Henriksson M, Bratt A, Folkman MJ, Spetz AL, et al. Horizontal transfer of oncogenes by uptake of apoptotic bodies. Proc Natl Acad Sci U S A. 2001;98(11):6407-11.

138. Savill J, Dransfield I, Gregory C, Haslett C. A blast from the past: clearance of apoptotic cells regulates immune responses. Nat Rev Immunol. 2002;2(12):965-75.

139. Bellone M, Iezzi G, Rovere P, Galati G, Ronchetti A, Protti MP, et al. Processing of engulfed apoptotic bodies yields T cell epitopes. J Immunol. 1997;159(11):5391-9.

140. Cocca BA, Cline AM, Radic MZ. Blebs and apoptotic bodies are B cell autoantigens. J Immunol. 2002;169(1):159-66.

141. Bellone M. Apoptosis, cross-presentation, and the fate of the antigen specific immune response. Apoptosis. 2000;5(4):307-14.

142. Muralidharan-Chari V, Clancy JW, Sedgwick A, D'Souza-Schorey C. Microvesicles: mediators of extracellular communication during cancer progression. J Cell Sci. 2010;123(Pt 10):1603-11.

143. Cocucci E, Racchetti G, Meldolesi J. Shedding microvesicles: artefacts no more. Trends Cell Biol. 2009;19(2):43-51.

144. D'Souza-Schorey C, Clancy JW. Tumor-derived microvesicles: shedding light on novel microenvironment modulators and prospective cancer biomarkers. Genes Dev. 2012;26(12):1287-99.

145. Chargaff E, West R. The biological significance of the thromboplastic protein of blood. J Biol Chem. 1946;166(1):189-97.

146. Antonyak MA, Cerione RA. Emerging picture of the distinct traits and functions of microvesicles and exosomes. Proc Natl Acad Sci U S A. 2015;112(12):3589-90.

147. Tauro BJ, Greening DW, Mathias RA, Ji H, Mathivanan S, Scott AM, et al. Comparison of ultracentrifugation, density gradient separation, and immunoaffinity capture methods for isolating human colon cancer cell line LIM1863-derived exosomes. Methods. 2012;56(2):293-304.

148. Kreimer S, Belov AM, Ghiran I, Murthy SK, Frank DA, Ivanov AR. Mass-spectrometry-based molecular characterization of extracellular vesicles: lipidomics and proteomics. J Proteome Res. 2015;14(6):2367-84.

149. Sluijter JP, Verhage V, Deddens JC, van den Akker F, Doevendans PA. Microvesicles and exosomes for intracardiac communication. Cardiovasc Res. 2014;102(2):302-11.

150. Xu R, Greening DW, Rai A, Ji H, Simpson RJ. Highly-purified exosomes and shed microvesicles isolated from the human colon cancer cell line LIM1863 by sequential centrifugal ultrafiltration are biochemically and functionally distinct. Methods. 2015;87:11-25.

151. Menck K, Scharf C, Bleckmann A, Dyck L, Rost U, Wenzel D, et al. Tumor-derived microvesicles mediate human breast cancer invasion through differentially glycosylated EMMPRIN. J Mol Cell Biol. 2015;7(2):143-53.

152. Arshad Malik MF. Influence of microvesicles in breast cancer metastasis and their therapeutic implications. Arch Iran Med. 2015;18(3):189-92.

153. McDaniel K, Correa R, Zhou T, Johnson C, Francis H, Glaser S, et al. Functional role of microvesicles in gastrointestinal malignancies. Ann Transl Med. 2013;1(1):4.

154. Jorfi S, Inal JM. The role of microvesicles in cancer progression and drug resistance. Biochem Soc Trans. 2013;41(1):293-8.

155. Dye JR, Ullal AJ, Pisetsky DS. The role of microparticles in the pathogenesis of rheumatoid arthritis and systemic lupus erythematosus. Scand J Immunol. 2013;78(2):140-8.

156. Lo Cicero A, Majkowska I, Nagase H, Di Liegro I, Troeberg L. Microvesicles shed by oligodendroglioma cells and rheumatoid synovial fibroblasts contain aggrecanase activity. Matrix Biol. 2012;31(4):229-33.

157. Sellam J, Proulle V, Jungel A, Ittah M, Miceli Richard C, Gottenberg JE, et al. Increased levels of circulating microparticles in primary Sjogren's syndrome, systemic lupus erythematosus and rheumatoid arthritis and relation with disease activity. Arthritis Res Ther. 2009;11(5):R156.

158. Xiong J, Miller VM, Li Y, Jayachandran M. Microvesicles at the crossroads between infection and cardiovascular diseases. J Cardiovasc Pharmacol. 2012;59(2):124-32.

159. Trams EG, Lauter CJ, Salem N, Jr., Heine U. Exfoliation of membrane ecto-enzymes in the form of micro-vesicles. Biochim Biophys Acta. 1981;645(1):63-70.

160. Harding C, Heuser J, Stahl P. Receptor-mediated endocytosis of transferrin and recycling of the transferrin receptor in rat reticulocytes. J Cell Biol. 1983;97(2):329-39.

161. Lane RE, Korbie D, Anderson W, Vaidyanathan R, Trau M. Analysis of exosome purification methods using a model liposome system and tunable-resistive pulse sensing. Sci Rep. 2015;5:7639.

162. Colombo M, Moita C, van Niel G, Kowal J, Vigneron J, Benaroch P, et al. Analysis of ESCRT functions in exosome biogenesis, composition and secretion highlights the heterogeneity of extracellular vesicles. J Cell Sci. 2013;126(Pt 24):5553-65.

163. Mathivanan S, Ji H, Simpson RJ. Exosomes: extracellular organelles important in intercellular communication. J Proteomics. 2010;73(10):1907-20.

164. Mathivanan S, Lim JW, Tauro BJ, Ji H, Moritz RL, Simpson RJ. Proteomics analysis of A33 immunoaffinity-purified exosomes released from the human colon tumor cell line LIM1215 reveals a tissue-specific protein signature. Mol Cell Proteomics. 2010;9(2):197-208.

165. De Toro J, Herschlik L, Waldner C, Mongini C. Emerging roles of exosomes in normal and pathological conditions: new insights for diagnosis and therapeutic applications. Front Immunol. 2015;6:203.

166. Suchorska WM, Lach MS. The role of exosomes in tumor progression and metastasis (Review). Oncol Rep. 2016;35(3):1237-44.

167. Greening DW, Gopal SK, Xu R, Simpson RJ, Chen W. Exosomes and their roles in immune regulation and cancer. Semin Cell Dev Biol. 2015;40:72-81.

168. Muller L, Mitsuhashi M, Simms P, Gooding WE, Whiteside TL. Tumor-derived exosomes regulate expression of immune function-related genes in human T cell subsets. Sci Rep. 2016;6:20254.

169. Thery C, Amigorena S, Raposo G, Clayton A. Isolation and characterization of exosomes from cell culture supernatants and biological fluids. Curr Protoc Cell Biol. 2006;Chapter 3:Unit 3.22.

170. Crescitelli R, Lasser C, Szabo TG, Kittel A, Eldh M, Dianzani I, et al. Distinct RNA profiles in subpopulations of extracellular vesicles: apoptotic bodies, microvesicles and exosomes. J Extracell Vesicles. 2013;2.

171. Witwer KW, Buzas EI, Bemis LT, Bora A, Lasser C, Lotvall J, et al. Standardization of sample collection, isolation and analysis methods in extracellular vesicle research. J Extracell Vesicles. 2013;2.

172. Lamparski HG, Metha-Damani A, Yao JY, Patel S, Hsu DH, Ruegg C, et al. Production and characterization of clinical grade exosomes derived from dendritic cells. J Immunol Methods. 2002;270(2):211-26.

173. Chiou N-T, Ansel KM. Improved exosome isolation by sucrose gradient fractionation of ultracentrifuged crude exosome pellets. Protocol Exchange. 2016.

174. Keller S, Ridinger J, Rupp AK, Janssen JW, Altevogt P. Body fluid derived exosomes as a novel template for clinical diagnostics. J Transl Med. 2011;9:86.

175. Cantin R, Diou J, Belanger D, Tremblay AM, Gilbert C. Discrimination between exosomes and HIV-1: purification of both vesicles from cell-free supernatants. J Immunol Methods. 2008;338(1-2):21-30.

176. Klimentova J, Stulik J. Methods of isolation and purification of outer membrane vesicles from gram-negative bacteria. Microbiol Res. 2015;170:1-9.

177. Bryzgunova OE, Zaripov MM, Skvortsova TE, Lekchnov EA, Grigor'eva AE, Zaporozhchenko IA, et al. Comparative Study of Extracellular Vesicles from the Urine of Healthy Individuals and Prostate Cancer Patients. PLoS One. 2016;11(6):e0157566.

178. Klein-Scory S, Tehrani MM, Eilert-Micus C, Adamczyk KA, Wojtalewicz N, Schnolzer M, et al. New insights in the composition of extracellular vesicles from pancreatic cancer cells: implications for biomarkers and functions. Proteome Sci. 2014;12(1):50.

179. de Menezes-Neto A, Saez MJ, Lozano-Ramos I, Segui-Barber J, Martin-Jaular L, Ullate JM, et al. Size-exclusion chromatography as a stand-alone methodology identifies novel markers in mass spectrometry analyses of plasma-derived vesicles from healthy individuals. J Extracell Vesicles. 2015;4:27378.

180. Müller G. Novel Tools for the Study of Cell Type-Specific Exosomes and Microvesicles | OMICS International. Journal of Bioanalysis & Biomedicine. 2012;4(4):46.

181. Taylor DD, Lyons KS, Gercel-Taylor C. Shed membrane fragment-associated markers for endometrial and ovarian cancers. Gynecol Oncol. 2002;84(3):443-8.

182. Gamez-Valero A, Monguio-Tortajada M, Carreras-Planella L, Franquesa M, Beyer K, Borras FE. Size-Exclusion Chromatography-based isolation minimally alters Extracellular Vesicles' characteristics compared to precipitating agents. Sci Rep. 2016;6:33641.

183. Corso G, Mager I, Lee Y, Gorgens A, Bultema J, Giebel B, et al. Reproducible and scalable purification of extracellular vesicles using combined bind-elute and size exclusion chromatography. Sci Rep. 2017;7(1):11561.

184. Yoo CE, Kim G, Kim M, Park D, Kang HJ, Lee M, et al. A direct extraction method for microRNAs from exosomes captured by immunoaffinity beads. Anal Biochem. 2012;431(2):96-8.

185. Ji H, Chen M, Greening DW, He W, Rai A, Zhang W, et al. Deep sequencing of RNA from three different extracellular vesicle (EV) subtypes released from the human LIM1863 colon cancer cell line uncovers distinct miRNA-enrichment signatures. PLoS One. 2014;9(10):e110314.

186. Greening DW, Xu R, Ji H, Tauro BJ, Simpson RJ. A protocol for exosome isolation and characterization: evaluation of ultracentrifugation, density-gradient separation, and immunoaffinity capture methods. Methods Mol Biol. 2015;1295:179-209.

187. Alvarez ML, Khosroheidari M, Kanchi Ravi R, DiStefano JK. Comparison of protein, microRNA, and mRNA yields using different methods of urinary exosome isolation for the discovery of kidney disease biomarkers. Kidney Int. 2012;82(9):1024-32.

188. Chen C, Skog J, Hsu CH, Lessard RT, Balaj L, Wurdinger T, et al. Microfluidic isolation and transcriptome analysis of serum microvesicles. Lab Chip. 2010;10(4):505-11.

189. Kanwar SS, Dunlay CJ, Simeone DM, Nagrath S. Microfluidic device (ExoChip) for on-chip isolation, quantification and characterization of circulating exosomes. Lab Chip. 2014;14(11):1891-900.

190. Ashcroft BA, de Sonneville J, Yuana Y, Osanto S, Bertina R, Kuil ME, et al. Determination of the size distribution of blood microparticles directly in plasma using atomic force microscopy and microfluidics. Biomed Microdevices. 2012;14(4):641-9.

191. Davies RT, Kim J, Jang SC, Choi EJ, Gho YS, Park J. Microfluidic filtration system to isolate extracellular vesicles from blood. Lab Chip. 2012;12(24):5202-10.

192. Wu M, Ouyang Y, Wang Z, Zhang R, Huang PH, Chen C, et al. Isolation of exosomes from whole blood by integrating acoustics and microfluidics. Proc Natl Acad Sci U S A. 2017;114(40):10584-9.

193. Roccaro AM, Sacco A, Maiso P, Azab AK, Tai YT, Reagan M, et al. BM mesenchymal stromal cell-derived exosomes facilitate multiple myeloma progression. J Clin Invest. 2013;123(4):1542-55.

194. Wu Y, Deng W, Klinke DJ, 2nd. Exosomes: improved methods to characterize their morphology, RNA content, and surface protein biomarkers. Analyst. 2015;140(19):6631-42.

195. Iwai K, Minamisawa T, Suga K, Yajima Y, Shiba K. Isolation of human salivary extracellular vesicles by iodixanol density gradient ultracentrifugation and their characterizations. J Extracell Vesicles. 2016;5:30829.

196. Hardij J, Cecchet F, Berquand A, Gheldof D, Chatelain C, Mullier F, et al. Characterisation of tissue factor-bearing extracellular vesicles with AFM: comparison of air-tapping-mode AFM and liquid Peak Force AFM. J Extracell Vesicles. 2013;2.

197. Filipe V, Hawe A, Jiskoot W. Critical evaluation of Nanoparticle Tracking Analysis (NTA) by NanoSight for the measurement of nanoparticles and protein aggregates. Pharm Res. 2010;27(5):796-810.

198. Dragovic RA, Gardiner C, Brooks AS, Tannetta DS, Ferguson DJ, Hole P, et al. Sizing and phenotyping of cellular vesicles using Nanoparticle Tracking Analysis. Nanomedicine. 2011;7(6):780-8.

199. Gardiner C, Shaw M, Hole P, Smith J, Tannetta D, Redman CW, et al. Measurement of refractive index by nanoparticle tracking analysis reveals heterogeneity in extracellular vesicles. J Extracell Vesicles. 2014;3:25361.

200. Momen-Heravi F, Balaj L, Alian S, Tigges J, Toxavidis V, Ericsson M, et al. Alternative methods for characterization of extracellular vesicles. Front Physiol. 2012;3:354.

201. van der Pol E, Hoekstra AG, Sturk A, Otto C, van Leeuwen TG, Nieuwland R. Optical and non-optical methods for detection and characterization of microparticles and exosomes. J Thromb Haemost. 2010;8(12):2596-607.

202. Lacroix R, Robert S, Poncelet P, Dignat-George F. Overcoming limitations of microparticle measurement by flow cytometry. Semin Thromb Hemost. 2010;36(8):807-18.

203. van der Vlist EJ, Nolte-'t Hoen EN, Stoorvogel W, Arkesteijn GJ, Wauben MH. Fluorescent labeling of nano-sized vesicles released by cells and subsequent quantitative and qualitative analysis by high-resolution flow cytometry. Nat Protoc. 2012;7(7):1311-26.

204. Nolte-'t Hoen EN, van der Vlist EJ, Aalberts M, Mertens HC, Bosch BJ, Bartelink W, et al. Quantitative and qualitative flow cytometric analysis of nanosized cell-derived membrane vesicles. Nanomedicine. 2012;8(5):712-20.

205. McVey MJ, Spring CM, Kuebler WM. Improved resolution in extracellular vesicle populations using 405 instead of 488 nm side scatter. J Extracell Vesicles. 2018;7(1):1454776.

206. Osteikoetxea X, Balogh A, Szabo-Taylor K, Nemeth A, Szabo TG, Paloczi K, et al. Improved characterization of EV preparations based on protein to lipid ratio and lipid properties. PLoS One. 2015;10(3):e0121184.

207. Nakai W, Yoshida T, Diez D, Miyatake Y, Nishibu T, Imawaka N, et al. A novel affinity-based method for the isolation of highly purified extracellular vesicles. Sci Rep. 2016;6:33935.

208. Logozzi M, De Milito A, Lugini L, Borghi M, Calabro L, Spada M, et al. High levels of exosomes expressing CD63 and caveolin-1 in plasma of melanoma patients. PLoS One. 2009;4(4):e5219.

209. Im H, Shao H, Park YI, Peterson VM, Castro CM, Weissleder R, et al. Label-free detection and molecular profiling of exosomes with a nano-plasmonic sensor. Nat Biotechnol. 2014;32(5):490-5.

210. Simpson RJ, Kalra H, Mathivanan S. ExoCarta as a resource for exosomal research. J Extracell Vesicles. 2012;1.

211. Kim DK, Kang B, Kim OY, Choi DS, Lee J, Kim SR, et al. EVpedia: an integrated database of high-throughput data for systemic analyses of extracellular vesicles. J Extracell Vesicles. 2013;2.

212. Kalra H, Simpson RJ, Ji H, Aikawa E, Altevogt P, Askenase P, et al. Vesiclepedia: a compendium for extracellular vesicles with continuous community annotation. PLoS Biol. 2012;10(12):e1001450.

213. Aatonen MT, Ohman T, Nyman TA, Laitinen S, Gronholm M, Siljander PR. Isolation and characterization of platelet-derived extracellular vesicles. J Extracell Vesicles. 2014;3.

214. MacKenzie A, Wilson HL, Kiss-Toth E, Dower SK, North RA, Surprenant A. Rapid secretion of interleukin-1beta by microvesicle shedding. Immunity. 2001;15(5):825-35.

215. Berda-Haddad Y, Robert S, Salers P, Zekraoui L, Farnarier C, Dinarello CA, et al. Sterile inflammation of endothelial cell-derived apoptotic bodies is mediated by interleukin-1alpha. Proc Natl Acad Sci U S A. 2011;108(51):20684-9.

216. Nardi Fda S, Michelon TF, Neumann J, Manvailer LF, Wagner B, Horn PA, et al. High levels of circulating extracellular vesicles with altered expression and function during pregnancy. Immunobiology. 2016;221(7):753-60.

217. Gulinelli S, Salaro E, Vuerich M, Bozzato D, Pizzirani C, Bolognesi G, et al. IL-18 associates to microvesicles shed from human macrophages by a LPS/TLR-4 independent mechanism in response to P2X receptor stimulation. Eur J Immunol. 2012;42(12):3334-45.

218. Hasegawa H, Thomas HJ, Schooley K, Born TL. Native IL-32 is released from intestinal epithelial cells via a non-classical secretory pathway as a membrane-associated protein. Cytokine. 2011;53(1):74-83.

219. Zhang HG, Liu C, Su K, Yu S, Zhang L, Zhang S, et al. A membrane form of TNF-alpha presented by exosomes delays T cell activation-induced cell death. J Immunol. 2006;176(12):7385-93.

220. Kandere-Grzybowska K, Letourneau R, Kempuraj D, Donelan J, Poplawski S, Boucher W, et al. IL-1 induces vesicular secretion of IL-6 without degranulation from human mast cells. J Immunol. 2003;171(9):4830-6.

221. Brouwers JF, Aalberts M, Jansen JW, van Niel G, Wauben MH, Stout TA, et al. Distinct lipid compositions of two types of human prostasomes. Proteomics. 2013;13(10-11):1660-6.

222. Trajkovic K, Hsu C, Chiantia S, Rajendran L, Wenzel D, Wieland F, et al. Ceramide triggers budding of exosome vesicles into multivesicular endosomes. Science. 2008;319(5867):1244-7.

223. Ikonen E. Roles of lipid rafts in membrane transport. Curr Opin Cell Biol. 2001;13(4):470-7.

224. Smaby JM, Momsen M, Kulkarni VS, Brown RE. Cholesterol-induced interfacial area condensations of galactosylceramides and sphingomyelins with identical acyl chains. Biochemistry. 1996;35(18):5696-704.

225. de Gassart A, Geminard C, Fevrier B, Raposo G, Vidal M. Lipid raft-associated protein sorting in exosomes. Blood. 2003;102(13):4336-44.

226. Del Conde I, Shrimpton CN, Thiagarajan P, Lopez JA. Tissue-factor-bearing microvesicles arise from lipid rafts and fuse with activated platelets to initiate coagulation. Blood. 2005;106(5):1604-11.

227. Laulagnier K, Motta C, Hamdi S, Roy S, Fauvelle F, Pageaux JF, et al. Mast cell- and dendritic cell-derived exosomes display a specific lipid composition and an unusual membrane organization. Biochem J. 2004;380(Pt 1):161-71.

228. Valadi H, Ekstrom K, Bossios A, Sjostrand M, Lee JJ, Lotvall JO. Exosome-mediated transfer of mRNAs and microRNAs is a novel mechanism of genetic exchange between cells. Nat Cell Biol. 2007;9(6):654-9.

229. Vojtech L, Woo S, Hughes S, Levy C, Ballweber L, Sauteraud RP, et al. Exosomes in human semen carry a distinctive repertoire of small non-coding RNAs with potential regulatory functions. Nucleic Acids Res. 2014;42(11):7290-304.

230. van Balkom BW, Eisele AS, Pegtel DM, Bervoets S, Verhaar MC. Quantitative and qualitative analysis of small RNAs in human endothelial cells and exosomes provides insights into localized RNA processing, degradation and sorting. J Extracell Vesicles. 2015;4:26760.

231. Cheng L, Sharples RA, Scicluna BJ, Hill AF. Exosomes provide a protective and enriched source of miRNA for biomarker profiling compared to intracellular and cell-free blood. J Extracell Vesicles. 2014;3.

232. Arroyo JD, Chevillet JR, Kroh EM, Ruf IK, Pritchard CC, Gibson DF, et al. Argonaute2 complexes carry a population of circulating microRNAs independent of vesicles in human plasma. Proc Natl Acad Sci U S A. 2011;108(12):5003-8.

233. Turchinovich A, Weiz L, Langheinz A, Burwinkel B. Characterization of extracellular circulating microRNA. Nucleic Acids Res. 2011;39(16):7223-33.

234. Shelke GV, Lasser C, Gho YS, Lotvall J. Importance of exosome depletion protocols to eliminate functional and RNA-containing extracellular vesicles from fetal bovine serum. J Extracell Vesicles. 2014;3.

235. Balaj L, Lessard R, Dai L, Cho YJ, Pomeroy SL, Breakefield XO, et al. Tumour microvesicles contain retrotransposon elements and amplified oncogene sequences. Nat Commun. 2011;2:180.

236. Garcia-Romero N, Carrion-Navarro J, Esteban-Rubio S, Lazaro-Ibanez E, Peris-Celda M, Alonso MM, et al. DNA sequences within glioma-derived extracellular vesicles can cross the intact blood-brain barrier and be detected in peripheral blood of patients. Oncotarget. 2017;8(1):1416-28.

237. Waterhouse M, Themeli M, Bertz H, Zoumbos N, Finke J, Spyridonidis A. Horizontal DNA transfer from donor to host cells as an alternative mechanism of epithelial chimerism after allogeneic hematopoietic cell transplantation. Biol Blood Marrow Transplant. 2011;17(3):319-29.

238. Guescini M, Genedani S, Stocchi V, Agnati LF. Astrocytes and Glioblastoma cells release exosomes carrying mtDNA. J Neural Transm (Vienna). 2010;117(1):1-4.

239. Guescini M, Guidolin D, Vallorani L, Casadei L, Gioacchini AM, Tibollo P, et al. C2C12 myoblasts release micro-vesicles containing mtDNA and proteins involved in signal transduction. Exp Cell Res. 2010;316(12):1977-84.

240. Torralba D, Baixauli F, Villarroya-Beltri C, Fernandez-Delgado I, Latorre-Pellicer A, Acin-Perez R, et al. Priming of dendritic cells by DNA-containing extracellular vesicles from activated T cells through antigen-driven contacts. Nat Commun. 2018;9(1):2658.

241. Tong M, Johansson C, Xiao F, Stone PR, James JL, Chen Q, et al. Antiphospholipid antibodies increase the levels of mitochondrial DNA in placental extracellular vesicles: Alarmin-g for preeclampsia. Sci Rep. 2017;7(1):16556.

242. Santonocito M, Vento M, Guglielmino MR, Battaglia R, Wahlgren J, Ragusa M, et al. Molecular characterization of exosomes and their microRNA cargo in human follicular fluid: bioinformatic analysis reveals that exosomal microRNAs control pathways involved in follicular maturation. Fertil Steril. 2014;102(6):1751-61.e1.

243. Al-Dossary AA, Strehler EE, Martin-Deleon PA. Expression and secretion of plasma membrane Ca2+-ATPase 4a (PMCA4a) during murine estrus: association with oviductal exosomes and uptake in sperm. PLoS One. 2013;8(11):e80181.

244. Flori F, Secciani F, Capone A, Paccagnini E, Caruso S, Ricci MG, et al. Menstrual cycle-related sialidase activity of the female cervical mucus is associated with exosome-like vesicles. Fertil Steril. 2007;88(4 Suppl):1212-9.

245. Uszynski W, Zekanowska E, Uszynski M, Zylinski A, Kuczynski J. New observations on procoagulant properties of amniotic fluid: microparticles (MPs) and tissue factor-bearing MPs (MPs-TF), comparison with maternal blood plasma. Thromb Res. 2013;132(6):757-60.

246. Admyre C, Johansson SM, Qazi KR, Filen JJ, Lahesmaa R, Norman M, et al. Exosomes with immune modulatory features are present in human breast milk. J Immunol. 2007;179(3):1969-78.

247. Machtinger R, Laurent LC, Baccarelli AA. Extracellular vesicles: roles in gamete maturation, fertilization and embryo implantation. Hum Reprod Update. 2016;22(2):182-93.

248. Hell L, Wisgrill L, Ay C, Spittler A, Schwameis M, Jilma B, et al. Procoagulant extracellular vesicles in amniotic fluid. Transl Res. 2017;184:12-20.e1.

249. Karlsson O, Rodosthenous RS, Jara C, Brennan KJ, Wright RO, Baccarelli AA, et al. Detection of long non-coding RNAs in human breastmilk extracellular vesicles: Implications for early child development. Epigenetics. 2016;11(10):721-9.

250. Aplin JD, Ruane PT. Embryo-epithelium interactions during implantation at a glance. J Cell Sci. 2017;130(1):15-22.

251. Wang H, Dey SK. Roadmap to embryo implantation: clues from mouse models. Nat Rev Genet. 2006;7(3):185-99.

252. Cheong Y, Boomsma C, Heijnen C, Macklon N. Uterine secretomics: a window on the maternal-embryo interface. Fertil Steril. 2013;99(4):1093-9.

253. Cha KY, Chian RC. Maturation in vitro of immature human oocytes for clinical use. Hum Reprod Update. 1998;4(2):103-20.

254. Reed BG, Carr BR. The Normal Menstrual Cycle and the Control of Ovulation. In: Feingold KR, Anawalt B, Boyce A, Chrousos G, Dungan K, Grossman A, et al., editors. Endotext. South Dartmouth (MA): MDText.com, Inc.; 2000.

255. Okabe M. The cell biology of mammalian fertilization. Development. 2013;140(22):4471-9.

256. Aplin JD. The cell biological basis of human implantation. Baillieres Best Pract Res Clin Obstet Gynaecol. 2000;14(5):757-64.

257. Hertig AT, Rock J, Adams EC. A description of 34 human ova within the first 17 days of development. Am J Anat. 1956;98(3):435-93.

258. Stricker R, Eberhart R, Chevailler MC, Quinn FA, Bischof P. Establishment of detailed reference values for luteinizing hormone, follicle stimulating hormone, estradiol, and progesterone during different phases of the menstrual cycle on the Abbott ARCHITECT analyzer. Clin Chem Lab Med. 2006;44(7):883-7.

259. Zamah AM, Hassis ME, Albertolle ME, Williams KE. Proteomic analysis of human follicular fluid from fertile women. Clin Proteomics. 2015;12(1):5.

260. Revelli A, Delle Piane L, Casano S, Molinari E, Massobrio M, Rinaudo P. Follicular fluid content and oocyte quality: from single biochemical markers to metabolomics. Reprod Biol Endocrinol. 2009;7:40.

261. Diez-Fraile A, Lammens T, Tilleman K, Witkowski W, Verhasselt B, De Sutter P, et al. Age-associated differential microRNA levels in human follicular fluid reveal pathways potentially determining fertility and success of in vitro fertilization. Hum Fertil (Camb). 2014;17(2):90-8.

262. Almiñana C. Snooping on a private conversation between the oviduct and gametes/embryos. Animal Reproduction. 2015;12(3):8.

263. Campoy I, Lanau L, Altadill T, Sequeiros T, Cabrera S, Cubo-Abert M, et al. Exosome-like vesicles in uterine aspirates: a comparison of ultracentrifugation-based isolation protocols. J Transl Med. 2016;14(1):180.

264. Griffiths GS, Galileo DS, Reese K, Martin-Deleon PA. Investigating the role of murine epididymosomes and uterosomes in GPI-linked protein transfer to sperm using SPAM1 as a model. Mol Reprod Dev. 2008;75(11):1627-36.

265. Franchi A, Cubilla M, Guidobaldi HA, Bravo AA, Giojalas LC. Uterosome-like vesicles prompt human sperm fertilizing capability. Mol Hum Reprod. 2016;22(12):833-41.

266. Laflamme J, Akoum A, Leclerc P. Induction of human sperm capacitation and protein tyrosine phosphorylation by endometrial cells and interleukin-6. Mol Hum Reprod. 2005;11(2):141-50.

267. Tannetta D, Collett G, Vatish M, Redman C, Sargent I. Syncytiotrophoblast extracellular vesicles - Circulating biopsies reflecting placental health. Placenta. 2017;52:134-8.

268. Mitchell MD, Peiris HN, Kobayashi M, Koh YQ, Duncombe G, Illanes SE, et al. Placental exosomes in normal and complicated pregnancy. Am J Obstet Gynecol. 2015;213(4 Suppl):S173-81.

269. Sarker S, Scholz-Romero K, Perez A, Illanes SE, Mitchell MD, Rice GE, et al. Placenta-derived exosomes continuously increase in maternal circulation over the first trimester of pregnancy. J Transl Med. 2014;12:204.

270. Salomon C, Torres MJ, Kobayashi M, Scholz-Romero K, Sobrevia L, Dobierzewska A, et al. A gestational profile of placental exosomes in maternal plasma and their effects on endothelial cell migration. PLoS One. 2014;9(6):e98667.

271. Tan KH, Tan SS, Sze SK, Lee WK, Ng MJ, Lim SK. Plasma biomarker discovery in preeclampsia using a novel differential isolation technology for circulating extracellular vesicles. Am J Obstet Gynecol. 2014;211(4):380.e1-13.

272. Hilfiker-Kleiner D, Sliwa K. Pathophysiology and epidemiology of peripartum cardiomyopathy. Nat Rev Cardiol. 2014;11(6):364-70.

273. Walenta K, Schwarz V, Schirmer SH, Kindermann I, Friedrich EB, Solomayer EF, et al. Circulating microparticles as indicators of peripartum cardiomyopathy. Eur Heart J. 2012;33(12):1469-79.

274. Takahashi T, Inaba Y, Somfai T, Kaneda M, Geshi M, Nagai T, et al. Supplementation of culture medium with L-carnitine improves development and cryotolerance of bovine embryos produced in vitro. Reprod Fertil Dev. 2013;25(4):589-99.

275. Zhang X, Wu XQ, Lu S, Guo YL, Ma X. Deficit of mitochondria-derived ATP during oxidative stress impairs mouse MII oocyte spindles. Cell Res. 2006;16(10):841-50.

276. Van Blerkom J, Davis P, Alexander S. Differential mitochondrial distribution in human pronuclear embryos leads to disproportionate inheritance between

blastomeres: relationship to microtubular organization, ATP content and competence. Hum Reprod. 2000;15(12):2621-33.

277. Stojkovic M, Westesen K, Zakhartchenko V, Stojkovic P, Boxhammer K, Wolf E. Coenzyme Q(10) in submicron-sized dispersion improves development, hatching, cell proliferation, and adenosine triphosphate content of in vitro-produced bovine embryos. Biol Reprod. 1999;61(2):541-7.

278. Team RC. R: A language and environment for statistical computing. Vienna, Austria: R Foundation for Statistical Computing; 2018.

279. Breuning MM, Kriegel H-P, Ng RT, Sander J. LOF:

Identifying density-based local outliers. Proceedings

of the ACM SIGMOD International Conference on Management of Data; June; Dallas, TX, USA2000. p. 93-104.

280. Hubert M, Rousseeuw PJ, Vanden Branden K. ROBPCA: A New Approach to Robust Principal Component Analysis. Technometrics. 2005;47(1):15.

281. Liu L, Zhang D, Liu H, Arendt C. Robust methods for population stratification in genome wide association studies. BMC Bioinformatics. 2013;14:132.

282. Lawrence M, Huber W, Pages H, Aboyoun P, Carlson M, Gentleman R, et al. Software for computing and annotating genomic ranges. PLoS Comput Biol. 2013;9(8):e1003118.

283. Zhang Y, Liu T, Meyer CA, Eeckhoute J, Johnson DS, Bernstein BE, et al. Model-based analysis of ChIP-Seq (MACS). Genome Biol. 2008;9(9):R137.

284. Stark R, Brown G. Differential Binding Analysis of ChIP-Seq Peak Data. Cambridge Research Institute - University of Cambridge: Bioconductor; 2011.

285. Van Deun J, Mestdagh P, Sormunen R, Cocquyt V, Vermaelen K, Vandesompele J, et al. The impact of disparate isolation methods for extracellular vesicles on downstream RNA profiling. J Extracell Vesicles. 2014;3.

286. Pantham P, Viall CA, Chen Q, Kleffmann T, Print CG, Chamley LW. Antiphospholipid antibodies bind syncytiotrophoblast mitochondria and alter the proteome of extruded syncytial nuclear aggregates. Placenta. 2015;36(12):1463-73.

287. Wlodkowic D, Telford W, Skommer J, Darzynkiewicz Z. Apoptosis and beyond: cytometry in studies of programmed cell death. Methods Cell Biol. 2011;103:55-98.

288. Bailey RW, Nguyen T, Robertson L, Gibbons E, Nelson J, Christensen RE, et al. Sequence of Physical Changes to the Cell Membrane During Glucocorticoid-Induced Apoptosis in S49 Lymphoma Cells. Biophys J. 962009. p. 2709-18.

289. Hugel B, Martinez MC, Kunzelmann C, Freyssinet JM. Membrane microparticles: two sides of the coin. Physiology (Bethesda). 2005;20:22-7.

290. Miyanishi M, Tada K, Koike M, Uchiyama Y, Kitamura T, Nagata S. Identification of Tim4 as a phosphatidylserine receptor. Nature. 2007;450(7168):435-9.

291. Kowal J, Arras G, Colombo M, Jouve M, Morath JP, Primdal-Bengtson B, et al. Proteomic comparison defines novel markers to characterize heterogeneous populations of extracellular vesicle subtypes. Proc Natl Acad Sci U S A. 2016;113(8):E968-77.

292. Svensson KJ, Christianson HC, Wittrup A, Bourseau-Guilmain E, Lindqvist E, Svensson LM, et al. Exosome uptake depends on ERK1/2-heat shock protein 27 signaling and lipid Raft-mediated endocytosis negatively regulated by caveolin-1. J Biol Chem. 2013;288(24):17713-24.

293. Adamczyk KA, Klein-Scory S, Tehrani MM, Warnken U, Schmiegel W, Schnolzer M, et al. Characterization of soluble and exosomal forms of the EGFR released from pancreatic cancer cells. Life Sci. 2011;89(9-10):304-12.

294. Mittelbrunn M, Gutierrez-Vazquez C, Villarroya-Beltri C, Gonzalez S, Sanchez-Cabo F, Gonzalez MA, et al. Unidirectional transfer of microRNA-loaded exosomes from T cells to antigen-presenting cells. Nat Commun. 2011;2:282.

295. Pols MS, Klumperman J. Trafficking and function of the tetraspanin CD63. Exp Cell Res. 2009;315(9):1584-92.

296. Nardi Fda S, Slowik R, Michelon T, Manvailer LF, Wagner B, Neumann J, et al. High Amounts of Total and Extracellular Vesicle-Derived Soluble HLA-G are Associated with HLA-G 14-bp Deletion Variant in Women with Embryo Implantation Failure. Am J Reprod Immunol. 2016;75(6):661-71.

297. Garte S, Gaspari L, Alexandrie AK, Ambrosone C, Autrup H, Autrup JL, et al. Metabolic gene polymorphism frequencies in control populations. Cancer Epidemiol Biomarkers Prev. 2001;10(12):1239-48.

298. Shi N, Guo X, Chen SY. Olfactomedin 2, a novel regulator for transforming growth factor-beta-induced smooth muscle differentiation of human embryonic stem cell-derived mesenchymal cells. Mol Biol Cell. 2014;25(25):4106-14.

299. Li S, Czubryt MP, McAnally J, Bassel-Duby R, Richardson JA, Wiebel FF, et al. Requirement for serum response factor for skeletal muscle growth and maturation revealed by tissue-specific gene deletion in mice. Proc Natl Acad Sci U S A. 2005;102(4):1082-7.

300. Liu S, Yan SJ, Lee YF, Liu NC, Ting HJ, Li G, et al. Testicular nuclear receptor 4 (TR4) regulates UV light-induced responses via Cockayne syndrome B protein-mediated transcription-coupled DNA repair. J Biol Chem. 2011;286(44):38103-8.

301. Collins LL, Lee YF, Heinlein CA, Liu NC, Chen YT, Shyr CR, et al. Growth retardation and abnormal maternal behavior in mice lacking testicular orphan nuclear receptor 4. Proc Natl Acad Sci U S A. 2004;101(42):15058-63.

302. Tanabe O, Shen Y, Liu Q, Campbell AD, Kuroha T, Yamamoto M, et al. The TR2 and TR4 orphan nuclear receptors repress Gata1 transcription. Genes Dev. 2007;21(21):2832-44.

303. Kim YS, Harry GJ, Kang HS, Goulding D, Wine RN, Kissling GE, et al. Altered cerebellar development in nuclear receptor TAK1/ TR4 null mice is associated with deficits in GLAST(+) glia, alterations in social behavior, motor learning, startle reactivity, and microglia. Cerebellum. 2010;9(3):310-23.

304. Bouchard M, Pfeffer P, Busslinger M. Functional equivalence of the transcription factors Pax2 and Pax5 in mouse development. Development. 2000;127(17):3703-13.

305. Urbanek P, Fetka I, Meisler MH, Busslinger M. Cooperation of Pax2 and Pax5 in midbrain and cerebellum development. Proc Natl Acad Sci U S A. 1997;94(11):5703-8.

306. Marlow FL. Maternal Control of Development in Vertebrates. 2010.

307. Wan LB, Pan H, Hannenhalli S, Cheng Y, Ma J, Fedoriw A, et al. Maternal depletion of CTCF reveals multiple functions during oocyte and preimplantation embryo development. Development. 2008;135(16):2729-38.

308. Moore JM, Rabaia NA, Smith LE, Fagerlie S, Gurley K, Loukinov D, et al. Loss of maternal CTCF is associated with peri-implantation lethality of Ctcf null embryos. PLoS One. 2012;7(4):e34915.

309. Fedoriw AM, Stein P, Svoboda P, Schultz RM, Bartolomei MS. Transgenic RNAi reveals essential function for CTCF in H19 gene imprinting. Science. 2004;303(5655):238-40.

310. Rubel CA, Franco HL, Jeong JW, Lydon JP, DeMayo FJ. GATA2 is expressed at critical times in the mouse uterus during pregnancy. Gene Expr Patterns. 2012;12(5-6):196-203.

311. Rubel CA, Wu SP, Lin L, Wang T, Lanz RB, Li X, et al. A Gata2 dependent transcription network regulates uterine progesterone responsiveness and endometrial function. Cell Rep. 2016;17(5):1414-25.

312. Simeonova E, Garstka M, Koziol-Lipinska J, Mostowska A. Monitoring the mitochondrial transmembrane potential with the JC-1 fluorochrome in programmed cell death during mesophyll leaf senescence. Protoplasma. 2004;223(2-4):143-53.

APPENDIX

Extracellular Vesicles in Human Reproduction in Health and Disease

Carlos Simon,[1,2,3,4]* David W. Greening,[5]* David Bolumar,[1,2]* Nuria Balaguer,[1,2] Lois A. Salamonsen,[6,7,8] and Felipe Vilella[1,2,4]

[1]Igenomix Foundation, 46980 Valencia, Spain; [2]Instituto de Investigación Sanitaria Hospital Clínico (INCLIVA), 46010 Valencia, Spain; [3]Department of Pediatrics, Obstetrics and Gynecology, School of Medicine, Valencia University, 46010 Valencia, Spain; [4]Department of Obstetrics and Gynecology, Stanford University, Palo Alto, California 94304; [5]Department of Biochemistry and Genetics, La Trobe Institute for Molecular Science, La Trobe University, Melbourne, Victoria 3086, Australia; [6]Centre for Reproductive Health, Hudson Institute of Medical Research, Clayton, Victoria 3168, Australia; [7]Department of Molecular and Translational Science, Monash University, Clayton, Victoria 3168, Australia; and [8]Department of Obstetrics and Gynaecology, Monash University, Clayton, Victoria 3168, Australia

ABSTRACT Extensive evidence suggests that the release of membrane-enclosed compartments, more commonly known as extracellular vesicles (EVs), is a potent newly identified mechanism of cell-to-cell communication both in normal physiology and in pathological conditions. This review presents evidence about the formation and release of different EVs, their definitive markers and cargo content in reproductive physiological processes, and their capacity to convey information between cells through the transfer of functional protein and genetic information to alter phenotype and function of recipient cells associated with reproductive biology. In the male reproductive tract, epididymosomes and prostasomes participate in regulating sperm motility activation, capacitation, and acrosome reaction. In the female reproductive tract, follicular fluid, oviduct/tube, and uterine cavity EVs are considered as vehicles to carry information during oocyte maturation, fertilization, and embryo–maternal crosstalk. EVs via their cargo might be also involved in the triggering, maintenance, and progression of reproductive- and obstetric-related pathologies such as endometriosis, polycystic ovarian syndrome, preeclampsia, gestational diabetes, and erectile dysfunction. In this review, we provide current knowledge on the present and future use of EVs not only as biomarkers, but also as therapeutic targeting agents, mainly as vectors for drug or compound delivery into target cells and tissues. ***(Endocrine Reviews 39: 292 – 332, 2018)***

ISSN Print: 0163-769X
ISSN Online: 1945-7189
Printed: in USA

Received: 13 October 2017
Accepted: 25 January 2018
First Published Online:
30 January 2018

Intercellular communication is an essential process both for multicellular organisms and for the relationship of unicellular organisms with the environment and hosts (1). Classically, communication has been identified as indirect as endocrine, paracrine, and autocrine or direct via cell-to-cell contact, secretion, release, and uptake of chemical moieties such as hormones, growth factors, or neurotransmitters (2, 3). According to the Human Protein Atlas, nearly 39% of the human protein-coding genes are annotated to give rise to membrane (28%) and secreted (15%) forms of signaling protein variants, some producing both isoforms and posttranslational modifications that can alter function. These molecules, which constitute potential therapeutic targets, include cytokines, growth factors, and coagulation factors, among others, playing physiological and pathological roles in processes such as immune defense, blood coagulation, or matrix remodeling. Of note, >500 of these proteins are currently known as pharmacological targets, with already approved druggable targets available commercially.

A new mechanism has recently been in the spotlight for cellular communication: the release of membrane-enclosed compartments, most commonly regarded as extracellular vesicles (EVs). EVs can act to convey molecules from one cell or tissue to another. Importantly, their contents (cargo) are protected from extracellular degradation or modification. They exert their biological roles by either direct interaction with cell surface receptors or by transmission of their contents by endocytosis, phagocytosis, or fusion with the membrane of the target cells. Recipient cell specificity appears to be driven

 doi: 10.1210/er.2017-00229

ESSENTIAL POINTS

- Extracellular vesicles are a newly identified mechanism of cell-to-cell communication, recently discovered as a communication between the mother and the embryo
- Extracellular vesicles play an important role in normal physiology and in pathological conditions in human reproduction
- Prostasomes participate in regulating sperm motility activation
- Different extracellular vesicles and their cargo are implicated in promoting oocyte development and maturation
- Exosomes and their cargo in microRNAs play an important role in embryo implantation
- Extracellular vesicles are involved in the triggering, maintenance, and progression of reproductive and obstetric pathologies
- The participation of extracellular vesicles in human reproductive health has made them appealing players as biomarkers and to carry therapeutic agents

by specific receptors between the target cells and EVs (4–6). EVs have been described in different body fluids, including semen (7), saliva (8), plasma (9), breast milk (10), urine (11), and amniotic fluid (12), among others (4).

EVs can be classified in different populations based on their biogenetic pathway, composition and physical characteristics, such as size or density, giving rise to three major categories: apoptotic bodies (ABs), microvesicles (MVs), and exosomes (EXOs) (5, 13, 14).

EV content is complex as a continually progressing field with new cargos being identified continually. Regrettably, owing to technical limitations in methods of isolation and differentiation of the different populations of EVs, mixed, heterogeneous populations are often used, making interpretation of their content and functionality difficult (15–17). This constitutes a salient notion in the field at present, that populations of EV subtypes must be considered when reviewing published literature. With homogeneous sample preparation and key developments in characterization of EVs, we now hold important insights into defining these selected communicators in far greater depth. With the implementation of high-resolution and sensitive instrumentation for characterization such as mass spectrometry and next generation deep sequencing, it has been possible to develop databases gathering information about protein, lipid, and RNA content of EVs from different sources, including ExoCarta (online source: www.exocarta.org) (18), EVpedia (online source: www.evpedia.info) (19), and Vesiclepedia (online source: www.microvesicles.org) (20).

In recent years, EVs have been shown to participate in different processes committed to the maintenance of the normal physiology of the organism such as tissue repair, maintenance of the stem cell status of progenitor cells, platelet and immune function, and nervous system homeostasis. The potential role of EVs in the pathogenesis of different diseases has also been studied, with cancer, autoimmunity, neurodegeneration, HIV-1 infection, and prion diseases being the widest studied areas (1, 6, 21). In all of these cases, EVs are unique, as they became small indicators of an organism's homeostasis that can stably travel over the body fluids. That their content reflects cell of origin and pathophysiological states highlights their usefulness as biomarkers. Importantly, EVs are attributed with the potential to cross tissue barriers, such as the blood–brain barrier, possibly by transcytosis. This fact makes them appealing targets for therapeutics development (22). EVs can be released in response to cell activation, pH changes, hypoxia, irradiation, injury, exposure to complement proteins, and cellular stress (23–25). Interestingly, EVs are also secreted by plant cells (26, 27), as well as pathogens (28, 29), including bacteria, mycobacteria, archaea, and fungi (30, 31), suggesting an important evolutionary conserved mechanism of intercellular signaling.

In the field of reproductive biology there is growing interest in understanding the role of EVs within the male and female reproductive tracts, as they may constitute a new mechanism of communication between the reproductive tract and the immature germ cells, or between the mother and the developing embryo. Such developments offer great potential implications in the establishment of a successful pregnancy or implications with understanding associated pathological conditions (32). In the present review, we address current knowledge on the existence and functionality of EVs as cell-to-cell messengers in normal human reproductive physiology, as well as their contribution in the triggering, maintenance, and/or progression of pathological conditions in the functionality of the reproductive tract. Furthermore, we discuss their usefulness as biomarkers of altered reproductive conditions such as preeclampsia, spontaneous preterm birth (SPB), or polycystic ovaries syndrome. Finally, we summarize current knowledge on the present and future of the use of EVs as therapeutic agents, mainly as vectors for drug or compounds delivery into target cells and tissues.

Types, Isolation, and Characterization of EVs and Cargo

EV heterogeneity

EVs can be classified into selected subtypes according to different criteria, that is, cellular origin, biophysical (density and size) and biochemical (biological markers) characteristics, biological function, and biogenetic pathway. According to their biogenetic mechanism of formation and release, three main classes of EVs are defined: ABs, MVs, and EXOs (Fig. 1).

Apoptotic bodies

ABs are EVs produced by plasma membrane blebbing in cells undergoing programmed cell death. This term was coined by Kerr *et al.* (33) who defined them as "small, roughly spherical or ovoid cytoplasmatic fragments, some of which contain pyknotic remnants of nuclei." Indeed, one of the events that characterizes ABs is the fragmentation and packaging of cellular organelles such as the nucleus, endoplasmic reticulum (ER), or Golgi apparatus into these vesicles (34, 35).

ABs have widely been described as 1 to 5 μm in diameter, thus overlapping with the size range of platelets (36, 37), although some groups extend this range to 50 nm (16, 38, 39). Their buoyant density in a sucrose gradient is in the range of 1.16 to 1.28 g/mL (40, 41).

This vesicle population is characterized by cytoskeletal and membrane alterations, including the translocation of phosphatidylserine (PS) from the inner to the outer leaflet of the lipid bilayer (42). In this way, PS serves as an "eat me" signal for phagocytes to target and clear apoptotic debris (43, 44). Moreover, PS can naturally be recognized by annexin V, which is a useful marker of ABs (45). Nevertheless, care should be taken when using annexin V for this purpose, as PS flipping can also be triggered by other stimuli such as mechanical disaggregation of tissues, enzymatic treatments for detachment of cells, electroporation, chemical transfections, or retroviral infections, and PS exposure has also been described in healthy cells (46). PS flipping also induces MV formation, so these can also be recognized by annexin V detection (47, 48). Another specific feature of ABs is the oxidation of surface molecules, creating sites for recognition of specific molecules such as thrombospondin (49) or C_3b complement protein (50), which are also useful as markers of ABs.

Included in newly identified potential molecular markers of ABs, VDAC1 is a protein that forms ionic channels in the mitochondrial membrane and has a role in the triggering of apoptosis. It proves to be a useful AB marker, as its biological function and subcellular localization are characteristic of this vesicular fraction (39). Calreticulin is an ER protein that could also work as an AB marker due to its subcellular localization (15), although it has also been observed in the smaller sized MV fraction (39). It is possible that, during the apoptosis process, the ER membrane is fragmented and forms vesicles smaller in size than ABs, which would contain calreticulin and would sediment at higher centrifugal forces (51, 52). Indeed, proteomic studies have related calreticulin with vesicular fractions across the full size range of MVs (53) and ABs (54).

Different functions have been attributed to ABs, although most are also features of other EVs. DNA can be horizontally transmitted between somatic cells, with possible integration of this DNA within the receptor cell where it can be functional (55). These vesicles are also a vehicle for the horizontal transfer of oncogenes, which are internalized by target cells and consequently increase their tumorigenic potential *in vivo* (56, 57). ABs have also been related to the immune response where they are associated with an underactivation of the immune system (58) and with antigen presentation with special regard to self-tolerance (59–61).

Microvesicles

MVs were reported for the first time by Chargaff and West (62) as being sedimented at high-speed centrifugation (31,000 × *g*) (not specifically at lower speeds such as 5000 × *g*). MVs are a population of EVs that are formed and released directly from the cell plasma membrane by outward budding and fission from viable cells (63, 64). Plasma membrane blebbing is triggered by different mechanisms that are accompanied by the remodeling of the membrane proteins and lipid redistribution, which modulate membrane rigidity and curvature (65). Such changes within the periphery of the plasma membrane have been associated with cargo sorting in MVs (66).

The size range of MVs has been classically established between 100 and 1000 nm (67), thus overlapping with that of bacteria (13). Some groups extend this range up to 1500 nm (68) or even 2000 nm (69–71). The buoyant density of MVs is not as clear as that of other vesicle populations: ~1.16 g/mL in sucrose gradient (71) or 1.04 to 1.07 g/mL (72). The flotation density in iodixanol gradient is between 1.18 and 1.19 g/mL (73).

As a proposed marker for MV populations, ARF6 is a guanosine triphosphate–binding protein that is implicated in the regulation of cargo sorting and promotion of the budding and release of MVs through activation of the phospholipase D metabolic pathway (65, 74). Additionally, data coming from our current knowledge on proteomic studies suggest numerous proteins (*e.g.*, KIF23, RACGAP1, exportin-2, chromosome segregation 1–like protein) as unique and/or enriched for MVs and potentially discriminatory markers (75). Nevertheless, care should be taken with these results, as different EV cell sources and

Figure 1. Main types of EVs present in body fluids and culture media. EVs are classified in three groups according to their biogenetic pathways. EXOs are produced in the endosomal pathway by invagination of the membrane of late endosomes to form intraluminal vesicles (ILVs) enclosed in multivesicular bodies (MVBs). MVBs can then fuse with lysosomes and degrade their content, or fuse with cell plasma membrane to release ILVs, now regarded as EXOs. MVs are produced directly from the cell plasma membrane by outward budding. ABs are generated as blebs in cells undergoing programmed cell death. EE, early endosome; ExV, exocytic vesicle; LE, late endosome.

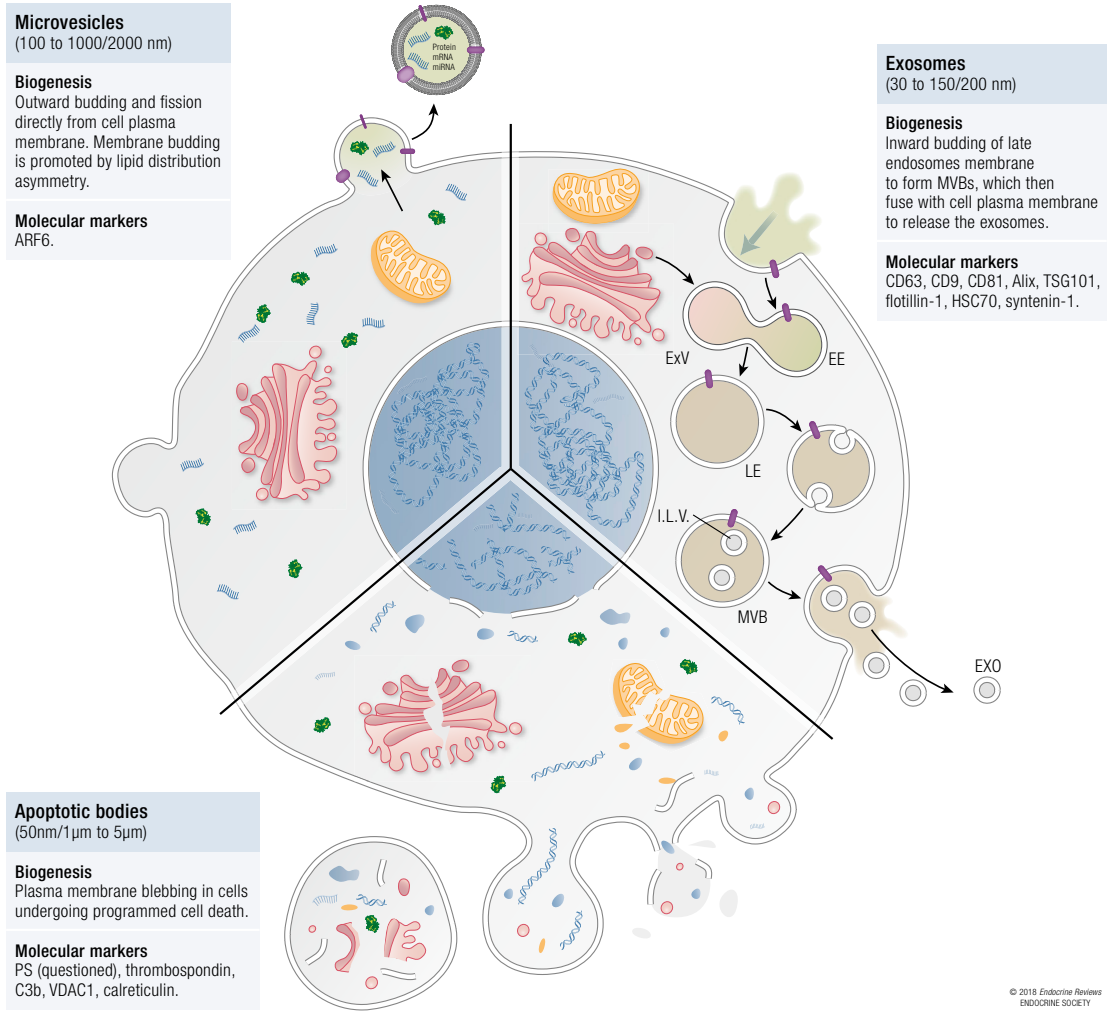

techniques to selectively enrich may lead to differences within EV populations.

Among the functions described for MVs are pivotal roles in cancer cell invasiveness (76, 77), transformation potential (78), progression (63, 79, 80), and drug resistance (81). MVs have also been implicated in autoimmune diseases (82–84), immune system modulation and coagulation (67, 85, 86), embryo–maternal crosstalk (87), and embryo self-regulation (88).

Exosomes

The first description of EXOs in 1981 described them as a second population of vesicles that appeared in the preparations of MVs, and the term "exosome" was coined (89). Two years later, their biogenetic pathway was formally described by transmission electron microscopy (TEM), trying to follow the pathway of uptake and trafficking of transferrin molecules within reticulocytes in an anemic mice model (90). EXOs constitute a population of nano-sized EVs that arise

and are trafficked through the endosomal pathway. Endosomal sorting complexes required for transport (ESCRTs) are important for the biogenesis of multivesicular bodies (MVBs, which include EXOs). MVB inward budding of the limiting membrane of late endosomes facilitates formation of intraluminal vesicles (ILVs) that remain enclosed inside the greater membrane compartment of MVBs. ESCRT-independent mechanisms, including neutral sphingomyelinase/ceramide formation and ARF6/PLD2, have been reported to also occur (73, 91). The formed MVBs can then be targeted to plasma membrane to release ILVs, now known as EXOs, or otherwise fuse with lysosomes to degrade their content (92). Members of the Rab guanosine triphosphatase (GTPase) family have been shown to modulate EXO secretion and are thought to act on different MVBs along ESCRT-dependent and -independent endocytic pathways. It is likely that ESCRT-dependent and ESCRT-independent MVB/EXO biogenesis machineries vary from tissue to tissue (or even cell type) depending on specific metabolic needs. There are several molecular mechanisms, both canonical and alternative, implicated in the formation, release, and extracellular fate of EXOs [see reviews in (5, 75)].

Most studies place EXOs in a size range of 30 to 150 nm (5, 93) or even 200 nm (94), thus establishing an overlap with viruses in terms of size (14). The buoyant density of EXOs in sucrose gradients has been set in a wide range of 1.10 to 1.21 g/mL (38, 95), and 1.10 to 1.12 g/mL in iodixanol gradients (96).

The classically associated markers of EXOs are molecules mainly implicated in the biogenesis of this population, which are incorporated during this process: tetraspanins (CD63, CD9, CD81), Alix, TSG101, and flotillin-1, among others (5, 95). Nonetheless, with the emerging interest in studying different EV populations as isolated entities, many of these classical markers have been identified as widespread between populations, although with different relative abundances. This is the case for at least CD9, CD63, HSC_70, and flotillin-1. Other molecules such as TSG101 and syntenin-1 have been ratified as markers of only this vesicle population (39). PS, while being described as a broad marker of EVs, has also been reported as exposed on the surface of EXOs produced by different cell types (92, 97). Accumulating evidence from *in vitro* studies using cells grown in culture and ex vivo body fluids indicates the existence of more than one EXO subtype (98–105). For example, EXOs contain subpopulations, including the study of EXOs derived from apical (EpCAM-Exos) or basolateral (A33-Exos) surfaces of highly polarized cancer cells, which indicated the presence of two distinct subtypes with distinct protein (98) and RNA cargo (99, 106). The biological significance of these findings awaits further investigation.

Because of the high expectations and efforts dedicated to the study of the role of EXOs in different biological processes, both in physiological or pathological conditions, the field of EXO biology has experienced an exponential growth in recent years, with a wide range of functions identified (1, 107). EXOs are implicated in cancer physiology, participating in tumor progression and maintenance, resistance, immune modulation, and angiogenesis (108). Their function in immune regulation has also been well studied in antigen presentation modulation, immune activation, and suppression (109, 110). Importantly, knowledge of the seminal role of EXOs in reproductive biology is expanding rapidly. Such studies and the molecular markers and mechanisms identified have the potential for use as markers to discriminate between EV subtypes, as well as various applications of EXOs in clinical diagnosis.

Methods of isolation and purification of EVs

The main experimental problem when studying EVs is to achieve a homogeneous separation with appropriate yield of the EV population of interest. Different methods of isolation and purification have been developed; however, to a varying extent, all carry the bias of providing completely homogeneous EV populations of any one vesicle type (summarized in Table 1). In the field, there is a pressing need to define EV surface-exposed proteins for the purpose of generating monoclonal antibodies that would allow discrimination of EV class or subtype (*i.e.*, stereotypical markers). Most rapid, one-step approaches for isolating EVs do not take into consideration that they are dealing with a possible mixture of vesicle classes or subtypes and coisolated contaminants such as high relative molecular mass protein oligomer and protein–RNA complexes (*e.g.*, high-density lipoprotein/low-density lipoprotein/AGO_2) complexes.

Serial differential centrifugation

Differential centrifugation is the most common and well-known method for the isolation of EVs. Although each group adapts the times and centrifugal speeds depending on their samples, the basic protocol as follows: (1) centrifugation at low speed for the elimination of cells (300 × *g*, 10 minutes), (2) centrifugation at up to 2000 × *g* for 10 minutes to pellet membrane debris and ABs, (3) centrifugation at 10,000 to 20,000 × *g* for 30 minutes to pellet MVs, and (4) a crude EXO preparation is pelleted by ultracentrifugation at 100,000 to 200,000 × *g* for 70 minutes. After steps 1 to 3 of centrifugation, supernatants are transferred to new tubes for the isolation of the subsequent EV type. Pellets (steps 2 to 4) containing different cell populations are washed by resuspension in phosphate-buffered saline (PBS) and recentrifugation under the same conditions. The

washing step removes some impurities, but also reduces EV yield.

Apart from vesicle size, centrifugation alone cannot achieve the separation of pure populations for various reasons: sedimentation of other particles in the supernatant depending on density, distance of the particles from the bottom of the tube, and vesicle/particle aggregation (111).

To improve EV population purity, a gradient step can be added to the centrifugation protocol. This system aims to avoid as far as possible the contamination of EV pellets with large protein/protein-RNA aggregates and proteins nonspecifically bound to EVs (4). The essentials of the technique are resuspension of the pellet from the previous serial differential centrifugation in a suitable buffer (*i.e.*, PBS), then loading on either the top or base of a prepared sucrose cushion (112, 113) or a sucrose gradient (114, 115). Following ultracentrifugation, vesicles are recovered either from the bottom of the tube (for cushions) or from a specific fraction of the gradient, depending on their buoyant density. Moreover, substitution of sucrose by a nonionic density gradient medium, called iodixanol (116), offers many advantages: better separation of viral particles from EVs; low toxicity toward biological material; is clinically applicable; and forms isosmotic solutions compatible with the size and shape of EVs in a wide range of densities (117–119).

Size exclusion methods: filtration and chromatography

Filtration for isolation of EVs is often used in combination with ultracentrifugation protocols to improve separation efficiency based on size. Filtration steps using 0.8-, 0.2-, or even 0.1-μm filters can be inserted between the centrifugation steps depending on the size of the desired population (112, 120, 121). Alternatively, ultrafiltration utilizes filtration units of different molecular mass cutoff membranes that are centrifuged at moderate centrifugal forces. They allow concentration of vesicles in the interface of the filters, from which they can be recovered by washing (122–125). All of these methods face several drawbacks. The pressure of the supernatant can cause the EVs to deform or break into smaller vesicles, and the filter membrane may decrease the yield. Gravity filtration has been proposed to cope with the problems associated with elevated pressures (120), but this can be time consuming and filters can become saturated.

Another option for EV isolation in conjunction with ultracentrifugation is based on size exclusion chromatography. In brief, the medium containing the vesicles is loaded into the chromatography device, generally a gel size exclusion column, equilibrated into the column, and eluted with PBS (126–128). The technique is usually coupled with previous low-speed centrifugation to remove larger debris and subsequent ultracentrifugation to wash and concentrate the vesicles from the different chromatography fractions (129, 142). Its advantages are enhanced separation of EVs from proteins and high-density lipoproteins, avoidance of protein and vesicle aggregate formation, reduced sensitivity to the viscosity of the vesicle media, compatibility with the biological properties and functionalities of the isolated vesicles, and preservation of the vesicular structure and conformation (126). Moreover, it offers shorter isolation times and relatively low cost. As a disadvantage, this technique offers reduced EV recovery yields in comparison with others such as ultracentrifugation or polymeric precipitation, although it is susceptible to scale-up (143, 144). Nevertheless, some studies indicate that a combination of size exclusion chromatography and ultrafiltration may produce a yield surpassing that of classical ultracentrifugation (145, 146).

Other approaches

Immunoaffinity uses microbeads coated with specific antibodies for the recognition of specific surface markers of EV populations. In brief, beads are incubated with the sample containing EVs, then beads linked to their epitopes on the EV surface are recovered by magnetism or low-speed centrifugation, depending on the nature of the beads (130, 131). The technique can follow centrifugation and/or filtration to clear large cellular products (96, 99, 132). This method differentiates EV populations based on surface markers regardless of their size. Nevertheless, care should be taken, as population-specific markers are not necessarily available, and the working surface of the beads is limiting, so the EVs may not have access when they are large or present at high concentrations (116).

Aiming for a quicker and simpler method to isolate EVs, a polymeric precipitation system (ExoQuick) was commercially developed. The experimental procedure is as simple as incubating the kit reagents with the EXO-containing media and recovering the resulting polymeric complex by low-speed centrifugation. A study with human ascite samples showed that ExoQuick could provide high concentrations and purity of exosomal RNA and that the high exosomal protein concentrations from the same samples compared well with other isolation methods such as ultracentrifugation, immunoaffinity isolation, and chromatography (133). Even though ultracentrifugation-based protocols are preferable for exosomal protein recovery and purity, ExoQuick obtains better results in terms of exosomal messenger RNA (mRNA) and microRNA (miRNA) yield and quality (134). The method has a series of limitations. Impurities such as lipoproteins are possibly coisolated along with EVs, and the method is unable to provide isolation of different EV subpopulations. It works ideally with small vesicles in the size range of 60 to 180 nm (111).

"Differential centrifugation is the most common and well-known method for the isolation of EVs."

Table 1. Classification of the Methods of Isolation of EVs Based on Their Principles

Method	Technique	Isolation Principle	General Workflow	Advantage	Limitation	References
Centrifugation	Serial differential centrifugation	Sedimentation velocity	Serial or differential centrifugation: (1) 300 × *g*, 10 min to remove cells → (2) 2000 × *g*, 10 min to remove cell debris, ABs → (3) 10,000/20,000 × *g*, 30 min to isolate MVs → (4) 100,000/200,000 × *g*, 70 min to isolate EXOs	• Broad application • Standardization • Ease of use • Reproducibility • Yield	• Sedimentation dependent on density, tube length, sample viscosity, concentration, and vesicle aggregation apart from size	(16, 112, 116, 138)
	Density gradient	Buoyant density	Generally introduced to further purify distinct types of EVs (*i.e.*, MVs or EXOs). Various different reagents, including sucrose or iodixanol. Crude EV populations loaded either on top (float down) or at bottom (float up) of gradient. Ultracentrifugation performed under pre-established conditions	• Purification: increases EV population purity from: protein aggregates, RNA–protein complexes, separation of EV subpopulations within the same type	• Yield	(4, 112–115, 117–119,139)
				• Soft isolation approach	• Reproducibility	
				• Clinically applicable medium (iodixanol)	• Trained user	
				• EV homogeneisty	• Time-consuming	
Size exclusion	Filtration	Size/shape	Generally interspersed within centrifugation steps: prior to centrifugation, supernatants are challenged through syringe filters of determined pore size	• Easy to use	• Yield loss within filtering membrane	(112, 120, 121)
				• Further stringency of the populations based on their canonical sized	• Risk of vesicles deformation or fragmentation.	
				• Reproducibility		
	Ultrafiltration	Size	Centrifugal filtration units of prefixed molecular size range that selectively retain vesicles Previous studies shown to isolate distinct subtypes of EVs using this strategy	• Easy to use	• Yield loss within filtering membrane.	(73, 122–125, 140)
				• Quick technique	• Risk of vesicles deformation or fragmentation.	
				• Reproducible		
	Chromatography	Size/charge	Purification of EVs based on surface charge or size	• High resolving power, improved purification of EVs from proteins and lipid particles	• Usually coupled to centrifugation to remove cell debris and recover EV containing fractions	(126–129, 142)
				• Limits EVs and protein aggregation based on buffer used	• Often issues with volume or buffer associated with elution	
				• Less sensitive to the viscosity of the media		
				• Respectful with EV functionalities and biological properties		
				• Shorter isolation times		

(*Continued*)

Table 1. *Continued*

Method	Technique	Isolation Principle	General Workflow	Advantage	Limitation	References
Immunoaffinity		Presence of specific EV surface molecules	Microbeads coupled to antibodies are incubated with EVs for specific surface markers recognition (*i.e.*, A33, EpCAM, CD63). Afterward, beads are washed and recovered by precipitation or magnetism.	• Separation based on specific molecules further than by size	• Sometimes coupled to centrifugation and/or filtration to initially remove larger cellular debris	(96, 98, 99, 130–132)
				• Selectivity	• Select surface markers of EVs are not always known or available	
				• Resolution	• Cost	
				• Speed of isolation	• Yield	
Polymeric precipitation		Weight increase to pellet at low centrifugal force	Incubation of polymerization kit reagents with EV solution and recovery by low-speed centrifugation	• High speed	• Possibility of coprecipitating impurities	(111, 133, 134)
				• Simple procedure	• Unable to separate EV fractions	
					• Ideal only for small (60 to 180 nm) EV populations	
Microfluidics		Different possible principles:	(1) EVs are passed through microfluidic system and EV-specific markers are recognized by antibodies in a device surface	• Reduced sample volume needed	• Habitually couple to centrifugation to remove undesired EV populations	(135–137, 141)
		(1) Presence of specific molecules	(2) Still not applicable for EVs	• Smaller processing times and costs, maintaining high sensitivity	• Unable to differentiate EVs populations	
		(2) Physical properties such as size	(3) Combination of microfluidics and polymer filter that allow passing EVs under a certain size	• Possibility to process, quantify. and image the samples within the system itself	• Still under development	
		(3) Microfluidic filtration				

A new technology based on microfluidic devices has recently been developed for the isolation of EVs. It allows the reduction of sample volumes, processing times, and costs while maintaining high sensitivity. The chip technology can be based on different principles. The first developed systems relied on the recognition of EVs by specific antibodies on the surface of the device (147). The surface of the flow system was coated with anti-CD63 antibodies. When EV-containing media was pumped through the system, EXOs were restrained. The system allows scanning electron microscopy (SEM) imaging and lysis of EVs for RNA isolation directly on the chip. However, it does not provide sufficient material for protein or functional analyses. Subsequently, the system was expanded with lipophilic staining of EXOs to allow simultaneous quantitation (135). A third microfluidic scheme used physical properties as the principle for EV isolation, separating microparticles based on their size within the micrometric size range (136). Clearly this method is not applicable to EV population analysis. This technology has also been combined with porous polymers, allowing purification of vesicles in the nanometric size range: the pore size can be modulated so that only EVs under a certain size can be filtered (148). A recent study introduced the concept of using a combination of acoustics and microfluidics for a high-purity degree of EXO isolation. The platform is composed of two sequential modules that remove larger components and other EV groups (MVs and ABs, respectively), allowing the direct use of undiluted body fluid samples (tested in whole blood) or conditioned media from cell cultures in a single step. The system is based on the combination of microfluidic channel conformation and adjusted acoustic pressure, which

make it possible to set the cutoff particle diameter (149).

The demands of clinical applications involving diagnostics and therapeutics such as low cost, reliability, and speed can eventually be met with modifications to existing technologies for improved scalability. Isolation of EVs from blood and urine is a challenge due to the presence of abundant and complex protein and lipoprotein networks, which undoubtedly will attenuate intrinsic EV protein/RNA signatures. Distinct clinically relevant strategies to isolate EVs are currently being investigated (75, 150, 151).

Methods for characterization of EVs

Characterization of EVs is fundamental to enable differentiation among the different subpopulations within the same biological sample, between vesicles of distinct cellular origin or even of the same origin in pathological vs physiologically normal conditions (summarized in Table 2).

Microscopy: morphology and size analysis

Electron microscopy techniques are the only method available to provide the appearance of EVs related to their size. Different variants offer different data to the user. TEM was initially used by Raposo *et al.* (152), who described EXOs as cup-shaped vesicles. Although different protocols can be used for TEM visualization, two general schemes offer different views. EVs can be resuspended in fixative media and laid into grids for staining and visualization. Alternatively, EV pellets from centrifugation and ultracentrifugation steps can be fixed, resin embedded, and cut into ultrathin slides, which are then stained and laid in grids. The first method is simpler and less time consuming, and it offers a view of the exterior of the EVs. The second method is more informative, shows the interior of the EVs, and allows immunogold staining of specific markers that are seen as electron-dense spots (153, 154). Cryo-electron microscopy allows direct visualization of frozen EVs without previous fixation and contrast steps. The structures are seen as close as possible to their native states (not dehydrated or fixed) and demonstrate variable EV morphology (155). Indeed, such analysis showed that the classical cup shape attributed to EXOs was an artifact of fixation (2). Finally, SEM offers three-dimensional imaging of the EVs for further morphological description (156, 157).

Atomic force microscopy (AFM) is an alternative for the analysis of size distribution and quantity of EVs within a sample and is based on the scanning of the sample by a mechanical probe, which physically touches the sample, providing topographical information. AFM allows imaging at the subnanometric level. It can be adjusted to air (dry samples) or liquid modes (aqueous samples), and differences in size or number measurements are negligible between them. The possibility of measuring samples in aqueous media is advantageous, as it permits the maintenance of EV physiological properties and structure (158–160). AFM has been efficiently combined with microfluidic isolation devices to provide consecutive isolation and characterization of EVs. Mica-microfluidic chips are also of interest, as they provide a nonconductive flat surface for *in situ* AFM analysis (137, 160).

Size distribution analysis techniques

Nanoparticle tracking analysis (NTA), a light-scattering technique, is now widely used for the assessment of EV size distributions and concentration in the range of 50 to 1000 nm. The principle of the technique is based in the inherent Brownian motion of the particles in a solution: EVs in suspension are irradiated by a laser beam, thus emitting dispersed light. This scattered light is captured by a microscope, and NTA software tracks the movement of each particle in a time lapse. Silica nanospheres have been proposed for standardization, as their refraction index (1.46) is similar to that observed for most EVs (refraction index of ~1.39) (161).

Dynamic light scattering is also used for the assessment of EV size distribution. Although the principle for size determination is also Brownian movement of particles in suspension, the way to attain these data varies from NTA technology. It has limitations when measuring polydisperse samples and those containing big EVs, because the bigger particles scatter more light, masking the smaller ones (162). It is also possible to calculate vesicle concentrations in the samples by direct extrapolation from the distribution representations using mathematical criteria (162).

Tunable resistive pulse sensing (or qNano by its IZON commercial name; Izon Science Ltd., New Zealand) is a novel and less expensive technique for the analysis of particle size distributions. The system is composed of a thermoplastic polyurethane membrane containing nanopores that are selected by size requirements. Currently, the system can measure individual particles in the size range of 30 nm to 10 μm and in the concentration range of 10^5 to 10^{12} particles per milliliter. Because the system analyzes the particles individually, multimodal populations can be studied. Alternatively, a configuration of only one pore type restricts measures to a narrow size range, which is particularly useful for analysis of a specific vesicle population. Combining pores of distinct size and geometry allows widening of this range and analysis of a greater volume of sample (163–165).

Flow cytometry has also been applied to the analysis of size distribution, concentration, and qualitative characteristics of the EVs within a sample. Light scatter flow cytometry allows the analysis of vesicles with a lower size limit of usually between 300 and 500 nm (166, 167), but small EVs, including EXOs,

cannot be studied by this method. However, innovative new flow cytometry technology and the use of fluorescent labeling of EVs has reduced the lower limit of detection to ~100 nm, and it is possible to discriminate between vesicles 100 to 200 nm in size (168, 169). Finally, EVs can be coupled via antibodies to their surface markers, to latex beads of greater size. In this way even nano-EVs can be analyzed, but no quantification or differentiation between vesicle populations is possible (170, 171).

Molecular marker characterization

The most effective and well-accepted approach to measure EV purity is the concentration of a specific EV surface marker antigen. Approaches including western immunoblotting, enzyme-linked immunosorbent assay (ELISA) using surface markers that can be used with adaptation for the quantitation of EVs within a sample (172, 173), and ExoScreen have been used (174).

Another approach for the characterization and quantitation of EVs is based on micronuclear magnetic resonance spectrometry (μNMR) (175) EV labeling with specific EV surface molecular marker antibodies coupled to magnetic nanoparticles enables specific detection by microfluidic μNMR. The technique offers a detection sensitivity level that greatly surpasses ELISA or flow cytometry.

Finally, transmission surface plasmon resonance can provide an alternative method for the molecular characterization and quantitation of EXOs in a system called nano-plasmonic EXO assay. This consists of a gold film patterned with a series of nanohole arrays, each of which is coated with specific monoclonal antibodies for the recognition of EXO-specific proteins. Compared with previous systems, the nano-plasmonic EXO assay is label free, easy to miniaturize and scalable for higher throughput detection, and improves detection sensitivity to a magnitude order lower than that for μNMR (176, 177).

During the past decade, recent studies and groups have used developments in proteomic profiling to characterize specific markers for highly purified EV subtypes (EXOs and MVs). Since the emergence of the interest in studying different vesicles populations as isolated entities, many of the classical markers of EXOs have been uncovered as widespread between populations, although with different relative abundances. This is the case of CD9, CD63, HSC70, EpCAM, and flotillin-1, among others (98, 100). Alternatively, some new molecular markers have been identified and ratified as markers of EXOs, including TSG101, syntenin-1, and Alix/PDCD6IP (39, 100). Numerous proteins found exclusively/enriched in MVs [*e.g.*, KIF23, RACGAP1, chromosome segregation 1–like protein, exportin-2 (CSE1L/CAS)] warrant further study as to their potential use as discriminatory markers for MVs. Furthermore, care should be taken when analyzing PS as a marker of ABs, as it has also been reported to be exposed in the surface of EXOs produced by different cell types (92, 97) and also MVs (47, 48). An in-depth review detailing proteomic insights into EV biology and defining markers for EV subtypes and understanding their trafficking and function was provided by Greening *et al.* (183).

EV cargo

Membrane receptors and cargo content are the most important feature of EVs, because they define their cellular selectively, target, uptake, and functionality, respectively. EV cargo includes proteins, bioactive lipids, various RNAs (including fusion gene and splice-variant transcripts), and DNAs (described later), as well as other cell regulatory molecules (1, 4). To date, most studies have focused on their genetic (particularly RNA and miRNA) and protein content, as sensitive methods exist for their comprehensive analysis and detection.

Protein contents in EVs have been widely studied since the application of mass spectrometry–based techniques (184). EVs have been shown as to be enriched in proteins from cytoskeleton, cytosol, plasma membrane, heat-shock proteins, and proteins involved in EVs biogenesis, whereas proteins from cellular organelles are less abundant (1). From initial studies, EVs were shown to carry commonly widespread EV proteins and a specific subset of proteins, depending on the cell, the type of vesicle, and the method of isolation (5). Moreover, it has been observed that EV number, protein content, and protein concentration vary depending on the stimuli for vesiculation, even in the same subpopulation of vesicles (185).

Cytokines have also been described to be carried by EVs (1). Interleukin (IL)-1β is among the examples of theses soluble mediators that are secreted in EVs. Indeed, secretion pathways of EVs may constitute an alternative to exocytosis for proteins that lack leader signal peptide (186). Another interesting example of cytokine cargo is IL-1α, which has been reported to be selectively carried by ABs but not by smaller-in-size vesicles ($<$1 μm) in endothelial cells (187), thus confirming the cargo sorting into different populations of EVs. Further examples of cytokines released into EVs are IL-18 (188), IL-32 (189), tumor necrosis factor (TNF)-α (190), and IL-6 (191), among many others. During pregnancy, EV cytokine cargo has been shown to be modified toward an increase in comparison with nonpregnancy, maybe contributing to the modulation of maternal immune response against the fetus. Levels of transforming growth factor-β1 and IL-10 were increased in EVs from pregnant women, along with an enhanced ability to induce caspase-3 activity in cytotoxic natural killer (NK) cells, thus promoting an immunosuppressive phenotype through the induction of apoptosis in these cells (192).

"The most effective and well-accepted approach to measure EV purity is the concentration of a specific EV surface marker antigen."

Table 2. Classification of the Methods of Characterization of EVs Based on Their Principles

Method	Technique	Principle	Main Features	Quantitative/Qualitative	References
Microscopy	TEM	Negitive staining of EVs with electron-dense molecules (heavy metals)	• Direct imaging of EV size	• Semiquantitative	(139, 152–154, 178)
			• Size distribution	• Dehydrating (fixation)	
			• Can be coupled to immunogold labeling to stain specific structures	• Possibility to take measures within the imaging field	
	SEM	Covering of molecules with microgold particles and electron reflection scanning	• Three-dimensional imaging of EV structures	• Semiquantitative	(156, 157, 179)
				• Possibility to take measuresments within the imaging field	
	Cryo-electron microscopy	Plunge-frozen in liquid ethane/nitrogen	• Avoids fixation and contrasting steps	• Semiquantitative	(2, 73, 155)
			• Allows seeing structures closer to their native states	• Possibility to take measures within the imaging field	
			• Size distribution	• Highly trained user	
	AFM	Use of a cantilever with a free end that touches the surface to obtain topographical information	• Resolution at the nanometric level	• Quantitative	(137, 158–160)
			• Possibility to analyze both dry and aqueous samples	• Size-distribution profile determination	
			• Can be combined with microfluidic isolation devices	• Require homogeneous EV purification	
			• It does not provide direct imaging of EVs		
Size distribution analysis techniques	NTA	Particles are challenged with a laser beam and forward scattered light is real-time captured by a microscope to calculate sizes based on particles using their Brownian motion.	• Size measures in the range of 50 to 1000 nm	• Qualitative: not only size populations but also EV markers can be analyzed by fluorescent labeling	(161, 180, 181)
			• Standardization is not needed but possible (interest for concentration assessments)	• Quantitative: possibility to get precise size distributions and their associated concentrations in 1-nm intervals	
			• Size distribution	• Cost	
			• Low sample use		
			• Compatibility of fluorescence detectors		
	Dynamic light scattering	Particles are challenged with a laser beam and reflected light is captured by a detector in a certain variable angle. The detector converts time-dependent fluctuations in the scattered light intensity into particle size data.	• Size measurements in the range of 1 to 6000 nm for EV concentrations from 10^6 to 10^9 particles/mL	• Mainly qualitative	(162, 182)
			• Samples can be recovered after the analysis	• Semiquantitative if standards are used	

(*Continued*)

Table 2. *Continued*

Method	Technique	Principle	Main Features	Quantitative/Qualitative	References
			• Limitations with polydisperse samples and those containing big EVs		
	Tunable resistive pulse sensing	A transmembrane voltage is established in a porous membrane. The crossing of EVs through the pores alters the electrophoretic flow causing a resistance that can be translated into size data.	• Size measurements in the range of 70 nm to 10 μm for EV concentrations from 10^5 to 10^{12} particles/mL	• Qualitative	(163–165)
			• Single EV measures that allow multimodal EV population studies	• Quantitative	
			• By modifying pore configuration, the analyzable EV size and sample volume can be regulated		
	Flow cytometry	EVs are swept along by a liquid stream to align them in single file in the center of the stream until the interrogation point, where they are excited by a laser beam. Laser scattered light is gathered by detectors situated 180° (size data) and 90° (morphology or fluorescently stained structure data) to the laser beam.	• Analysis of EVs with a lower size limit of 250 to 500 nm and ability to distinguish vesicles that differ 200 nm in size	• Qualitative: not only size populations but also EV markers can be analyzed	(166–171)
			• New technological developments have reduced the limit of detection to ~100 nm and the discrimination power to 100 to 200 nm	• Quantitative	
			• Possibility to coupling to latex beads for easy marker analysis		
			• No sorting capacity		
			• Dependent on EV surface markers or use of EV fluorescent labels		
Molecular marker characterization techniques	Western blotting/ ELISA	Both techniques share the same principle: proteins are attached to support (membranes or plates, respectively) and challenge with antibodies carrying a certain label.	• Easy to perform	• Qualitative	(39, 172, 173)
			• Cheap and available	• Semiquantitative in the case of western blot and quantitative for ELISA	
			• Relatively quick		
	ExoScreen	ELISA sandwich-like system with modifications in the detection tandem. The method relies on that all the components of the system must stay closed (~200 nm, within the same vesicle) for laser stimuli transfer and detection.	• Reduced time consumption	• Qualitative	(174)
			• Increased sensitivity	• Quantitative	
			• EV isolation is not mandatory		
			• Little sample volumes are required		
	μNMR	Labeling of specific EV surface molecular markers with antibodies coupled to magnetic nanoparticles and detection by microfluidic μNMR	• Greatly higher sensitivity	• Qualitative	(175)
				• Quantitative	
	Nano-plasmonic EXO assay	A gold film with nanoholes coated with specific antibodies for the recognition of exosomal proteins is light-excited, generating surface plasmons. Joining of EVs to the antibodies causes plasmon intensity changes that are proportional to the amount of joined EVs.	• Label-free	• Qualitative	(176, 177)
			• Easy to miniaturize	• Quantitative	
			• Scalable for higher throughput detection		
			• A magnitude order more detection sensitivity than μNMR		

Abbreviations: ELISA, enzyme-linked immunosorbent assay; μNMR, micronuclear magnetic resonance spectrometry.

Lipid content of EVs has been much less studied. However, some groups have shown that EVs are enriched in certain types of lipids in comparison with their parent cells, demonstrating the sorting of these molecules. Specifically, vesicles are enriched in sphingomyelin, cholesterol, PS (193, 194), ceramide and its derivate, and, in general, saturated fatty acids (195). It is also remarkable that the lipid/protein ratios are higher in vesicles than in parent cells. In contrast, phospatidylinositols, phospatidylglycerols, phosphatidylcholine, and phosphatidylethanolamines are more present in parent cells than in vesicles (193). Recently, when using mass spectrometry, quantitative lipidomic combinations of three lipid species were shown to distinguish cancer patients from healthy controls (196).

RNAs in EVs were first described by Valadi *et al.* (197) in mast cells. They found that EXOs released by these cells contained mRNAs and miRNAs and were able to transfer their content to other cells, where mRNA was functional and could be translated into protein. More recent studies using high-throughput sequencing techniques have shown that EXOs contain various classes of small noncoding RNAs in addition to mRNA, that is, miRNA, small interfering RNA (siRNA), small nucleolar RNA, Y RNA, vault RNA, ribosomal RNA, transfer RNA (tRNA), long noncoding RNA, and piwi-interacting RNA (198–200). Ng *et al.* (171) showed that endometrial epithelial cells cultured *in vitro* produced EVs containing a different miRNA profile from that of parent cells, thus suggesting a sorting mechanism of these miRNAs into EXOs. This could constitute a mechanism for communication between the mother and the embryo with potential implications in embryo implantation. Indeed, bioinformatic studies on the EV miRNAs showed that some of the genes targeted by the miRNAs are involved in implantation. More recently, our investigation group deepened the knowledge of maternal–embryo crosstalk and demonstrated that EXOs containing miR-30d were actively transferred from endometrial epithelial cells to trophoblastic cells, were the miRNA was subsequently internalized (156).

A major problem concerning RNA analysis from EVs is the variability of the results depending on the methodology used for isolation of cells and obtaining data. One of the major factors affecting this variability is the possibility that the RNA present in the medium, for example, from lysed cells, could stick to the external EV walls, thus being isolated along with internal RNA. In this sense, RNase A treatment previous to EV RNA isolation should be conducted (201). Even with this procedure, it has been stated that extravesicular RNAs associated with proteins, such as miRNAs in complex with argonaute proteins, can circumvent RNase A degradation, thus leading to bias in interpretation of results. This protective role of protein complexes has been reported in extravesicular medium (202, 203) and inside EVs (204). To overcome complex protection, treatment with proteinase K has been proposed for dissociation of RNA–protein complexes (205). Nevertheless, negative impact in EV yields should be investigated, as proteases may provoke vesicle lysis.

Less has been reported regarding DNA content in EVs. Some studies have currently reported the presence of double-stranded DNA in EVs (206, 207), even distinguishing a different pattern of content among EV subpopulations (208). A previous study conducted in a similar way in tumor cells, using DNase to cleave extravesicular DNA, showed that EV DNA was more abundant in MVs from tumor cells than from normal cells and that this DNA was mainly single stranded (209). It has been shown that mitochondrial DNA can also be transported between cells inside EXOs, possibly constituting a pathway to transmit altered mitochondrial DNA and associated pathologies (210). This may serve as evidence of a *trans*-acting function of DNA, being able to have functional effects on the recipient cells.

Of note, both the amount and content of EV genetic cargo can be hormonally regulated in EXOs from target cells: this is of particular relevance to reproductive tissues and is further discussed later.

EV mechanism of recognition and uptake

Mechanisms of EV uptake

For EVs to act in cell–cell signaling, they must recognize their specific cellular target, bind to that cell, and undergo internalization (Fig. 2).

Target cell recognition. EVs may interact with recipient cells by direct signaling through ligand/receptor molecules on their respective surfaces or by direct fusion of EV and recipient cell plasma membranes (211) through lipid raft–, clathrin-, and calveolae-dependent endocytosis, micropinocytosis, and phagocytosis (212–217).

Cell surface and integral membrane/adhesion proteins on distinct EVs are important in mediating associated cell recognition and adhesion. These include integrin pairs: for example, distinct EXO integrin repertoires, specifically integrins $\alpha_6\beta_4$ and $\alpha_6\beta_1$, were identified as associated with lung metastasis, whereas EXO integrin $\alpha_v\beta_5$ associated with liver metastasis (218). The integrin profile of each EXO subtype permits selective cellular targeting.

Differences in EXO tetraspanin complexes also appear to influence target cell interaction *in vitro* and *in vivo*, possibly by modulating the functions of associated integrin adhesion molecules (219). EXO capture by dendritic cells was reduced by 5% to 30% following coincubation with blocking antibodies specific for various integrins, adhesion molecules, or tetraspanins (212). Other membrane proteins reported as important in targeting selected EVs to recipient cells

Figure 2. Pathways shown to participate in EV uptake by target cells. EVs transport signals between cells and facilitate selective reprogramming. EVs have been shown to be internalized by cells through (1) phagocytosis and (2) clathrin- and (3) caveolin-mediated endocytosis. There is also evidence to support their interaction with (4) lipid rafts resulting in EV uptake. Lipid rafts are involved in both clathrin- and caveolin-mediated endocytosis. EVs may also deliver their protein, mRNA, and miRNA content by (5) fusion with the plasma membrane. EVs can be internalized by (6) macropinocytosis where membrane protrusions or blebs extend from the cell, fold backward around the EVs, and enclose them into the lumen of a macropinosome; (7) alternatively, EVs are macropinocytosed after becoming caught in membrane ruffles. On the other hand, (8) intraluminal EVs may fuse with the endosomal limiting membrane following endocytosis to deliver their protein, mRNA, and miRNA cargo and elicit a phenotypic response.

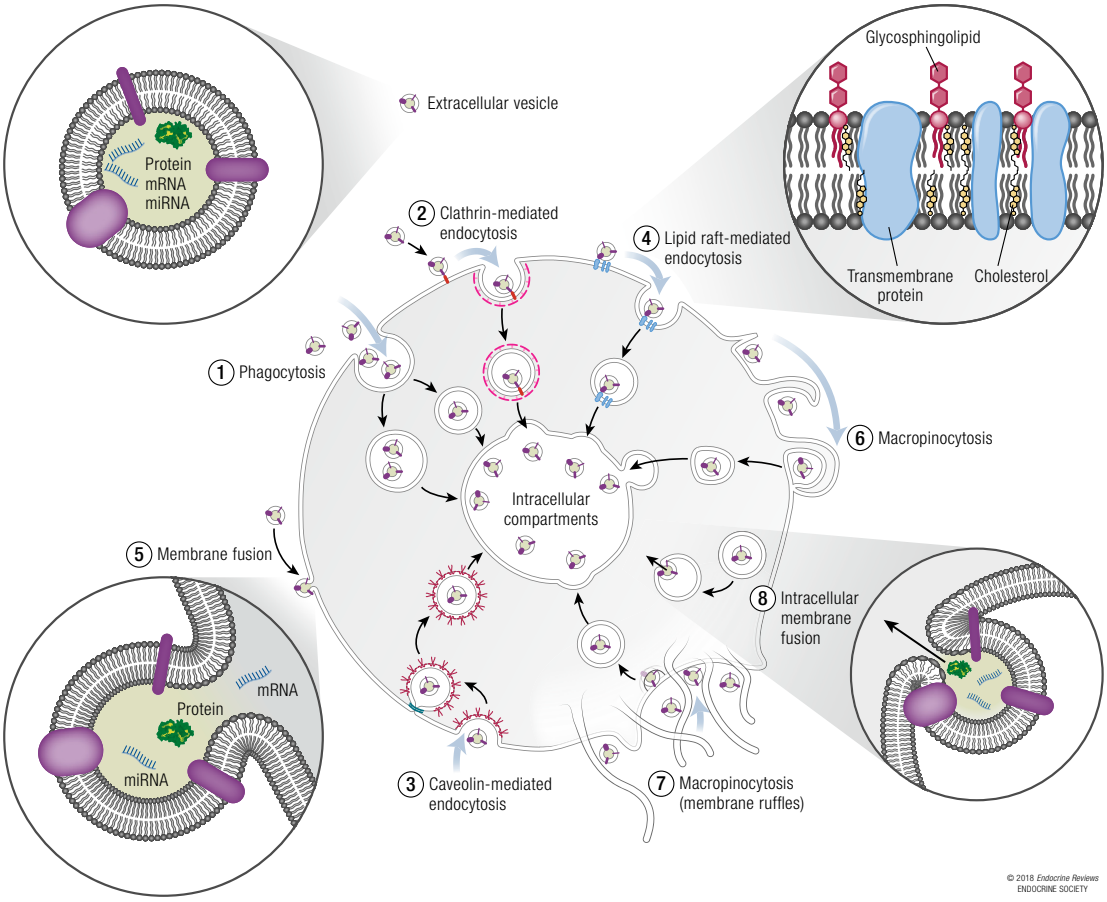

include intercellular adhesion molecule 1 and milk fat globule–epidermal growth factor VIII protein (220, 221). Furthermore, the delivery efficiency of EXOs to cells is reported to be directly related to rigidity of cargo lipids, including sphingomyelin and (*N*-acetylneuraminyl)galactosylglucosylceramide (23).

Recent new data indicate that proteoglycans and lectins can participate in EXO binding and internalization. Proteoglycans are cell surface proteins, whereas lectins, such as galectins 1, 3, and 5, which recognize and bind proteoglycans, are identified on EVs. Indeed, proteoglycan receptors along the plasma membranes of cells and proteoglycans on EXO surfaces have been shown to promote docking (222).

Exosome uptake and release of cargo. EV internalization by recipient cells is reported to occur via multiple processes such as phagocytosis (197, 212, 213), clathrin-mediated endocytosis (223), macropinocytosis (217), receptor interaction (224), and direct fusion (23). However, a better understanding of the underlying mechanisms and, importantly, whether EV subtypes have distinct mechanisms of uptake at their target cell specificity is required (225–229) [reviewed in (230)].

EV uptake is readily demonstrated in cell culture using fluorescently labeled EVs (91). Uptake and cargo

release occur very rapidly, within minutes to hours. However, such techniques do not absolutely prove release, as it is possible that the transfer and spread of fluorescence results from the culture conditions and lipid/membrane transfer.

Recent developments in modification of EVs have also facilitated monitoring and tracking their behavior, interaction, and transfer *in vivo* (231). Intracellular probes are used to fluorescently label mRNA within EVs to monitor EV-borne mRNA encoding luciferase. Developments in transgenic mice enable visualization of EV transfer to cells associated with tumor stroma (232) and immune cells (233, 234), whereas EV-mediated transfer of donor genomic DNA to recipient cells supports a mechanism for genetic influence between cells (235). Such *in vivo* approaches have not specifically shown whether transfer involves a direct fusion of EVs with the recipient cells, formation of gap junctions or nanotubes, or phagocytosis of live or apoptotic cell–derived EVs by the recipient cell.

Low pH is important for EXO uptake. There appears to be elevated stability and lipid/cholesterol content of exosomal membranes in an acidic environment (23).

Understanding recipient cell function and regulation by EXOs needs to focus on specific mechanisms of targeting and delivery, uptake, and transfer, including modulation of key signaling pathways in various recipient cells both *in vitro* and *in vivo*. Processes that control target cell recognition and EV uptake are not well understood.

Inhibiting EV recognition and uptake

Although several uptake mechanisms have been proposed for EVs, detailed knowledge regarding the key steps in EV target cell definition and definitive mechanisms of uptake is required (230) particularly because variability is found between cell types in vesicle internalization (236). The use of inhibitors is proving useful in elucidating cell type–specific mechanisms.

As discussed, using fluorescently labeled EVs, internalization can be readily observed *in vitro* within a short period of time (91, 237). Treatment with inhibitory agents such as chlorpromazine to examine clathrin-dependent uptake (214) and specific RGD inhibitory peptides (238) to target integrin-mediated EV uptake allows identification of selective processes of internalization. The efficacy of EV exchange between cells probably depends on their surface antigen repertoires because partial digestion of membrane proteins exposed on EVs with proteinase K can significantly decrease their uptake (214), and blockage of selected integrins or tetraspanins with monoclonal antibodies also has suppressive effects on EV internalization (212). Furthermore, the use of cytochalasin D, which interferes with actin polymerization and endocytosis, significantly reduces the uptake of EVs (214, 215). Similarly, the inhibition or knockout of dynamin, a GTPase responsible for formation of endosomal vesicles, significantly suppresses EV uptake (216). Further research is needed to understand the precise mechanisms that underpin distinct EV entry into selected target cells and importantly how to control this process.

EVs as Messengers in Reproductive Physiology

Normal reproductive processes are highly dynamic, with well-characterized stages. The considerable intercellular interactions involved at each stage have prompted the study of the involvement of EVs in both the male and female reproductive tracts, from preconception to birth. EVs associated with reproductive biology have been specifically identified and studied in different fluids such as prostatic and epididymal fluid (239), seminal fluid (7, 155), follicular fluid (240, 241) oviductal fluid (242, 243), cervical mucus (244), uterine fluid (156, 171), amniotic fluid (115, 245), and breast milk (246), as well as the originating tissues [reviewed in (247)] (summarized Table 3).

There are currently increasing data pointing to EVs as key regulators of different reproduction processes such as sperm and ovum maturation, coordination of capacitation/acrosome reaction, prevention of polyspermy, endometrial embryo crosstalk, and even communication between *in vitro*–cocultured embryos leading to quorum improved development (291). In these initial steps of the reproductive process (*e.g.*, preconception) EVs are widely produced by different organs and show specific functions. Once implantation has taken place, production of EVs continues throughout pregnancy, with the placenta being the main source of EVs. During early pregnancy, EVs are released by the extravillous trophoblast (EVT). Later on, the syncytiotrophoblast (STB) is formed and establishes contact with maternal blood flow. From here on, STBs constitute the main site of EV generation, and these EVs get access to the maternal systemic vasculature, where they show important roles in immune modulation, either for the innate or the adaptive response (32). Of note, EVs are also found in amniotic fluid, where they are attributed to inflammatory and procoagulant activities (292), and in maternal breast milk. In the latter case, an important influence of EV recovery procedure has been detected on subsequent analysis (293). Among attributed roles, milk EVs have been involved in bone formation, immune modulation, and gene expression regulation, with special emphasis for long noncoding RNAs (246, 294).

EVs in the male reproductive tract: epididymis and prostate

After leaving the seminiferous tubules, spermatozoa (SPZ) are still immature cells. SPZ are stored in the epididymis where they undergo a series of morphological and biochemical modifications that provide them with motility and fertilization ability in their transit from the caput to the cauda, a process called sperm maturation (295, 296). During ejaculation, SPZ mix with seminal fluid from the seminal vesicles, the prostate, and the bulbourethral gland to form the ejaculated semen, which is ejected into the vaginal cavity. Seminal fluid composition is crucial in promoting sperm motility and genomic stability (295, 297). Moreover, it contributes to the establishment of maternal immune tolerance (298, 299). Subsequently, as SPZ travel through the female reproductive tract to the upper fallopian tube where fertilization occurs, they interact with the endometrial and tubal milieu. Finally, to achieve successful fertilization, SPZ undergo capacitation: sperm head membranes undergo a series of biochemical modifications that enable the acrosome reaction when the spermatozoon reaches the zona pellucida of the oocyte. This leads to the release of enzymes that allow SPZ to penetrate the zona pellucida and fuse with the oocyte plasma membrane (300–302). In this context, secretions from the different components of the male and female reproductive tracts have been proposed to play a sequential role in programming sperm function (303).

Epididymosomes

Epididymosomes (EVs originating from the epididymis) were first described in 1967 by Pikó (304) in the Chinese hamster as having diameters between 20 and 100 nm and being associated with the SPZ acrosomal membrane (305). More recently, it has been shown that epididymosomes are a population of roughly spherical bilayered vesicles that display heterogeneity both in size and content that varies between the different segments of the epididymis. Their sizes range from 50 to 800 nm or even to 2 to 10 μm in the first segments of the caput (239). Their lipidic composition also varies: indeed, an increase in sphingomyelin and a general decrease in the other phospholipids and in the proportion of cholesterol occurs with epididymal progression from the caput to the cauda. This is in contrast to SPZ, where the proportions remain more constant. Epididymosomes also have an increased ratio of saturated/unsaturated fatty acids from the caput to the cauda, whereas the opposite situation is found in SPZ. Taken together, these data indicate that epididymosomes tend to gain membrane rigidity whereas SPZ membranes tend to become more fluid (239).

Two main classes of epididymosomes have been identified: CD9-positive epididymosomes, which preferentially bind live SPZ, and ELSPBP1-enriched epididymosomes, which present higher affinity for dead SPZ (306). CD9-positive epididymosomes are EVs of size ranging from 20 to 150 nm (307). These were recovered by ultracentrifugation from the total epididymal fluid EVs, specifically in the epididymis cauda. CD9-positive epididymal cargo transferred to SPZ includes proteins involved in sperm maturation, namely P25b, GliPr1L1, and MIF (248–250), in contrast to ELSPBP1, which was widespread between all EVs. Moreover, CD9, in cooperation with CD26, plays a role in promoting this transfer (307).

ELSPBP1-enriched epididymosomes constitute a subpopulation of vesicles obtained from the epididymal fluid by high-speed ultracentrifugation (120,000 × *g*) after SPZ and debris removal at 4000 × *g* (308). It had been suggested that ELSPBP1 allowed distinction between dead and viable SPZ, as it was only detectable in the dead SPZ population (309). Later, the same group demonstrated that epididymosomes were the only path for the transmission of molecules including ELSPBP1 to dead SPZ (307, 308). Interestingly, ELSPBP and biliverdin reductase A (BLVRA) can associate and bind in tandem to dead SPZ, concurrently with the epididymal maturation of SPZ, a process during which these cells cease producing BLVRA. Therefore, BLVRA could act as a quencher of reactive oxygen species generated by dead and immature SPZ, protecting viable SPZ from oxidative stress. Moreover, BLVRA may be involved in hemic protein catabolism, changes also important in the SPZ maturation process (251, 306).

Because the epididymis brings SPZ to functional maturity before they enter the vas deferens, it is not surprising that epididymosomes serve as a means for protein transfer into SPZ during their transit in the epididymal duct. Some epididymosomal proteins have proven roles in sperm maturation: these include P25b, MIF, or sperm adhesion molecule (SPAM1), among others (252, 310). SPAM1 is a hyaluronidase with roles in both fertilization and sperm maturation. It is transferred to SPZ from epididymosomes, increasing their ability for penetrating the oocyte cumulus (253). Another protein transferred to SPZ by this mechanism is ADAM7, which is important for sperm motility, morphology, and establishment of membrane correct protein composition (254, 255). Of note is the transfer of the plasma membrane ATPase 4 (PMCA4), a major Ca^{2+} efflux pump, into epididymosomes: this plays a pivotal role in SPZ maturation and motility (253). Glutathione peroxidase 5 associates with SPZ during its transit through the epididymis, protecting them from lipid peroxidation stress and, independently, is transferred to SPZ via epididymosomes (256). Finally, components of the Notch pathway are described

"Normal reproductive processes are highly dynamic, with well-characterized stages."

Table 3. Main Functions of EVs in Reproductive Physiology Classified by Their Origin

EV Type	Main Features	Target	Function	References
Epididymosomes	First described by Pikó in 1967	SPZ	Transfer of molecules involved in sperm maturation (P25b, GliPr1L1, MIF, SPAM1, PMCA4)	(248–250, 252, 253)
	Sizes: 50 to 8000 nm or even 2 to 10 μm		Protection from oxidative stress (BLVRA)	(251)
			Protection from lipid peroxidation (glutathione peroxidase 5)	(256)
	Two main classes: CD9-positive (affinity for live SPZ) and ELSPBP1-enriched (affinity for dead SPZ) epididymosomes		Morphology and membrane composition regulation (ADAM7)	(254, 255)
			Sperm motility (ADAM7, PMCA4)	(253–255)
			Small RNA regulation of gene expression	(257, 258, 291)
Prostasomes	First described by Ronquist *et al.* in 1978	SPZ	Enhancement of sperm motility (progesterone receptors, Ca^{2+} cascade signaling components, aminopeptidase N)	(261, 263, 264, 265, 266)
			Protection from acidic female reproductive tract environment	(262)
	Sizes: 30 to 500 nm		Protection from oxidative stress (PMCA4)	(264)
	Unusual lipid composition that provides them with increased ordered structure, rigidity, and viscosity		Prevention of premature capacitation and acrosome reaction (cholesterol)	(260, 267–269)
			Posterior induction of capacitation, SPZ hypermotility, and acrosome reaction at the moment of fertilization (cAMP, progesterone receptors, hydrolases, lipoxygenases)	(270– 274)
			Protection from the hostile female reproductive tract: immunity, oxidative stress, bacteria	(259, 260, 270)
Uterine microenvironment EVs	Wide variety of origins: serum transudates, residues from womb cell apoptosis, endometrial epithelial cells, and conceptus	Endometrium: endometrial origin	Promotion of embryo implantation (specific miRNA cargo)	(171)
	Variations throughout the menstrual cycle	Endometrium: embryo origin	Regulation of endometrial angiogenesis (specific miRNA and protein cargo) and uterine spiral arteries remodeling	(285, 286)
	—	Embryo: endometrial origin	Embryo development (enJSRV *env* gene RNA) and subsequent priming of the endometrium for embryo harboring	(282–284)
			Promotion of embryo implantation (miR-30d, specific protein cargo, influenced by uterine hormones—functional with trophoderm)	(91, 156)
		Embryo: embryo origin	Enhancing of trophoblast cells migratory ability and implantation efficiency (laminin, fibronectin)	(88)
		SPZ	Sperm maturation (SPAM1)	(287)
			Capacitation, acrosome reaction and motility promotion (PMCA4)	(243, 288)
Oviductal EVs	First described for their implications in SPZ final competence acquisition	SPZ	Regulation of SPZ storage and promotion of capacitation, acrosome reaction, and hypermotility (PMCA4a)	(243, 279, 280, 289)
			Regulation of molecule delivery into SPZ (integrins $\alpha_5\beta_1$ and $\alpha_v\beta_3$)	(242)
		Embryo	Enhancement of embryo quality and early development	(281)

(*Continued*)

Table 3. *Continued*

EV Type	Main Features	Target	Function	References
Follicular EVs	First described by da Silvera *et al.* in 2012	Cumulus–oocyte complex	Follicle development and oocyte growth (specific miRNA cargo, ACVR1, ID2)	(275, 277)
	miRNA cargo variation with female age and reproductive aging		Follicle maturation: proliferation of small follicles and inflammatory response of large developed follicles (specific miRNA signatures)	(276)
			Cumulus–oocyte complex expansion and related genes upregulation	(278)

Abbreviation: SPZ, spermatozoa.

in epididymosomes, suggesting that these vesicles transmit Notch signaling at a distance between epididymal epithelial cells, but also between the epididymis and SPZ with important implications for sperm motility (311).

Epididymosomes also convey miRNAs within the epididymal duct. As with proteins, distinct regions of the epididymis produce EVs with a specific set of miRNA whose profiles differ from those of parent cells, suggesting a sorting mechanism (290). Indeed, it has been proposed that epididymosomes may act as modulators of gene expression between sections of the epididymal duct (290). Recent analysis confirmed that they contain >350 miRNA, showing a different profile from that of parent cells and dependent on the region of the epididymis from which they originate. Finally, it was demonstrated that many of these miRNAs are transported into the SPZ (312).

An emerging concept is the transfer of traits to the offspring by epigenomic modifications. In this respect, tRNA has been attributed a new function as a modulator of genetic expression. It was initially discovered that a respiratory syncytial virus infection of lung and kidney cell lines led to the production of specific tRNA fragments (tRFs) that are able to repress the expression of specific mRNAs in the cytoplasm to favor viral replication and survival (313). Subsequently, further examples of tRFs have been described with potential implications in pathological processes, such as cell proliferation in cancer (314). Mature molecules corresponding to tRNA fragments are highly enriched in mature sperm. Interestingly, these fragments are produced by sequence-specific cleavage, giving place to fragments corresponding to the tRNA 5′ end (257). Recently, the transfer of tRFs to maturing SPZ in epididymosomes was demonstrated in mice (258), providing an explanation for the scarcity of these molecules in testicular SPZ but with an increase with SPZ maturation. A tRF (tRF-Gly-GCC) has been identified as transferred to SPZ by epididymosomes. This tRF represses MERVL, an endogenous retroelement that positively regulates a set of genes that are highly expressed in preimplantation embryos. Interestingly, male mice treated with a low-protein diet have a trend (nonsignificant) to increased tRF-Gly-GCC in mature SPZ and to downregulate tRF-Gly-GCC targets in embryos at the two-cell stage. This evidence supports that parental diet can affect the offspring epigenome; however, these preliminary data require confirmation (258).

Prostasomes

Prostasomes were first described as vesicles recovered from human prostatic fluid by centrifugation that were associated with Mg^{2+}- and Ca^{2+}-dependent ATPase activity (315). They are now considered a population of EVs produced by the prostate epithelial cells that interact with SPZ, epididymal, and seminal secretions at the time of ejaculation. They are EVs that range from 30 to 500 nm and are surrounded by lipoprotein bilaminar or multilaminar membranes (259, 316). It is likely that a population of prostasomes is exosomal, as they originate from structures resembling MVBs and exhibit classical EXO markers (317). The lipid composition of prostasomes is unusual and provides them with a characteristic highly ordered structure, rigidity, and viscosity due to several factors: a high cholesterol/phospholipid ratio reaching values of 2, which greatly surpasses the values for most of biological cholesterol-rich membranes; phospholipid composition domination by sphingomyelin, which accounts for almost a half of the phospholipids found in prostasomes (318); and finally prostasomes show a strongly saturated fatty acid profile in comparison with SPZ membranes (319). It has been reported that prostasome uptake decreases the fluidity of SPZ membranes by transfer of lipids directly dependent on the prostasome/SPZ ratio (316, 320). This decrement is crucial, as it stands as a regulator of the acrosome reaction, preventing a premature response (260).

Different roles have been attributed to prostasomes in sperm maturation and function, either directly or indirectly. These include protection of SPZ from the female acidic environment and immune surveillance modulation of SPZ motility, capacitation, acrosome reaction, and fertilizing ability, among others (259, 260, 316, 317).

SPZ motility is vital for a successful fertilizing ability, especially for traversing the cervical mucus and zona pellucida (321). One of the first roles attributed to prostasomes was the enhancement of SPZ motility (261) in a pH-dependent manner, suggesting that prostasomes might alleviate the negative effects of the vaginal acidic microenvironment on SPZ motility, thus showing a protective effect (262). Ca^{2+} has been well known as the major ion promoting SPZ motility and fertility, from initial studies carried out in the hamster (322). Increased SPZ Ca^{2+} levels have been linked to prostasomal delivery, directly depending on the extent of fusion/prostasome concentration and influenced by pH (323). However, it took a decade to identify a mechanism. Park *et al.* (263) showed that a progesterone-triggered long-term sustained Ca^{2+} stimulus is involved in SPZ motility promotion via fusion of (acidic) pH-dependent prostasomes. Specifically, prostasomes transferred progesterone receptors and different Ca^{2+} signaling cascade components to the SPZ neck region where, following progesterone stimulation, they triggered the release of Ca^{2+} from SPZ internal acidic stores to promote SPZ motility (263). Other proteins involved in intracellular Ca^{2+} homeostasis are also transported into SPZ in prostasomes, including PMCA4 (264), which along with nitric oxide synthases (NOSs) are delivered into SPZ by prostasomes. PMCA4 and NOS activity is stimulated by Ca^{2+} ions (324) and, indeed, NOS spatially interacts with PMCA4 to a degree positively related to Ca^{2+} concentration levels. This supports the theory that PMCA4 expels Ca^{2+} from SPZ in the presence of NOS to reduce nitric oxide production and thus oxidative stress, which could reduce SPZ viability, resulting in asthenozoospermia (264). Prostasomes also carry aminopeptidase N, a protein involved in modulating sperm motility, which acts through the regulation of endogenous opioid peptides, such as enkephalins, once in SPZ (265, 266).

Interestingly, EXO-like EVs found in cervical mucus have been reported to carry sialidase activity, which reaches a maximum during the ovulatory phase in healthy women. This is likely involved in modifying the properties of the highly glycoslyated mucus to favor SPZ access to the uterine cavity and tubes (244).

There are scarce data on the nucleic acid cargo of prostasomes and its implications for male reproductive physiology. Prostasomes contain various coding and regulatory RNAs, with potential modulatory functions (199). Interestingly, mRNA and miRNA do not represent most of the prostasomal RNA (317), and it has been postulated that mRNA in semen is predominantly transported inside vesicles whereas miRNA is mostly contained in the vesicle-free fraction of the semen, forming complexes with proteins (204). DNA inside prostasomes apparently represents random regions of the genome and is effectively transported into SPZ (325, 326). Nevertheless, this DNA may be a contaminant from ABs in the semen (327).

Capacitation is a cyclic adenosine monophosphate (cAMP)–regulated process, whose production is in turn promoted by bicarbonate and Ca^{2+} ions and influenced by membrane dynamic changes mainly due to cholesterol composition (259, 317). It has been proposed that prostasomes may act as inhibitors of the capacitation process and acrosomal reaction, mainly through transfer of cholesterol (267, 268). Indeed, this might represent a mechanism to avoid premature capacitation and acrosome reaction (260, 269). A switch between positive and negative regulation exerted by prostasomes may be influenced by the environment or even determined by specific prostasome subpopulations. cAMP promotes capacitation through the protein kinase A (PKA) axis by the simultaneous tyrosine phosphorylation of specific downstream proteins and plasma membrane protein and lipid remodeling. This remodeling breaks down plasma membrane asymmetry, exposing cholesterol molecules to external acceptors to trigger the capacitation process (270). In this context, coincubation of equine SPZ with prostasomes led to increased cAMP levels and tyrosine phosphorylation of PKA cascade proteins, in addition to the prostasome endogenous PKA activity described in previous reports. However, these changes were not correlated with increased capacitation and acrosome reaction rates and reverted after 3 hours of coincubation in capacitating conditions (267). Interestingly, Aalberts *et al.* (270) observed that at least a subpopulation of prostasomes is able to bind to live SPZ only when capacitation-inducing conditions are established, probably to promote hypermotility and acrosome reaction at the precise moment it is needed. Nonetheless, care should be taken when interpolating these results into humans, as they were obtained from a stallion model, a species that deposits its ejaculate directly in the uterus.

Following capacitation, SPZ need to undergo an acrosome reaction to enable penetration of the zona pellucida of the oocyte and fusion of plasma membranes. The zona pellucida glycoprotein ZP3 is mandatory for this process, as it facilitates sperm binding, triggering the acrosome reaction. Nevertheless, the acrosome reaction begins before the SPZ contacts the zona pellucida, probably due to the progesterone-dependent stimulus produced by cumulus cells (328). Conversely, prostasomes have been proposed as inhibitors of the acrosome reaction through the transference of cholesterol to the SPZ (268, 329) or as inducers by facilitating progesterone uptake by the SPZ (271), most likely by the transfer of progesterone receptors (263). Other studies also supporting the promotion of the acrosome reaction via prostasomes include delivery of molecules to the SPZ membrane in a pig model

(272), or progesterone priming, acting via the Ca^{2+} signaling axis (330). Other acrosome reaction–promoting molecules in prostasomes include hydrolases (273) and lipoxygenases (274).

In summary, the role of prostasomes in sperm-fertilizing ability in humans is most likely the result of orchestrated actions. Initially, prostasomes would attach to SPZ after mixing during ejaculation, favored by the acidic environment of the vagina, thus transferring cholesterol to stabilize SPZ membranes and prevent premature capacitation and acrosome reaction. This would enable prostasomes to pass the barrier of cervical mucus adhered to SPZ with subsequent fusion and transfer of their content to the SPZ when the SPZ first contacts the oocyte. At this time, the progesterone secreted by the cumulus cells would activate Ca^{2+}-dependent pathways that promote the capacitation process and acrosome reaction (259).

Finally, of note is the role of prostasomes in protecting SPZ from the potentially hostile female genital tract. They appear to exert roles as protectors from female immunity, antioxidants, antibacterial agents, and the process of semen liquefaction [see reviews in (259, 260, 270)].

EVs in the female reproductive tract: follicular fluid, oviduct/tube, and uterine cavity

Contemporarily with sperm maturation, coordinate oocyte development must be taking place so that both gametes can meet at the appropriate location and time inside the female reproductive tract. Developing oocytes are arrested in prophase I of meiosis in primordial follicles from the fetal period until female reproductive maturity. From this moment, cohorts of these oocytes cyclically restart growth, forming the zona pellucida, while granulosa cells proliferate to form the cumulus, which will support posterior egg fertilization. Concomitantly, meiosis is reinitiated, extruding the first polar body and arresting again at metaphase II during ovulation (331). The resumption of meiosis is stimulated by the luteinizing hormone peak, which in turn is initiated by a surge in estradiol-17β levels due to the secretion by granulosa cells from the preovulatory follicle and results in ovulation 36 hours later (332). After ovulation, the extracellular matrix of the cumulus cells serves as an adhesion dock for the fallopian tubes, through which the eggs travel as far as the ampulla where they await SPZ for fertilization (333). Following fertilization, embryo development to the blastocyst stage proceeds as the embryo passages through the fallopian tubes, reaching the uterine cavity ~4 days after ovulation. The blastocyst undergoes final preparation for implantation into the maternal endometrium in the microenvironment of uterine fluid with implantation occurring 6 to 10 days after ovulation (334).

The process of embryo implantation can only occur during a short period of time during the luteal phase of the menstrual cycle, which has been classically regarded as the window of implantation and that typically extends from 5.5 to 9.5 days after ovulation in healthy normal cycling women (334, 335). At this point, different factors affect and limit embryo implantation, namely embryo quality, endometrial receptivity and embryo–endometrial crosstalk (336), where EVs stand as important potential mediators.

During this process, EVs carry out many different supporting actions: they assist follicle and oocyte development and maturation at the initial stages, and they further assist early embryo development and implantation as the conceptus reaches the uterus. Furthermore, female tract EVs contribute in preparing endometrial vascular net, promote embryo implantation, and prime the endometrium for harboring the embryo. Moreover, these EVs also contribute to SPZ maturity, capacitation, and acrosome reaction coordination, support SPZ storage while waiting for the oocyte, and regulate molecule delivery into SPZ during this period. All of these concepts are discussed in the following sections.

Follicular fluid EVs

Oocyte maturation occurs within the microenvironment of follicular fluid (337). The easy availability of this fluid during oocyte retrieval in assisted reproductive techniques makes it attractive in the search of biomarkers for oocyte quality (338). EVs (resembling EXOs and MVs) were first identified in follicular fluid by da Silveira *et al.* (339), who demonstrated follicular fluid EV uptake by granulosa cells, both *in vivo* and *in vitro*, and their protein and miRNA cargo. EV miRNAs were also present in the surrounding granulosa and cumulus cells, thus suggesting EVs as a vehicle for biomolecule transfer within the ovary. Of particular interest, the miRNA signature of follicular EVs varied with the age of the female, suggesting EV miRNA cargo as an indicative and possible predictor of age-related decline in oocyte quality (339). Subsequently, EV miRNAs were further evaluated and a set of four differentially expressed miRNAs based on age (young/old) was defined. However, these age-related miRNAs were studied in complete follicular fluid samples and as such cannot be confidently attributed to EVs (340).

"Following capacitation, SPZ need to undergo an acrosome reaction to enable penetration of the zona pellucida."

The miRNA of bovine follicular fluid is present both as free miRNAs and in EXOs, each with different composition (275). The EXOs were taken up by granulosa cells *in vitro*, resulting in increased miRNA content and variations in mRNA profiles: some of the affected genes are involved in follicle development. Moreover, some of the miRNA within EXOs may also contribute to oocyte growth, as they were differentially expressed in follicles containing oocytes at different maturation stages (275). A more exhaustive characterization of the EV content of bovine follicular fluid demonstrated variation in number, protein markers,

and miRNA contents depending on the developmental stage of the follicles. What is more interesting, variation in the miRNA signature suggested a switch in genetic programming concurrent with follicular maturation. As such, EV miRNAs from small follicles preferentially promoted cell proliferation pathways whereas those from large follicles related to inflammatory response pathways (276). A possible role in follicle development through the TGFB/BMP axis by follicular fluid–derived exosomes was demonstrated when granulosa cells were exposed to follicular fluid exosomes *in vitro*. It was proposed that these effects were triggered by the direct delivery of ACVR1 and ACRV1 regulatory miRNA within follicular EXOs to granulosa cells (277).

Cumulus–oocyte complex expansion is a critical process for ovulation. In this context, *in vitro* coculture experiments using bovine follicular fluid–derived EXOs and cumulus–oocyte complexes from mice and cattle revealed that follicular EVs are taken up by cumulus cells, promoting both cumulus expansion and related expansion of genes (278).

Oviduct/tubal EVs

Fertilization of the oocyte by SPZ occurs within the fallopian tubes/oviduct. After capacitation, SPZ must undergo an acrosome reaction and maintain hyperactivated motility to fuse with the oocyte, with both functions being regulated by high intracellular Ca^{2+} concentration levels. In this context, the major murine Ca^{2+} efflux pump PMCA4, and particularly its splicing variant PMCA4a, is predominant in oviductal fluid, compared with uterine and vaginal fluids, and is totally associated with EVs. Moreover, these PMCA4a-carrying vesicles had exosomal characteristics and were taken up by SPZ, where the efflux pump was functionally relocated to their membranes. This was the first study describing the presence of EXOs in the oviducts and introduced the relevance of PMCA4 as a tool for the maintenance of Ca^{2+} homeostasis and SPZ viability during SPZ storage, regulating capacitation and acrosome reaction timing and SPZ motility (242, 243, 279, 280). Subsequently, the same authors discovered that integrins ($\alpha_5\beta_1$ and $\alpha_v\beta_3$) in oviductal EVs were transferred to SPZ and were involved in EV–SPZ fusion for cargo delivery. Although the oviductal EVs include both MVs and EXOs, the former appeared to be more efficient in fusing with SPZ (242).

Bovine oviductal EVs produced *in vitro* by cell lines have beneficial effects on the quality and development of *in vitro*–cocultured bovine embryos, suggesting a functional communication between the oviduct and embryo during the early stages of embryo development (281). However, these results must be treated with caution, as oviductal EVs produced *in vitro* have been observed to carry a different cargo compared with *in vivo*–produced EVs. This is the case, for example, for OVGP and HSPA8, oviductal proteins known to be important in the fertilization process and early pregnancy. Whereas HSPA8 was found in both *in vitro* and *in vivo* EXOs, OVGP was absent in EXOs of *in vitro* origin (341).

Uterine EVs

Endometrial fluid is a viscous liquid secreted by the endometrial epithelial cells from the glands into the uterine cavity. Because the endometrium is a hormonally regulated organ, the molecular composition of the fluid varies depending on the phase of the menstrual cycle (342). Uterine fluid, a biologically and clinically relevant sample source (343), also contains contributions from the oviductal fluid and a large cohort of plasma proteins along with other factors differentially exudated from the blood (344). Importantly, this uterine fluid carries information that mirrors maternal environmental exposure and possibly relays such information to the embryo, subsequently generating long-term epigenetic effects on the offspring via embryonic and placental programming.

To date, EVs have been reported throughout menstrual/estrous cycles in the endometrial fluid of different species, including humans (156, 171) and sheep (282–284, 345), and they are also released by endometrial epithelial cells in culture (156, 171).

Ng *et al.* (171) first described the production of EVs by human endometrial epithelial cells in primary culture and by the endometrial epithelial cell line ECC1. These EVs contained a specific subset of miRNAs, not detectable in the parent cells. Bioinformatic analysis revealed that some of the target genes of the EV miRNAs are relevant to processes involved in embryo implantation. Importantly, they also verified the presence of EVs in human uterine fluid and the associated mucus (171).

Greening *et al.* (91) demonstrated that the proteome of highly purified EXOs derived from human endometrial epithelial cells is regulated by steroid hormones and thus varies with the progression of the menstrual cycle. Under follicular phase hormonal conditions, when estrogen constitutes the main hormonal stimulus, the EXO proteome was enriched in proteins related to cytoskeletal reorganization and signaling cascades, coinciding with the phase of endometrial restoration. Importantly, after ovulation, when progesterone is the dominant hormone driving endometrial receptivity, the proteome altered with changes indicating enrichment in extracellular matrix reorganization and embryo implantation. As in other systems, the exosomal protein profiles were shown to be distinct from parental cells. Importantly, this study demonstrated that endometrial EXOs were transferred and internalized by human HTR-8 trophoblast cells, enhancing their adhesive capacity, partially through focal adhesion kinase (FAK) signaling (91). This was

significantly higher when the EXOs were derived from cells subjected to both estrogen and progesterone to mimic the receptive phase of the menstrual cycle.

Embryonic and trophectodermal EVs

Interestingly, murine embryonic stem cells from the inner cell mass generate MVs that reach the trophectodermal layer and enhance the migration ability of trophoblast cells in culture, either as isolated cells or in the whole embryo. The presence of laminin and fibronectin in the cargo of the inner cell mass EVs enabled attachment to the integrins on the trophoblast cell surfaces and stimulated c-Jun N-terminal kinase and FAK cascades, increasing trophoblast migration. Furthermore, injection of these EVs inside the blastocoele cavity of day 3.5 blastocysts increased their implantation efficiency (88). Importantly, note that this mechanism may be particular to the mouse and to other species in which the inner cell mass is distal to the site of trophectoderm attachment to the endometrial surface: in women this is the reverse, with the extracellular matrix tightly aligned with the attaching trophectoderm.

EVs produced by ungulate trophectoderm participate in crosstalk with the maternal endometrium (283). Bidarimath *et al.* (285) observed that EVs from a porcine trophectodermal cell line stimulated the proliferation of endothelial cells *in vitro*, thus being potential regulators of maternal endometrial angiogenesis. These vesicles contained an miRNA and protein cargo likely to annotate functions in the angiogenesis process. Again, care should be taken with these data, as they were retrieved from cell lines cultured *in vitro*. Furthermore, the pig is a species with epitheliochorial placentation, and thus the *in utero* development is very different from that of the human (285). Nevertheless, study of human EVT cell (HTR-8/SVneo and Jeg3)–derived EXOs similarly showed that these vesicles promote vascular smooth muscle cells migration, which is important during human uterine spiral artery remodeling in successful pregnancies (346). Importantly, the two trophoblast cell lines (which are different stages along their differentiation pathway) produced differential migration results, raising the likelihood that cell origin as well as content and bioactivity of the exosomal cargo are of considerable importance, emphasizing the need to keep models as close to the physiological situation as possible.

EVs as vehicles for embryo–maternal crosstalk. The first indication that the endometrium produced EVs with unique cargo was that the human endometrial epithelial cell model ECC1 (which best represents luminal epithelium) released EVs containing a different miRNA profile from that of parent cells (171). These EVs could provide a mechanism for communication between the mother and the embryo with potential implications in embryo implantation. Indeed, bioinformatic analyses on the EV miRNAs showed predominance of the genes targeted by the miRNAs as involved in implantation. Furthermore, interrogation of the proteome of ECC1 EVs, cultured under conditions to represent the proliferative (estrogen-dominant) and secretory (estrogen plus progesterone) phases of the cycle, showed that the protein cargo of EVs is hormone specific, enriched with 254 and 126 proteins, respectively (91). Importantly, 35% of the endometrial EV proteome had not been previously reported, indicating the unique cargo of endometrial EVs. These findings were validated in EVs from primary endometrial epithelial cells. Functionally, the EVs were internalized by human trophoblast cells, inducing increased adhesive capacity, that was at least partially mediated through active FAK signaling, indicating a likely role in promoting embryo implantation (109). Interestingly, among the implantation-related proteome of these endometrial EXOs were the cell surface metalloproteinases ADAM10 and matrix metalloproteinase-14 (a membrane-bound matrix metalloproteinase), for which there are abundant substrates on the trophectoderm.

Another study showed that endometrial epithelial-derived EVs in the uterine fluid contain hsa-miR-30d during the receptive phase of the cycle. This EXO-associated hsa-miR-30d was internalized by mouse embryos via the trophectoderm, resulting in an indirect overexpression of genes encoding for certain molecules involved in the murine embryonic adhesion phenomenon—*Itgb3*, *Itga7*, and *Cdh5*. Functionally, *in vitro* treatment of murine embryos with miR-30d resulted in a notable increase in embryo adhesion, again indicating how maternal endometrial miRNAs might act as transcriptomic modifiers of the preimplantation embryo (156).

"Fertilization of the oocyte by SPZ occurs within the fallopian tubes/oviduct."

Implications of EVs in Reproductive Pathology

Given their seminal functional role and presence in various aspects of reproductive biology, a growing field of evidence is uncovering potential roles for EVs in regulating reproductive pathological conditions, including endometriosis, polycystic ovaries syndrome, erectile dysfunction (ED), early pregnancy loss, hypertension, preeclampsia (PE), and gestational diabetes (GD) mellitus (summarized Table 4). Given this importance of EVs during maternal environment and development, significant efforts are now focused on evaluating prognostic value and applicability of EVs as diagnostic and therapeutic agents (107, 370).

EVs in endometriosis

Endometriosis is an estrogen-dependent inflammatory disease that is characterized by the deposition and growth of endometrial cells outside the uterine cavity,

Table 4. Involvement of EVs in Reproduction-Related Pathologies

Disease	EV Pathogenic Role			References
Endometriosis	Promotion of endometriotic lesions invasion and progression			(347, 348, 350)
	Enhancement of angiogenic potential			(347, 349)
Polycystic ovaries syndrome	miRNA expression regulation toward PCOS phenotype			(351)
ED	Promotion of endothelial dysfunction, vascular damage, and atherogenesis			(352, 353)
Early pregnancy loss	Induction of an excessive procoagulant activity			(354, 355, 368)
	Promotion of endothelial dysfunction			(356)
PE	Placental origin	Promotion of abnormal remodeling of uterine spiral arteries		(333)
		Enhancement of angiogenic failure and subsequent endothelial dysfunction		(358)
		Stimulation of proinflammatory and procoagulant activities		(357–360, 366)
		Generation of oxidative stress into the placenta and mother vasculature		(361, 362)
	Maternal origin	General	Transportation of PE risk factors	(363)
			Failure to ensure appropriate vascular development	(367)
		Platelet EVs	Unleashing of thrombo-inflammatory placental response	(364)
		Leukocyte EVs	Promotion of proinflammatory cytokines release by the placenta	(365)
GD mellitus	Promotion of proinflammatory cytokines production by endothelial cells			(369)

Abbreviation: PCOS, polycystic ovarian syndrome.

with the pelvic peritoneum and ovaries being the most common sites for ectopic growth (371). For this reason, endometriosis is considered a benign metastasizing disease (372).

Endometriosis is characterized in part by an increase in the expression of angiogenic factors and metalloproteinases. Patients with endometriosis show higher levels of these molecules in endometriotic lesions than in eutopic endometrium, and eutopic endometrium of endometriosis patients shows higher levels than in healthy endometrial controls (347). Indeed, by inhibiting metalloproteinases it is possible to avoid the establishment of ectopic endometriotic cysts (373). In this context, EMMPRIN, a metalloproteinase inducer, is carried in EVs produced by uterine epithelial cells and stimulates the expression of metalloproteinases in stromal fibroblasts. The secretion of both EMMPRIN and metalloproteinases is positively regulated by IL-1β/α, whose secretion is increased in women under endometriosis conditions in whom there is a proinflammatory peritoneal environment. This would allow the increase of metalloproteinase production by fibroblasts to trigger endometriotic lesion invasion (348).

In terms of EV RNA cargo, EVs from endometrial stromal cells from women with endometriosis vs women without the disorder showed different profiles of exosomal miRNA content between EVs derived from eutopic and ectopic endometrium from endometriosis subjects and between eutopic endometrium from women without or with disease (349). Moreover, there was a differential miRNA signature between eutopic endometriotic and control EXOs. Among these miRNAs, miR21 is already known for a role in angiogenesis. It remains to be established whether miR-21 can promote angiogenesis following EV uptake (349).

Ectonucleotidases are enzymes involved in inflammatory processes and previously reported as expressed in the endometrium. Teixidó *et al.* (350) investigated ectonucleotidase activity from endometriotic cysts (endometriomas) on the ovary, one of the common sites for endometriotic lesion development. Ectonucleotidases were highly enriched in endometriomas compared with simple cysts. Interestingly, the ectonucleotidase activity was also contained by EXOs derived from endometriomas and simple cyst fluids, but it was significantly higher for EXOs from endometriomas.

Polycystic ovarian syndrome

Polycystic ovarian syndrome (PCOS) is one of the most common hormonal disorders affecting women, characterized by androgen excess and insulin resistance, leading to androgenism, high risk of glucose intolerance, diabetes, and lipid abnormalities (374). Its complex phenotypic manifestation was formally described nearly a century ago as the concurrence in

women of amenorrhea, hirsutism, obesity, and typical polycystic appearance of the ovaries (375).

Koiou *et al.* (376) observed that platelet MVs in plasma from PCOS affected women (defined by elevated circulating androgens and insulin resistance markers) were at higher levels than in healthy controls. Moreover, there was a significant positive correlation between MVs and numbers of follicles in the ovaries of these women. Subsequent confirmation of the increase in EV levels (mainly of exosomal size) in PCOS also demonstrated a direct correlation with insulin resistance markers. Furthermore, polycystic ovary–derived EVs showed a higher content in annexin V along with 16 miRNAs that are normally expressed at low levels, being increased with PCOS (377).

Sang *et al.* (351) described EVs in the human follicular fluid and identified 120 miRNAs within their cargo, 11 of which were highly expressed and with target genes in pathways involved in reproduction, endocrine, and metabolic processes. Two of these miRNAs, miR-132 and miR-320, were significantly decreased in the follicular fluid EVs from PCOS patients compared with nonaffected controls (351). Of note, miR-132 and miR-320 have HMGA2 and RAB5B, respectively, as target genes: these were associated with key roles in the etiology of PCOS in a previous genome-wide association study (378).

DENND1A is a PCOS candidate locus, characterized in a number of genome-wide association studies (378, 379). DENND1A variants at two levels, both at the protein and mRNA levels, were increased in theca cells of PCOS patients compared with healthy controls. In agreement with these results, mRNA for this locus was significantly increased in EXOs extracted from the urine of PCOS-affected women in comparison with normal-cycling controls. In this sense, the exosomal miRNA profile is proposed to reflect the physiological status of the source cells, providing a potential biomarker of PCOS (380). Further studies are needed to uncover the roles of EVs in the triggering and development of PCOS.

Erectile dysfunction

ED is the most studied sexual problem worldwide and mainly affects men >40 years of age. It costs up to £7 million in the United Kingdom and $15 billion in the United States. The prevalence of this condition varies greatly throughout the world, highlighting the Middle East (45.1%), United States (37.7%), and especially mainland China (varying from 17.1% to 92.3%), according to a retrospective study carried out on men of different ages (381).

Microparticles have been proposed as involved in endothelial dysfunction and atherogenesis, with special regard to ED. Initially, microparticles defined as membrane vesicles, apoptotic or not, <1.5 μm were recovered from plasma after platelet depletion at 900 × *g* and measured by flow cytometry using specific markers (352). These circulating endothelial-derived microparticles were increased in type 2 diabetic men with ED, compared with controls, and a positive correlation between microparticle counts and ED severity, determined by the International Index of Erectile Function, was shown. However, diabetes risk factors did not influence microparticle levels, and thus these were postulated to be independently linked to ED severity. Finally, microparticles were proposed as possible links between endothelial dysfunction and ED (352). Retrospectively, a molecular signature identified in microparticles enabled discrimination between diabetes and ED. The marker CD31 in microparticles was mainly related to diabetes, whereas CD62E was directly linked to ED, without diabetes. The CD31/CD62 ratio could be used to evaluate endothelial function, with a high ratio being related to endothelial activation and a low ratio associated with apoptosis. In the study, diabetic men with ED showed lower ratios, possibly indicating a cooperative effect of the two disorders. Finally, levels of $CD31^+$ microparticles were directly correlated with ED aggressiveness (382).

La Vignera *et al.* (353) increased the centrifugal force to achieve a better clearance of platelets from serum (13,000 × *g*). They confirmed an increase in endothelial-derived microparticle levels in ED patients with arterial etiology, in comparison with patients with ED of psychogenic origin. Because a positive correlation was observed with typical ED metabolic parameters, they proposed endothelial dysfunction as the cause underlying ED and reasserted microparticles as predictors of the condition. Furthermore, their levels were directly related to the aggressiveness of arterial ED (383): a combination of disorders leading to greater vascular damage was associated with more severe ED and endothelial dysfunction, and correlated with increasing levels of endothelial microparticles (384).

ED is associated with increased endothelial apoptosis, and both can be, in part, reverted by treatment with a type 5 phosphodiesterase inhibitor such as tadalafil (385). Treatment benefits were maintained for 4 weeks after the cessation of a 1-year treatment in almost half of the analyzed cases (386). Subsequently, the effect of tadalafil treatment and discontinuation on the production of apoptotic endothelial-derived microparticles was examined. ED patients had increased levels of apoptotic microparticles compared with controls before the start of the treatment. Ninety days of tadalafil administration improved International Index of Erectile Function score and endothelial parameters and reduced apoptotic microparticle levels, although not to control levels. These improvements reverted by 6 months after treatment discontinuation (387). Interestingly, complementation of tadalafil treatment with an antioxidant maintained the tadalafil effects at least until 6 months after treatment cessation, prolonging the duration of the antiapoptotic effect within the endothelium (388). This is in accord with

other studies implicating oxidative stress in endothelial dysfunction (389, 390). Patients with greater severity and duration of ED, associated with the concurrence of high cardiovascular risk profiles, were nonresponders to sildenafil, another type 5 phosphodiesterase inhibitor.

Androgen deficiency has also been proposed to contribute to the development of cardiovascular disease and endothelial function impairment (391). Six months of androgen replacement therapy (testosterone) improved endothelial and ED features and decreased endothelial derived microparticle levels in patients of ED and late onset hypogonadism (a new vascular risk factor) (392). Indeed, late-onset hypogonadism worsened metabolic parameters and increased the already high endothelial microparticle levels in ED patients (393).

Pregnancy complications

EVs from a variety of sources (epididymis, prostate, cervical mucus, ovarian follicle, embryo, and endometrium) have potential roles in both the establishment and development of a successful pregnancy. However, from the sixth week of gestation (394), placenta-derived EVs mainly of STB origin represent the main source of vesicles with potential implication in feto–maternal communication (32, 87). Their concentrations in maternal plasma increase gradually as pregnancy progresses (286). Their release and bioactivity are favored by both low oxygen tensions (395) and high D-glucose concentrations (396). Changes in concentration, composition, and bioactivity of placental and nonplacental EVs have been reported in pregnancy disorders (397). Notably, the secretion of EVs is increased in the two main EV-related pregnancy complications, that is, GD (398) and PE (399).

EVs in early pregnancy loss

Early pregnancy loss is a common complication that affects ~15% of the gestations and shows recurrence rates of 2% to 3%. Importantly, up to 50% of these cases are usually of idiopathic etiology (400). Interestingly, the levels of plasma endothelial microparticles are decreased in pregnancy loss, especially in cases with recurrent miscarriage, compared with controls (401). However, these results should be viewed with caution, as in healthy pregnancy (their controls) there is also an increase in EV levels, mainly due to the contribution of placenta-derived EVs (394).

In pregnancy, the hemostatic balance shifts toward upregulated procoagulant activity, with increased clotting factors and fibrinogen, and concurrently decreased anticoagulant factors and fibrinolytic activity (402). An excessive procoagulant response leading to thrombosis of the uteroplacental vasculature and subsequent hypoxia has been proposed as a factor accounting for an important part of the fetal loss cases (403). In this regard, blood microparticles with procoagulant activity are increased in miscarriage cases, in parallel with the enhanced coagulation-promoting activity. These microparticles may play a role in this outcome by favoring the thrombotic phenomena (354, 355). Furthermore, pregnancy loss–affected women present with lower levels of platelet microparticles and higher levels of endothelial microparticles than do controls; although this could not be directly related to the hypercoagulation phenotype, it was suggested to reflect endothelial dysfunction (356). In contrast, plasma platelet-derived microparticles were increased in women with recurrent miscarriage compared with controls (376). However, these results may be biased by the small size of the study population (404), and the controls may be inappropriate due to the contribution of the placenta to the total EV content.

EVs in gestational vascular complications

Gestational vascular complications, which include hypertension and PE, are prevalent causes of maternal and fetal morbidity and mortality. Hypertension may appear as a consequence of abnormal placentation into the maternal uterus, and it may lead to the development of impaired liver function, progressive renal insufficiency, pulmonary edema, and the new onset of cerebral or visual disturbances that might end in the hemolysis, elevated liver enzymes, and low platelet count syndrome and/or eclampsia (405). PE is a complex disorder causing preterm birth, intrauterine growth restriction, and maternal death (406). In general, different studies point toward an increase in endothelial microparticle shedding within gestational vascular complication conditions, thus suggesting vascular injury (407).

Preeclampsia

PE is a pregnancy-related syndrome affecting between 2% and 8% of pregnancies and is characterized by a variety of systemic symptoms. It is detected by new-onset hypertension and proteinuria after the 20th week of gestation. Its etiology is not well known, but the pathogenesis of PE is conceptualized in a two-stage model with the placental defect precipitating an abnormal vascular maternal response that manifests as the signs of this pathological condition. Early PE appears before 34 weeks of gestation and involves the fetus, showing reduced placental perfusion, possibly due to abnormal trophoblast invasion and/or uterine spiral artery remodeling. Late PE appears after 34 weeks, and the maternal manifestations appear; a series of inflammatory, metabolic, and thrombotic responses compromise vascular function up to the point of producing systemic organ damage (408).

Several published studies have attempted to elucidate the relevance of EVs of both maternal and placental STB origin in the pathophysiology of PE. Changes in EV concentration and cargo affect PE

development via proinflammatory and procoagulatory activity enhancement. In this section, we summarize current knowledge of EVs in relationship to PE.

Placenta-derived EVs. The placenta plays a critical role and is undoubtedly the source of PE development. PE can develop even in the absence of a fetus, provided that trophoblast tissues are established, forming the characteristic mass known as a hydatidiform mole, a tissue abnormality formed by the distension of some or all of the chorionic villi (409).

STB-derived EXOs and MVs (STBMs) are increased in PE compared with normal pregnancies (357), perhaps in part owing to the hypoxia that results from abnormal placentation (346). This increase occurs specifically in early-onset PE cases but not in late-onset PE or normotensive intrauterine growth restriction (410, 411). Importantly, early-onset PE is established in the first trimester when trophoblast invasion and vascular remodeling occur (346), emphasizing the importance of STBMs in these processes. Furthermore, variations in protein (399, 412, 413), lipid (414), and miRNA (399) cargo of STBMs may explain the specific roles of STBMs in PE, including immune response, coagulation, oxidative stress, and apoptosis.

One of the main characteristics of PE is abnormal remodeling of the uterine spiral arteries, which in normal pregnancies ensures enough maternal blood flow to support fetal growth and development. Thus, a role for EVT-derived EVs has been proposed in PE development. Variations in concentration, cargo, and bioactivity of EVT-derived EVs as indicated above may result from a proinflammatory environment, inducing these changes, impairing their physiological roles in vascular/smooth muscle tissue remodeling, and thus stimulating the emergence of PE (346, 415). In PE, increased amounts of proinflammatory cytokines (IL-18, IL-12, TNF-α) are released by monocytes and lymphocytes. PE-increased STBMs can bind monocytes to promote the production of more inflammatory cytokines, perpetuating the proinflammatory environment and hence stimulation of EV alterations and endothelial cell damage (357). Furthermore, villous cytotrophoblast-derived EXOs carry syncytin-1 and syncytin-2, which are involved in EXO fusion with the target cells. Importantly, syncytin-2 content was reduced in EXOs derived from serum of PE patients (416).

Antiangiogenic factors, such as sFlt1 and sEng, appear to participate in PE through a series of mechanisms that lead to the imbalance of angiogenic factors and finally to the generation of endothelial dysfunction and the maternal syndrome of PE. Increasing levels of sFLT and sEng can predict PE and directly correlate with the aggressiveness of this syndrome (417). PAI-1 and, to a lesser extent, PAI-2, which is predominant in placenta, are important inhibitors of fibrinolysis. Their overactivation results in the establishment of fibrin deposits that occlude placental vasculature and spiral arteries, leading to hypertension and endothelial damage causing PE. Moreover, increasing levels of PAI-1 in plasma directly correlate with PE severity (418). Eng and PAI-2 are highly expressed and localized to the surface of STBM MVs and EXOs, and thus can readily influence the development of PE (358). Additionally, STBMs from PE patients possess increased tissue factor activity compared with normotensive patients (359), and this could increase fibrin deposition. Coagulation may be enhanced by STBM action directly by direct association with platelets leading to activation: such activity is increased in PE-derived STBMs and correlates with PE-associated thrombotic risk. Moreover, treatment with aspirin, which is usually prescribed for PE women to reduce platelet aggregation, also inhibits STBM-induced platelet aggregation (360).

Cell-free hemoglobin (HbF) is released by the placenta, and increased hemoglobin expression as well as HbF accumulation in the vascular lumen of PE placentas have been reported (419). Indeed, HbF has been proposed as an important factor marking the transition between the first and second stages of PE. HbF causes placental damage similar to that observed in PE by inducing oxidative stress, which affects the blood–placenta barrier integrity (420). Blood–placenta barrier disruption may lead to the release of placental factors, including HbF, which leak into the maternal circulation, contributing to the maternal manifestations of PE. Moreover, levels of HbF correlate with PE severity symptoms (421). Placental HbF can provoke differential alterations in STBM miRNA cargo between EV populations: three miRNAs were specifically downregulated in MV populations under HbF influence. STBMs may also transport HbF itself, although these data may be an artifact of the external HbF perfusion (361). Furthermore, STBMs from PE pregnancies exacerbated the production of superoxide radicals by neutrophils in a dose-dependent manner, also correlating with PE severity. In this way, STBMs display multiple mechanisms to cause vascular damage and dysfunction in women with PE (362).

Maternally derived EVs. Even before pregnancy, maternal risk factors for PE are obesity, diabetes mellitus, hypertension, and systemic lupus erythematous. Pro-PE EVs have altered concentrations and modified molecular contents that may alter the functioning of maternal tissues prior to pregnancy. In particular, changes in endothelial cells and leukocyte- and platelet-derived EVs are associated with the risk of PE. All share the common feature of a general increase in endothelial and platelet-derived EV levels [see review in (363)].

Once pregnancy is established, maternal EVs of different cellular origin interact with embryonic tissues with potential implications in PE pathogenesis. Platelets have crucial roles in PE development, and

"Early pregnancy loss is a common complication that affects ~15% of the gestations and shows recurrence rates of 2% to 3%."

several studies report decreased platelet-derived EV levels in pregnancy compared with nonpregnancy, with a further decrease in PE (363). EVs of maternal endothelial and platelet origin appear to unleash a thrombo-inflammatory response in the placenta. EVs cause activated platelet aggregation and inflammasome activation within the placental vascular and trophoblastic cells, triggering a PE-like phenotype. Furthermore, inhibition of inflammasome or platelet activation components within the placenta abrogated the PE-like phenotype (364).

In contrast to platelets, leukocytes and certain derived EVs populations are increased in PE in comparison with normotensive pregnancies, mainly those EVs of granulocyte and monocyte origin (422). Interestingly, low levels of NK cell–derived EVs are observed in PE, linking with PE-associated maternal immune tolerance disorders (NK cell death activity dysfunction) (423). Of interest, Holder *et al.* (365) showed that human placenta is able to internalize EXOs from macrophages via endocytosis. Importantly, macrophage EXO uptake induced the release of proinflammatory cytokines by the placenta. Previously, the same group had reported that EXOs from PE placenta can activate peripheral blood mononuclear cells, inducing a proinflammatory response to a greater extent than EVs from normal placenta, and related to their cytokine content, mainly IL-1β. Moreover, PE-derived EVs stimulated an enhanced response of peripheral blood mononuclear cells to external pathogen-associated molecular patterns such as lipopolysaccharide (365). Such outcomes may be triggered by direct stimulation by EVs of Toll-like receptor, the signal subsequently internalized via nuclear factor κB (366). Taken together, these studies indicate a potential positive feedback loop by which an inflammatory response is overstimulated under PE conditions via EVs. Endothelial-derived EV levels correlate with the increment of the antiangiogenic factor sFLt1 and the sFLt1/P1GF ratio. This combined evidence suggests that apoptosis of endothelia occurs along with inhibition of angiogenesis and correlates with PE-characteristic endothelial damage, which persists between $<$1 week (424) and 72 hours postpartum (425).

Regarding obesity, a link between EXO release and the progression of PE is emerging. A recent study has observed that the levels of EXOs in maternal blood are correlated with maternal body mass index (BMI). A positive correlation of BMI with EXO levels was established, leading to the decrease of placenta-derived EXO proportions throughout gestation. These increased EXO levels contributed to a further exacerbated release of IL-6, IL-8, and TFN-α from endothelial cells, thus leading to worsened systemic inflammation in a BMI-dependent manner (426).

Finally, it has been observed that serum MVs from healthy pregnant women can reduce caspase activity and stimulate migration and tube formation in endothelial cells, whereas this is abrogated when the MVs are derived from patients with gestational vascular complications such as PE and hypertension. Furthermore, similar opposing actions on early-stage trophoblast of these vesicles was observed (367).

EVs in gestational diabetes

GD is defined as a carbohydrate intolerance of variable severity that appears or is first recognized during pregnancy. Along with PE, GD represents the most common metabolic complication of pregnancy, affecting between 1% and 15% of all pregnancies and increasing concurrently with obesity rates. It is characterized by pancreatic β cell–insufficient insulin production, usually due to pregnancy and characteristic insulin resistance, and is associated with maternal and fetal morbidity. Moreover, women with GD have increased risks of developing type II diabetes in the future (427, 428).

To date, little is known about the contribution of EVs in this pathophysiology. Salomon *et al.* (369) showed increased serum placenta-derived EXOs in GD pregnancies compared with control pregnancies, regardless of gestational age. *In vitro*, GD EXOs increased the release of proinflammatory cytokines from endothelial cells contributing to the enhanced proinflammatory state in pregnancy under GD conditions.

Clinical and Therapeutic Applications of EVs

The involvement of EVs in a wide variety of pathophysiological processes has made them appealing players as biomarkers and to carry therapeutic agents. This may also be the case when considering reproductive disorders.

EVs as biomarkers

EVs have been proposed as potential biomarkers of disorders of reproductive organs. The placenta releases EVs from the sixth week of pregnancy with steady increase as pregnancy proceeds, peaking at term (360). Importantly, their release is modulated by a number of factors that arise from the placenta; hence, EVs may provide mirrors of placental/fetal health and evolution (397). Because maternal blood is the primary source of placental EXOs, it will contain both maternal and placenta-specific EV populations and thus placental alkaline phosphatase (PLAP) has been proposed as a marker for the placental EVs, because it is restricted to placental cell lineages (394).

Alterations in both the levels and cargo of placenta-derived EXOs during pregnancy are associated with different pregnancy complications. A proteomic signature of 62 proteins in microparticles was developed from plasma samples of women at 10 to 12 weeks of

gestation (363). This signature was able to predict and differentiate SPBs from normal term births. Functional enrichment analyses showed processes related with preterm birth, such as inflammation, fibrinolysis, immune modulation, the coagulation cascade, or steroid metabolism. Currently, the only tool for evaluation of risk of spontaneous preterm birth is measurement of cervical length by ultrasound (364). A retrospective study on plasma samples of women at early gestational age (prior to 18 weeks) demonstrated potential for EXOs in the diagnosis of PE and SPB with higher (but not significant) levels of EXOs in both pathological conditions vs normal pregnancies. More interestingly, a specific exosomal miRNA signature could differentiate between the three conditions, being more similar between normal pregnancy and SPB compared with that of PE. When these miRNA profiles were compared with those from the EVT HTR-8/SVneo cell line cultured under normal and low-oxygen tension (LOT) conditions there was a strong correlation between the SPB and LOT conditions, with a common variation in >45% of the SPB condition miRNA profile. Placental–exosomal miRNA cargo was related to cell migration potential and inflammatory cytokine production. Particularly, LOT EXOs decreased endothelial cell migration potential and increased their TNF-α production, which could negatively impact spiral artery remodeling during placentation. Thus, under circumstances that favor a proinflammatory environment or a reduction of oxygen tension such as advanced gestational age, placental EVs may be negatively altered, impacting spiral artery remodeling and resulting in development of pathologies such as PE or SPB (422). In this sense, placental EVs may be potential early biomarkers of PE/SPB or as targets for directed therapy. Finally, both total and placenta-derived EVs are increased in women delivering low birth weight babies compared with those with normal birth weight deliveries (429).

EVs have been further investigated as biomarkers of PE. Recent publications debate the usefulness of the content of EVs for their predictive value in the diagnosis of PE. As an example, Tan *et al.* (430) analyzed three candidate biomarkers, TIMP-1, PAI-1, and P1GF, for their predictive ability in a large cohort of low-risk PE women from EVs isolated from bank plasma samples. They concluded that measurement of TIMP-1 and PAI-1 reinforced the value of the classical P1GF for PE prediction. Indeed, TIMP-1 and PAI-1 were analyzed in specific subgroups of EVs that can be retrieved thanks to their affinity to cholera toxin B and annexin V, both of which had been described previously in the search for PE biomarkers. In this study, EVs were purified from plasma of women at ~32 weeks of pregnancy, using immunoadsorption to the surface proteins, GM1 ganglioside (binds to cholera toxin B chain), and PS (binds to annexin V). Using these two populations of EVs (one from each marker), a specific protein signature was identified in women with PE compared with healthy pregnant controls. Importantly, note that such biomarker discovery is highly dependent on the selected conditions, providing a possible limitation. Indeed, in this study, large cellular debris was not removed from samples prior to the immunoadsorption step, providing a major potential source of error (431). In another study, different subtypes of MVs were evaluated in plasma, compared with cord blood from normal women and those with PE. Microparticles were more abundant and had altered coagulation-related factors in cord blood in PE compared with no PE (432). Recently, Salomon *et al.* (433) investigated whether EXOs and their miRNA cargo might provide early biomarkers of PE. More than 300 miRNAs were identified in total and placenta-derived EXOs in maternal plasma across gestation with hsa-miR-486-1-5p and hsa-miR-486-2-5 being identified as candidates for further study. Functional analysis showed that these miRNAs are involved in migration, placental development, and angiogenesis. Because PLAP is a marker of serum placenta-derived EXOs, which trend upwards with gestational age, exosomal content of PLAP has been proposed as a potential biomarker of PE in saliva and gingival cervical fluid (434). Finally, reduced EV-associated endothelial nitric oxide synthase expression and activity, a common feature of PE, was elevated in EVs from PE placentas (defined by PLAP) in both serum and placental perfusates, compared with healthy controls (435). Importantly, considering the above information, note that current biomarkers of pregnancy complications, such as PE or gestational diabetes mellitus, allow us to diagnose these states only once the pathologies are established and when the clinical management is limited. In this sense, to advance the field, efforts should focus on discovery of new biomarkers during early gestation.

EVs have also been proposed as biomarkers of peripartum cardiomyopathy (PPCM). PPCM is an idiopathic form of cardiomyopathy characterized by left ventricular systolic dysfunction (the ejaculation fraction is reduced normally <45%) and subsequent heart failure. It usually appears around the end of pregnancy and in the next few months and it is currently only diagnosed by exclusion of other heart failure causes (436), making a search for new biomarkers of considerable importance. Initially, Walenta *et al.* (437) reported increased levels of blood-derived activated endothelial microparticles in PPCM when compared with healthy postpartum, pregnant, and nonpregnant control but also with patients of ischemic cardiomyopathy and stable coronary arterial disease. These microparticles in PPCM were mainly platelet derived and monocyte microparticles. Treatment with bromocriptine, a therapy proven to work in animal models and human patients, significantly reduced endothelial and platelet-derived microparticles in

"EVs have also been proposed as biomarkers of peripartum cardiomyopathy (PPCM)."

PPCM compared with patients treated with standard undirected heart failure therapy. Thus, specific microparticle profiles may provide biomarkers that can distinguish PPCM from normal pregnancy, vascular diseases, and heart failure of different origin. miR146a has also been identified as a possible EXO-associated biomarker for PPCM. The 16-kDa N-terminal prolactin fragment, the primary known trigger of PPCM, stimulates the packaging of miR-146a into EXOs from human umbilical vein endothelial cells, which then are able to reach cardiomyocytes and trigger PPCM. Thus, miR-146a may provide a biomarker and therapeutic target for PPCM (438).

Placental EVs may provide indicators of infectious diseases during pregnancy. Both total and placental-derived EVs are increased in plasma from pregnant women with HIV infection compared with noninfected controls. In contrast, there were no changes in the level of plasma EVs due to malaria infection, neither for placental malaria nor for its peripheral variant. Nonetheless, miR-517c was found to be increased in microparticles from plasma of women with active placental malaria compared with noninfected controls (429).

Clinical and therapeutic aspects of EVs in reproductive biology

Intercellular transfer of genetic and protein material mediated by EVs could facilitate new diagnostic and therapeutic tools in the field of reproductive biology. As discussed, EVs are stable, versatile, cell-derived nanovesicles with target-homing specificity and the ability to transfer through *in vivo* biological barriers and they hold promise for the development of new approaches in drug delivery (75). Specifically, bioengineered EVs are being successfully deployed to deliver potent drugs and the capacity for select cellular reprogramming (6, 41). Recently, members of the International Society for Extracellular Vesicles and the Society for Clinical Research and Translation of Extracellular Vesicles presented a framework for challenges associated with development of EV-based therapeutics at the preclinical and clinical levels (439). This discussion addresses development of best practice models and current outlook for EV therapies.

Engineered or modified EVs can be designed for cell-specific targeting and delivery (440, 441). A seminal study has demonstrated that the selective cellular uptake of EVs surpasses that of more traditional carriers such as liposomes or nanoparticles, taking advantage of the natural characteristics of EVs to deliver molecules to target cells (442). Such insights provide future possibilities for clinical applications of EVs based on their ability to circumvent the limitations of various drug delivery systems of mucosal and blood–brain barrier traversal. The physicochemical configuration of EVs can also be modified to enable extended clearance compared with synthetic nanoparticles and spatiotemporal localization (ligand and cell type–specific targeting) and controlled release (238, 443–445). With respect to modifying EV cargo, a recent, comprehensive study compared various passive and active drug-loading methods, including electroporation, saponin treatment, extrusion, and dialysis, and used porphyrins of various hydrophobicities as model drugs (446). A comprehensive overview of EV cargo loading strategies, including electroporation, sonication, direct transfection, and cellular engineering, is provided in the literature (447, 448).

The potential functional roles of EVs in human embryo development have only recently been demonstrated. Embryos may generate their own microenvironment by secreting soluble factors and membrane vesicles, which constitute a secretome with selected autocrine and paracrine signaling (91, 449–453). In reproductive biology, nanoparticles have been used experimentally to load sperm with exogenous genetic material that is subsequently transferred to the oocyte during fertilization (454, 455). EVs have been identified in uterine fluid during the estrous/menstrual cycles, including humans, sheep, and mice (75, 156, 171, 282, 456). Indeed, EVs derived from the maternal endometrium contain multiple subtypes, including mixtures of EVs, EXOs and packaged different proteins, miRNAs and endogenous retrovirus mRNA (91, 156, 282–284, 287, 348). In the broader context of trophectodermal preparation for implantation, EVs have been shown to mediate communication between the inner cell mass and the trophectoderm (88). EV-encapsulated cargo is protected from degradation and is highly stable in biological fluids. Such unique properties may greatly facilitate the translation of EVs and their selected bioactive cargo and surface ligands into clinical applications. The study of EVs in reproduction has the potential for expanding our current understanding of the normal physiology of reproduction and pathological conditions such as implantation failure (452). Recent studies have provided key insights into the functional capacity of maternal EVs and how the protein cargo is directly modulated by uterine hormones during implantation to subsequently modulate trophoblast adhesive capacity (91). This study further validated selected components in primary human endometrial cells under hormonal control.

Recent studies have observed the ability of EVs to undergo cell-selective fusion (457) and tissue-specific tropism (228, 238, 458, 459), as well as their capacity to transverse the blood–brain barrier (460) and penetrate dense structural tissue (461). Importantly, based on their surface composition, EVs may be directed to specific tissues and organs (219, 238, 458, 459). Imaging of EVs in selected targeted organs has indeed demonstrated that the interactions of EVs with target cells are highly dynamic (232, 462). Such unique

properties of circulating EVs make them promising applications for the delivery of therapeutic cargo. Several studies support the utility of EVs as a novel path for drug delivery and as new drug targets. Alvarez-Erviti *et al.* (462), in an *in vivo* study, demonstrated that systemically injected neuron-targeted EXOs loaded with BACE1 siRNAs were able to significantly reduce BACE mRNA and protein, specifically in neurons (463). Furthermore, EXOs loaded with artificial siRNA against MAPK efficiently knocked down MAPK1 upon their delivery into monocytes and lymphocytes *in vitro* (464). Similarly, EXOs from induced pluripotent stem cells have been shown to deliver siRNA to attenuate expression of intercellular adhesion molecule 1 and neutrophil adhesion in pulmonary microvascular endothelial cells (465). Exosomes have further been applied for drug delivery to target a small-molecule, anti-inflammatory drug to selected organs and immune cells (466). These studies have demonstrated the capacity for EV-mediated targeted and delivery capacity and importantly the ability for EXOs to deliver and modulate multiple pathways simultaneously in the targeted cells. All of these studies are examples showing how EV cargo can be manipulated in a way that may be useful for target-based drug development for successful *in vivo* drug delivery.

Recent reviews have discussed the rationale to aim for selective silencing of EVs that promote unwanted functional effects. However, this is still an emerging concept in the field. Some of the strategies for specific silencing of EV subtypes (cell specific) are likely to require careful and detailed mechanistic studies. There are inherent difficulties in avoiding the blocking of all EV types indiscriminately, which may interfere with and perturb physiological intercellular communication. Some examples of systems for abrogating EV formation and targeting/recipient cell uptake [reviews include (222, 230, 448, 467)]: (1) inhibition of EXO formation, including treatment with dimethyl amiloride; (2) inhibition of the endolysosomal compartment functions, including proton pump inhibitors, (3) blocking of EXO release (for example, silencing GTPase Rab11/27A/35 using siRNA or targeting ESCRT proteins and/or GTPases involved in trafficking of EXOs); and (4) prevention of fusion or uptake of EXOs by target cells, which can be done using a variety of reagents that block phosphatidyl serine such as diannexin, heparin to inhibit endocytosis (heparan sulfate proteoglycans), cytochalasin D to inhibit endocytosis and micropinocytosis, chlorpromazine to inhibit clathrin-dependent endocytosis, EIPA and LY294002 to block micropinocytosis, annexin V to inhibit phagocytosis and macropinocytosis, methyl-β-cyclodextrin, simvastatin, and filipin III to target lipid raft–mediated endocytosis, nystatin to target caveolae-mediated endocytosis, dynasore to inhibit clathrin-independent endocytosis (calveolae), and nystatin to perturb lipid raft–mediated endocytosis.

Future studies are required toward investigating EVs from primary tissues and biofluids and incorporating state-of-the-art quantitative analyses, including quantitative proteomics (183, 468) and sequencing technology that could be exploited to study protein and gene regulation during pregnancy. These would enable identification and monitoring of functional or low-abundant EV cargo, as well as cellular drivers of implantation and signaling, that hitherto have been unreported or functionally masked. Unlike small-molecule pharmaceutical compounds, there are no defined parameters or assays for current safety testing of EV-based therapeutics (469). Understanding biodistribution patterns and circulating timeframe of locally and systemically administered EVs is important to assessing safety, in addition to techniques that enable reproducible monitoring and safety testing of selected EV marker cargo. Targeted studies using EVs (modified or engineered) will hold the potential to develop novel nanodiagnostics and nanotherapeutics to increase the success of pregnancy rates during assisted reproductive technologies or *in vitro* fertilization. Recent work on targetable biodegradable delivery platforms for transporting biological cargo into gametes and embryos [reviewed in (470)] emphasizes the need to understand how EVs enter cells. We anticipate that future investigations into the use of EVs for the intentional targeted delivery of molecular compounds will provide new horizons for reproductive science and clinical assisted reproductive technologies, ultimately leading to improvements in pregnancy success.

"Recent reviews have discussed the rationale to aim for selective silencing of EVs that promote unwanted functional effects."

Concluding Remarks

Considering the body of evidence treated in the present review, there is no doubt that the field of EVs and its implication in reproduction is rapidly evolving and promises a further understanding of the processes that lead to a successful pregnancy, as well as markers of correct or compromised reproductive function. Nonetheless, there is still a difficult path to negotiate. First, there is an unavoidable need to firmly define standard methods for EVs isolation, because these define the fractions considered as different EV populations and, as such, may lead to ambiguous results that cannot be compared among studies. New challenges associated with standardization of methods for isolation, quantification, and analysis of EVs from complex tissues such as blood, as well as the stability of EVs within such biofluid samples, need to be overcome before the EV field can provide reliable tools for diagnosis and therapy.

It is also necessary to define the extent to which EVs are important participants in the reproductive events that lead to the delivery of healthy normal newborns, as this knowledge will lead to new therapies and clinical tests to ensure good pregnancy outcomes. Sample availability is maybe one of the main limiting factors that hinders such progress. In this sense, much more is known about epididymal and prostatic EV regulation of sperm compared with embryo maternal crosstalk through EVs. Nevertheless, EV communication may provide a cornerstone to enable better understanding of the conception and implantation

processes. This is important as it paves the way to deal with those patients in which the present assisted reproductive techniques fail.

Finally, data regarding the involvement of EVs in the triggering, maintenance, and progression of reproductive and obstetric-related disorders is still in its infancy and further key investigations utilizing homogeneous and human-specific material are needed. The use of EVs as disease biomarkers provides the opportunity for diagnostic potential with reduced invasiveness, as they can be retrieved from body fluid instead of tissue biopsies. This is vital for embryo diagnoses, where the possibility of getting STBMs from mother blood flow appears as an interesting alternative to invasive amniocentesis and chorionic villi sampling, further offering the possibility of an earlier diagnosis. Regarding EVs used as therapeutic agents, many different variants could be exploited. EVs could be used as vectors to deliver drugs and biological compounds in a targeted manner. Nevertheless, they could potentially be used as therapeutic targets if they are produced by affected cells and present disease-promoting characteristics. This may be achieved by inhibiting EV biosynthesis, by capturing them once produced, or by blocking their uptake by target cells, and this may be applicable in diseases such as PE. Furthermore, they could be used as natural therapeutic agents when experimental strategies rely on their natural features. Understanding cell type specificity and the long-term effects of EV remodeling, the potential of EVs to impart transgenerational consequences on the offspring's health, ranging from metabolism to sex determination, and potential epigenetic changes affecting the mother's fertility and altering the offspring's fertility are key factors to be addressed as the field moves forward. EVs derived from the immune cells including dendritic cells within the reproductive tissues also need examination, since such cells, once stimulated, may trigger detrimental immune responses. Advances in research on noncoding RNAs contained in EVs must also be considered (471). Understanding all these molecular signaling networks, utilizing advances in quantitative proteomics and sequencing technology, and mediated by EVs that coordinate strategies for successful implantation, may lead to approaches to improve the outcomes of natural pregnancy and pregnancy achieved using reproductive technologies.

References

1. Yáñez-Mó M, Siljander PRM, Andreu Z, Zavec AB, Borràs FE, Buzás EI, Buzas K, Casal E, Cappello F, Carvalho J, Colás E, Cordeiro-da Silva A, Fais S, Falcon-Perez JM, Ghobrial IM, Giebel B, Gimona M, Graner M, Gursel I, Gursel M, Heegaard NHH, Hendrix A, Kierulf P, Kokubun K, Kosanovic M, Kralj-Iglic V, Krämer-Albers E-M, Laitinen S, Lässer C, Lener T, Ligeti E, Linē A, Lipps G, Llorente A, Lötvall J, Manček-Keber M, Marcilla A, Mittelbrunn M, Nazarenko I, Nolte-'t Hoen ENM, Nyman TA, O'Driscoll L, Olivan M, Oliveira C, Pállinger É, Del Portillo HA, Reventós J, Rigau M, Rohde E, Sammar M, Sánchez-Madrid F, Santarém N, Schallmoser K, Ostenfeld MS, Stoorvogel W, Stukelj R, Van der Grein SG, Vasconcelos MH, Wauben MHM, De Wever O. Biological properties of extracellular vesicles and their physiological functions. *J Extracell Vesicles*. 2015;**4**(1):27066.
2. Raposo G, Stoorvogel W. Extracellular vesicles: exosomes, microvesicles, and friends. *J Cell Biol*. 2013; **200**(4):373–383.
3. Hardie DG. *Biochemical Messengers: Hormones, Neurotransmitters, and Growth Factors*. New York, NY: Chapman & Hall; 1991.
4. Zaborowski MP, Balaj L, Breakefield XO, Lai CP. Extracellular vesicles: composition, biological relevance, and methods of study. *Bioscience*. 2015;**65**(8): 783–797.
5. Colombo M, Raposo G, Théry C. Biogenesis, secretion, and intercellular interactions of exosomes and other extracellular vesicles. *Annu Rev Cell Dev Biol*. 2014;**30**(1):255–289.
6. EL Andaloussi S, Mäger I, Breakefield XO, Wood MJA. Extracellular vesicles: biology and emerging therapeutic opportunities. *Nat Rev Drug Discov*. 2013;**12**(5):347–357.
7. Ronquist G, Brody I. The prostasome: its secretion and function in man. *Biochim Biophys Acta*. 1985; **822**(2):203–218.
8. Ogawa Y, Kanai-Azuma M, Akimoto Y, Kawakami H, Yanoshita R. Exosome-like vesicles with dipeptidyl peptidase IV in human saliva. *Biol Pharm Bull*. 2008;**31**(6):1059–1062.
9. Caby M-P, Lankar D, Vincendeau-Scherrer C, Raposo G, Bonnerot C. Exosomal-like vesicles are present in human blood plasma. *Int Immunol*. 2005; **17**(7):879–887.
10. Lässer C, Alikhani VS, Ekström K, Eldh M, Paredes PT, Bossios A, Sjöstrand M, Gabrielsson S, Lötvall J, Valadi H. Human saliva, plasma and breast milk exosomes contain RNA: uptake by macrophages. *J Transl Med*. 2011;**9**(1):9.
11. Pisitkun T, Shen R-F, Knepper MA. Identification and proteomic profiling of exosomes in human urine. *Proc Natl Acad Sci USA*. 2004;**101**(36): 13368–13373.
12. Asea A, Jean-Pierre C, Kaur P, Rao P, Linhares IM, Skupski D, Witkin SS. Heat shock protein-containing exosomes in mid-trimester amniotic fluids. *J Reprod Immunol*. 2008;**79**(1):12–17.
13. Akers JC, Gonda D, Kim R, Carter BS, Chen CC. Biogenesis of extracellular vesicles (EV): exosomes, microvesicles, retrovirus-like vesicles, and apoptotic bodies. *J Neurooncol*. 2013;**113**(1):1–11.
14. György B, Szabó TG, Pásztói M, Pál Z, Misják P, Aradi B, László V, Pállinger E, Pap E, Kittel A, Nagy G, Falus A, Buzás EI. Membrane vesicles, current state-of-the-art: emerging role of extracellular vesicles. *Cell Mol Life Sci*. 2011;**68**(16):2667–2688.
15. Van Deun J, Mestdagh P, Sormunen R, Cocquyt V, Vermaelen K, Vandesompele J, Bracke M, De Wever O, Hendrix A. The impact of disparate isolation methods for extracellular vesicles on downstream RNA profiling. *J Extracell Vesicles*. 2014;**3**(1):24858.
16. Szatanek R, Baran J, Siedlar M, Baj-Krzyworzeka M. Isolation of extracellular vesicles: determining the correct approach. [Review] *Int J Mol Med*. 2015; **36**(1):11–17.
17. Tkach M, Théry C. Communication by extracellular vesicles: where we are and where we need to go. *Cell*. 2016;**164**(6):1226–1232.
18. Simpson RJ, Kalra H, Mathivanan S. ExoCarta as a resource for exosomal research. *J Extracell Vesicles*. 2012;**1**(1):18374.
19. Kim D-K, Kang B, Kim OY, Choi D-S, Lee J, Kim SR, Go G, Yoon YJ, Kim JH, Jang SC, Park K-S, Choi E-J, Kim KP, Desiderio DM, Kim Y-K, Lötvall J, Hwang D, Gho YS. EVpedia: an integrated database of high-throughput data for systemic analyses of extracellular vesicles. *J Extracell Vesicles*. 2013;**2**(1):20384.
20. Kalra H, Simpson RJ, Ji H, Aikawa E, Altevogt P, Askenase P, Bond VC, Borràs FE, Breakefield X, Budnik V, Buzas E, Camussi G, Clayton A, Cocucci E, Falcon-Perez JM, Gabrielsson S, Gho YS, Gupta D, Harsha HC, Hendrix A, Hill AF, Inal JM, Jenster G, Krämer-Albers E-M, Lim SK, Llorente A, Lötvall J, Marcilla A, Mincheva-Nilsson L, Nazarenko I, Nieuwland R, Nolte-'t Hoen ENM, Pandey A, Patel T, Piper MG, Pluchino S, Prasad TSK, Rajendran L, Raposo G, Record M, Reid GE, Sánchez-Madrid F, Schiffelers RM, Siljander P, Stensballe A, Stoorvogel W, Taylor D, Théry C, Valadi H, van Balkom BWM, Vázquez J, Vidal M, Wauben MHM, Yáñez-Mó M, Zoeller M, Mathivanan S. Vesiclepedia: a compendium for extracellular vesicles with continuous community annotation. *PLoS Biol*. 2012;**10**(12):e1001450.

21. Budnik V, Ruiz-Cañada C, Wendler F. Extracellular vesicles round off communication in the nervous system. *Nat Rev Neurosci*. 2016;**17**(3):160–172.
22. Maas SLN, Breakefield XO, Weaver AM. Extracellular vesicles: unique intercellular delivery vehicles. *Trends Cell Biol*. 2017;**27**(3):172–188.
23. Parolini I, Federici C, Raggi C, Lugini L, Palleschi S, De Milito A, Coscia C, Iessi E, Logozzi M, Molinari A, Colone M, Tatti M, Sargiacomo M, Fais S. Microenvironmental pH is a key factor for exosome traffic in tumor cells. *J Biol Chem*. 2009;**284**(49):34211–34222.
24. Mittelbrunn M, Gutiérrez-Vázquez C, Villarroya-Beltri C, González S, Sánchez-Cabo F, González MÁ, Bernad A, Sánchez-Madrid F. Unidirectional transfer of microRNA-loaded exosomes from T cells to antigen-presenting cells. *Nat Commun*. 2011;**2**:282.
25. Kucharzewska P, Belting M. Emerging roles of extracellular vesicles in the adaptive response of tumour cells to microenvironmental stress. *J Extracell Vesicles*. 2013;**2**(1):20304.
26. An Q, van Bel AJ, Hückelhoven R. Do plant cells secrete exosomes derived from multivesicular bodies? *Plant Signal Behav*. 2007;**2**(1):4–7.
27. Rutter BD, Innes RW. Extracellular vesicles isolated from the leaf apoplast carry stress-response proteins. *Plant Physiol*. 2017;**173**(1):728–741.
28. Silverman JM, Clos J, de'Oliveira CC, Shirvani O, Fang Y, Wang C, Foster LJ, Reiner NE. An exosome-based secretion pathway is responsible for protein export from *Leishmania* and communication with macrophages. *J Cell Sci*. 2010;**123**(Pt 6):842–852.
29. Regev-Rudzki N, Wilson DW, Carvalho TG, Sisquella X, Coleman BM, Rug M, Bursac D, Angrisano F, Gee M, Hill AF, Baum J, Cowman AF. Cell-cell communication between malaria-infected red blood cells via exosome-like vesicles. *Cell*. 2013;**153**(5):1120–1133.
30. Brown L, Wolf JM, Prados-Rosales R, Casadevall A. Through the wall: extracellular vesicles in Gram-positive bacteria, mycobacteria and fungi. *Nat Rev Microbiol*. 2015;**13**(10):620–630.
31. Deatherage BL, Cookson BT. Membrane vesicle release in bacteria, eukaryotes, and archaea: a conserved yet underappreciated aspect of microbial life. *Infect Immun*. 2012;**80**(6):1948–1957.
32. Tannetta D, Dragovic R, Alyahyaei Z, Southcombe J. Extracellular vesicles and reproduction-promotion of successful pregnancy. *Cell Mol Immunol*. 2014;**11**(6):548–563.
33. Kerr JF, Wyllie AH, Currie AR. Apoptosis: a basic biological phenomenon with wide-ranging implications in tissue kinetics. *Br J Cancer*. 1972;**26**(4):239–257.
34. Taylor RC, Cullen SP, Martin SJ. Apoptosis: controlled demolition at the cellular level. *Nat Rev Mol Cell Biol*. 2008;**9**(3):231–241.
35. Elmore S. Apoptosis: a review of programmed cell death. *Toxicol Pathol*. 2007;**35**(4):495–516.
36. Atkin-Smith GK, Tixeira R, Paone S, Mathivanan S, Collins C, Liem M, Goodall KJ, Ravichandran KS, Hulett MD, Poon IKH. A novel mechanism of generating extracellular vesicles during apoptosis via a beads-on-a-string membrane structure. *Nat Commun*. 2015;**6**(1):7439.
37. Hristov M, Erl W, Linder S, Weber PC. Apoptotic bodies from endothelial cells enhance the number and initiate the differentiation of human endothelial progenitor cells in vitro. *Blood*. 2004;**104**(9):2761–2766.
38. Willms E, Johansson HJ, Mäger I, Lee Y, Blomberg KEM, Sadik M, Alaarg A, Smith CIE, Lehtiö J, El Andaloussi S, Wood MJA, Vader P. Cells release subpopulations of exosomes with distinct molecular and biological properties. *Sci Rep*. 2016;**6**(1):22519.
39. Jeppesen DK, Hvam ML, Primdahl-Bengtson B, Boysen AT, Whitehead B, Dyrskjøt L, Orntoft TF, Howard KA, Ostenfeld MS. Comparative analysis of discrete exosome fractions obtained by differential centrifugation. *J Extracell Vesicles*. 2014;**3**(1):25011.
40. Osteikoetxea X, Németh A, Sódar BW, Vukman KV, Buzás EI. Extracellular vesicles in cardiovascular disease: are they Jedi or Sith? *J Physiol*. 2016;**594**(11):2881–2894.
41. van der Pol E, Böing AN, Harrison P, Sturk A, Nieuwland R. Classification, functions, and clinical relevance of extracellular vesicles. *Pharmacol Rev*. 2012;**64**(3):676–705.
42. van Engeland M, Kuijpers HJ, Ramaekers FC, Reutelingsperger CP, Schutte B. Plasma membrane alterations and cytoskeletal changes in apoptosis. *Exp Cell Res*. 1997;**235**(2):421–430.
43. Hochreiter-Hufford A, Ravichandran KS. Clearing the dead: apoptotic cell sensing, recognition, engulfment, and digestion. *Cold Spring Harb Perspect Biol*. 2013;**5**(1):a008748.
44. Wu Y, Tibrewal N, Birge RB. Phosphatidylserine recognition by phagocytes: a view to a kill. *Trends Cell Biol*. 2006;**16**(4):189–197.
45. Fadok VA, Bratton DL, Henson PM. Phagocyte receptors for apoptotic cells: recognition, uptake, and consequences. *J Clin Invest*. 2001;**108**(7):957–962.
46. Wlodkowic D, Telford W, Skommer J, Darzynkiewicz Z. Apoptosis and beyond: cytometry in studies of programmed cell death. *Methods Cell Biol*. 2011;**103**:55–98.
47. Bailey RW, Nguyen T, Robertson L, Gibbons E, Nelson J, Christensen RE, Bell JP, Judd AM, Bell JD. Sequence of physical changes to the cell membrane during glucocorticoid-induced apoptosis in S49 lymphoma cells. *Biophys J*. 2009;**96**(7):2709–2718.
48. Hugel B, Martínez MC, Kunzelmann C, Freyssinet J-M. Membrane microparticles: two sides of the coin. *Physiology (Bethesda)*. 2005;**20**:22–27.
49. Friedl P, Vischer P, Freyberg MA. The role of thrombospondin-1 in apoptosis. *Cell Mol Life Sci*. 2002;**59**(8):1347–1357.
50. Takizawa F, Tsuji S, Nagasawa S. Enhancement of macrophage phagocytosis upon iC3b deposition on apoptotic cells. *FEBS Lett*. 1996;**397**(2–3):269–272.
51. Abas L, Luschnig C. Maximum yields of microsomal-type membranes from small amounts of plant material without requiring ultracentrifugation. *Anal Biochem*. 2010;**401**(2):217–227.
52. Lavoie C, Lanoix J, Kan FW, Paiement J. Cell-free assembly of rough and smooth endoplasmic reticulum. *J Cell Sci*. 1996;**109**(Pt 6):1415–1425.
53. Tong M, Kleffmann T, Pradhan S, Johansson CL, DeSousa J, Stone PR, James JL, Chen Q, Chamley LW. Proteomic characterization of macro-, micro- and nano-extracellular vesicles derived from the same first trimester placenta: relevance for feto-maternal communication. *Hum Reprod*. 2016;**31**(4):687–699.
54. Pantham P, Viall CA, Chen Q, Kleffmann T, Print CG, Chamley LW. Antiphospholipid antibodies bind syncytiotrophoblast mitochondria and alter the proteome of extruded syncytial nuclear aggregates. *Placenta*. 2015;**36**(12):1463–1473.
55. Holmgren L, Szeles A, Rajnavölgyi E, Folkman J, Klein G, Ernberg I, Falk KI. Horizontal transfer of DNA by the uptake of apoptotic bodies. *Blood*. 1999;**93**(11):3956–3963.
56. Ehnfors J, Kost-Alimova M, Persson NL, Bergsmedh A, Castro J, Levchenko-Tegnebratt T, Yang L, Panaretakis T, Holmgren L. Horizontal transfer of tumor DNA to endothelial cellsin vivo. *Cell Death Differ*. 2009;**16**(5):749–757.
57. Bergsmedh A, Szeles A, Henriksson M, Bratt A, Folkman MJ, Spetz AL, Holmgren L. Horizontal transfer of oncogenes by uptake of apoptotic bodies. *Proc Natl Acad Sci USA*. 2001;**98**(11):6407–6411.
58. Savill J, Dransfield I, Gregory C, Haslett C. A blast from the past: clearance of apoptotic cells regulates immune responses. *Nat Rev Immunol*. 2002;**2**(12):965–975.
59. Bellone M, Iezzi G, Rovere P, Galati G, Ronchetti A, Protti MP, Davoust J, Rugarli C, Manfredi AA. Processing of engulfed apoptotic bodies yields T cell epitopes. *J Immunol*. 1997;**159**(11):5391–5399.
60. Cocca BA, Cline AM, Radic MZ. Blebs and apoptotic bodies are B cell autoantigens. *J Immunol*. 2002;**169**(1):159–166.
61. Bellone M. Apoptosis, cross-presentation, and the fate of the antigen specific immune response. *Apoptosis*. 2000;**5**(4):307–314.
62. Chargaff E, West R. The biological significance of the thromboplastic protein of blood. *J Biol Chem*. 1946;**166**(1):189–197.
63. Muralidharan-Chari V, Clancy JW, Sedgwick A, D'Souza-Schorey C. Microvesicles: mediators of extracellular communication during cancer progression. *J Cell Sci*. 2010;**123**(Pt 10):1603–1611.
64. Cocucci E, Racchetti G, Meldolesi J. Shedding microvesicles: artefacts no more. *Trends Cell Biol*. 2009;**19**(2):43–51.
65. Tricarico C, Clancy J, D'Souza-Schorey C. Tricarico C, Clancy J, D'Souza-Schorey C. Biology and biogenesis of shed microvesicles. *Small GTPases*. 2017;**8**(4):220–232.
66. D'Souza-Schorey C, Clancy JW. Tumor-derived microvesicles: shedding light on novel microenvironment modulators and prospective cancer biomarkers. *Genes Dev*. 2012;**26**(12):1287–1299.
67. Théry C, Ostrowski M, Segura E. Membrane vesicles as conveyors of immune responses. *Nat Rev Immunol*. 2009;**9**(8):581–593.
68. Antonyak MA, Cerione RA. Emerging picture of the distinct traits and functions of microvesicles and exosomes. *Proc Natl Acad Sci USA*. 2015;**112**(12):3589–3590.
69. Lawson C, Vicencio JM, Yellon DM, Davidson SM. Microvesicles and exosomes: new players in metabolic and cardiovascular disease. *J Endocrinol*. 2016;**228**(2):R57–R71.
70. Vader P, Breakefield XO, Wood MJA. Extracellular vesicles: emerging targets for cancer therapy. *Trends Mol Med*. 2014;**20**(7):385–393.
71. Kreimer S, Belov AM, Ghiran I, Murthy SK, Frank DA, Ivanov AR. Mass-spectrometry-based molecular characterization of extracellular vesicles: lipidomics and proteomics. *J Proteome Res*. 2015;**14**(6):2367–2384.
72. Sluijter JPG, Verhage V, Deddens JC, van den Akker F, Doevendans PA. Microvesicles and exosomes for intracardiac communication. *Cardiovasc Res*. 2014;**102**(2):302–311.
73. Xu R, Greening DW, Rai A, Ji H, Simpson RJ. Highly-purified exosomes and shed microvesicles isolated from the human colon cancer cell line LIM1863 by sequential centrifugal ultrafiltration are biochemically and functionally distinct. *Methods*. 2015;**87**:11–25.
74. Muralidharan-Chari V, Clancy J, Plou C, Romao M, Chavrier P, Raposo G, D'Souza-Schorey C. ARF6-regulated shedding of tumor cell-derived plasma membrane microvesicles. *Curr Biol*. 2009;**19**(22):1875–1885.

75. Xu R, Greening DW, Zhu H-J, Takahashi N, Simpson RJ. Extracellular vesicle isolation and characterization: toward clinical application. *J Clin Invest*. 2016; **126**(4):1152–1162.
76. Clancy JW, Sedgwick A, Rosse C, Muralidharan-Chari V, Raposo G, Method M, Chavrier P, D'Souza-Schorey C. Regulated delivery of molecular cargo to invasive tumour-derived microvesicles. *Nat Commun*. 2015;**6**(1):6919.
77. Menck K, Scharf C, Bleckmann A, Dyck L, Rost U, Wenzel D, Dhople VM, Siam L, Pukrop T, Binder C, Klemm F. Tumor-derived microvesicles mediate human breast cancer invasion through differentially glycosylated EMMPRIN. *J Mol Cell Biol*. 2015;**7**(2): 143–153.
78. Antonyak MA, Li B, Boroughs LK, Johnson JL, Druso JE, Bryant KL, Holowka DA, Cerione RA. Cancer cell-derived microvesicles induce transformation by transferring tissue transglutaminase and fibronectin to recipient cells. *Proc Natl Acad Sci USA*. 2011; **108**(12):4852–4857.
79. Arshad Malik MF. Influence of microvesicles in breast cancer metastasis and their therapeutic implications. *Arch Iran Med*. 2015;**18**(3):189–192.
80. McDaniel K, Correa R, Zhou T, Johnson C, Francis H, Glaser S, Venter J, Alpini G, Meng F. Functional role of microvesicles in gastrointestinal malignancies. *Ann Transl Med*. 2013;**1**(1):4.
81. Jorfi S, Inal JM. The role of microvesicles in cancer progression and drug resistance. *Biochem Soc Trans*. 2013;**41**(1):293–298.
82. Dye JR, Ullal AJ, Pisetsky DS. The role of microparticles in the pathogenesis of rheumatoid arthritis and systemic lupus erythematosus. *Scand J Immunol*. 2013;**78**(2):140–148.
83. Lo Cicero A, Majkowska I, Nagase H, Di Liegro I, Troeberg L. Microvesicles shed by oligodendroglioma cells and rheumatoid synovial fibroblasts contain aggrecanase activity. *Matrix Biol*. 2012;**31**(4): 229–233.
84. Sellam J, Proulle V, Jüngel A, Ittah M, Miceli Richard C, Gottenberg J-E, Toti F, Benessiano J, Gay S, Freyssinet J-M, Mariette X. Increased levels of circulating microparticles in primary Sjögren's syndrome, systemic lupus erythematosus and rheumatoid arthritis and relation with disease activity. *Arthritis Res Ther*. 2009;**11**(5):R156.
85. Nomura S, Shimizu M. Clinical significance of procoagulant microparticles. *J Intensive Care*. 2015; **3**(1):2.
86. Xiong J, Miller VM, Li Y, Jayachandran M. Microvesicles at the crossroads between infection and cardiovascular diseases. *J Cardiovasc Pharmacol*. 2012;**59**(2):124–132.
87. Tong M, Chamley LW. Placental extracellular vesicles and feto-maternal communication. *Cold Spring Harb Perspect Med*. 2015;**5**(3):a023028.
88. Desrochers LM, Bordeleau F, Reinhart-King CA, Cerione RA, Antonyak MA. Microvesicles provide a mechanism for intercellular communication by embryonic stem cells during embryo implantation. *Nat Commun*. 2016;**7**:11958.
89. Trams EG, Lauter CJ, Salem N Jr, Heine U. Exfoliation of membrane ecto-enzymes in the form of microvesicles. *Biochim Biophys Acta*. 1981;**645**(1):63–70.
90. Harding C, Heuser J, Stahl P. Receptor-mediated endocytosis of transferrin and recycling of the transferrin receptor in rat reticulocytes. *J Cell Biol*. 1983;**97**(2):329–339.
91. Greening DW, Nguyen HPT, Elgass K, Simpson RJ, Salamonsen LA. Human endometrial exosomes contain hormone-specific cargo modulating trophoblast adhesive capacity: insights into endometrial-embryo interactions. *Biol Reprod*. 2016; **94**(2):38.
92. Théry C, Zitvogel L, Amigorena S. Exosomes: composition, biogenesis and function. *Nat Rev Immunol*. 2002;**2**(8):569–579.
93. Lane RE, Korbie D, Anderson W, Vaidyanathan R, Trau M. Analysis of exosome purification methods using a model liposome system and tunable-resistive pulse sensing. *Sci Rep*. 2015;**5**(1):7639.
94. Colombo M, Moita C, van Niel G, Kowal J, Vigneron J, Benaroch P, Manel N, Moita LF, Théry C, Raposo G. Analysis of ESCRT functions in exosome biogenesis, composition and secretion highlights the heterogeneity of extracellular vesicles. *J Cell Sci*. 2013; **126**(Pt 24):5553–5565.
95. Mathivanan S, Ji H, Simpson RJ. Exosomes: extracellular organelles important in intercellular communication. *J Proteomics*. 2010;**73**(10):1907–1920.
96. Mathivanan S, Lim JWE, Tauro BJ, Ji H, Moritz RL, Simpson RJ. Proteomics analysis of A33 immunoaffinity-purified exosomes released from the human colon tumor cell line LIM1215 reveals a tissue-specific protein signature. *Mol Cell Proteomics*. 2010;**9**(2): 197–208.
97. Miyanishi M, Tada K, Koike M, Uchiyama Y, Kitamura T, Nagata S. Identification of Tim4 as a phosphatidylserine receptor. *Nature*. 2007; **450**(7168):435–439.
98. Tauro BJ, Greening DW, Mathias RA, Mathivanan S, Ji H, Simpson RJ. Two distinct populations of exosomes are released from LIM1863 colon carcinoma cell-derived organoids. *Mol Cell Proteomics*. 2013;**12**(3):587–598.
99. Ji H, Chen M, Greening DW, He W, Rai A, Zhang W, Simpson RJ. Deep sequencing of RNA from three different extracellular vesicle (EV) subtypes released from the human LIM1863 colon cancer cell line uncovers distinct miRNA-enrichment signatures. *PLoS One*. 2014;**9**(10):e110314.
100. Kowal J, Arras G, Colombo M, Jouve M, Morath JP, Primdal-Bengtson B, Dingli F, Loew D, Tkach M, Théry C. Proteomic comparison defines novel markers to characterize heterogeneous populations of extracellular vesicle subtypes. *Proc Natl Acad Sci USA*. 2016;**113**(8):E968–E977.
101. Lai RC, Tan SS, Yeo RWY, Choo ABH, Reiner AT, Su Y, Shen Y, Fu Z, Alexander L, Sze SK, Lim SK. MSC secretes at least 3 EV types each with a unique permutation of membrane lipid, protein and RNA. *J Extracell Vesicles*. 2016;**5**(1):29828.
102. Tkach M, Kowal J, Zucchetti AE, Enserink L, Jouve M, Lankar D, Saitakis M, Martin-Jaular L, Théry C. Qualitative differences in T-cell activation by dendritic cell-derived extracellular vesicle subtypes. *EMBO J*. 2017;**36**(20):3012–3028.
103. Ogawa Y, Miura Y, Harazono A, Kanai-Azuma M, Akimoto Y, Kawakami H, Yamaguchi T, Toda T, Endo T, Tsubuki M, Yanoshita R. Proteomic analysis of two types of exosomes in human whole saliva. *Biol Pharm Bull*. 2011;**34**(1):13–23.
104. Aalberts M, van Dissel-Emiliani FMF, van Adrichem NPH, van Wijnen M, Wauben MHM, Stout TAE, Stoorvogel W. Identification of distinct populations of prostasomes that differentially express prostate stem cell antigen, annexin A1, and GLIPR2 in humans. *Biol Reprod*. 2012;**86**(3):82.
105. Laulagnier K, Javalet C, Hemming FJ, Chivet M, Lachenal G, Blot B, Chatellard C, Sadoul R. Amyloid precursor protein products concentrate in a subset of exosomes specifically endocytosed by neurons. *Cell Mol Life Sci*. 2018;**75**(4):757–773.
106. Chen M, Xu R, Ji H, Greening DW, Rai A, Izumikawa K, Ishikawa H, Takahashi N, Simpson RJ. Transcriptome and long noncoding RNA sequencing of three extracellular vesicle subtypes released from the human colon cancer LIM1863 cell line. *Sci Rep*. 2016;**6**(1):38397.
107. De Toro J, Herschlik L, Waldner C, Mongini C. Emerging roles of exosomes in normal and pathological conditions: new insights for diagnosis and therapeutic applications. *Front Immunol*. 2015;**6**:203.
108. Suchorska WM, Lach MS. The role of exosomes in tumor progression and metastasis. [Review] *Oncol Rep*. 2016;**35**(3):1237–1244.
109. Greening DW, Gopal SK, Xu R, Simpson RJ, Chen W. Exosomes and their roles in immune regulation and cancer. *Semin Cell Dev Biol*. 2015;**40**:72–81.
110. Muller L, Mitsuhashi M, Simms P, Gooding WE, Whiteside TL. Tumor-derived exosomes regulate expression of immune function-related genes in human T cell subsets. *Sci Rep*. 2016;**6**(1):20254.
111. Witwer KW, Buzás EI, Bemis LT, Bora A, Lässer C, Lötvall J, Nolte-'t Hoen EN, Piper MG, Sivaraman S, Skog J, Théry C, Wauben MH, Hochberg F. Standardization of sample collection, isolation and analysis methods in extracellular vesicle research. *J Extracell Vesicles*. 2013;**2**(1):20360.
112. Théry C, Amigorena S, Raposo G, Clayton A. Isolation and characterization of exosomes from cell culture supernatants and biological fluids. *Curr Protoc Cell Biol*. 2006;Chapter 3:Unit 3.22. doi: https://doi.org/10.1002/0471143030.cb0322s30.
113. Lamparski HG, Metha-Damani A, Yao J-Y, Patel S, Hsu D-H, Ruegg C, Le Pecq J-B. Production and characterization of clinical grade exosomes derived from dendritic cells. *J Immunol Methods*. 2002; **270**(2):211–226.
114. Chiou N-T, Ansel KM. Improved exosome isolation by sucrose gradient fractionation of ultracentrifuged crude exosome pellets. Protocol Exchange. Available at: www.nature.com/protocolexchange/protocols/5035.
115. Keller S, Ridinger J, Rupp A-K, Janssen JWG, Altevogt P. Body fluid derived exosomes as a novel template for clinical diagnostics. *J Transl Med*. 2011;**9**(1):86.
116. Greening DW, Xu R, Ji H, Tauro BJ, Simpson RJ. A protocol for exosome isolation and characterization: evaluation of ultracentrifugation, density-gradient separation, and immunoaffinity capture methods. *Methods Mol Biol*. 2015;**1295**:179–209.
117. Cantin R, Diou J, Bélanger D, Tremblay AM, Gilbert C. Discrimination between exosomes and HIV-1: purification of both vesicles from cell-free supernatants. *J Immunol Methods*. 2008;**338**(1–2):21–30.
118. Klimentová J, Stulík J. Methods of isolation and purification of outer membrane vesicles from gram-negative bacteria. *Microbiol Res*. 2015;**170**:1–9.
119. Ford T, Graham J, Rickwood D. Iodixanol: a nonionic iso-osmotic centrifugation medium for the formation of self-generated gradients. *Anal Biochem*. 1994;**220**(2):360–366.
120. György B, Módos K, Pállinger E, Pálóczi K, Pásztói M, Misják P, Deli MA, Sipos A, Szalai A, Voszka I, Polgár A, Tóth K, Csete M, Nagy G, Gay S, Falus A, Kittel A, Buzás EI. Detection and isolation of cell-derived microparticles are compromised by protein complexes resulting from shared biophysical parameters. *Blood*. 2011;**117**(4):e39–e48.
121. Bryzgunova OE, Zaripov MM, Skvortsova TE, Lekchnov EA, Grigor'eva AE, Zaporozhchenko IA, Morozkin ES, Ryabchikova EI, Yurchenko YB, Voitsitskiy VE, Laktionov PP. Comparative study of extracellular vesicles from the urine of healthy individuals and prostate cancer patients. *PLoS One*. 2016;**11**(6):e0157566.
122. Lobb RJ, Becker M, Wen SW, Wong CSF, Wiegmans AP, Leimgruber A, Möller A. Optimized exosome

isolation protocol for cell culture supernatant and human plasma. *J Extracell Vesicles*. 2015;**4**(1):27031.
123. Klein-Scory S, Tehrani MM, Eilert-Micus C, Adamczyk KA, Wojtalewicz N, Schnölzer M, Hahn SA, Schmiegel W, Schwarte-Waldhoff I. New insights in the composition of extracellular vesicles from pancreatic cancer cells: implications for biomarkers and functions. *Proteome Sci*. 2014;**12**(1):50.
124. Cheruvanky A, Zhou H, Pisitkun T, Kopp JB, Knepper MA, Yuen PST, Star RA. Rapid isolation of urinary exosomal biomarkers using a nanomembrane ultrafiltration concentrator. *Am J Physiol Renal Physiol*. 2007;**292**(5):F1657–F1661.
125. Merchant ML, Powell DW, Wilkey DW, Cummins TD, Deegens JK, Rood IM, McAfee KJ, Fleischer C, Klein E, Klein JB. Microfiltration isolation of human urinary exosomes for characterization by MS. *Proteomics Clin Appl*. 2010;**4**(1):84–96.
126. Böing AN, van der Pol E, Grootemaat AE, Coumans FAW, Sturk A, Nieuwland R. Single-step isolation of extracellular vesicles by size-exclusion chromatography. *J Extracell Vesicles*. 2014;**3**(1):23430.
127. de Menezes-Neto A, Sáez MJF, Lozano-Ramos I, Segui-Barber J, Martin-Jaular L, Ullate JME, Fernandez-Becerra C, Borrás FE, Del Portillo HA. Size-exclusion chromatography as a stand-alone methodology identifies novel markers in mass spectrometry analyses of plasma-derived vesicles from healthy individuals. *J Extracell Vesicles*. 2015;**4**(1):27378.
128. Lozano-Ramos I, Bancu I, Oliveira-Tercero A, Armengol MP, Menezes-Neto A, Del Portillo HA, Lauzurica-Valdemoros R, Borràs FE. Size-exclusion chromatography-based enrichment of extracellular vesicles from urine samples. *J Extracell Vesicles*. 2015; **4**(1):27369.
129. Taylor DD, Lyons KS, Gerçel-Taylor Ç. Shed membrane fragment-associated markers for endometrial and ovarian cancers. *Gynecol Oncol*. 2002; **84**(3):443–448.
130. Hong CS, Muller L, Boyiadzis M, Whiteside TL. Isolation and characterization of $CD34^+$ blast-derived exosomes in acute myeloid leukemia. *PLoS One*. 2014;**9**(8):e103310.
131. Yoo CE, Kim G, Kim M, Park D, Kang HJ, Lee M, Huh N. A direct extraction method for microRNAs from exosomes captured by immunoaffinity beads. *Anal Biochem*. 2012;**431**(2):96–98.
132. Clayton A, Court J, Navabi H, Adams M. Analysis of antigen presenting cell derived exosomes, based on immuno-magnetic isolation and flow cytometry. *J Immunol Methods*. 2001;**247**(1–2):163–174.
133. Taylor DD, Zacharias W, Gercel-Taylor C. Exosome isolation for proteomic analyses and RNA profiling. *Methods Mol Biol*. 2011;**728**:235–246.
134. Alvarez ML, Khosroheidari M, Kanchi Ravi R, DiStefano JK. Comparison of protein, microRNA, and mRNA yields using different methods of urinary exosome isolation for the discovery of kidney disease biomarkers. *Kidney Int*. 2012;**82**(9):1024–1032.
135. Kanwar SS, Dunlay CJ, Simeone DM, Nagrath S. Microfluidic device (ExoChip) for on-chip isolation, quantification and characterization of circulating exosomes. *Lab Chip*. 2014;**14**(11):1891–1900.
136. Bhagat AAS, Kuntaegowdanahalli SS, Papautsky I. Continuous particle separation in spiral microchannels using Dean flows and differential migration. *Lab Chip*. 2008;**8**(11):1906–1914.
137. Ashcroft BA, de Sonneville J, Yuana Y, Osanto S, Bertina R, Kuil ME, Oosterkamp TH. Determination of the size distribution of blood microparticles directly in plasma using atomic force microscopy and microfluidics. *Biomed Microdevices*. 2012;**14**(4): 641–649.
138. Crescitelli R, Lässer C, Szabó TG, Kittel A, Eldh M, Dianzani I, Buzás EI, Lötvall J. Distinct RNA profiles in subpopulations of extracellular vesicles: apoptotic bodies, microvesicles and exosomes. *J Extracell Vesicles*. 2013;**2**(1):20677.
139. Ji H, Greening DW, Barnes TW, Lim JW, Tauro BJ, Rai A, Xu R, Adda C, Mathivanan S, Zhao W, Xue Y, Xu T, Zhu H-J, Simpson RJ. Proteome profiling of exosomes derived from human primary and metastatic colorectal cancer cells reveal differential expression of key metastatic factors and signal transduction components. *Proteomics*. 2013; **13**(10–11):1672–1686.
140. Xu R, Simpson RJ, Greening DW. A protocol for isolation and proteomic characterization of distinct extracellular vesicle subtypes by sequential centrifugal ultrafiltration. *Methods Mol Biol*. 2017;**1545**: 91–116.
141. Chen X, Gao C, Li H, Huang L, Sun Q, Dong Y, Tian C, Gao S, Dong H, Guan D, Hu X, Zhao S, Li L, Zhu L, Yan Q, Zhang J, Zen K, Zhang C-Y. Identification and characterization of microRNAs in raw milk during different periods of lactation, commercial fluid, and powdered milk products. *Cell Res*. 2010; **20**(10):1128–1137.
142. Müller G. Novel tools for the study of cell type-specific exosomes and microvesicles. *J Bioanal Biomed*. 2012;**4**(4):40–60.
143. Gámez-Valero A, Monguió-Tortajada M, Carreras-Planella L, Franquesa M, Beyer K, Borràs FE. Size-exclusion chromatography-based isolation minimally alters extracellular vesicles' characteristics compared to precipitating agents. *Sci Rep*. 2016;**6**(1): 33641.
144. Corso G, Mäger I, Lee Y, Görgens A, Bultema J, Giebel B, Wood MJA, Nordin JZ, Andaloussi SE. Reproducible and scalable purification of extracellular vesicles using combined bind-elute and size exclusion chromatography. *Sci Rep*. 2017;**7**(1):11561.
145. Benedikter BJ, Bouwman FG, Vajen T, Heinzmann ACA, Grauls G, Mariman EC, Wouters EFM, Savelkoul PH, Lopez-Iglesias C, Koenen RR, Rohde GGU, Stassen FRM. Ultrafiltration combined with size exclusion chromatography efficiently isolates extracellular vesicles from cell culture media for compositional and functional studies. *Sci Rep*. 2017; **7**(1):15297.
146. Nordin JZ, Lee Y, Vader P, Mäger I, Johansson HJ, Heusermann W, Wiklander OPB, Hällbrink M, Seow Y, Bultema JJ, Gilthorpe J, Davies T, Fairchild PJ, Gabrielsson S, Meisner-Kober NC, Lehtiö J, Smith CIE, Wood MJA, El Andaloussi S. Ultrafiltration with size-exclusion liquid chromatography for high yield isolation of extracellular vesicles preserving intact biophysical and functional properties. *Nanomedicine (Lond)*. 2015;**11**(4):879–883.
147. Chen C, Skog J, Hsu C-H, Lessard RT, Balaj L, Wurdinger T, Carter BS, Breakefield XO, Toner M, Irimia D. Microfluidic isolation and transcriptome analysis of serum microvesicles. *Lab Chip*. 2010; **10**(4):505–511.
148. Davies RT, Kim J, Jang SC, Choi E-J, Gho YS, Park J. Microfluidic filtration system to isolate extracellular vesicles from blood. *Lab Chip*. 2012;**12**(24): 5202–5210.
149. Wu M, Ouyang Y, Wang Z, Zhang R, Huang P-H, Chen C, Li H, Li P, Quinn D, Dao M, Suresh S, Sadovsky Y, Huang TJ. Isolation of exosomes from whole blood by integrating acoustics and microfluidics. *Proc Natl Acad Sci USA*. 2017;**114**(40): 10584–10589.
150. Li P, Kaslan M, Lee SH, Yao J, Gao Z. Progress in exosome isolation techniques. *Theranostics*. 2017; **7**(3):789–804.
151. Willis GR, Kourembanas S, Mitsialis SA. Toward exosome-based therapeutics: isolation, heterogeneity, and fit-for-purpose potency. *Front Cardiovasc Med*. 2017;**4**:63.
152. Raposo G, Nijman HW, Stoorvogel W, Liejendekker R, Harding CV, Melief CJ, Geuze HJ. B lymphocytes secrete antigen-presenting vesicles. *J Exp Med*. 1996; **183**(3):1161–1172.
153. Melo SA, Luecke LB, Kahlert C, Fernandez AF, Gammon ST, Kaye J, LeBleu VS, Mittendorf EA, Weitz J, Rahbari N, Reissfelder C, Pilarsky C, Fraga MF, Piwnica-Worms D, Kalluri R. Glypican-1 identifies cancer exosomes and detects early pancreatic cancer. *Nature*. 2015;**523**(7559):177–182.
154. Roccaro AM, Sacco A, Maiso P, Azab AK, Tai Y-T, Reagan M, Azab F, Flores LM, Campigotto F, Weller E, Anderson KC, Scadden DT, Ghobrial IM. BM mesenchymal stromal cell-derived exosomes facilitate multiple myeloma progression. *J Clin Invest*. 2013;**123**(4):1542–1555.
155. Höög JL, Lötvall J. Diversity of extracellular vesicles in human ejaculates revealed by cryo-electron microscopy. *J Extracell Vesicles*. 2015;**4**(1):28680.
156. Vilella F, Moreno-Moya JM, Balaguer N, Grasso A, Herrero M, Martínez S, Marcilla A, Simón C. Hsa-miR-30d, secreted by the human endometrium, is taken up by the pre-implantation embryo and might modify its transcriptome. *Development*. 2015; **142**(18):3210–3221.
157. Wu Y, Deng W, Klinke DJ II. Exosomes: improved methods to characterize their morphology, RNA content, and surface protein biomarkers. *Analyst (Lond)*. 2015;**140**(19):6631–6642.
158. Iwai K, Minamisawa T, Suga K, Yajima Y, Shiba K. Isolation of human salivary extracellular vesicles by iodixanol density gradient ultracentrifugation and their characterizations. *J Extracell Vesicles*. 2016;**5**(1): 30829.
159. Hardij J, Cecchet F, Berquand A, Gheldof D, Chatelain C, Mullier F, Chatelain B, Dogné J-M. Characterisation of tissue factor-bearing extracellular vesicles with AFM: comparison of air-tapping-mode AFM and liquid peak force AFM. *J Extracell Vesicles*. 2013;**2**(1):21045.
160. Yuana Y, Oosterkamp TH, Bahatyrova S, Ashcroft B, Garcia Rodriguez P, Bertina RM, Osanto S. Atomic force microscopy: a novel approach to the detection of nanosized blood microparticles. *J Thromb Haemost*. 2010;**8**(2):315–323.
161. Gardiner C, Ferreira YJ, Dragovic RA, Redman CWG, Sargent IL. Extracellular vesicle sizing and enumeration by nanoparticle tracking analysis. *J Extracell Vesicles*. 2013;**2**(1):19671.
162. Filipe V, Hawe A, Jiskoot W. Critical evaluation of nanoparticle tracking analysis (NTA) by NanoSight for the measurement of nanoparticles and protein aggregates. *Pharm Res*. 2010;**27**(5):796–810.
163. van der Pol E, Coumans FAW, Grootemaat AE, Gardiner C, Sargent IL, Harrison P, Sturk A, van Leeuwen TG, Nieuwland R. Particle size distribution of exosomes and microvesicles determined by transmission electron microscopy, flow cytometry, nanoparticle tracking analysis, and resistive pulse sensing. *J Thromb Haemost*. 2014;**12**(7):1182–1192.
164. Momen-Heravi F, Balaj L, Alian S, Tigges J, Toxavidis V, Ericsson M, Distel RJ, Ivanov AR, Skog J, Kuo WP. Alternative methods for characterization of extracellular vesicles. *Front Physiol*. 2012;**3**:354.
165. Garza-Licudine E, Deo D, Yu S, Uz-Zaman A, Dunbar WB. Portable nanoparticle quantization using a resizable nanopore instrument—the IZON qNano™. *Conf Proc IEEE Eng Med Biol Soc*. 2010; **2010**:5736–5739.

166. van der Pol E, Hoekstra AG, Sturk A, Otto C, van Leeuwen TG, Nieuwland R. Optical and non-optical methods for detection and characterization of microparticles and exosomes. *J Thromb Haemost*. 2010;**8**(12):2596–2607.
167. Lacroix R, Robert S, Poncelet P, Dignat-George F. Overcoming limitations of microparticle measurement by flow cytometry. *Semin Thromb Hemost*. 2010;**36**(8):807–818.
168. van der Vlist EJ, Nolte-'t Hoen ENM, Stoorvogel W, Arkesteijn GJA, Wauben MHM. Fluorescent labeling of nano-sized vesicles released by cells and subsequent quantitative and qualitative analysis by high-resolution flow cytometry. *Nat Protoc*. 2012;**7**(7):1311–1326.
169. Nolte-'t Hoen ENM, van der Vlist EJ, Aalberts M, Mertens HCH, Bosch BJ, Bartelink W, Mastrobattista E, van Gaal EVB, Stoorvogel W, Arkesteijn GJA, Wauben MHM. Quantitative and qualitative flow cytometric analysis of nanosized cell-derived membrane vesicles. *Nanomedicine (Lond)*. 2012;**8**(5):712–720.
170. Osteikoetxea X, Balogh A, Szabó-Taylor K, Németh A, Szabó TG, Pálóczi K, Sódar B, Kittel Á, György B, Pállinger É, Matkó J, Buzás EI. Improved characterization of EV preparations based on protein to lipid ratio and lipid properties. *PLoS One*. 2015;**10**(3):e0121184.
171. Ng YH, Rome S, Jalabert A, Forterre A, Singh H, Hincks CL, Salamonsen LA. Endometrial exosomes/microvesicles in the uterine microenvironment: a new paradigm for embryo-endometrial cross talk at implantation. *PLoS One*. 2013;**8**(3):e58502.
172. Nakai W, Yoshida T, Diez D, Miyatake Y, Nishibu T, Imawaka N, Naruse K, Sadamura Y, Hanayama R. A novel affinity-based method for the isolation of highly purified extracellular vesicles. *Sci Rep*. 2016;**6**(1):33935.
173. Logozzi M, De Milito A, Lugini L, Borghi M, Calabrò L, Spada M, Perdicchio M, Marino ML, Federici C, Iessi E, Brambilla D, Venturi G, Lozupone F, Santinami M, Huber V, Maio M, Rivoltini L, Fais S. High levels of exosomes expressing CD63 and caveolin-1 in plasma of melanoma patients. *PLoS One*. 2009;**4**(4):e5219.
174. Yoshioka Y, Kosaka N, Konishi Y, Ohta H, Okamoto H, Sonoda H, Nonaka R, Yamamoto H, Ishii H, Mori M, Furuta K, Nakajima T, Hayashi H, Sugisaki H, Higashimoto H, Kato T, Takeshita F, Ochiya T. Ultra-sensitive liquid biopsy of circulating extracellular vesicles using ExoScreen. *Nat Commun*. 2014;**5**:3591.
175. Shao H, Chung J, Balaj L, Charest A, Bigner DD, Carter BS, Hochberg FH, Breakefield XO, Weissleder R, Lee H. Protein typing of circulating microvesicles allows real-time monitoring of glioblastoma therapy. *Nat Med*. 2012;**18**(12):1835–1840.
176. Im H, Shao H, Weissleder R, Castro CM, Lee H. Nano-plasmonic exosome diagnostics. *Expert Rev Mol Diagn*. 2015;**15**(6):725–733.
177. Im H, Shao H, Park YI, Peterson VM, Castro CM, Weissleder R, Lee H. Label-free detection and molecular profiling of exosomes with a nano-plasmonic sensor. *Nat Biotechnol*. 2014;**32**(5):490–495.
178. Carrasco-Ramírez P, Greening DW, Andrés G, Gopal SK, Martín-Villar E, Renart J, Simpson RJ, Quintanilla M. Podoplanin is a component of extracellular vesicles that reprograms cell-derived exosomal proteins and modulates lymphatic vessel formation. *Oncotarget*. 2016;**7**(13):16070–16089.
179. Gopal SK, Greening DW, Hanssen EG, Zhu H-J, Simpson RJ, Mathias RA. Oncogenic epithelial cell-derived exosomes containing Rac1 and PAK2 induce angiogenesis in recipient endothelial cells. *Oncotarget*. 2016;**7**(15):19709–19722.
180. Dragovic RA, Gardiner C, Brooks AS, Tannetta DS, Ferguson DJP, Hole P, Carr B, Redman CWG, Harris AL, Dobson PJ, Harrison P, Sargent IL. Sizing and phenotyping of cellular vesicles using nanoparticle tracking analysis. *Nanomedicine (Lond)*. 2011;**7**(6):780–788.
181. Gardiner C, Shaw M, Hole P, Smith J, Tannetta D, Redman CW, Sargent IL. Measurement of refractive index by nanoparticle tracking analysis reveals heterogeneity in extracellular vesicles. *J Extracell Vesicles*. 2014;**3**(1):25361.
182. Palmieri V, Lucchetti D, Gatto I, Maiorana A, Marcantoni M, Maulucci G, Papi M, Pola R, De Spirito M, Sgambato A. Dynamic light scattering for the characterization and counting of extracellular vesicles: a powerful noninvasive tool. *J Nanopart Res*. 2014;**16**(9):2583.
183. Greening DW, Xu R, Gopal SK, Rai A, Simpson RJ. Proteomic insights into extracellular vesicle biology—defining exosomes and shed microvesicles. *Expert Rev Proteomics*. 2017;**14**(1):69–95.
184. Théry C, Regnault A, Garin J, Wolfers J, Zitvogel L, Ricciardi-Castagnoli P, Raposo G, Amigorena S. Molecular characterization of dendritic cell-derived exosomes. Selective accumulation of the heat shock protein hsc73. *J Cell Biol*. 1999;**147**(3):599–610.
185. Aatonen MT, Ohman T, Nyman TA, Laitinen S, Grönholm M, Siljander PRM. Isolation and characterization of platelet-derived extracellular vesicles. *J Extracell Vesicles*. 2014;**3**(1):24692.
186. MacKenzie A, Wilson HL, Kiss-Toth E, Dower SK, North RA, Surprenant A. Rapid secretion of interleukin-1β by microvesicle shedding. *Immunity*. 2001;**15**(5):825–835.
187. Berda-Haddad Y, Robert S, Salers P, Zekraoui L, Farnarier C, Dinarello CA, Dignat-George F, Kaplanski G. Sterile inflammation of endothelial cell-derived apoptotic bodies is mediated by interleukin-1α. *Proc Natl Acad Sci USA*. 2011;**108**(51):20684–20689.
188. Gulinelli S, Salaro E, Vuerich M, Bozzato D, Pizzirani C, Bolognesi G, Idzko M, Di Virgilio F, Ferrari D. IL-18 associates to microvesicles shed from human macrophages by a LPS/TLR-4 independent mechanism in response to P2X receptor stimulation. *Eur J Immunol*. 2012;**42**(12):3334–3345.
189. Hasegawa H, Thomas HJ, Schooley K, Born TL. Native IL-32 is released from intestinal epithelial cells via a non-classical secretory pathway as a membrane-associated protein. *Cytokine*. 2011;**53**(1):74–83.
190. Zhang H-G, Liu C, Su K, Yu S, Zhang L, Zhang S, Wang J, Cao X, Grizzle W, Kimberly RP. A membrane form of TNF-alpha presented by exosomes delays T cell activation-induced cell death. *J Immunol*. 2006;**176**(12):7385–7393.
191. Kandere-Grzybowska K, Letourneau R, Kempuraj D, Donelan J, Poplawski S, Boucher W, Athanassiou A, Theoharides TC. IL-1 induces vesicular secretion of IL-6 without degranulation from human mast cells. *J Immunol*. 2003;**171**(9):4830–4836.
192. Nardi FS, Michelon TF, Neumann J, Manvailer LFS, Wagner B, Horn PA, Bicalho MG, Rebmann V. High levels of circulating extracellular vesicles with altered expression and function during pregnancy. *Immunobiology*. 2016;**221**(7):753–760.
193. Llorente A, Skotland T, Sylvänne T, Kauhanen D, Róg T, Orłowski A, Vattulainen I, Ekroos K, Sandvig K. Molecular lipidomics of exosomes released by PC-3 prostate cancer cells. *Biochim Biophys Acta*. 2013;**1831**(7):1302–1309.
194. Brouwers JF, Aalberts M, Jansen JWA, van Niel G, Wauben MH, Stout TAE, Helms JB, Stoorvogel W. Distinct lipid compositions of two types of human prostasomes. *Proteomics*. 2013;**13**(10–11):1660–1666.
195. Trajkovic K, Hsu C, Chiantia S, Rajendran L, Wenzel D, Wieland F, Schwille P, Brügger B, Simons M. Ceramide triggers budding of exosome vesicles into multivesicular endosomes. *Science*. 2008;**319**(5867):1244–1247.
196. Skotland T, Ekroos K, Kauhanen D, Simolin H, Seierstad T, Berge V, Sandvig K, Llorente A. Molecular lipid species in urinary exosomes as potential prostate cancer biomarkers. *Eur J Cancer*. 2017;**70**:122–132.
197. Valadi H, Ekström K, Bossios A, Sjöstrand M, Lee JJ, Lötvall JO. Exosome-mediated transfer of mRNAs and microRNAs is a novel mechanism of genetic exchange between cells. *Nat Cell Biol*. 2007;**9**(6):654–659.
198. Huang X, Yuan T, Tschannen M, Sun Z, Jacob H, Du M, Liang M, Dittmar RL, Liu Y, Liang M, Kohli M, Thibodeau SN, Boardman L, Wang L. Characterization of human plasma-derived exosomal RNAs by deep sequencing. *BMC Genomics*. 2013;**14**(1):319.
199. Vojtech L, Woo S, Hughes S, Levy C, Ballweber L, Sauteraud RP, Strobl J, Westerberg K, Gottardo R, Tewari M, Hladik F. Exosomes in human semen carry a distinctive repertoire of small non-coding RNAs with potential regulatory functions. *Nucleic Acids Res*. 2014;**42**(11):7290–7304.
200. van Balkom BWM, Eisele AS, Pegtel DM, Bervoets S, Verhaar MC. Quantitative and qualitative analysis of small RNAs in human endothelial cells and exosomes provides insights into localized RNA processing, degradation and sorting. *J Extracell Vesicles*. 2015;**4**(1):26760.
201. Cheng L, Sharples RA, Scicluna BJ, Hill AF. Exosomes provide a protective and enriched source of miRNA for biomarker profiling compared to intracellular and cell-free blood. *J Extracell Vesicles*. 2014;**3**(1):23743.
202. Arroyo JD, Chevillet JR, Kroh EM, Ruf IK, Pritchard CC, Gibson DF, Mitchell PS, Bennett CF, Pogosova-Agadjanyan EL, Stirewalt DL, Tait JF, Tewari M. Argonaute2 complexes carry a population of circulating microRNAs independent of vesicles in human plasma. *Proc Natl Acad Sci USA*. 2011;**108**(12):5003–5008.
203. Turchinovich A, Weiz L, Langheinz A, Burwinkel B. Characterization of extracellular circulating microRNA. *Nucleic Acids Res*. 2011;**39**(16):7223–7233.
204. Li H, Huang S, Guo C, Guan H, Xiong C. Cell-free seminal mRNA and microRNA exist in different forms. *PLoS One*. 2012;**7**(4):e34566.
205. Shelke GV, Lässer C, Gho YS, Lötvall J. Importance of exosome depletion protocols to eliminate functional and RNA-containing extracellular vesicles from fetal bovine serum. *J Extracell Vesicles*. 2014;**3**(1):24783.
206. Thakur BK, Zhang H, Becker A, Matei I, Huang Y, Costa-Silva B, Zheng Y, Hoshino A, Brazier H, Xiang J, Williams C, Rodriguez-Barrueco R, Silva JM, Zhang W, Hearn S, Elemento O, Paknejad N, Manova-Todorova K, Welte K, Bromberg J, Peinado H, Lyden D. Double-stranded DNA in exosomes: a novel biomarker in cancer detection. *Cell Res*. 2014;**24**(6):766–769.
207. Waldenström A, Gennebäck N, Hellman U, Ronquist G. Cardiomyocyte microvesicles contain DNA/RNA and convey biological messages to target cells. *PLoS One*. 2012;**7**(4):e34653.
208. Lázaro-Ibáñez E, Sanz-Garcia A, Visakorpi T, Escobedo-Lucea C, Siljander P, Ayuso-Sacido A, Yliperttula M.

Different gDNA content in the subpopulations of prostate cancer extracellular vesicles: apoptotic bodies, microvesicles, and exosomes. *Prostate*. 2014; **74**(14):1379–1390.
209. Balaj L, Lessard R, Dai L, Cho Y-J, Pomeroy SL, Breakefield XO, Skog J. Tumour microvesicles contain retrotransposon elements and amplified oncogene sequences. *Nat Commun*. 2011;**2**:180.
210. Guescini M, Genedani S, Stocchi V, Agnati LF. Astrocytes and glioblastoma cells release exosomes carrying mtDNA. *J Neural Transm (Vienna)*. 2010; **117**(1):1–4.
211. Montecalvo A, Larregina AT, Shufesky WJ, Stolz DB, Sullivan MLG, Karlsson JM, Baty CJ, Gibson GA, Erdos G, Wang Z, Milosevic J, Tkacheva OA, Divito SJ, Jordan R, Lyons-Weiler J, Watkins SC, Morelli AE. Mechanism of transfer of functional microRNAs between mouse dendritic cells via exosomes. *Blood*. 2012;**119**(3):756–766.
212. Morelli AE, Larregina AT, Shufesky WJ, Sullivan MLG, Stolz DB, Papworth GD, Zahorchak AF, Logar AJ, Wang Z, Watkins SC, Falo LD Jr, Thomson AW. Endocytosis, intracellular sorting, and processing of exosomes by dendritic cells. *Blood*. 2004;**104**(10): 3257–3266.
213. Feng D, Zhao W-L, Ye Y-Y, Bai X-C, Liu R-Q, Chang L-F, Zhou Q, Sui S-F. Cellular internalization of exosomes occurs through phagocytosis. *Traffic*. 2010;**11**(5):675–687.
214. Escrevente C, Keller S, Altevogt P, Costa J. Interaction and uptake of exosomes by ovarian cancer cells. *BMC Cancer*. 2011;**11**(1):108.
215. Svensson KJ, Christianson HC, Wittrup A, Bourseau-Guilmain E, Lindqvist E, Svensson LM, Mörgelin M, Belting M. Exosome uptake depends on ERK1/2-heat shock protein 27 signaling and lipid Raft-mediated endocytosis negatively regulated by caveolin-1. *J Biol Chem*. 2013;**288**(24):17713–17724.
216. Nanbo A, Kawanishi E, Yoshida R, Yoshiyama H. Exosomes derived from Epstein-Barr virus-infected cells are internalized via caveola-dependent endocytosis and promote phenotypic modulation in target cells. *J Virol*. 2013;**87**(18):10334–10347.
217. Fitzner D, Schnaars M, van Rossum D, Krishnamoorthy G, Dibaj P, Bakhti M, Regen T, Hanisch U-K, Simons M. Selective transfer of exosomes from oligodendrocytes to microglia by macropinocytosis. *J Cell Sci*. 2011; **124**(Pt 3):447–458.
218. Paolillo M, Schinelli S. Integrins and exosomes, a dangerous liaison in cancer progression. *Cancers (Basel)*. 2017;**9**(8):E95.
219. Rana S, Yue S, Stadel D, Zöller M. Toward tailored exosomes: the exosomal tetraspanin web contributes to target cell selection. *Int J Biochem Cell Biol*. 2012;**44**(9):1574–1584.
220. Segura E, Guérin C, Hogg N, Amigorena S, Théry C. $CD8^+$ dendritic cells use LFA-1 to capture MHC-peptide complexes from exosomes in vivo. *J Immunol*. 2007;**179**(3):1489–1496.
221. Hanayama R, Tanaka M, Miwa K, Shinohara A, Iwamatsu A, Nagata S. Identification of a factor that links apoptotic cells to phagocytes. *Nature*. 2002; **417**(6885):182–187.
222. French KC, Antonyak MA, Cerione RA. Extracellular vesicle docking at the cellular port: extracellular vesicle binding and uptake. *Semin Cell Dev Biol*. 2017; **67**:48–55.
223. Tian T, Zhu Y-L, Zhou Y-Y, Liang G-F, Wang Y-Y, Hu F-H, Xiao Z-D. Exosome uptake through clathrin-mediated endocytosis and macropinocytosis and mediating miR-21 delivery. *J Biol Chem*. 2014; **289**(32):22258–22267.
224. Christianson HC, Svensson KJ, van Kuppevelt TH, Li J-P, Belting M. Cancer cell exosomes depend on cell-surface heparan sulfate proteoglycans for their internalization and functional activity. *Proc Natl Acad Sci USA*. 2013;**110**(43):17380–17385.
225. Camussi G, Deregibus M-C, Bruno S, Grange C, Fonsato V, Tetta C. Exosome/microvesicle-mediated epigenetic reprogramming of cells. *Am J Cancer Res*. 2011;**1**(1):98–110.
226. Hong BS, Cho J-H, Kim H, Choi E-J, Rho S, Kim J, Kim JH, Choi D-S, Kim Y-K, Hwang D, Gho YS. Colorectal cancer cell-derived microvesicles are enriched in cell cycle-related mRNAs that promote proliferation of endothelial cells. *BMC Genomics*. 2009;**10**(1):556.
227. Hood JL, San RS, Wickline SA. Exosomes released by melanoma cells prepare sentinel lymph nodes for tumor metastasis. *Cancer Res*. 2011;**71**(11): 3792–3801.
228. Peinado H, Alečković M, Lavotshkin S, Matei I, Costa-Silva B, Moreno-Bueno G, Hergueta-Redondo M, Williams C, García-Santos G, Ghajar C, Nitadori-Hoshino A, Hoffman C, Badal K, Garcia BA, Callahan MK, Yuan J, Martins VR, Skog J, Kaplan RN, Brady MS, Wolchok JD, Chapman PB, Kang Y, Bromberg J, Lyden D. Melanoma exosomes educate bone marrow progenitor cells toward a pro-metastatic phenotype through MET. *Nat Med*. 2012;**18**(6): 883–891.
229. Sheldon H, Heikamp E, Turley H, Dragovic R, Thomas P, Oon CE, Leek R, Edelmann M, Kessler B, Sainson RCA, Sargent I, Li J-L, Harris AL. New mechanism for Notch signaling to endothelium at a distance by Delta-like 4 incorporation into exosomes. *Blood*. 2010;**116**(13):2385–2394.
230. Mulcahy LA, Pink RC, Carter DRF. Routes and mechanisms of extracellular vesicle uptake. *J Extracell Vesicles*. 2014;**3**(1):24641.
231. Lai CP, Kim EY, Badr CE, Weissleder R, Mempel TR, Tannous BA, Breakefield XO. Visualization and tracking of tumour extracellular vesicle delivery and RNA translation using multiplexed reporters. *Nat Commun*. 2015;**6**(1):7029.
232. Zomer A, Maynard C, Verweij FJ, Kamermans A, Schäfer R, Beerling E, Schiffelers RM, de Wit E, Berenguer J, Ellenbroek SIJ, Wurdinger T, Pegtel DM, van Rheenen J. In vivo imaging reveals extracellular vesicle-mediated phenocopying of metastatic behavior. *Cell*. 2015;**161**(5):1046–1057.
233. Ridder K, Sevko A, Heide J, Dams M, Rupp A-K, Macas J, Starmann J, Tjwa M, Plate KH, Sültmann H, Altevogt P, Umansky V, Momma S. Extracellular vesicle-mediated transfer of functional RNA in the tumor microenvironment. *Oncolmmunology*. 2015; **4**(6):e1008371.
234. Ridder K, Keller S, Dams M, Rupp A-K, Schlaudraff J, Del Turco D, Starmann J, Macas J, Karpova D, Devraj K, Depboylu C, Landfried B, Arnold B, Plate KH, Höglinger G, Sültmann H, Altevogt P, Momma S. Extracellular vesicle-mediated transfer of genetic information between the hematopoietic system and the brain in response to inflammation. *PLoS Biol*. 2014;**12**(6):e1001874.
235. Cai J, Han Y, Ren H, Chen C, He D, Zhou L, Eisner GM, Asico LD, Jose PA, Zeng C. Extracellular vesicle-mediated transfer of donor genomic DNA to recipient cells is a novel mechanism for genetic influence between cells. *J Mol Cell Biol*. 2013;**5**(4): 227–238.
236. Keller S, König A-K, Marmé F, Runz S, Wolterink S, Koensgen D, Mustea A, Sehouli J, Altevogt P. Systemic presence and tumor-growth promoting effect of ovarian carcinoma released exosomes. *Cancer Lett*. 2009;**278**(1):73–81.
237. Christianson HC, Belting M. Heparan sulfate proteoglycan as a cell-surface endocytosis receptor. *Matrix Biol*. 2014;**35**:51–55.
238. Hoshino A, Costa-Silva B, Shen T-L, Rodrigues G, Hashimoto A, Tesic Mark M, Molina H, Kohsaka S, Di Giannatale A, Ceder S, Singh S, Williams C, Soplop N, Uryu K, Pharmer L, King T, Bojmar L, Davies AE, Ararso Y, Zhang T, Zhang H, Hernandez J, Weiss JM, Dumont-Cole VD, Kramer K, Wexler LH, Narendran A, Schwartz GK, Healey JH, Sandstrom P, Labori KJ, Kure EH, Grandgenett PM, Hollingsworth MA, de Sousa M, Kaur S, Jain M, Mallya K, Batra SK, Jarnagin WR, Brady MS, Fodstad O, Müller V, Pantel K, Minn AJ, Bissell MJ, Garcia BA, Kang Y, Rajasekhar VK, Ghajar CM, Matei I, Peinado H, Bromberg J, Lyden D. Tumour exosome integrins determine organotropic metastasis. *Nature*. 2015;**527**(7578): 329–335.
239. Rejraji H, Sion B, Prensier G, Carreras M, Motta C, Frenoux J-M, Vericel E, Grizard G, Vernet P, Drevet JR. Lipid remodeling of murine epididymosomes and spermatozoa during epididymal maturation. *Biol Reprod*. 2006;**74**(6):1104–1113.
240. Franz C, Böing AN, Montag M, Strowitzki T, Markert UR, Mastenbroek S, Nieuwland R, Toth B. Extracellular vesicles in human follicular fluid do not promote coagulation. *Reprod Biomed Online*. 2016; **33**(5):652–655.
241. Santonocito M, Vento M, Guglielmino MR, Battaglia R, Wahlgren J, Ragusa M, Barbagallo D, Borzì P, Rizzari S, Maugeri M, Scollo P, Tatone C, Valadi H, Purrello M, Di Pietro C. Molecular characterization of exosomes and their microRNA cargo in human follicular fluid: bioinformatic analysis reveals that exosomal microRNAs control pathways involved in follicular maturation. *Fertil Steril*. 2014; **102**(6):1751–1761.e1.
242. Al-Dossary AA, Bathala P, Caplan JL, Martin-DeLeon PA. Oviductosome-sperm membrane interaction in cargo delivery: detection of fusion and underlying molecular players using three-dimensional super-resolution structured illumination microscopy (SR-SIM). *J Biol Chem*. 2015;**290**(29):17710–17723.
243. Al-Dossary AA, Strehler EE, Martin-DeLeon PA. Expression and secretion of plasma membrane Ca2+-ATPase 4a (PMCA4a) during murine estrus: association with oviductal exosomes and uptake in sperm. *PLoS ONE*. 2013;**8**(11):e80181.
244. Flori F, Secciani F, Capone A, Paccagnini E, Caruso S, Ricci MG, Focarelli R. Menstrual cycle-related sialidase activity of the female cervical mucus is associated with exosome-like vesicles. *Fertil Steril*. 2007;**88**(4, Suppl):1212–1219.
245. Uszyński W, Zekanowska E, Uszyński M, Zyliński A, Kuczyński J. New observations on procoagulant properties of amniotic fluid: microparticles (MPs) and tissue factor-bearing MPs (MPs-TF), comparison with maternal blood plasma. *Thromb Res*. 2013; **132**(6):757–760.
246. Admyre C, Johansson SM, Qazi KR, Filén J-J, Lahesmaa R, Norman M, Neve EPA, Scheynius A, Gabrielsson S. Exosomes with immune modulatory features are present in human breast milk. *J Immunol*. 2007;**179**(3):1969–1978.
247. Foster BP, Balassa T, Benen TD, Dominovic M, Elmadjian GK, Florova V, Fransolet MD, Kestlerova A, Kmiecik G, Kostadinova IA, Kyvelidou C, Meggyes M, Mincheva MN, Moro L, Pastuschek J, Spoldi V, Wandernoth P, Weber M, Toth B, Markert UR. Extracellular vesicles in blood, milk and body fluids of the female and male urogenital tract and with special regard to reproduction. *Crit Rev Clin Lab Sci*. 2016;**53**(6):379–395.
248. Frenette G, Sullivan R. Prostasome-like particles are involved in the transfer of P25b from the bovine epididymal fluid to the sperm surface. *Mol Reprod Dev*. 2001;**59**(1):115–121.

249. Caballero J, Frenette G, D'Amours O, Belleannée C, Lacroix-Pépin N, Robert C, Sullivan R. Bovine sperm raft membrane associated glioma pathogenesis-related 1-like protein 1 (GliPr1L1) is modified during the epididymal transit and is potentially involved in sperm binding to the zona pellucida. *J Cell Physiol*. 2012;**227**(12):3876–3886.
250. Frenette G, Lessard C, Madore E, Fortier MA, Sullivan R. Aldose reductase and macrophage migration inhibitory factor are associated with epididymosomes and spermatozoa in the bovine epididymis. *Biol Reprod*. 2003;**69**(5):1586–1592.
251. D'Amours O, Frenette G, Caron P, Belleannée C, Guillemette C, Sullivan R. Evidences of biological functions of biliverdin reductase A in the bovine epididymis. *J Cell Physiol*. 2016;**231**(5):1077–1089.
252. Sullivan R, Frenette G, Girouard J. Epididymosomes are involved in the acquisition of new sperm proteins during epididymal transit. *Asian J Androl*. 2007;**9**(4):483–491.
253. Martin-DeLeon PA. Epididymosomes: transfer of fertility-modulating proteins to the sperm surface. *Asian J Androl*. 2015;**17**(5):720–725.
254. Oh JS, Han C, Cho C. ADAM7 is associated with epididymosomes and integrated into sperm plasma membrane. *Mol Cells*. 2009;**28**(5):441–446.
255. Choi H, Han C, Jin S, Kwon JT, Kim J, Jeong J, Kim J, Ham S, Jeon S, Yoo YJ, Cho C. Reduced fertility and altered epididymal and sperm integrity in mice lacking ADAM7. *Biol Reprod*. 2015;**93**(3):70.
256. Taylor A, Robson A, Houghton BC, Jepson CA, Ford WCL, Frayne J. Epididymal specific, selenium-independent GPX5 protects cells from oxidative stress-induced lipid peroxidation and DNA mutation. *Hum Reprod*. 2013;**28**(9):2332–2342.
257. Peng H, Shi J, Zhang Y, Zhang H, Liao S, Li W, Lei L, Han C, Ning L, Cao Y, Zhou Q, Chen Q, Duan E. A novel class of tRNA-derived small RNAs extremely enriched in mature mouse sperm. *Cell Res*. 2012; **22**(11):1609–1612.
258. Sharma U, Conine CC, Shea JM, Boskovic A, Derr AG, Bing XY, Belleannée C, Kucukural A, Serra RW, Sun F, Song L, Carone BR, Ricci EP, Li XZ, Fauquier L, Moore MJ, Sullivan R, Mello CC, Garber M, Rando OJ. Biogenesis and function of tRNA fragments during sperm maturation and fertilization in mammals. *Science*. 2016;**351**(6271):391–396.
259. Saez F, Sullivan R. Prostasomes, post-testicular sperm maturation and fertility. *Front Biosci*. 2016; **21**(7):1464–1473.
260. Burden HP, Holmes CH, Persad R, Whittington K. Prostasomes—their effects on human male reproduction and fertility. *Hum Reprod Update*. 2006; **12**(3):283–292.
261. Stegmayr B, Ronquist G. Promotive effect on human sperm progressive motility by prostasomes. *Urol Res*. 1982;**10**(5):253–257.
262. Arienti G, Carlini E, Nicolucci A, Cosmi EV, Santi F, Palmerini CA. The motility of human spermatozoa as influenced by prostasomes at various pH levels. *Biol Cell*. 1999;**91**(1):51–54.
263. Park K-H, Kim B-J, Kang J, Nam T-S, Lim JM, Kim HT, Park JK, Kim YG, Chae S-W, Kim U-H. Ca^{2+} signaling tools acquired from prostasomes are required for progesterone-induced sperm motility. *Sci Signal*. 2011;**4**(173):ra31.
264. Andrews RE, Galileo DS, Martin-DeLeon PA. Plasma membrane Ca^{2+}-ATPase 4: interaction with constitutive nitric oxide synthases in human sperm and prostasomes which carry Ca^{2+}/CaM-dependent serine kinase. *Mol Hum Reprod*. 2015;**21**(11): 832–843.
265. Subirán N, Agirregoitia E, Valdivia A, Ochoa C, Casis L, Irazusta J. Expression of enkephalin-degrading enzymes in human semen and implications for sperm motility. *Fertil Steril*. 2008;**89**(5, Suppl): 1571–1577.
266. Arienti G, Carlini E, Verdacchi R, Cosmi EV, Palmerini CA. Prostasome to sperm transfer of CD13/aminopeptidase N (EC 3.4.11.2). *Biochim Biophys Acta*. 1997;**1336**(3):533–538.
267. Pons-Rejraji H, Artonne C, Sion B, Brugnon F, Canis M, Janny L, Grizard G. Prostasomes: inhibitors of capacitation and modulators of cellular signalling in human sperm. *Int J Androl*. 2011;**34**(6 Pt 1):568–580.
268. Cross NL, Mahasreshti P. Prostasome fraction of human seminal plasma prevents sperm from becoming acrosomally responsive to the agonist progesterone. *Arch Androl*. 1997;**39**(1):39–44.
269. Bechoua S, Rieu I, Sion B, Grizard G. Prostasomes as potential modulators of tyrosine phosphorylation in human spermatozoa. *Syst Biol Reprod Med*. 2011; **57**(3):139–148.
270. Aalberts M, Sostaric E, Wubbolts R, Wauben MWM, Nolte-'t Hoen ENM, Gadella BM, Stout TAE, Stoorvogel W. Spermatozoa recruit prostasomes in response to capacitation induction. *Biochim Biophys Acta*. 2013;**1834**(11):2326–2335.
271. Palmerini CA, Saccardi C, Carlini E, Fabiani R, Arienti G. Fusion of prostasomes to human spermatozoa stimulates the acrosome reaction. *Fertil Steril*. 2003; **80**(5):1181–1184.
272. Siciliano L, Marcianò V, Carpino A. Prostasome-like vesicles stimulate acrosome reaction of pig spermatozoa. *Reprod Biol Endocrinol*. 2008;**6**(1):5.
273. Minelli A, Allegrucci C, Liguori L, Ronquist G. Ectodiadenosine polyphosphates hydrolase activity on human prostasomes. *Prostate*. 2002;**51**(1):1–9.
274. Oliw EH, Fabiani R, Johansson L, Ronquist G. Arachidonic acid 15-lipoxygenase and traces of E prostaglandins in purified human prostasomes. *J Reprod Fertil*. 1993;**99**(1):195–199.
275. Sohel MMH, Hoelker M, Noferesti SS, Salilew-Wondim D, Tholen E, Looft C, Rings F, Uddin MJ, Spencer TE, Schellander K, Tesfaye D. Exosomal and non-exosomal transport of extra-cellular microRNAs in follicular fluid: implications for bovine oocyte developmental competence. *PLoS One*. 2013; **8**(11):e78505.
276. Navakanitworakul R, Hung W-T, Gunewardena S, Davis JS, Chotigeat W, Christenson LK. Characterization and small RNA content of extracellular vesicles in follicular fluid of developing bovine antral follicles. *Sci Rep*. 2016; **6**(1):25486.
277. da Silveira JC, Carnevale EM, Winger QA, Bouma GJ. Regulation of ACVR1 and ID2 by cell-secreted exosomes during follicle maturation in the mare. *Reprod Biol Endocrinol*. 2014;**12**(1):44.
278. Hung W-T, Hong X, Christenson LK, McGinnis LK. Extracellular vesicles from bovine follicular fluid support cumulus expansion. *Biol Reprod*. 2015;**93**(5): 117.
279. Schuh K, Cartwright EJ, Jankevics E, Bundschu K, Liebermann J, Williams JC, Armesilla AL, Emerson M, Oceandy D, Knobeloch K-P, Neyses L. Plasma membrane Ca^{2+} ATPase 4 is required for sperm motility and male fertility. *J Biol Chem*. 2004;**279**(27): 28220–28226.
280. Okunade GW, Miller ML, Pyne GJ, Sutliff RL, O'Connor KT, Neumann JC, Andringa A, Miller DA, Prasad V, Doetschman T, Paul RJ, Shull GE. Targeted ablation of plasma membrane Ca^{2+}-ATPase (PMCA) 1 and 4 indicates a major housekeeping function for PMCA1 and a critical role in hyperactivated sperm motility and male fertility for PMCA4. *J Biol Chem*. 2004;**279**(32):33742–33750.
281. Lopera-Vásquez R, Hamdi M, Fernandez-Fuertes B, Maillo V, Beltrán-Breña P, Calle A, Redruello A, López-Martín S, Gutierrez-Adán A, Yañez-Mó M, Ramírez MÁ, Rizos D. Extracellular vesicles from BOEC in in vitro embryo development and quality. *PLoS One*. 2016;**11**(2):e0148083.
282. Burns GW, Brooks KE, Spencer TE. Extracellular vesicles originate from the conceptus and uterus during early pregnancy in sheep. *Biol Reprod*. 2016; **94**(3):56.
283. Burns G, Brooks K, Wildung M, Navakanitworakul R, Christenson LK, Spencer TE. Extracellular vesicles in luminal fluid of the ovine uterus. *PLoS ONE*. 2014; **9**(3):e90913.
284. Ruiz-González I, Xu J, Wang X, Burghardt RC, Dunlap KA, Bazer FW. Exosomes, endogenous retroviruses and Toll-like receptors: pregnancy recognition in ewes. *Reproduction*. 2015;**149**(3):281–291.
285. Bidarimath M, Khalaj K, Kridli RT, Kan FWK, Koti M, Tayade C. Extracellular vesicle mediated intercellular communication at the porcine maternal-fetal interface: A new paradigm for conceptus-endometrial cross-talk. *Sci Rep*. 2017;**7**:40476.
286. Salomon C, Torres MJ, Kobayashi M. A gestational profile of placental exosomes in maternal plasma and their effects on endothelial cell migration. *PLoS ONE*. 2014;**9**(6):e98667.
287. Griffiths GS, Galileo DS, Reese K, Martin-Deleon PA. Investigating the role of murine epididymosomes and uterosomes in GPI-linked protein transfer to sperm using SPAM1 as a model. *Mol Reprod Dev*. 2008;**75**(11):1627–1636.
288. Franchi A, Cubilla M, Guidobaldi HA, Bravo AA, Giojalas LC. Uterosome-like vesicles prompt human sperm fertilizing capability. *Mol Hum Reprod*. 2016; **22**(12):833–841.
289. Al-Dossary AA, Martin-Deleon PA. Role of exosomes in the reproductive tract Oviductosomes mediate interactions of oviductal secretion with gametes/early embryo. *Front Biosci*. 2016;**21**(6): 1278–1285.
290. Belleannée C, Calvo É, Caballero J, Sullivan R. Epididymosomes convey different repertoires of microRNAs throughout the bovine epididymis. *Biol Reprod*. 2013;**89**(2):30.
291. Machtinger R, Laurent LC, Baccarelli AA. Extracellular vesicles: roles in gamete maturation, fertilization and embryo implantation. *Hum Reprod Update*. 2016;**22**(2):182–193.
292. Hell L, Wisgrill L, Ay C, Spittler A, Schwameis M, Jilma B, Pabinger I, Altevogt P, Thaler J. Procoagulant extracellular vesicles in amniotic fluid. *Transl Res*. 2017;**184**:12–20.e1.
293. Wang X. Isolation of extracellular vesicles from breast milk. *Methods Mol Biol*. 2017;**1660**: 351–353.
294. Karlsson O, Rodosthenous RS, Jara C, Brennan KJ, Wright RO, Baccarelli AA, Wright RJ. Detection of long non-coding RNAs in human breastmilk extracellular vesicles: implications for early child development. *Epigenetics*. 2016:0. doi:10.1080/15592294.2016.1216285.
295. Sullivan R, Saez F. Epididymosomes, prostasomes, and liposomes: their roles in mammalian male reproductive physiology. *Reproduction*. 2013;**146**(1): R21–R35.
296. Schoysman RJ, Bedford JM. The role of the human epididymis in sperm maturation and sperm storage as reflected in the consequences of epididymovasostomy. *Fertil Steril*. 1986;**46**(2):293–299.
297. Owen DH, Katz DF. A review of the physical and chemical properties of human semen and the formulation of a semen simulant. *J Androl*. 2005; **26**(4):459–469.

298. Sisti G, Kanninen TT, Witkin SS. Maternal immunity and pregnancy outcome: focus on preconception and autophagy. *Genes Immun*. 2016;**17**(1):1–7.
299. Robertson SA, Sharkey DJ. The role of semen in induction of maternal immune tolerance to pregnancy. *Semin Immunol*. 2001;**13**(4):243–254.
300. Ickowicz D, Finkelstein M, Breitbart H. Mechanism of sperm capacitation and the acrosome reaction: role of protein kinases. *Asian J Androl*. 2012;**14**(6): 816–821.
301. Fraser LR. Sperm capacitation and the acrosome reaction. *Hum Reprod*. 1998;**13**(Suppl 1):9–19.
302. Zaneveld LJD, De Jonge CJ, Anderson RA, Mack SR. Human sperm capacitation and the acrosome reaction. *Hum Reprod*. 1991;**6**(9):1265–1274.
303. Zhu J, Barratt CL, Lippes J, Pacey AA, Cooke ID. The sequential effects of human cervical mucus, oviductal fluid, and follicular fluid on sperm function. *Fertil Steril*. 1994;**61**(6):1129–1135.
304. Pikó L. Immunological phenomena in the reproductive process. *Int J Fertil*. 1967;**12**(4):377–383.
305. Yanagimachi R, Kamiguchi Y, Mikamo K, Suzuki F, Yanagimachi H. Maturation of spermatozoa in the epididymis of the Chinese hamster. *Am J Anat*. 1985; **172**(4):317–330.
306. Sullivan R. Epididymosomes: a heterogeneous population of microvesicles with multiple functions in sperm maturation and storage. *Asian J Androl*. 2015;**17**(5):726–729.
307. Caballero JN, Frenette G, Belleannée C, Sullivan R. CD9-positive microvesicles mediate the transfer of molecules to bovine spermatozoa during epididymal maturation. *PLoS One*. 2013;**8**(6):e65364.
308. D'Amours O, Frenette G, Bordeleau L-J, Allard N, Leclerc P, Blondin P, Sullivan R. Epididymosomes transfer epididymal sperm binding protein 1 (ELSPBP1) to dead spermatozoa during epididymal transit in bovine. *Biol Reprod*. 2012;**87**(4):94.
309. D'Amours O, Bordeleau L-J, Frenette G, Blondin P, Leclerc P, Sullivan R. Binder of sperm 1 and epididymal sperm binding protein 1 are associated with different bull sperm subpopulations. *Reproduction*. 2012;**143**(6):759–771.
310. Thimon V, Frenette G, Saez F, Thabet M, Sullivan R. Protein composition of human epididymosomes collected during surgical vasectomy reversal: a proteomic and genomic approach. *Hum Reprod*. 2008;**23**(8):1698–1707.
311. Murta D, Batista M, Silva E, Trindade A, Henrique D, Duarte A, Lopes-da-Costa L. Notch signaling in the epididymal epithelium regulates sperm motility and is transferred at a distance within epididymosomes. *Andrology*. 2016;**4**(2):314–327.
312. Reilly JN, McLaughlin EA, Stanger SJ, Anderson AL, Hutcheon K, Church K, Mihalas BP, Tyagi S, Holt JE, Eamens AL, Nixon B. Characterisation of mouse epididymosomes reveals a complex profile of microRNAs and a potential mechanism for modification of the sperm epigenome. *Sci Rep*. 2016;**6**(1): 31794.
313. Wang Q, Lee I, Ren J, Ajay SS, Lee YS, Bao X. Identification and functional characterization of tRNA-derived RNA fragments (tRFs) in respiratory syncytial virus infection. *Mol Ther*. 2013;**21**(2): 368–379.
314. Lee YS, Shibata Y, Malhotra A, Dutta A. A novel class of small RNAs: tRNA-derived RNA fragments (tRFs). *Genes Dev*. 2009;**23**(22):2639–2649.
315. Ronquist G, Brody I, Gottfries A, Stegmayr B. An Mg^{2+} and Ca^{2+}-stimulated adenosine triphosphatase in human prostatic fluid: part I. *Andrologia*. 1978;**10**(4):261–272.
316. Kravets FG, Lee J, Singh B, Trocchia A, Pentyala SN, Khan SA. Prostasomes: current concepts. *Prostate*. 2000;**43**(3):169–174.
317. Aalberts M, Stout TAE, Stoorvogel W. Prostasomes: extracellular vesicles from the prostate. *Reproduction*. 2013;**147**(1):R1–R14.
318. Arvidson G, Ronquist G, Wikander G, Ojteg AC. Human prostasome membranes exhibit very high cholesterol/phospholipid ratios yielding high molecular ordering. *Biochim Biophys Acta*. 1989;**984**(2): 167–173.
319. Arienti G, Carlini E, Polci A, Cosmi EV, Palmerini CA. Fatty acid pattern of human prostasome lipid. *Arch Biochem Biophys*. 1998;**358**(2):391–395.
320. Carlini E, Palmerini CA, Cosmi EV, Arienti G. Fusion of sperm with prostasomes: effects on membrane fluidity. *Arch Biochem Biophys*. 1997;**343**(1):6–12.
321. Saez F, Frenette G, Sullivan R. Epididymosomes and prostasomes: their roles in posttesticular maturation of the sperm cells. *J Androl*. 2003;**24**(2):149–154.
322. Suarez SS, Dai X. Intracellular calcium reaches different levels of elevation in hyperactivated and acrosome-reacted hamster sperm. *Mol Reprod Dev*. 1995;**42**(3):325–333.
323. Palmerini CA, Carlini E, Nicolucci A, Arienti G. Increase of human spermatozoa intracellular Ca^{2+} concentration after fusion with prostasomes. *Cell Calcium*. 1999;**25**(4):291–296.
324. Knowles RG, Moncada S. Nitric oxide synthases in mammals. *Biochem J*. 1994;**298**(Pt 2):249–258.
325. Ronquist GK, Larsson A, Ronquist G, Isaksson A, Hreinsson J, Carlsson L, Stavreus-Evers A. Prostasomal DNA characterization and transfer into human sperm. *Mol Reprod Dev*. 2011;**78**(7):467–476.
326. Ronquist KG, Ronquist G, Carlsson L, Larsson A. Human prostasomes contain chromosomal DNA. *Prostate*. 2009;**69**(7):737–743.
327. Ronquist G. Prostasomes: their characterisation: implications for human reproduction: prostasomes and human reproduction. *Adv Exp Med Biol*. 2015; **868**:191–209.
328. Jin M, Fujiwara E, Kakiuchi Y, Okabe M, Satouh Y, Baba SA, Chiba K, Hirohashi N. Most fertilizing mouse spermatozoa begin their acrosome reaction before contact with the zona pellucida during in vitro fertilization. *Proc Natl Acad Sci USA*. 2011; **108**(12):4892–4896.
329. Cross NL. Effect of cholesterol and other sterols on human sperm acrosomal responsiveness. *Mol Reprod Dev*. 1996;**45**(2):212–217.
330. Arienti G, Carlini E, Saccardi C, Palmerini CA. Nitric oxide and fusion with prostasomes increase cytosolic calcium in progesterone-stimulated sperm. *Arch Biochem Biophys*. 2002;**402**(2):255–258.
331. Cha K-Y, Chian RC. Maturation in vitro of immature human oocytes for clinical use. *Hum Reprod Update*. 1998;**4**(2):103–120.
332. Reed BG, Carr BR. The normal menstrual cycle and the control of ovulation. In: De Groot LJ, Chrousos G, Dungan K, Feingold KR, Grossman A, Hershman JM, Koch C, Korbonits M, McLachlan R, New M, Purnell J, Rebar R, Singer F, Vinik A, eds. Endotext [Internet]. South Dartmouth, MA: MDText.com, Inc. Available at: https://www.ncbi.nlm.nih.gov/books/NBK279054/. Accessed 22 May 2015.
333. Okabe M. The cell biology of mammalian fertilization. *Development*. 2013;**140**(22):4471–4479.
334. Hertig AT, Rock J, Adams EC. A description of 34 human ova within the first 17 days of development. *Am J Anat*. 1956;**98**(3):435–493.
335. Aplin JD. The cell biological basis of human implantation. *Baillieres Best Pract Res Clin Obstet Gynaecol*. 2000;**14**(5):457–464.
336. Wang H, Dey SK. Roadmap to embryo implantation: clues from mouse models. *Nat Rev Genet*. 2006; **7**(3):185–199.
337. Zamah AM, Hassis ME, Albertolle ME, Williams KE. Proteomic analysis of human follicular fluid from fertile women. *Clin Proteomics*. 2015;**12**(1):5.
338. Revelli A, Delle Piane L, Casano S, Molinari E, Massobrio M, Rinaudo P. Follicular fluid content and oocyte quality: from single biochemical markers to metabolomics. *Reprod Biol Endocrinol*. 2009;**7**(1): 40.
339. da Silveira JC, Veeramachaneni DNR, Winger QA, Carnevale EM, Bouma GJ. Cell-secreted vesicles in equine ovarian follicular fluid contain miRNAs and proteins: a possible new form of cell communication within the ovarian follicle. *Biol Reprod*. 2012; **86**(3):71.
340. Diez-Fraile A, Lammens T, Tilleman K, Witkowski W, Verhasselt B, De Sutter P, Benoit Y, Espeel M, D'Herde K. Age-associated differential microRNA levels in human follicular fluid reveal pathways potentially determining fertility and success of in vitro fertilization. *Hum Fertil (Camb)*. 2014;**17**(2): 90–98.
341. Almiñana C. Snooping on a private conversation between the oviduct and gametes/embryos. *Anim Reprod*. 2015;**12**(3):366–374.
342. Li M-Q, Jin L-P. Ovarian stimulation for in vitro fertilization alters the protein profile expression in endometrial secretion. *Int J Clin Exp Pathol*. 2013; **6**(10):1964–1971.
343. Zhang Y, Wang Q, Wang H, Duan E. Uterine fluid in pregnancy: a biological and clinical outlook. *Trends Mol Med*. 2017;**23**(7):604–614.
344. Salamonsen LA, Nie G, Hannan NJ, Dimitriadis E. Society for Reproductive Biology Founders' Lecture 2009. Preparing fertile soil: the importance of endometrial receptivity. *Reprod Fertil Dev*. 2009;**21**(7): 923–934.
345. Campoy I, Lanau L, Altadill T, Sequeiros T, Cabrera S, Cubo-Abert M, Pérez-Benavente A, Garcia A, Borrós S, Santamaria A, Ponce J, Matias-Guiu X, Reventós J, Gil-Moreno A, Rigau M, Colás E. Exosome-like vesicles in uterine aspirates: a comparison of ultracentrifugation-based isolation protocols. *J Transl Med*. 2016;**14**(1):180.
346. Salomon C, Yee SW, Mitchell MD, Rice GE. The possible role of extravillous trophoblast-derived exosomes on the uterine spiral arterial remodeling under both normal and pathological conditions. *Biomed Res Int*. 2014;**2014**:693157.
347. Di Carlo C, Bonifacio M, Tommaselli GA, Bifulco G, Guerra G, Nappi C. Metalloproteinases, vascular endothelial growth factor, and angiopoietin 1 and 2 in eutopic and ectopic endometrium. *Fertil Steril*. 2009;**91**(6):2315–2323.
348. Braundmeier AG, Dayger CA, Mehrotra P, Belton RJ Jr, Nowak RA. EMMPRIN is secreted by human uterine epithelial cells in microvesicles and stimulates metalloproteinase production by human uterine fibroblast cells. *Reprod Sci*. 2012;**19**(12): 1292–1301.
349. Harp D, Driss A, Mehrabi S, Chowdhury I, Xu W, Liu D, Garcia-Barrio M, Taylor RN, Gold B, Jefferson S, Sidell N, Thompson W. Exosomes derived from endometriotic stromal cells have enhanced angiogenic effects in vitro. *Cell Tissue Res*. 2016;**365**(1): 187–196.
350. Texidó L, Romero C, Vidal A, García-Valero J, Fernández Montoli ME, Baixeras N, Condom E, Ponce J, García-Tejedor A, Martín-Satué M. Ecto-nucleotidases activities in the contents of ovarian endometriomas: potential biomarkers of endometriosis. *Mediators Inflamm*. 2014;**2014**:120673.

351. Sang Q, Yao Z, Wang H, Feng R, Wang H, Zhao X, Xing Q, Jin L, He L, Wu L, Wang L. Identification of microRNAs in human follicular fluid: characterization of microRNAs that govern steroidogenesis in vitro and are associated with polycystic ovary syndrome in vivo. *J Clin Endocrinol Metab*. 2013; **98**(7):3068–3079.
352. Esposito K, Ciotola M, Giugliano F, Schisano B, Improta L, Improta MR, Beneduce F, Rispoli M, De Sio M, Giugliano D. Endothelial microparticles correlate with erectile dysfunction in diabetic men. *Int J Impot Res*. 2007;**19**(2):161–166.
353. La Vignera S, Condorelli R, Vicari E, D'Agata R, Calogero AE. Arterial erectile dysfunction: reliability of new markers of endothelial dysfunction. *J Endocrinol Invest*. 2011;**34**(10):e314–e320.
354. Patil R, Ghosh K, Satoskar P, Shetty S. Elevated procoagulant endothelial and tissue factor expressing microparticles in women with recurrent pregnancy loss. *PLoS One*. 2013;**8**(11):e81407.
355. Laude I, Rongières-Bertrand C, Boyer-Neumann C, Wolf M, Mairovitz V, Hugel B, Freyssinet JM, Frydman R, Meyer D, Eschwège V. Circulating procoagulant microparticles in women with unexplained pregnancy loss: a new insight. *Thromb Haemost*. 2001;**85**(1):18–21.
356. Pasquier E, De Saint Martin L, Bohec C, Collet M. Unexplained pregnancy loss: a marker of basal endothelial dysfunction?. *Fertil Steril*. 2013;**100**(4): 1013–1017.
357. Germain SJ, Sacks GP, Sooranna SR, Sargent IL, Redman CW. Systemic inflammatory priming in normal pregnancy and preeclampsia: the role of circulating syncytiotrophoblast microparticles. *J Immunol*. 2007;**178**(9):5949–5956.
358. Guller S, Tang Z, Ma YY, Di Santo S, Sager R, Schneider H. Protein composition of microparticles shed from human placenta during placental perfusion: potential role in angiogenesis and fibrinolysis in preeclampsia. *Placenta*. 2011;**32**(1):63–69.
359. Gardiner C, Tannetta DS, Simms CA, Harrison P, Redman CWG, Sargent IL. Syncytiotrophoblast microvesicles released from pre-eclampsia placentae exhibit increased tissue factor activity. *PLoS One*. 2011;**6**(10):e26313.
360. Tannetta DS, Hunt K, Jones CI, Davidson N, Coxon CH, Ferguson D, Redman CW, Gibbins JM, Sargent IL, Tucker KL. Syncytiotrophoblast extracellular vesicles from pre-eclampsia placentas differentially affect platelet function. *PLoS One*. 2015;**10**(11): e0142538.
361. Cronqvist T, Saljé K, Familari M, Guller S, Schneider H, Gardiner C, Sargent IL, Redman CW, Mörgelin M, Åkerström B, Gram M, Hansson SR. Syncytiotrophoblast vesicles show altered micro-RNA and haemoglobin content after ex-vivo perfusion of placentas with haemoglobin to mimic pre-eclampsia. *PLoS One*. 2014;**9**(2):e90020.
362. Aly AS, Khandelwal M, Zhao J, Mehmet AH, Sammel MD, Parry S. Neutrophils are stimulated by syncytiotrophoblast microvillous membranes to generate superoxide radicals in women with pre-eclampsia. *Am J Obstet Gynecol*. 2004;**190**(1): 252–258.
363. Gilani SI, Weissgerber TL, Garovic VD, Jayachandran M. Preeclampsia and extracellular vesicles. *Curr Hypertens Rep*. 2016;**18**(9):68.
364. Kohli S, Ranjan S, Hoffmann J, Kashif M, Daniel EA, Al-Dabet MM, Bock F, Nazir S, Huebner H, Mertens PR, Fischer K-D, Zenclussen AC, Offermanns S, Aharon A, Brenner B, Shahzad K, Ruebner M, Isermann B. Maternal extracellular vesicles and platelets promote preeclampsia via inflammasome activation in trophoblasts. *Blood*. 2016;**128**(17): 2153–2164.
365. Holder B, Jones T, Sancho Shimizu V, Rice TF, Donaldson B, Bouqueau M, Forbes K, Kampmann B. Macrophage exosomes induce placental inflammatory cytokines: a novel mode of maternal–placental messaging. *Traffic*. 2016;**17**(2):168–178.
366. Holder BS, Tower CL, Jones CJP, Aplin JD, Abrahams VM. Heightened pro-inflammatory effect of preeclamptic placental microvesicles on peripheral blood immune cells in humans. *Biol Reprod*. 2012; **86**(4):103.
367. Shomer E, Katzenell S, Zipori Y, Sammour RN, Isermann B, Brenner B, Aharon A. Microvesicles of women with gestational hypertension and preeclampsia affect human trophoblast fate and endothelial function. *Hypertension*. 2013;**62**(5): 893–898.
368. Kaptan K, Beyan C, Ifran A, Pekel A. Platelet-derived microparticle levels in women with recurrent spontaneous abortion. *Int J GYnecol Obstet*. 2008; **102**:271–274.
369. Salomon C, Scholz-Romero K, Sarker S, Sweeney E, Kobayashi M, Correa P, Longo S, Duncombe G, Mitchell MD, Rice GE, Illanes SE. Gestational diabetes mellitus is associated with changes in the concentration and bioactivity of placenta-derived exosomes in maternal circulation across gestation. *Diabetes*. 2016;**65**(3):598–609.
370. Yuana Y, Sturk A, Nieuwland R. Extracellular vesicles in physiological and pathological conditions. *Blood Rev*. 2013;**27**(1):31–39.
371. Bulun SE. Endometriosis. *N Engl J Med*. 2009;**360**(3): 268–279.
372. Tarin D. Cell and tissue interactions in carcinogenesis and metastasis and their clinical significance. *Semin Cancer Biol*. 2011;**21**(2):72–82.
373. Bruner-Tran KL, Eisenberg E, Yeaman GR, Anderson TA, McBean J, Osteen KG. Steroid and cytokine regulation of matrix metalloproteinase expression in endometriosis and the establishment of experimental endometriosis in nude mice. *J Clin Endocrinol Metab*. 2002;**87**(10):4782–4791.
374. Ehrmann DA. Polycystic ovary syndrome. *N Engl J Med*. 2005;**352**(12):1223–1236.
375. Stein IF, Leventhal ML. Amenorrhea associated with bilateral polycystic ovaries. *Am J Obstet Gynecol*. 1935;**29**(2):181–191.
376. Koiou E, Tziomalos K, Katsikis I, Papadakis E, Kandaraki EA, Panidis D. Platelet-derived microparticles in overweight/obese women with the polycystic ovary syndrome. *Gynecol Endocrinol*. 2013; **29**(3):250–253.
377. Willis GR, Connolly K, Ladell K, Davies TS, Guschina IA, Ramji D, Miners K, Price DA, Clayton A, James PE, Rees DA. Young women with polycystic ovary syndrome have raised levels of circulating annexin V–positive platelet microparticles. *Hum Reprod*. 2014;**29**(12):2756–2763.
378. Shi Y, Zhao H, Shi Y, Cao Y, Yang D, Li Z, Zhang B, Liang X, Li T, Chen J, Shen J, Zhao J, You L, Gao X, Zhu D, Zhao X, Yan Y, Qin Y, Li W, Yan J, Wang Q, Zhao J, Geng L, Ma J, Zhao Y, He G, Zhang A, Zou S, Yang A, Liu J, Li W, Li B, Wan C, Qin Y, Shi J, Yang J, Jiang H, Xu J-E, Qi X, Sun Y, Zhang Y, Hao C, Ju X, Zhao D, Ren C-E, Li X, Zhang W, Zhang Y, Zhang J, Wu D, Zhang C, He L, Chen Z-J. Genome-wide association study identifies eight new risk loci for polycystic ovary syndrome. *Nat Genet*. 2012;**44**(9): 1020–1025.
379. Chen Z-J, Zhao H, He L, Shi Y, Qin Y, Shi Y, Li Z, You L, Zhao J, Liu J, Liang X, Zhao X, Zhao J, Sun Y, Zhang B, Jiang H, Zhao D, Bian Y, Gao X, Geng L, Li Y, Zhu D, Sun X, Xu J-E, Hao C, Ren C-E, Zhang Y, Chen S, Zhang W, Yang A, Yan J, Li Y, Ma J, Zhao Y. Genome-wide association study identifies susceptibility loci for polycystic ovary syndrome on chromosome 2p16.3, 2p21 and 9q33.3. *Nat Genet*. 2011;**43**(1):55–59.
380. McAllister JM, Modi B, Miller BA, Biegler J, Bruggeman R, Legro RS, Strauss JF III. Overexpression of a DENND1A isoform produces a polycystic ovary syndrome theca phenotype. *Proc Natl Acad Sci USA*. 2014;**111**(15):E1519–E1527.
381. Wang W, Fan J, Huang G, Zhu X, Tian Y, Tan H, Su L. Meta-analysis of prevalence of erectile dysfunction in mainland China: evidence based on epidemiological surveys. *Sex Med*. 2017;**5**(1):e19–e30.
382. Esposito K, Ciotola M, Giugliano F, Sardelli L, Giugliano F, Maiorino MI, Beneduce F, De Sio M, Giugliano D. Phenotypic assessment of endothelial microparticles in diabetic and nondiabetic men with erectile dysfunction. *J Sex Med*. 2008;**5**(6): 1436–1442.
383. La Vignera S, Vicari E, Condorelli RA, Di Pino L, Calogero AE. Arterial erectile dysfunction: reliability of penile Doppler evaluation integrated with serum concentrations of late endothelial progenitor cells and endothelial microparticles. *J Androl*. 2012;**33**(3): 412–419.
384. Condorelli RA, Calogero AE, Vicari E, di Pino L, Giacone F, Mongioì L, la Vignera S. Arterial erectile dysfunction and peripheral arterial disease: reliability of a new phenotype of endothelial progenitor cells and endothelial microparticles. *J Androl*. 2012;**33**(6):1268–1275.
385. Park K, Ryu KS, Li WJ, Kim SW, Paick J-S. Chronic treatment with a type 5 phosphodiesterase inhibitor suppresses apoptosis of corporal smooth muscle by potentiating Akt signalling in a rat model of diabetic erectile dysfunction. *Eur Urol*. 2008;**53**(6): 1282–1289.
386. Porst H, Glina S, Ralph D, Zeigler H, Wong DG, Woodward B. Durability of response following cessation of tadalafil taken once daily as treatment for erectile dysfunction. *J Sex Med*. 2010;**7**(10): 3487–3494.
387. La Vignera S, Condorelli RA, Vicari E, D'Agata R, Calogero AE. Endothelial apoptosis decrease following tadalafil administration in patients with arterial ED does not last after its discontinuation. *Int J Impot Res*. 2011;**23**(5):200–205.
388. La Vignera S, Condorelli R, Vicari E, D'Agata R, Calogero AE. Endothelial antioxidant compound prolonged the endothelial antiapoptotic effects registered after tadalafil treatment in patients with arterial erectile dysfunction. *J Androl*. 2012;**33**(2): 170–175.
389. Schulz E, Gori T, Münzel T. Oxidative stress and endothelial dysfunction in hypertension. *Hypertens Res*. 2011;**34**(6):665–673.
390. Higashi Y, Noma K, Yoshizumi M, Kihara Y. Endothelial function and oxidative stress in cardiovascular diseases. *Circ J*. 2009;**73**(3):411–418.
391. Francomano D, Bruzziches R, Natali M, Aversa A, Spera G. Cardiovascular effect of testosterone replacement therapy in aging male. *Acta Biomed*. 2010;**81**(Suppl 1):101–106.
392. La Vignera S, Condorelli R, Vicari E, D'Agata R, Calogero A. Original immunophenotype of blood endothelial progenitor cells and microparticles in patients with isolated arterial erectile dysfunction and late onset hypogonadism: effects of androgen replacement therapy. *Aging Male*. 2011;**14**(3):183–189.
393. La Vignera S, Condorelli RA, Vicari E, D'Agata R, Calogero AE. New immunophenotype of blood endothelial progenitor cells and endothelial microparticles in patients with arterial erectile

dysfunction and late-onset hypogonadism. *J Androl*. 2011;**32**(5):509–517.
394. Sarker S, Scholz-Romero K. Placenta-derived exosomes continuously increase in maternal circulation over the first trimester of pregnancy. *J Transl Med*. 2014;**12**:204.
395. Salomon C, Kobayashi M, Ashman K, Sobrevia L. Hypoxia-induced changes in the bioactivity of cytotrophoblast-derived exosomes. *PLoS ONE*. 2013; **8**(11):e79636.
396. Rice GE, Scholz-Romero K, Sweeney E, Peiris H, Kobayashi M, Duncombe G, Mitchell MD, Salomon C. The effect of glucose on the release and bioactivity of exosomes from first trimester trophoblast cells. *J Clin Endocrinol Metab*. 2015;**100**(10): E1280–E1288.
397. Mitchell MD, Peiris HN, Kobayashi M, Koh YQ. Placental exosomes in normal and complicated pregnancy. *Am J Obstet Gynecol*. 2015;**213**(4 Suppl): S173–S181.
398. Salomon C, Sobrevia L, Ashman K, Illanes S, Mitchell MD, Rice GE. The role of placental exosomes in gestational diabetes mellitus. In: Sobrevia L, ed. *Gestational Diabetes–Causes, Diagnosis and Treatment*. Available at: https://doi.org/10.5772/55298. Accessed 24 April 2017.
399. Redman C, Tannetta DS, Dragovic RA, Gardiner C. Review: does size matter? Placental debris and the pathophysiology of pre-eclampsia. *Placenta*. 2012; **33**:S48–S54.
400. Ford HB, Schust DJ. Recurrent pregnancy loss: etiology, diagnosis, and therapy. *Rev Obstet Gynecol*. 2009;**2**(2):76–83.
401. Alijotas-Reig J, Palacio-Garcia C, Farran-Codina I, Zarzoso C, Cabero-Roura L, Vilardell-Tarres M. Circulating cell-derived microparticles in women with pregnancy loss. *Am J Reprod Immunol*. 2011; **66**(3):199–208.
402. Katz D, Beilin Y. Disorders of coagulation in pregnancy. *Br J Anaesth*. 2015;**115**(Suppl 2):ii75–ii88.
403. Rai R. Is miscarriage a coagulopathy? *Curr Opin Obstet Gynecol*. 2003;**15**(3):265–268.
404. Katzenell S, Shomer E, Zipori Y, Zylberfisz A, Brenner B, Aharon A. Characterization of negatively charged phospholipids and cell origin of microparticles in women with gestational vascular complications. *Thromb Res*. 2012;**130**(3):479–484.
405. Karthikeyan VJ, Lip GYH. Endothelial damage/dysfunction and hypertension in pregnancy. *Front Biosci (Elite Ed)*. 2011;**3**:1100–1108.
406. Uzan J, Carbonnel M, Piconne O, Asmar R, Ayoubi JM. Pre-eclampsia: pathophysiology, diagnosis, and management. *Vasc Health Risk Manag*. 2011;**7**: 467–474.
407. Aharon A. The role of extracellular vesicles in placental vascular complications. *Thromb Res*. 2015; **135**(Suppl 1):S23–S25.
408. Jeyabalan A. Epidemiology of preeclampsia: impact of obesity. *Nutr Rev*. 2013;**71**(Suppl 1):S18–S25.
409. Roberts JM, Escudero C. The placenta in pre-eclampsia. *ScienceDirect. Pregnancy Hypertens*. 2012; **2**(2):72–83.
410. Chen Y, Huang Y, Jiang R, Teng Y. Syncytiotrophoblast-derived microparticle shedding in early-onset and late-onset severe pre-eclampsia. *Int J Gynaecol Obstet*. 2012; **119**(3):234–238.
411. Goswami D, Tannetta DS, Magee LA, Fuchisawa A, Redman CWG, Sargent IL, von Dadelszen P. Excess syncytiotrophoblast microparticle shedding is a feature of early-onset pre-eclampsia, but not normotensive intrauterine growth restriction. *Placenta*. 2006;**27**(1):56–61.
412. Li H, Han L, Yang Z, Huang W, Zhang X, Gu Y, Li Y, Liu X, Zhou L, Hu J, Yu M, Yang J, Li Y, Zheng Y, Guo J, Han J, Li L. Differential proteomic analysis of syncytiotrophoblast extracellular vesicles from early-onset severe preeclampsia, using 8-plex iTRAQ labeling coupled with 2D nano LC-MS/MS. *Cell Physiol Biochem*. 2015;**36**(3):1116–1130.
413. Baig S, Kothandaraman N, Manikandan J, Rong L, Ee KH, Hill J, Lai CW, Tan WY, Yeoh F, Kale A, Su LL, Biswas A, Vasoo S, Choolani M. Proteomic analysis of human placental syncytiotrophoblast microvesicles in preeclampsia. *Clin Proteomics*. 2014;**11**(1):40.
414. Baig S, Lim JY, Fernandis AZ, Wenk MR, Kale A, Su LL, Biswas A, Vasoo S, Shui G, Choolani M. Lipidomic analysis of human placental syncytiotrophoblast microvesicles in adverse pregnancy outcomes. *Placenta*. 2013;**34**(5):436–442.
415. Truong G, Guanzon D, Kinhal V, Elfeky O, Lai A, Longo S, Nuzhat Z, Palma C, Scholz-Romero K, Menon R, Mol BW, Rice GE, Salomon C. Oxygen tension regulates the miRNA profile and bioactivity of exosomes released from extravillous trophoblast cells—liquid biopsies for monitoring complications of pregnancy. *PLoS ONE*. 2017;**12**(3): e0174514.
416. Vargas A, Zhou S, Éthier-Chiasson M, Flipo D, Lafond J, Gilbert C, Barbeau B. Syncytin proteins incorporated in placenta exosomes are important for cell uptake and show variation in abundance in serum exosomes from patients with preeclampsia. *FASEB J*. 2014;**28**(8):3703–3719.
417. Levine RJ, Lam C, Qian C, Yu KF, Maynard SE, Sachs BP, Sibai BM, Epstein FH, Romero R, Thadhani R, Karumanchi SA; CPEP Study Group. Soluble endoglin and other circulating antiangiogenic factors in preeclampsia. *N Engl J Med*. 2006;**355**(10): 992–1005.
418. Estellés A, Gilabert J, Keeton M, Eguchi Y, Aznar J, Grancha S, Espña F, Loskutoff DJ, Schleef RR. Altered expression of plasminogen activator inhibitor type 1 in placentas from pregnant women with pre-eclampsia and/or intrauterine fetal growth retardation. *Blood*. 1994;**84**(1):143–150.
419. Centlow M, Carninci P, Nemeth K, Mezey E, Brownstein M, Hansson SR. Placental expression profiling in preeclampsia: local overproduction of hemoglobin may drive pathological changes. *Fertil Steril*. 2008;**90**(5):1834–1843.
420. May K, Rosenlöf L, Olsson MG, Centlow M, Mörgelin M, Larsson I, Cederlund M, Rutardottir S, Siegmund W, Schneider H, Akerström B, Hansson SR. Perfusion of human placenta with hemoglobin introduces preeclampsia-like injuries that are prevented by α_1-microglobulin. *Placenta*. 2011;**32**(4): 323–332.
421. Olsson MG, Centlow M, Rutardóttir S, Stenfors I, Larsson J, Hosseini-Maaf B, Olsson ML, Hansson SR, Akerström B. Increased levels of cell-free hemoglobin, oxidation markers, and the antioxidative heme scavenger α_1-microglobulin in preeclampsia. *Free Radic Biol Med*. 2010;**48**(2):284–291.
422. Lok CAR, Jebbink J, Nieuwland R, Faas MM, Boer K, Sturk A, Van Der Post JAM. Leukocyte activation and circulating leukocyte-derived microparticles in preeclampsia. *Am J Reprod Immunol*. 2009;**61**(5): 346–359.
423. Mikhailova VA, Ovchinnikova OM, Zainulina MS, Sokolov DI, Sel'kov SA. Detection of microparticles of leukocytic origin in the peripheral blood in normal pregnancy and preeclampsia. *Bull Exp Biol Med*. 2014;**157**(6):751–756.
424. Joerger-Messerli MS, Hoesli IM, Rusterholz C, Lapaire O. Stimulation of monocytes by placental microparticles involves Toll-like receptors and nuclear factor κ-light-chain-enhancer of activated B cells. *Front Immunol*. 2014;**5**:173.
425. Ling L, Huang H, Zhu L, Mao T, Shen Q, Zhang H. Evaluation of plasma endothelial microparticles in pre-eclampsia. *J Int Med Res*. 2014;**42**(1): 42–51.
426. Elfeky O, Longo S, Lai A, Rice GE, Salomon C. Influence of maternal BMI on the exosomal profile during gestation and their role on maternal systemic inflammation. *Placenta*. 2017;**50**:60–69.
427. Chen L, Mayo R, Chatry A, Hu G. Gestational diabetes mellitus: its epidemiology and implication beyond pregnancy. *Curr Epidemiol Rep*. 2016;**3**(1):1–11.
428. Erem C, Kuzu UB, Deger O, Can G. Prevalence of gestational diabetes mellitus and associated risk factors in Turkish women: the Trabzon GDM Study. *Arch Med Sci*. 2015;**11**(4):724–735.
429. Moro L, Bardají A, Macete E, Barrios D, Morales-Prieto DM, España C, Mandomando I, Sigaúque B, Dobaño C, Markert UR, Benitez-Ribas D, Alonso PL, Menéndez C, Mayor A. Placental microparticles and microRNAs in pregnant women with *Plasmodium falciparum* or HIV infection. *PLoS One*. 2016;**11**(1): e0146361.
430. Tan KH, Tan SS, Ng MJ, Tey WS, Sim WK, Allen JC, Lim SK. Extracellular vesicles yield predictive pre-eclampsia biomarkers. *J Extracell Vesicles*. 2017;**6**(1): 1408390.
431. Tan KH, Tan SS, Sze SK, Lee WKR, Ng MJ, Lim SK. Plasma biomarker discovery in preeclampsia using a novel differential isolation technology for circulating extracellular vesicles. *Am J Obstet Gynecol*. 2014;**211**(4):380.e1–380.e13.
432. Campello E, Spiezia L, Radu CM, Dhima S, Visentin S, Valle FD, Tormene D, Woodhams B, Cosmi E, Simioni P. Circulating microparticles in umbilical cord blood in normal pregnancy and pregnancy with pre-eclampsia. *Thromb Res*. 2015;**136**(2):427–431.
433. Chaparro A, Gaedechens D, Ramírez V, Zuñiga E, Kusanovic JP, Inostroza C, Varas-Godoy M, Silva K, Salomon C, Rice G, Illanes SE. Placental biomarkers and angiogenic factors in oral fluids of patients with preeclampsia. *Prenat Diagn*. 2016;**36**(5):476–482.
434. Salomon C, Guanzon D, Scholz-Romero K, Longo S, Correa P, Illanes SE, Rice GE. Placental exosomes as early biomarker of preeclampsia: potential role of exosomal microRNAs across gestation. *J Clin Endocrinol Metab*. 2017;**102**(9):3182–3194.
435. Motta-Mejia C, Kandzija N, Zhang W, Mhlomi V, Cerdeira AS, Burdujan A, Tannetta D, Dragovic R, Sargent IL, Redman CW, Kishore U, Vatish M. Placental vesicles carry active endothelial nitric oxide synthase and their activity is reduced in preeclampsia. *Hypertension*. 2017;**70**(2):372–381.
436. Hilfiker-Kleiner D, Sliwa K. Pathophysiology and epidemiology of peripartum cardiomyopathy. *Nat Rev Cardiol*. 2014;**11**(6):364–370.
437. Walenta K, Schwarz V, Schirmer SH, Kindermann I, Friedrich EB, Solomayer EF, Sliwa K, Labidi S, Hilfiker-Kleiner D, Böhm M. Circulating microparticles as indicators of peripartum cardiomyopathy. *Eur Heart J*. 2012;**33**(12):1469–1479.
438. Halkein J, Tabruyn SP, Ricke-Hoch M, Haghikia A, Nguyen N-Q-N, Scherr M, Castermans K, Malvaux L, Lambert V, Thiry M, Sliwa K, Noel A, Martial JA, Hilfiker-Kleiner D, Struman I. MicroRNA-146a is a therapeutic target and biomarker for peripartum cardiomyopathy. *J Clin Invest*. 2013;**123**(5):2143–2154.
439. Reiner AT, Witwer KW, van Balkom BWM, de Beer J, Brodie C, Corteling RL, Gabrielsson S, Gimona M, Ibrahim AG, de Kleijn D, Lai CP, Lötvall J, Del Portillo HA, Reischl IG, Riazifar M, Salomon C, Tahara H, Toh WS, Wauben MHM, Yang VK, Yang Y, Yeo RWY, Yin H, Giebel B, Rohde E, Lim SK. Concise review: developing best-practice models for the therapeutic

use of extracellular vesicles. *Stem Cells Transl Med*. 2017;**6**(8):1730–1739.
440. Jang SC, Kim OY, Yoon CM, Choi D-S, Roh T-Y, Park J, Nilsson J, Lötvall J, Kim Y-K, Gho YS. Bioinspired exosome-mimetic nanovesicles for targeted delivery of chemotherapeutics to malignant tumors. *ACS Nano*. 2013;**7**(9):7698–7710.
441. Tan S, Li X, Guo Y, Zhang Z. Lipid-enveloped hybrid nanoparticles for drug delivery. *Nanoscale*. 2013;**5**(3): 860–872.
442. Haney MJ, Klyachko NL, Zhao Y, Gupta R, Plotnikova EG, He Z, Patel T, Piroyan A, Sokolsky M, Kabanov AV, Batrakova EV. Exosomes as drug delivery vehicles for Parkinson's disease therapy. *J Control Release*. 2015;**207**: 18–30.
443. Tian Y, Li S, Song J, Ji T, Zhu M, Anderson GJ, Wei J, Nie G. A doxorubicin delivery platform using engineered natural membrane vesicle exosomes for targeted tumor therapy. *Biomaterials*. 2014;**35**(7):2383–2390.
444. Ohno S, Takanashi M, Sudo K, Ueda S, Ishikawa A, Matsuyama N, Fujita K, Mizutani T, Ohgi T, Ochiya T, Gotoh N, Kuroda M. Systemically injected exosomes targeted to EGFR deliver antitumor microRNA to breast cancer cells. *Mol Ther*. 2013;**21**(1): 185–191.
445. Kooijmans SAA, Aleza CG, Roffler SR, van Solinge WW, Vader P, Schiffelers RM. Display of GPI-anchored anti-EGFR nanobodies on extracellular vesicles promotes tumour cell targeting. *J Extracell Vesicles*. 2016;**5**(1):31053.
446. Fuhrmann G, Serio A, Mazo M, Nair R, Stevens MM. Active loading into extracellular vesicles significantly improves the cellular uptake and photodynamic effect of porphyrins. *J Control Release*. 2015; **205**:35–44.
447. Ohno S, Drummen GPC, Kuroda M. Focus on extracellular vesicles: development of extracellular vesicle-based therapeutic systems. *Int J Mol Sci*. 2016;**17**(2):172.
448. Syn NL, Wang L, Chow EK-H, Lim CT, Goh B-C. Exosomes in cancer nanomedicine and immunotherapy: prospects and challenges. *Trends Biotechnol*. 2017;**35**(7):665–676.
449. Katz-Jaffe MG, Schoolcraft WB, Gardner DK. Analysis of protein expression (secretome) by human and mouse preimplantation embryos. *Fertil Steril*. 2006;**86**(3):678–685.
450. Ratajczak J, Miekus K, Kucia M, Zhang J, Reca R, Dvorak P, Ratajczak MZ. Embryonic stem cell-derived microvesicles reprogram hematopoietic progenitors: evidence for horizontal transfer of mRNA and protein delivery. *Leukemia*. 2006;**20**(5):847–856.
451. Saadeldin IM, Kim SJ, Choi YB, Lee BC. Improvement of cloned embryos development by co-culturing with parthenotes: a possible role of exosomes/microvesicles for embryos paracrine communication. *Cell Reprogram*. 2014;**16**(3):223–234.
452. Nguyen HPT, Simpson RJ, Salamonsen LA, Greening DW. Extracellular vesicles in the intrauterine environment: challenges and potential functions. *Biol Reprod*. 2016;**95**(5):109.
453. Greening DW, Nguyen HPT, Evans J, Simpson RJ, Salamonsen LA. Modulating the endometrial epithelial proteome and secretome in preparation for pregnancy: the role of ovarian steroid and pregnancy hormones. *J Proteomics*. 2016;**144**:99–112.
454. Kim TS, Lee SH, Gang GT, Lee YS, Kim SU, Koo DB, Shin MY, Park CK, Lee DS. Exogenous DNA uptake of boar spermatozoa by a magnetic nanoparticle vector system. *Reprod Domest Anim*. 2010;**45**(5):e201–e206.
455. Campos VF, de Leon PMM, Komninou ER, Dellagostin OA, Deschamps JC, Seixas FK, Collares T. NanoSMGT: transgene transmission into bovine embryos using halloysite clay nanotubes or nanopolymer to improve transfection efficiency. *Theriogenology*. 2011;**76**(8):1552–1560.
456. Liang X, Zhang L, Wang S, Han Q, Zhao RC. Exosomes secreted by mesenchymal stem cells promote endothelial cell angiogenesis by transferring miR-125a. *J Cell Sci*. 2016;**129**(11):2182–2189.
457. Lösche W, Scholz T, Temmler U, Oberle V, Claus RA. Platelet-derived microvesicles transfer tissue factor to monocytes but not to neutrophils. *Platelets*. 2004; **15**(2):109–115.
458. Costa-Silva B, Aiello NM, Ocean AJ, Singh S, Zhang H, Thakur BK, Becker A, Hoshino A, Mark MT, Molina H, Xiang J, Zhang T, Theilen T-M, García-Santos G, Williams C, Ararso Y, Huang Y, Rodrigues G, Shen T-L, Labori KJ, Lothe IMB, Kure EH, Hernandez J, Doussot A, Ebbesen SH, Grandgenett PM, Hollingsworth MA, Jain M, Mallya K, Batra SK, Jarnagin WR, Schwartz RE, Matei I, Peinado H, Stanger BZ, Bromberg J, Lyden D. Pancreatic cancer exosomes initiate pre-metastatic niche formation in the liver. *Nat Cell Biol*. 2015;**17**(6):816–826.
459. Fong MY, Zhou W, Liu L, Alontaga AY, Chandra M, Ashby J, Chow A, O'Connor STF, Li S, Chin AR, Somlo G, Palomares M, Li Z, Tremblay JR, Tsuyada A, Sun G, Reid MA, Wu X, Swiderski P, Ren X, Shi Y, Kong M, Zhong W, Chen Y, Wang SE. Breast-cancer-secreted miR-122 reprograms glucose metabolism in premetastatic niche to promote metastasis. *Nat Cell Biol*. 2015;**17**(2):183–194.
460. Wood MJ, O'Loughlin AJ, Samira L. Exosomes and the blood–brain barrier: implications for neurological diseases. *Ther Deliv*. 2011;**2**(9):1095–1099.
461. Headland SE, Jones HR, Norling LV, Kim A, Souza PR, Corsiero E, Gil CD, Nerviani A, Dell'Accio F, Pitzalis C, Oliani SM, Jan LY, Perretti M. Neutrophil-derived microvesicles enter cartilage and protect the joint in inflammatory arthritis. *Sci Transl Med*. 2015;**7**(315): 315ra190.
462. Suetsugu A, Honma K, Saji S, Moriwaki H, Ochiya T, Hoffman RM. Imaging exosome transfer from breast cancer cells to stroma at metastatic sites in orthotopic nude-mouse models. *Adv Drug Deliv Rev*. 2013;**65**(3):383–390.
463. Alvarez-Erviti L, Seow Y, Yin H, Betts C, Lakhal S, Wood MJA. Delivery of siRNA to the mouse brain by systemic injection of targeted exosomes. *Nat Biotechnol*. 2011;**29**(4):341–345.
464. Wahlgren J, De L Karlson T, Brisslert M, Vaziri Sani F, Telemo E, Sunnerhagen P, Valadi H. Plasma exosomes can deliver exogenous short interfering RNA to monocytes and lymphocytes. *Nucleic Acids Res*. 2012;**40**(17):e130.
465. Ju Z, Ma J, Wang C, Yu J, Qiao Y, Hei F. Exosomes from iPSCs delivering siRNA attenuate intracellular adhesion molecule-1 expression and neutrophils adhesion in pulmonary microvascular endothelial cells. *Inflammation*. 2017;**40**(2):486–496.
466. Sun D, Zhuang X, Xiang X, Liu Y, Zhang S, Liu C, Barnes S, Grizzle W, Miller D, Zhang H-G. A novel nanoparticle drug delivery system: the anti-inflammatory activity of curcumin is enhanced when encapsulated in exosomes. *Mol Ther*. 2010; **18**(9):1606–1614.
467. Luan X, Sansanaphongpricha K, Myers I, Chen H, Yuan H, Sun D. Engineering exosomes as refined biological nanoplatforms for drug delivery. *Acta Pharmacol Sin*. 2017;**38**(6):754–763.
468. Gopal SK, Greening DW, Rai A, Chen M, Xu R, Shafiq A, Mathias RA, Zhu H-J, Simpson RJ. Extracellular vesicles: their role in cancer biology and epithelial-mesenchymal transition. *Biochem J*. 2017;**474**(1): 21–45.
469. Lener T, Gimona M, Aigner L, Börger V, Buzas E, Camussi G, Chaput N, Chatterjee D, Court FA, Del Portillo HA, O'Driscoll L, Fais S, Falcon-Perez JM, Felderhoff-Mueser U, Fraile L, Gho YS, Görgens A, Gupta RC, Hendrix A, Hermann DM, Hill AF, Hochberg F, Horn PA, de Kleijn D, Kordelas L, Kramer BW, Krämer-Albers E-M, Laner-Plamberger S, Laitinen S, Leonardi T, Lorenowicz MJ, Lim SK, Lötvall J, Maguire CA, Marcilla A, Nazarenko I, Ochiya T, Patel T, Pedersen S, Pocsfalvi G, Pluchino S, Quesenberry P, Reischl IG, Rivera FJ, Sanzenbacher R, Schallmoser K, Slaper-Cortenbach I, Strunk D, Tonn T, Vader P, van Balkom BWM, Wauben M, Andaloussi SE, Théry C, Rohde E, Giebel B. Applying extracellular vesicles based therapeutics in clinical trials—an ISEV position paper. *J Extracell Vesicles*. 2015;**4**(1):30087.
470. Barkalina N, Jones C, Wood MJA, Coward K. Extracellular vesicle-mediated delivery of molecular compounds into gametes and embryos: learning from nature. *Hum Reprod Update*. 2015;**21**(5):627–639.
471. Sousa C, Pereira I, Santos AC, Carbone C, Kovačević AB, Silva AM, Souto EB. Targeting dendritic cells for the treatment of autoimmune disorders. *Colloids Surf B Biointerfaces*. 2017;**158**:237–248.

Acknowledgments

We thank Fernando Ibañez from Contextos Culturales for help in the final edition of the figures for this review.

Financial Support: This work was supported by MINECO/FEDER Grant SAF2015-67154-R to C.S; La Trobe Institute for Molecular Science Fellowship, La Trobe University Leadership Research Focus grant, and La Trobe University Start-up Fund to D.W.G; MECD Grant FPU15/02248 to D.B; Atracció de Talent Program ultraviolet-INV-PREDOC14-178329 to N.B; National Health and Medical Research Council of Australia Project Grant 1002028 and the Victorian Government's infrastructure support funding to the Hudson Institute to L.A.S.; and by Miguel Servet Program Type I of ISCIII (CP13/00038) and FIS project (PI14/00545) to F.V.

Correspondence and Reprint Requests: Felipe Vilella, PhD, Igenomix Foundation/INCLIVA, Narcis de Monturiol Estarriol 11, Parcela B, Paterna, 46980 Valencia, Spain. E-mail: felipe.vilella@igenomix.com.

Disclosure Summary: The authors have nothing to disclose.

*These authors contributed equally to this work.

Abbreviations

AB, apoptotic body; AFM, atomic force microscopy; BLVRA, biliverdin reductase A; BMI, body mass index; cAMP, cyclic adenosine monophosphate; ED, erectile dysfunction; ELISA, enzyme-linked immunosorbent assay; ER, endoplasmic reticulum; ESCRT, endosomal sorting complex required for transport; EV, extracellular vesicle; EVT, extravillous trophoblast; EXO, exosome; FAK, focal adhesion kinase; GD, gestational diabetes; GTPase, guanosine triphosphatase; HbF, cell-free hemoglobin; IL, interleukin; ILV, intraluminal vesicle; LOT, low-oxygen tension; miRNA, microRNA; mRNA, messenger RNA; MV, microvesicle; MVB, multivesicular body; NK, natural killer; NOS, nitric oxide synthase; NTA, nanoparticle tracking analysis; PBS, phosphate-buffered saline; PCOS, polycystic ovarian syndrome; PE, preeclampsia; PKA, protein kinase A; PLAP, placental alkaline phosphatase; PPCM, peripartum cardiomyopathy; PS, phosphatidylserine; SEM, scanning electron microscopy; siRNA, small interfering RNA; SPAM1, sperm adhesion molecule 1; SPB, spontaneous preterm birth; SPZ, spermatozoa; STB, syncytiotrophoblast; STBM, syncytiotrophoblast-derived exosome and microvesicle; TEM, transmission electron microscopy; TNF, tumor necrosis factor; tRF, transfer RNA fragment; tRNA, transfer RNA; μ.NMR, micronuclear magnetic resonance spectrometry.

genes

MDPI

Article

Identification and Characterization of Extracellular Vesicles and Its DNA Cargo Secreted During Murine Embryo Development

Blanca Simon [1,2,†], David Bolumar [1,2,†], Alicia Amadoz [3], Jorge Jimenez-Almazán [3], Diana Valbuena [3], Felipe Vilella [1,*] and Inmaculada Moreno [1,3,*]

1 Igenomix Foundation-INCLIVA Biomedical Research Institute, Ronda de Narcís Monturiol, 11B, 46980 Paterna, Spain; blansi@alumni.uv.es (B.S.); david.bolumar@igenomix.com (D.B.)
2 Department of Pediatrics, Obstetrics and Gynecology, School of Medicine, University of Valencia, Av. de Blasco Ibáñez, 15, 46010 Valencia, Spain
3 Igenomix, R&D, Parque Tecnológico de Paterna, Ronda de Narcís Monturiol, 11B, 46980 Paterna, Spain; alicia.amadoz@igenomix.com (A.A.); jorge.jimenez@igenomix.com (J.J.-A.); diana.valbuena@igenomix.com (D.V.)
* Correspondence: felipe.vilella@igenomix.com (F.V.); Inmaculada.moreno@igenomix.com (I.M.); Tel.: +34-963905310 (F.V. & I.M.)
† These authors contributed equally to this study.

Received: 7 January 2020; Accepted: 12 February 2020; Published: 17 February 2020

Abstract: Extracellular vesicles (EVs) are known to transport DNA, but their implications in embryonic implantation are unknown. The aim of this study was to investigate EVs production and secretion by preimplantation embryos and assess their DNA cargo. Murine oocytes and embryos were obtained from six- to eight-week-old females, cultured until E4.5 and analyzed using transmission electron microscopy to examine EVs production. EVs were isolated from E4.5-day conditioned media and quantified by nanoparticle tracking analysis, characterized by immunogold, and their DNA cargo sequenced. Multivesicular bodies were observed in murine oocytes and preimplantation embryos together with the secretion of EVs to the blastocoel cavity and blastocyst spent medium. Embryo-derived EVs showed variable electron-densities and sizes (20–500 nm) and total concentrations of $1.74 \times 10^7 \pm 2.60 \times 10^6$ particles/mL. Embryo secreted EVs were positive for CD63 and ARF6. DNA cargo sequencing demonstrated no differences in DNA between apoptotic bodies or smaller EVs, although they showed significant gene enrichment compared to control medium. The analysis of sequences uniquely mapping the murine genome revealed that DNA contained in EVs showed higher representation of embryo genome than vesicle-free DNA. Murine blastocysts secrete EVs containing genome-wide sequences of DNA to the medium, reinforcing the relevance of studying these vesicles and their cargo in the preimplantation moment, where secreted DNA may help the assessment of the embryo previous to implantation.

Keywords: extracellular vesicles; exosomes; microvesicles; apoptotic bodies; DNA; preimplantation embryos; murine blastocysts

1. Introduction

Embryo-endometrial communication is mediated by different mechanisms including extracellular vesicles (EVs) with a plethora of molecules released to this interface. EVs constitute a novel bidirectional form of cross-talk during embryo implantation, as they are secreted by both the endometrium [1,2], and the embryo [3,4] contributing to new functional perspectives as their cargo is composed by virtually all sorts of biomolecules. In fact, EVs have been described to participate in several reproductive processes,

such as gametogenesis, fertilization, embryo development and implantation, and fetal development throughout term (for review see [5]).

EVs are secreted by cells of different human tissues and organs and can be isolated in a variety of biological fluids including blood [6], urine [7], saliva [8], breast milk [9], amniotic fluid [10], ascitic fluid [11], cerebrospinal fluid [12], bile [13], semen [14], and endometrial fluid [2].

Three major types of EVs have been described based on their biogenetic pathway, composition, and physical characteristics such as size or density, namely, apoptotic bodies (ABs), microvesicles (MVs), and exosomes (EXOs) [15,16]. ABs result from the outward budding of the plasma membrane in the context of programmed cell death and their diameter ranges from 50–5000 nm [17,18]. MVs are produced directly by outward budding of the plasma membrane. They are in the size range from 100–1000 nm and are associated to the GTP-binding protein ARF6, which is used for their identification [19]. EXOs originate from the endosomal pathway as late endosomes that evolve into multivesicular bodies and migrate from the perinuclear region to the cell surface by fusion [20,21]. Their sizes range between 30–150 nm and are identified by classical molecular markers such as tetraspanins (CD63, CD9, CD81), flotillin-1, or heat shock 70-kDa proteins, although recent reports considered that other EVs might share these markers [22]. Their cargo portrays their functionality in regulating communication by means of proteins, cytokines, lipids, RNA, or DNA [23].

The embryo also secretes EVs that participate in both the dialogue with the maternal endometrium [24], and in self-paracrine regulation [4]. EVs are secreted by a trophectoderm cell line in the pig model [25], and in the human model [26] stimulating the proliferation of endothelial cells in vitro, thus becoming potential regulators of maternal endometrial angiogenesis. Regarding the nucleic acid cargo of embryo derived EVs, several papers have described the RNA cargo of trophoblast-derived EVs, mainly focusing on miRNA [25], linking miRNA signature with successful pregnancy [27], nevertheless, the DNA cargo of embryo derived EVs has received little attention. The aim of the present study is to identify and characterize embryo derived EVs secreted during murine embryo development, and to analyze their DNA cargo comparatively among the different EVs subpopulations.

2. Materials and Methods

2.1. Mouse Embryo Isolation and Culture

Female B6C3H1/Crl mice of 8-weeks of age (Charles River Laboratories International, Wilmington, MA, USA) were stimulated using 10 IU of Foligon/PMSG (MSD Animal Health, Madrid, Spain) followed by administration of 10 IU of Ovitrelle/hCG (Merck Serono, Darmstadt, Germany) 48 h later. Female mice were mated with males overnight and sacrificed by cervical dislocation 24 h after vaginal plug was observed. At embryonic day 1.5 (E1.5), embryos were extracted by flushing the oviduct with PBS using a 30G syringe needle. Non-fertilized metaphase II (MII) oocytes were also collected. Mouse embryos were washed and cultured in oxygenated G2-Plus media (Vitrolife, Västra Frölunda, Sweden) at 37 °C and 5% CO2 in groups of 40 embryos per well (Nunc 4-well plates, ThermoFisher Scientific, Whaltham, MA, USA) until day E4.5, reaching the stage of hatching/hatched blastocysts. MII oocytes, embryos at different developmental stages (E2.5, E3.5, and E4.5) and spent culture media from them were collected and preserved accordingly to the objective of the investigation.

The total number of females used was 80. Embryos from 10 animals were used for identification and phenotypic characterization of EVs using electron microscopy and immunogold. Ten animals were used in triplicates (n = 30) for quantification by nanoparticle tracking analysis and 10 in quadruplicates (n = 40) for sequencing experiments. An average of 32 embryos were obtained per female, 50% of them achieved hatching/hatched blastocyst stage by day E4.5. All animal experimentation was conducted at the animal facility located in the School of Pharmacy at the University of Valencia under the protocol code 2015/VSC/PEA/00048, approved by the Ethics Committee of Animal Welfare on 12 March 2015.

2.2. Isolation and Purification of EVs Secreted by Murine Embryos

Conditioned media from embryo culture was collected at day E4.5 and centrifuged at low speed (300× *g*, 10 min) to remove larger debris. The resulting supernatant was centrifuged at 2,000× *g* for 10 min to recover ABs as previously described [28]. It was subsequently ultracentrifuged at 185,000× *g* for 70 min in a P50A3 Hitachi rotor (Hitachi, Tokio, Japan) to collect non-apoptotic EVs (naEVs) that includes MVs and EXOs in the same fraction. All centrifugations were conducted at 4 °C.

2.3. Transmission Electron Microscopy and Immunogold

Oocytes and embryos at different developmental stages (E2.5, E3.5, and E4.5) and pellets containing EVs from spent culture media were fixed overnight in Karnovsky's solution (2.5% glutaraldehyde/2% formaldehyde in phosphate buffer 0.1 M, pH 7.4), washed in PBS and encapsulated in 2% agar in distilled water. Samples were then washed 5 times in PBS for 5 min and stained in a 2% osmium tetroxide 0.2 M PBS solution for 2 h. Then, dehydrated following the next sequence: three washes of 5 min in distilled water at 4 °C, 5-min wash in 30° ethanol, 10-min wash in 50° ethanol, 10-min wash in 70° ethanol twice, 45-min wash in 2:1 90° ethanol + LR-white twice, 45-min wash in 2:1 100° ethanol + LR-White, and O/N wash in 1:2 100° ethanol + LR-white in continuous shaking. Ethanol was let to evaporate, and wash media was changed by 100% LR-White in continuous shaking, for a 30-min incubation. Finally, samples were allowed to polymerize for 1 day at 60 °C, protecting them from the air. Resin-embedded samples were ultrasectioned in 60 nm slices, incubated for 1 h on formvar carbon-coated cooper (regular visualization) and nickel (immunogold visualization) grids, and contrasted with uranyl acetate. Ultrathin cuts were done using a UC6 Leica ultramicrotome (Leica, Wetzlar, Germany) equipped with an Ultra 45° diamond blade (Diatome, Hatfield, PA, USA). Prepared samples were observed using a JEM-1010 transmission electron microscope (Jeol Korea Ltd., Seoul, South Korea) at 80 kV, using a digital camera MegaView III and Olympus Image Analysis Software.

For the immunogold labelling assays, 60 nm sections from previous resin blocks were processed as described by Marcilla and collaborators [29]. Specifically, two different combinations of primary antibodies were used: rabbit α-CD63 (Abcam, ref: ab118307), rabbit α-ARF6 (Abcam, ref: ab77581), and mouse α-DNA (Millipore, Burlington, MA, USA ref: CBL186). All the antibodies were diluted in PBS/0.5% BSA following the manufacturer's datasheets. Then, the grids were washed in PBS/0.5% BSA and incubated with gold-coupled secondary antibodies [goat α-mouse coupled to 10 nm gold particles (BBI solutions, Crumlin, UK, ref: 15736) and goat α-rabbit coupled to 18 nm gold particles (Jackson Immunoresearch, Ely, UK) at 1:20 dilution in PBS/0.5% BSA for 30 min, following datasheets specifications. In parallel, paired grids were incubated only with the secondary antibodies as negative controls. Finally, grids were stained with 2% uranyl acetate and imaged by TEM as previously described.

2.4. Nanoparticle Tracking Analysis

Nanoparticle tracking analysis (NTA) was performed using a NanoSight300 (NS300, Malvern Instruments ltd, Malvern, UK). The naEVs fraction isolated from E4.5 spent media was resuspended in 1 mL of sterile PBS w/o Ca2+/Mg2+ (Biowest, Nuaillé, France, ref. L0615-500). In parallel, an aliquot of fresh embryo culture media was processed as a blank control. Three 60 sec videos were recorded under the static flow conditions for each sample with camera level set at 11. Videos were analyzed with NTA software version 3.2 Dev Build 3.2.16 to determine mean size and estimated concentration of measured particles with corresponding standard error. The NS300 system was calibrated with silica microspheres 100, 167, and 300 nm (Bangs Laboratories, Inc.; Fishers, IN, USA) prior to analysis, as previously demonstrated [30], auto settings were used for blur, minimum track length, and minimum expected particle size.

2.5. DNA Amplification and Sequencing of EVs Derived from Murine Embryos

Sequencing analysis was conducted to assess whether a specific DNA cargo is loaded into EVs secreted by the embryo, namely, ABs and naEVs. Mouse embryos representing the whole murine genome and EVs-depleted supernatant fraction after isolation of EVs (SN) were also sequenced. Because ABs are the result of dying cells, it is expected to have a representation of the total embryo DNA in this fraction. Sequencing of the DNA of ABs was used as an internal control. The negative control was blank medium that had not been in contact with murine embryos (blank). Groups of 10 mice were used to obtain the samples (embryo, ABs, naEVs, SN) in four independent sequencing experiments. DNase treatment of the different EV populations was conducted to evaluate and remove external DNA contamination and its potential bias in the analysis. The samples corresponding to DNase treated and untreated ABs from one of the four replicates were lost due to technical reasons, so only DNA from embryos, treated and untreated naEVs, and SN were included in the analysis for this biological replicate.

Embryos for DNA sequencing corresponding to E4.5 stage, were snap-frozen for initial DNA extraction and kept at −80 °C until processing. At this point, embryos were diluted in nuclease-free water (Ambion, ThermoFisher Scientific, Waltham , MA, USA) at a rate of 1 embryo/µL. DNA from pooled SN from all embryo culture wells and an equal volume of fresh blank media (G2-Plus) was extracted using QIAamp DNA mini kit (Qiagen, Hilden, Germany), eluting in 30 µL of nuclease free-water. For DNase treatment, ABs and naEVs were separated in two equivalent aliquots from pooled spent embryo culture media at the beginning of the isolation process. Once isolated, EVs were resuspended in nuclease-free water and, in the case of DNase treatment, 50 U/mL DNaseI (Sigma-Aldrich, San Luis, MO, USA) in 20 mM Tris-HCl (Thermo Fisher Scientific), 10 mM MgCl2 (Thermo Fisher Scientific), and 1 mM CaCl2 (Sigma-Aldrich, ref. 21115-100ML) were added to a final volume of 5 µL. Samples were then incubated at 37 °C for 30 min for DNase digestion followed by 10 min at 75 °C for DNase inactivation.

Immediately after, DNA amplification was performed using DOPlify whole genome amplification platform (RHS Ltd., Thebarton, Australia) following the manufacturer's instruction. Then, DNA was purified by using AMPure XP (Beckman Coulter, Brea, CA, USA) at a final concentration of 1.8X, in order to recover small-sized DNA fragments, and eluted in a final volume of 20 µL of nuclease-free water. Subsequently, the amplified DNA profiles were analysed by TapeStation 4200 (Agilent, Santa Clara, CA, USA). Finally, samples were sequentially diluted to 0.5 and 0.2 ng/µL to meet libraries kit DNA input requirements by Qubit dsDNA HS Assay (TermoFisher Scientific, Waltham, MA, USA). DNA libraries were built using Nextera XT DNA Library Prep Kit, specifically designed for samples with low DNA input. The experimental procedure was conducted following the protocol provided by the manufacturer, adjusting AMPure XP purification to 1.8X proportion. Then, libraries were pooled and sequenced using a 300 cycles-NextSeq 500/550 v2 High Output cartridge in a NextSeq 550 platform (Illumina, San Diego, CA, USA). To do so, 5 µL of the libraries pool, normalized by the bead method, were diluted in 995 µL of HT1 buffer. Then, 750 µL of the dilution was rediluted in 750 µL of HT1 buffer. The resulting dilution was denaturalized at 98 °C for 4 min, cooled in ice for 5 min and loaded into the sequencing cartridge for sequencing.

2.6. Computational Analysis of Sequencing Results

Raw data pre-processing: Raw data from pair-ended Illumina sequencing was downloaded from Illumina BaseSpace and converted into FASTQ files using bcl2fastq (version 2.16.0.10). Then, each sample was aligned to the mouse reference genome (mm10) using BWA (version 0.7.10) [31]. Reads with mapping quality lower than 10 were filtered out using Samtools (version 1.1) [32] and duplicates were removed with PICARD software (version 1.119). Finally, the coverage of each genome feature was obtained with Bedtools (version 2.17.0) [33] using Ensembl Biomart mm10 annotations. The raw genomic sequences generated in this study are deposited in the SRA database under the accession number PRJNA547453.

Murine-specific DNA sequences: A greater than expected quantity of valid reads were observed in blank media. Using the blank media for a background subtraction with the count per million (CPM) of each gene feature to decrease the background noise is not usually recommended because this data transformation may break the statistical assumptions of later steps. Therefore, the approach used here was to identify and filter murine-specific reads in a common manner for all samples. Then, background noise is considered as a background population (blank) and included in the analysis as another comparison group, whose results could be considered as differences with the background. To identify murine-specific reads, pre-processed data was mapped to the human reference genome (Hg19) using BWA. Then, unmapped reads were filtered using Samtools [32] and read ids were retrieved. Murine-specific reads were retrieved from pre-processed data by read id using PICARD software. Finally, the coverage of each genomic feature was obtained with Bedtools using Ensembl Biomart mm10 annotations.

Differential DNA enrichment of vesicles' cargo: The approach used for the differential DNA enrichment analysis is based on the edgeR methodology [34–36] that uses read counts of genomic features obtained from massively parallel sequencing technologies such as Illumina, 454, or ABI SOLiD applied to different types of experiments such as RNA-seq or ChIP-seq. edgeR can be applied to differential abundance analysis at the gene, exon, transcript, or tag level. In fact, read counts can be summarized by any genomic feature.

Here, differential DNA enriched regions were obtained using the following approach. In order to filter out lowly enriched regions, genomic features with greater than 1 cpm reads mapped in at least 1.5 samples (half of the mean of groups sizes) were kept for the following analyses. Raw counts were normalized using TMM method from edgeR R package [34]. A differential enrichment analysis of genome features was done using a generalized linear model approach for pairwise comparisons between sample types (embryo, ABs, naEVs, SN, blank). Experimental set and treatment were taken as factors in the additive model in order to adjust for differences between groups.

3. Results

3.1. Identification of EVs in Murine Oocytes and Embryos

Ultrastructural visualization of murine oocytes using TEM identified the existence of multivesicular bodies (MVBs) in the cytoplasm. These MVBs showed bilipid membrane vesicles containing smaller vesicular structures of different electron densities and sizes that would give rise to EXOs upon fusion of the MVBs with the oocyte plasma membrane. These structures were identified by their lower electron density, and vesicles of different sizes were observed entering the zona pellucida (Figure 1A). The presence of MVBs was also observed in the blastomeres at different embryo developmental stages (E2.5 and E3.5), migrating from the cytoplasm to the plasma membrane where their content was secreted outwards through the zona pellucida (Figure 1B). Interestingly, large vesicles including complex structures were also observed in the intercellular space (Figure 1C). At the blastocyst stage (day E4.5), the secretion of vesicular structures was observed both into the extracellular medium through the zona pellucida (zp), as well as into the blastocoel (bl) cavity (Figure 1D).

3.2. EVs Isolated from Blastocyst Culture Media

In order to study naEVs-including MVs and EXOs-produced and released by murine blastocysts, spent media at developmental day E4.5 was ultracentrifuged and gathered naEVs where quantified by NTA. The vesicular fraction showed vesicle profiles compatible in size with that of EXOs and MVs. The total concentration of naEVs from spent media was $1.74 \cdot 10^7 \pm 2.60 \cdot 10^6$ particles/mL, with a size profile showing two main populations. A first population extended from approximately 50–170 nm and accounted for $9.87 \times 10^6 \pm 7.55 \times 10^5$ particles/mL (56.72%) while the second extended from 180–310 nm and were represented by $6.75 \times 10^6 \pm 1.57 \times 10^6$ particles/mL (38.83%) to the total (Figure 2A).

Importantly, standard error of measurements showed that only a small amount of these particles remained constant among replicates (Figure 2A).

Finally, morphological analysis of EVs isolated from spent culture media by TEM showed vesicles of variable appearance, electron densities, and sizes ranging from 20 nm–500 nm, suggesting that EVs secreted by the embryo constitute a heterogenous population including different types of EVs (Figure 2B).

3.3. Phenotypic Characterization of Embryo Secreted EVs

Phenotypic characterization of the EVs secreted by murine embryos to the spent medium was performed using immunohistochemistry coupled to gold nanoparticles using specific surface markers for EXOs (CD63) or MVs (ARF6). As a negative control, paired grids of E4.5 blastocyst were incubated with the secondary antibodies only. Positive ARF6 staining was consistent with an active vesicular biogenesis through phospholipase D pathway in embryos, a mechanism described for inward budding of MVBs membrane in EXOs biogenetic pathway [37] and outward budding of cell plasma membrane in MVs formation [38]. Positivity for CD63, a tetraspanin involved in the formation of EXOs, was considered as canonical marker for these types of EVs that originate from the endosomal pathway (Figure 3A).

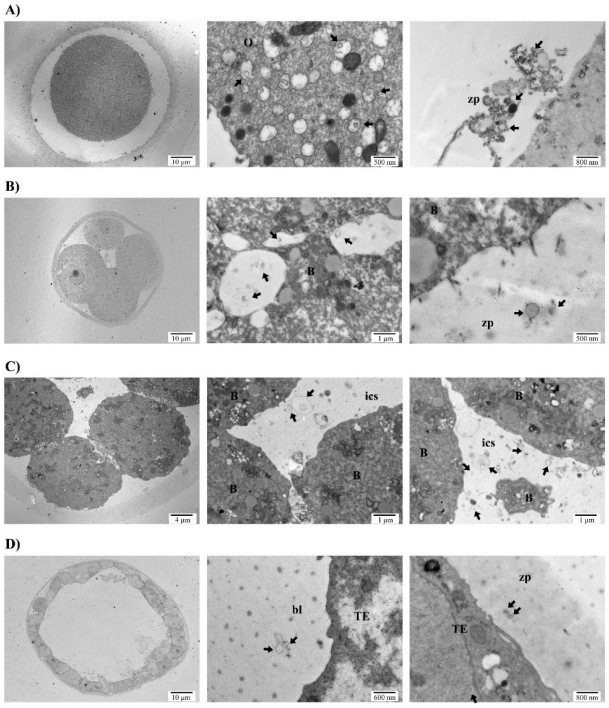

Figure 1. Vesicle production and secretion by murine embryos at different developmental stages shown by TEM. (**A**) Mouse oocyte (left) with magnifications of the production of multivesicular bodies (MVBs) in the cellular cytoplasm (center) and secretion of their content towards the zona pellucida (right). (**B**) E2.5 embryo (left) with magnifications of the cytoplasm containing MVBs (center) and the secretion of extracellular vesicles (EVs) through the zona pellucida (right). (**C**) E3.5 mouse embryo (left) showing MVB secreted to the intercellular space. (**D**) E4.5 blastocyst (left) secreting EVs into the zona pellucida (center) and blastocoel cavity (right). Abbreviations: B, blastomere; bl, blastocoel; O, oocyte; TE, trophectoderm cell; zp, zona pellucida.

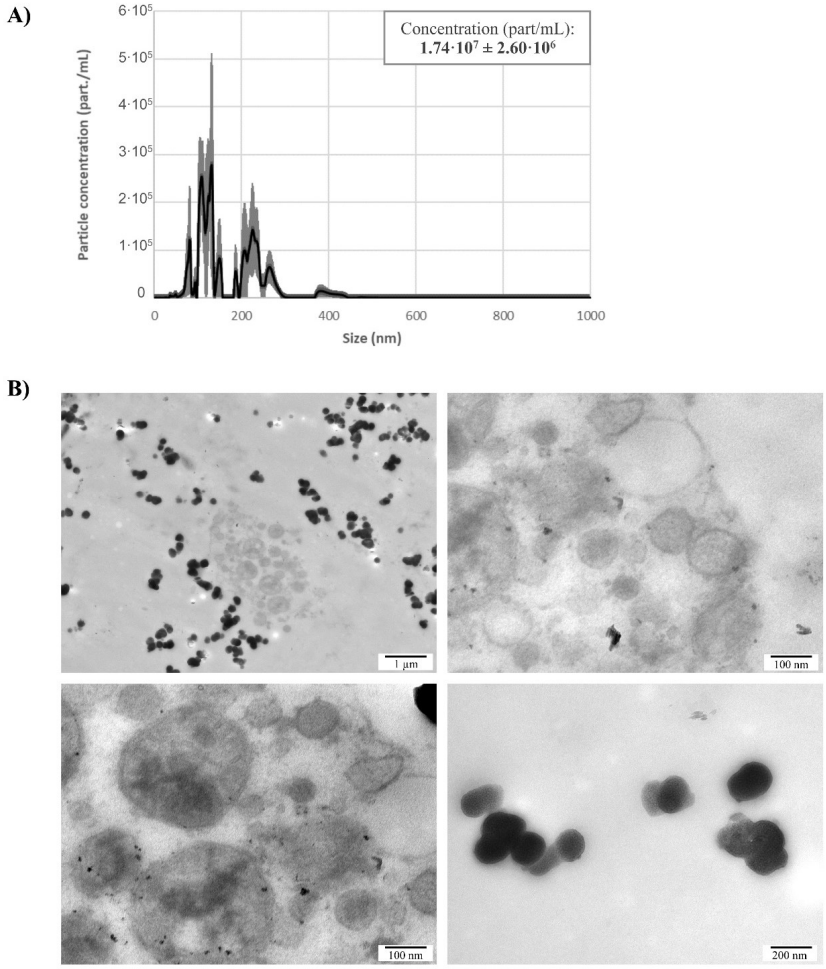

Figure 2. Isolation of naEVs from E4.5 blastocyst spent media. (**A**) Size distribution and quantification using nanoparticle tracking analysis of naEVs isolated from spent blastocyst media. Net particle concentration was calculated after subtracting particles found in the same volume of blank media. Values represent the mean of three independent experiments ±SEM. (**B**) Different images showing morphological characterization of naEVs in spent culture media by TEM. Particles of different aspects, electron densities and sizes ranging from 20–500 nm were observed.

Additionally, immunogold was performed on ultrathin sections to assess the presence of ARF6 and CD63 in naEVs fraction isolated by ultracentrifugation from E4.5 blastocyst spent media. In parallel, to study the potential cargo of DNA in naEVs, DNA targeting antibodies were used. The results revealed positivity for the microvesicular marker ARF6, exosomal marker CD63, and DNA (Figure 3B), thus suggesting the presence of DNA cargo in the EVs secreted by the embryos. Particularly, in our experimental set in which 702 single naEVs were studied, 16.1% of DNA positive EVs were identified.

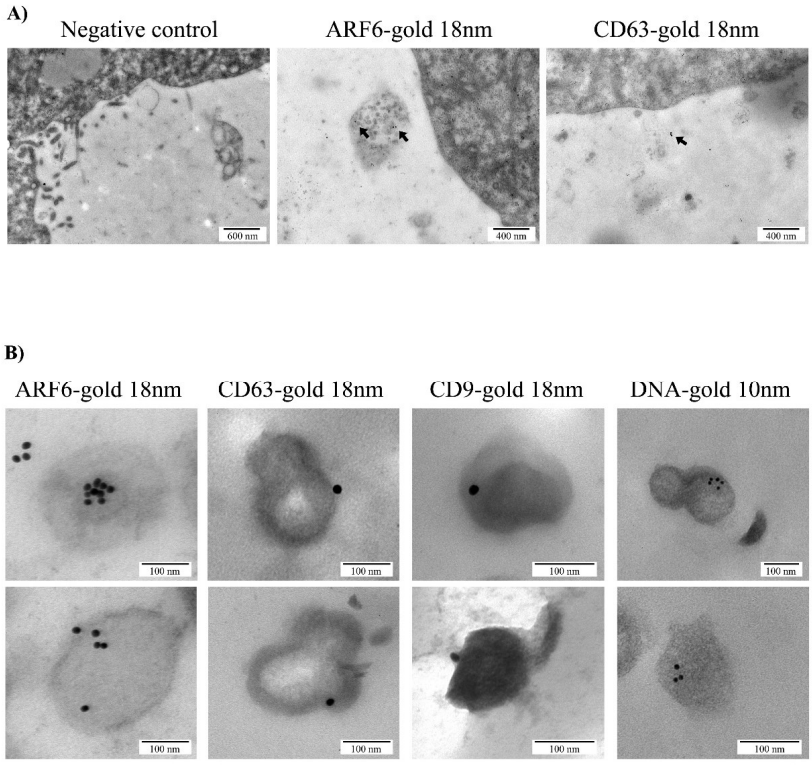

Figure 3. Phenotypic characterization of EVs using immunogold staining. (**A**) Vesicles secreted by the trophoectodermal (TE) cells of murine embryo blastocyst showed positive staining for microvesicles (MVs) and exosomes (EXOs) markers, ARF6 and CD63, respectively. (**B**) Immunogold detection of ARF6, CD63 and DNA in naEVs isolated from spent media of E4.5 blastocysts. ARF6 and CD63 are coupled to 18 nm gold particles; DNA is coupled to 10 nm gold particles. Bars represent 100 μm. Two representative images for each immunogold labeling experiment are included in the figure.

3.4. Characterization of the DNA Cargo of the EVs Secreted by the Embryo

EVs secreted by the embryo, classified as ABs or naEVs, were sequenced and compared. First, DNase treatment was applied to ABs and naEVs fractions and compared to untreated controls to discard the existence of DNA attached to the external membrane of vesicles that could confound with the real cargo. Genomic DNA from the embryos originating the EVs was used as a positive control, SN after the isolation of EVs from the spent media was included as an EVs depleted fraction and oxygenated blank media (G2-plus) as a negative control. Sequencing coverage and mapping statistics are detailed in Table S1. Sequencing of the DNA from different subpopulations revealed no differences among them (Figure 4A). However, DNase treated samples showed a different read count distribution and were differentiated into a separate cluster (Figure 4B, Figure S1), suggesting the existence of external DNA attached to the membrane of vesicles. Paired comparisons of untreated samples showed no statistical differences between the DNA regions observed in ABs and naEVs fractions, neither with the embryo genomic DNA or the EV-depleted SN, but all of them showed significant enrichment in a reduced number of gene sequences compared to the blank media (Figure 4C,D). Eleven of these differential sequences were commonly enriched in all the embryonic fractions against the blank, but no differences among the spent media derived fractions were observed. The complete list of enriched sequences is shown in Table 1 and Tables S2–S5.

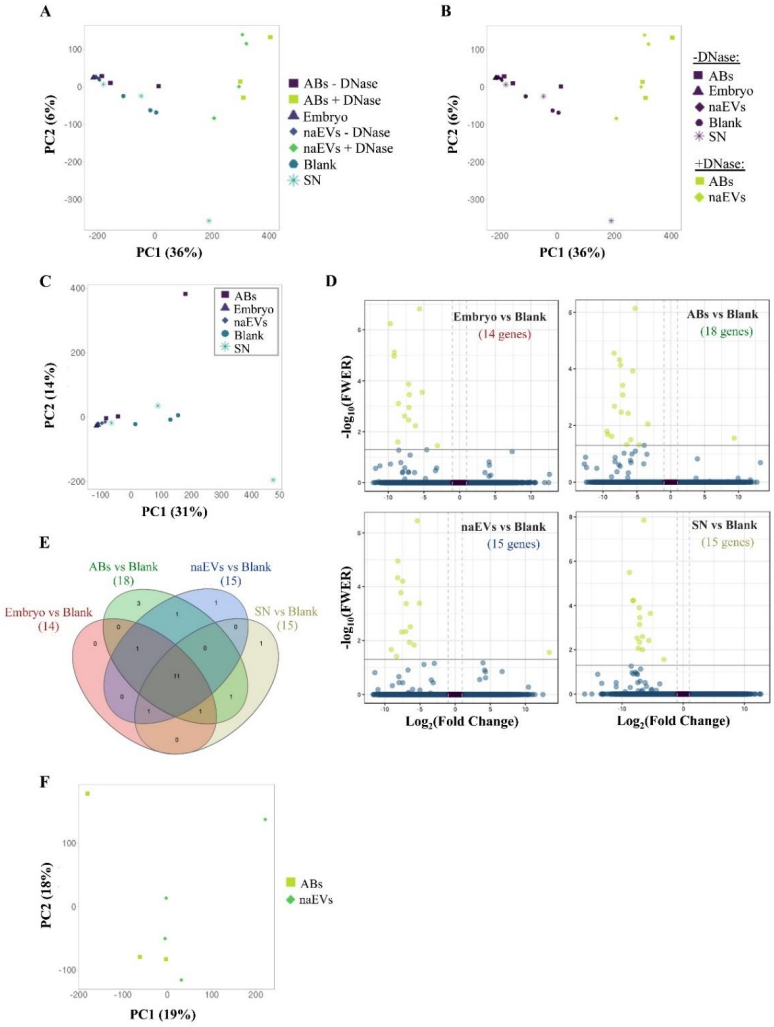

Figure 4. Analysis of the DNA produced and released by the murine embryo to the culture media. (**A**) PCA showing similarity between samples using normalized counts of 27,207 genomic features of the DNase treated and untreated EVs fractions produced by the embryo, the culture media as a negative control (blank), the embryo itself as a positive control, and the SN as an EVs free fraction. (**B**) PCA showing sample distribution by treatment showing separated clusters by treatment. (**C**) PCA of separate analysis using DNase untreated samples, including embryo, Abs, naEVs, SN, and blank control (normalized counts of 26,997 genomic features). PCA shows the similarity between fractions and replicates. (**D**) Volcano plots showing differential enriched genes in the studied fractions (embryo, ABs, naEVs, or SN) compared to the blank control. Negative FC values (left) indicate genes that are enriched in each fraction with respect to the blank medium, while positive values (right) correspond to genes enriched in the blank medium compared to the studied sample. The number of differentially enriched genes is shown in brackets for each comparison. (**E**) Venn diagram showing common and specific enriched genes in pairwise comparisons. (**F**) PCA of DNase treated replicates showed no differences between DNA content in the treated vesicle subpopulations. Abbreviations: AB, apoptotic bodies; naEVs, smaller in size extracellular vesicles (including microvesicles and exosomes); SN, supernatant.

Table 1. Genes enriched in the comparison of the different DNase untreated samples (embryo, ABs, naEVs and SN) against the blank culture medium.

Gene ID	Chr	Embryo vs. Blank		ABs vs. Blank		naEVs vs. Blank		SN vs. Blank	
		log(FC)	FWER	log(FC)	FWER	log(FC)	FWER	log(FC)	FWER
2610005L07Rik	8	7.04	3.50×10^4	7.10	3.79×10^4	6.97	4.26×10^4	7.11	3.48×10^4
Gm10715	9	9.17	1.08×10^5	7.09	8.17×10^4	7.71	1.67×10^4	8.24	6.06×10^5
Gm10717	9	7.71	2.44×10^3	5.89	3.18×10^2	6.50	1.15×10^2	7.13	4.57×10^3
Gm13822	5	7.14	1.35×10^4	7.42	7.34×10^5	7.47	6.25×10^5	7.18	1.27×10^4
Gm17535	9	9.71	5.68×10^7	7.57	4.76×10^5	8.15	1.11×10^5	8.77	3.19×10^6
Gm26624	4	5.22	2.83×10^4	5.62	1.17×10^4	5.09	4.09×10^4	5.37	2.29×10^4
Gm26804	8	7.15	3.47×10^3	7.30	3.35×10^3	7.03	4.63×10^3	6.66	9.83×10^3
Gm7120	13	6.20	5.84×10^3	6.29	3.69×10^3	6.39	3.04×10^3	7.14	7.15×10^4
Pisd-ps1	11	9.14	7.51×10^6	8.38	2.77×10^5	8.17	4.65×10^5	8.12	5.83×10^5
Pisd-ps2	17	8.56	7.81×10^4	8.31	2.08×10^3	7.61	4.78×10^3	7.34	8.52×10^3
Sfi1	11	5.61	1.49×10^7	5.26	7.32×10^7	5.38	3.56×10^7	6.42	1.40×10^8
C230088H06Rik	4	3.10	3.53×10^2	3.38	8.85×10^3			3.18	2.73×10^2
Gm10720	9	7.09	1.11×10^3			5.84	1.44×10^2	6.64	2.54×10^3
Gm14412	2	8.66	2.51×10^2	8.70	2.41×10^2	8.35	3.86×10^2		
C130026I21Rik	1			4.64	4.84×10^2			5.61	3.80×10^3
Gm13251	4			9.41	1.60×10^2	9.08	2.15×10^2		
Cd2bp2	7			−9.38	2.77×10^2				
Fbxw18	9							7.53	2.98×10^3
Gm10306	4					−13.38	2.75×10^2		
Gm13154	4			6.50	4.66×10^2				
Leprot	4			9.29	2.04×10^2				

Abbreviations: ABs, Apoptotic Bodies; Chr, Chromosome; FC, Fold Change; FWER, Family-Wise Error Rate; naEVs, smaller in size extracellular vesicles (including microvesicles and exosomes); SN, supernatant.

DNase treated ABs and naEVs were compared to evaluate their DNA cargo after removal of external DNA. PCA analysis did not cluster separately for both populations and differential enrichment analysis did not evidence any result either (Figure 4F). The absence of differences after DNase treatment may be due to the scarce amount of DNA remaining after treatment, which resulted in poor sequencing outputs (Figure S1, panel C).

Considering these results, the culture media itself was assessed to test whether it could contain contaminating DNA that aligns to the murine genome, masking the results. To evaluate this effect, the reads were aligned to both human and murine genomes. Approximately, 80% of the reads from all the samples, including unused blank media, were able to map both human and murine reference genomes, while only 20% of the reads could be uniquely matched to the murine genome (Figure S2). This fact constituted an important hindrance for the analysis of murine-derived DNA in samples with reduced input and made it impossible to get complete DNA enrichment analyses.

In this context, those DNA sequences that uniquely map the murine genome were analyzed and only those comparisons of murine DNA isolated from embryos or EVs compared to the blank negative controls were considered. PCA analysis of murine-unique sequences showed again a wide dispersion of the different fractions analyzed (Figure 5A) and only DNase treated versus untreated samples clustered separately (Figure 5B and Figure S1, panels D–F). No major differences in DNA regions were found among DNase untreated fractions (Figure 5C). However, a higher amount of gene sequences was found in all the fractions compared to the blank media (Figure 5D) which only showed artefactual mapping to murine DNA (Figure S3). In this case, 169 gene sequences representing all murine chromosomes were found in the different samples studied (embryo, ABs, naEVs, or SN) compared to the blank, while 25 of them were common to all the comparisons. The individual assessment of each fraction compared to the blank rendered a total of 2, 14, 8, and 92 genes enriched in embryo, ABs, naEVs, and SN, respectively. (Figure 5E, Tables S6–S9). Interestingly, the enriched genes found in vesicles were more similar to the DNA found in the embryo, while the SN showed a different pattern of enriched genes compared to embryo, EVs, and blank media (Figure 5E and Table S10).

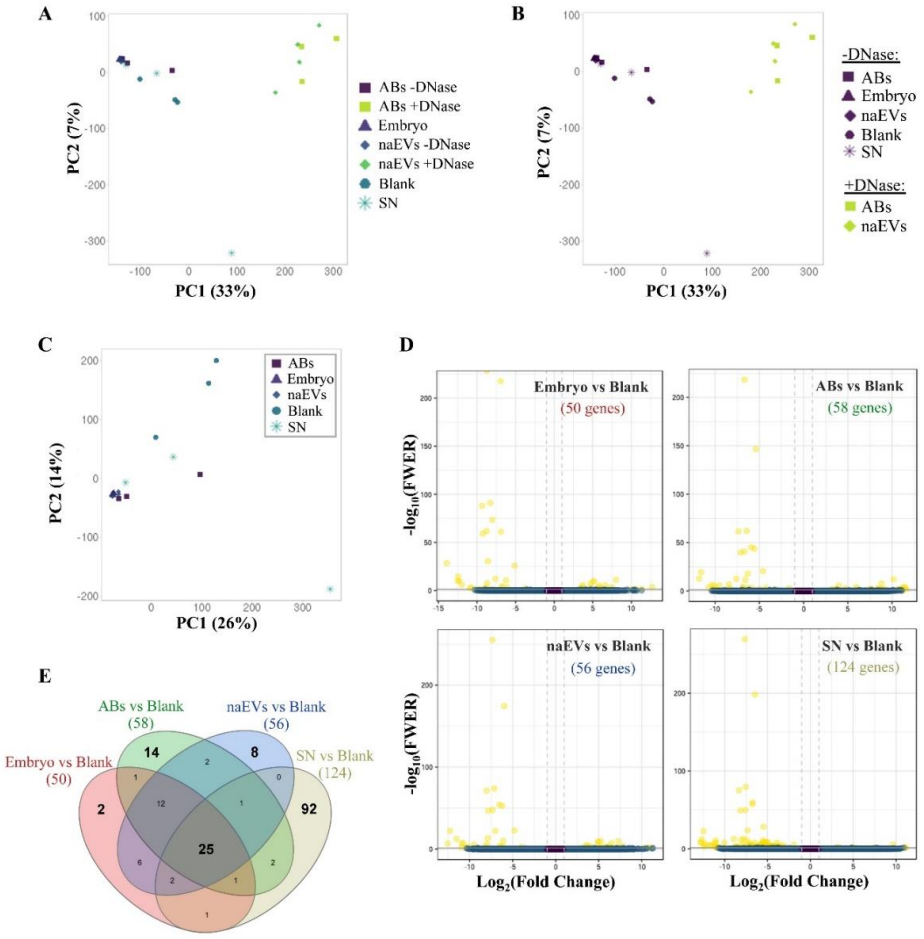

Figure 5. Analysis of murine-specific DNA sequences secreted by the embryo to the culture media. Study of DNA sequences uniquely mapping to Mus musculus reference genome secreted by the murine embryo to the spent media in EVs or as a free form. (**A**) PCA showing similarity between samples using normalized counts of 27,970 genomic features after filtering out human-homologous reads. (**B**) PCA grouping samples by DNase treatment. (**C**) Separate PCA of DNase untreated samples using normalized counts of 27,824 genomic features after filtering out human-homologous reads. (**D**) Volcano plots showing differential enriched genes in the studied fractions (embryo, ABs, naEVs, or SN) compared to the blank control. Negative FC values (left) indicate genes that are enriched in each fraction with respect to the blank medium, while positive values (right) correspond to genes enriched in the blank medium compared to the studied sample. The number of differentially enriched genes is shown in brackets for each comparison. (**E**) Venn diagram showing common and specific enriched genes in pairwise comparisons. Abbreviations: AB, apoptotic bodies; naEVs, smaller in size extracellular vesicles (including microvesicles and exosomes); SN, supernatant.

4. Discussion

The production and secretion of EVs by the embryo have been reported in different species from bovine [39], pig [40], mouse [41], and human [3]. Although different size ranges have been demonstrated among species, all shared phenotypic markers such as CD63 and CD9 [42]. The

achievement of blastocyst/hatching stage is key for the release of EVs to the extracellular medium [43]. In humans, the presence of EVs in conditioned media of in vitro cultured human embryos from day three to day five has been previously described as well as their uptake by the maternal side [3]. A similar event occurs in the sheep model, where EVs coming from the conceptus were observed to be internalized by the uterine epithelia, but not in other maternal tissues [24]. Also, of importance is the delivery of EVs between embryo compartments. Particularly, MVs have been observed to be produced by the inner cell mass reaching the trophectoderm, thus promoting its migration and implantation abilities [4]. Our results showed oocytes and embryos in different developmental stages with MVB produced by the blastomeres, as well as secreted vesicles of different sizes (Figure 1A–D). Of note, the existence of large vesicles with complex structures and contents in the intercellular space of the developing embryos was reported, which is in line with Desrochers' group observations (Figure 1C, D). NTA allows a precise measurement and quantification of EVs by their light scattering properties measured directly by a camera. Results showed a polydisperse population with varying sizes (Figure 2A), which were confirmed by deposition, staining, and TEM visualization of the vesicles (Figure 2B). Regarding molecular markers, immunogold staining of ultrathin cuts from EVs produced by the embryos showed the presence of CD63 and CD9 in the EVs, but also of ARF6, a GTP-binding protein involved in MVs synthesis through the phospholipase D pathway [38]. Importantly, gold labelling also revealed the presence of DNA cargo within these EVs (Figure 3). All-in-all, this initial analysis served us to confirm the production of varying in-size/phenotype EVs by the murine embryos to the culture media, and to associate them with EXOs and MVs markers as well as with DNA cargo. However, the quantification of positive vesicles may be impacted by the method used for the isolation of such vesicles. As high recovery methods may result in a great population of vesicles with low purity showing a low percentage of positive vesicles, while methods that yield a very pure population of vesicles may present a higher degree of positivity while missing other vesicular subtypes that may present a different phenotype. In this work, EVs were recovered using high-speed differential ultracentrifugation after intermediate speed apoptotic bodies removal and washes. This is considered an intermediate recovery and intermediate specificity method [44]. Nonetheless, positivity in our experimental set-up is only descriptive as we analyzed immunogold labelling on ultrathin sections, and only a small representation of the total vesicle fraction has been stained and visualized for this purpose.

Different molecules can be analyzed from the spent media with potential different diagnostic usefulness, including RNA [43] and DNA, both nuclear and mitochondrial [45]. DNA content of EVs is currently a developing field of research. Although different studies coincide in that embryo material in the spent medium may be greatly masked by maternal contamination coming from cumulus cells, its putative clinical usefulness has already been proposed for embryo chromosomal non-invasive diagnosis [43,46–50]. DNA secreted by cells can be single or double stranded at the extracellular medium in its free form, but also externally stuck or included in EVs where it is protected from the enzymes present in the medium [51]. Also, it has been reported that different subpopulations of EVs contain different DNA cargo [16], including mtDNA [52]. It was even observed that EVs' DNA can be transported into target cells in either the cytoplasm or nuclei [53] where it serves a function [54]. Nevertheless, there is not much information about the DNA content of EVs produced by preimplantation embryos in culture. A recent study reported the presence of DNA in embryo-derived EVs by flow cytometry, associating higher concentrations of DNA-containing EVs with higher rates of implantation failure after embryo transfer. Nevertheless, this may be explained by the fact that these DNA-containing EVs were mainly apoptotic bodies, thus reflecting poor embryo quality [55]. To our knowledge, there are still no works addressing the potential diagnostic value of embryo derived EVs for the detection of DNA mutations/polymorphisms in the cells of origin, but some works in different biofluids, such as blood, urine, or seminal fluid, have done so, highlighting EVs as potential biomarkers for pathological mutations [56]. In order to go one step further into the analysis of the DNA secreted by the preimplantation embryo, the present study analyzes whether any specific cargo was transported inside the EVs released to the spent media during early embryo development.

Pairwise comparisons of embryo fractions—consisting of full-embryos, ABs, MVs, EXOs and SN—against blank media were performed. Differentially enriched genes were observed in all the fractions analyzed and compared to the blank media (Figure 4), although the number of enriched genes was lower than expected. We hypothesized that the small differences found in the DNA enrichment analysis could be influenced by genetic material present in the blank control. G2-plus is a commercial medium supplemented with human serum albumin, which is a blood derived molecule and so it may drag residual DNA from the original source. The possibility of human–mouse cross-species mapping is not trite since 90% of the mouse and human genomes can be partitioned into corresponding regions of conserved synteny. At the nucleotide level, approximately 40% of the human genome, likely representing most of the orthologous sequences, can be aligned to the mouse genome. Around 80% of the mouse genes have a single identifiable orthologue in the human, while only 1% does not have a known homologue [57]. Our hypothesis was confirmed with 80% of the total reads corresponding to blank media aligning both the human and the murine genomes (Figure S2). The analysis of murine-specific DNA sequences in the blanks evidenced poor DNA size and quality and supported the consideration of these samples as background noise (Figure S3). Under this situation, human-homologous reads were filtered out and pairwise comparisons with murine-specific reads were recalculated (Figure 5). New comparisons provided richer results and even a trend was observed showing a high similarity between EVs and embryo DNA regions, while the SN presented a differential DNA pattern. This would introduce the concept of two differentiated embryo DNA sources: vesicular and cell-free DNA, deserving future analysis. Far from intending to establish any functional conclusion and considering the technical limitations of the data analysis, the results presented herein demonstrate the possibility of detecting specific DNA sequences secreted by the murine embryo over the inherent masking of blank medium and point at a differential DNA profile between EVs and SN, which may be of importance and should be further investigated.

Because DNA potentially stuck to the external surface of EVs may influence the results of the sequencing analysis, paired fractions of ABs and naEVs populations were treated with DNase prior to sequencing. Despite having control for human-homologous sequences effect, no statistically significant genes or DNA regions were obtained when comparing specific subtypes of EVs (ABs and naEVs) after DNase treatment. This may be due to the scarce DNA material left for sequencing after the harsh DNase treatment. Further studies starting from a higher number of vesicles and/or using defined embryo culture media might shed light on this point.

5. Conclusions

Our results demonstrate the existence of EVs produced by the murine oocyte and embryo throughout embryo development. These EVs are secreted to the extracellular space, and can be found in the intercellular space, the blastocoel or even in the spent culture media, after crossing the zona pellucida. The analysis of the different EVs collected from blastocyst spent media showed the presence of DNA representing the full murine genome, with no differences in DNA cargos between the different fractions (ABs and naEVs). Also, vesicle-free DNA was found in the EVs-depleted supernatant of embryo culture. These findings demonstrate that embryo DNA is randomly secreted to the spent culture medium under physiological conditions without the need of aneuploidy or apoptotic events. Furthermore, our results reinforce the relevance of cellular communication between the conceptus and maternal endometrium during implantation and to support the feasibility of non-invasive testing of pre-implantation embryos.

Supplementary Materials: The following are available online at http://www.mdpi.com/2073-4425/11/2/203/s1, Figure S1: DNA sequencing read counts and normalization of the different fractions. Plots showing normalization of samples sequencing reads previous (A, B, C) and after (D, E, F) filtering by specific murine genome. (A and D). All samples populations. (B and E) DNase untreated samples. (C and F) DNase treated EVs. Abbreviations: ABs: Apoptotic bodies; CPM, Counts per million; naEVs: non-apoptotic EVs (including microvesicles and exosomes); SN: supernatant; Figure S2: Mouse-Human cross-mapping. Normalized plot showing the percentages of reads for each sample able to map both to the human and murine reference genomes (purple) and those mapping

uniquely to the murine genome (yellow). Abbreviations: ABs: Apoptotic bodies; naEVs: non-apoptotic EVs (including microvesicles and exosomes); SN: supernatant; Figure S3: Quality control of murine specific DNA sequences. (A) Murine genomic sequences detected in blank samples showed poor mapping quality (MAPQ score) compared to embryo-derived samples. Murine genes differentially enriched in the experimental setting showed poor mapping quality (B) and insert insert size (C) in blank samples compared to embryo-derived fractions; Table S1: DNA sequencing reads, and mapping statistics; Table S2: Sequencing analysis data for the enriched genes in the comparison Embryo vs blank control for total gene sequences; Table S3: Sequencing analysis data for the enriched genes in the comparison ABs vs blank control for total gene sequences; Table S4: Sequencing analysis data for the enriched genes in the comparison naEVs vs blank control for total gene sequences; Table S5: Sequencing analysis data for the enriched genes in the comparison SN vs blank control for total gene sequences; Table S6: Sequencing analysis data for the enriched genes in the comparison Embryo vs blank control for gene sequences uniquely binding the Mus musculus reference genome; Table S7: Sequencing analysis data for the enriched genes in the comparison ABs vs blank control for gene sequences uniquely binding the Mus musculus reference genome; Table S8: Sequencing analysis data for the enriched genes in the comparison naEVs vs blank control for gene sequences uniquely binding the Mus musculus reference genome; Table S9: Sequencing analysis data for the enriched genes in the comparison SN vs blank control for gene sequences uniquely binding the Mus musculus reference genome; Table S10: Gene sequences uniquely mapping to the Mus musculus reference genome enriched in the comparisons of the different DNase untreated samples (embryo genomic DNA, ABs, naEVs and SN) vs the blank control. Abbreviations: ABs, Apoptotic Bodies; Chr, Chromosome; FC, FoldChange; FWER, Family-Wise Error Rate; naEVs, non-apoptotic EVs; SN, Supernatant.

Author Contributions: Conceptualization, F.V. and I.M.; methodology, B.S., D.B., and D.V.; software, A.A. and J.J.-A.; validation, D.B., F.V., and I.M.; formal analysis, B.S., D.B., A.A., J.J.-A., D.V., F.V., and I.M.; data curation, A.A. and J.J.-A.; writing—original draft preparation, B.S., D.B., and I.M.; writing—review and editing, B.S., D.B., A.A., J.J.-A., D.V., F.V., and I.M.; funding acquisition, D.B. and F.V. All authors have read and agreed to the published version of the manuscript.

Funding: This research was funded by Igenomix Foundation. D.B. is supported by the grant FPU15/02248 from the Spanish Ministry of Education, Culture and Sports. FV is supported by Instituto de Salud Carlos III through Miguel Servet Program Type II [CPII18/00020] and FIS project [PI18/00957].

Conflicts of Interest: A.A., J.J.-A., D.V. and I.M. are full-time or part-time employed by Igenomix S.L. B.S., D.B. and F.V. declare no competing financial interests.

References

1. Ng, Y.H.; Rome, S.; Jalabert, A.; Forterre, A.; Singh, H.; Hincks, C.L.; Salamonsen, L.A. Endometrial exosomes/microvesicles in the uterine microenvironment: A new paradigm for embryo-endometrial cross talk at implantation. *PLoS ONE* **2013**, *8*, e58502. [CrossRef] [PubMed]
2. Vilella, F.; Moreno-Moya, J.M.; Balaguer, N.; Grasso, A.; Herrero, M.; Martínez, S.; Marcilla, A.; Simón, C. Hsa-miR-30d, secreted by the human endometrium, is taken up by the pre-implantation embryo and might modify its transcriptome. *Development* **2015**, *142*, 3210–3221. [CrossRef] [PubMed]
3. Giacomini, E.; Vago, R.; Sanchez, A.M.; Podini, P.; Zarovni, N.; Murdica, V.; Rizzo, R.; Bortolotti, D.; Candiani, M.; Viganò, P. Secretome of in vitro cultured human embryos contains extracellular vesicles that are uptaken by the maternal side. *Sci. Rep.* **2017**, *7*, 880. [CrossRef] [PubMed]
4. Desrochers, L.M.; Bordeleau, F.C.O.; Reinhart-King, C.A.; Antonyak, M.A.; Cerione, R.A. Microvesicles provide a mechanism for intercellular communication by embryonic stem cells during embryo implantation. *Nat Commun.* **2016**, *7*, 1–11. [CrossRef] [PubMed]
5. Simón, C.; Greening, D.W.; Bolumar, D.; Balaguer, N.; Salamonsen, L.A.; Vilella, F. Extracellular Vesicles in Human Reproduction in Health and Disease. *Endocr. Rev.* **2018**, *39*, 292–332. [CrossRef] [PubMed]
6. Caby, M.-P.; Lankar, D.; Vincendeau-Scherrer, C.; Raposo, G.; Bonnerot, C. Exosomal-like vesicles are present in human blood plasma. *Int. Immunol.* **2005**, *17*, 879–887. [CrossRef] [PubMed]
7. Pisitkun, T.; Shen, R.-F.; Knepper, M.A. Identification and proteomic profiling of exosomes in human urine. *Proc. Natl. Acad. Sci. USA* **2004**, *101*, 13368–13373. [CrossRef]
8. Ogawa, Y.; Miura, Y.; Harazono, A.; Kanai-Azuma, M.; Akimoto, Y.; Kawakami, H.; Yamaguchi, T.; Toda, T.; Endo, T.; Tsubuki, M.; et al. Proteomic analysis of two types of exosomes in human whole saliva. *Biol. Pharm. Bull* **2011**, *34*, 13–23. [CrossRef]
9. Admyre, C.; Johansson, S.M.; Qazi, K.R.; Filén, J.-J.; Lahesmaa, R.; Norman, M.; Neve, E.P.A.; Scheynius, A.; Gabrielsson, S. Exosomes with immune modulatory features are present in human breast milk. *J. Immunol.* **2007**, *179*, 1969–1978. [CrossRef]

10. Asea, A.; Jean-Pierre, C.; Kaur, P.; Rao, P.; Linhares, I.M.; Skupski, D.; Witkin, S.S. Heat shock protein-containing exosomes in mid-trimester amniotic fluids. *J. Reprod. Immunol.* **2008**, *79*, 12–17. [CrossRef]
11. Andre, F.; Schartz, N.E.C.; Movassagh, M.; Flament, C.; Pautier, P.; Morice, P.; Pomel, C.; Lhomme, C.; Escudier, B.; Le Chevalier, T.; et al. Malignant effusions and immunogenic tumour-derived exosomes. *Lancet* **2002**, *360*, 295–305. [CrossRef]
12. Vella, L.J.; Sharples, R.A.; Lawson, V.A.; Masters, C.L.; Cappai, R.; Hill, A.F. Packaging of prions into exosomes is associated with a novel pathway of PrP processing. *J. Pathol.* **2007**, *211*, 582–590. [CrossRef] [PubMed]
13. Masyuk, A.I.; Huang, B.Q.; Ward, C.J.; Gradilone, S.A.; Banales, J.M.; Masyuk, T.V.; Radtke, B.; Splinter, P.L.; LaRusso, N.F. Biliary exosomes influence cholangiocyte regulatory mechanisms and proliferation through interaction with primary cilia. *Am. J. Physiol. Gastrointest. Liver Physiol.* **2010**, *299*, G990–G999. [CrossRef] [PubMed]
14. Ronquist, G.; Brody, I. The prostasome: Its secretion and function in man. *Biochim. Biophys. Acta* **1985**, *822*, 203–218. [CrossRef]
15. Akers, J.C.; Gonda, D.; Kim, R.; Carter, B.S.; Chen, C.C. Biogenesis of extracellular vesicles (EV): Exosomes, microvesicles, retrovirus-like vesicles, and apoptotic bodies. *J. Neurooncol.* **2013**, *113*, 1–11. [CrossRef]
16. Lázaro-Ibáñez, E.; Sanz-Garcia, A.; Visakorpi, T.; Escobedo-Lucea, C.; Siljander, P.; Ayuso-Sacido, Á.; Yliperttula, M. Different gDNA content in the subpopulations of prostate cancer extracellular vesicles: Apoptotic bodies, microvesicles, and exosomes. *Prostate* **2014**, *74*, 1379–1390. [CrossRef]
17. Hochreiter-Hufford, A.; Ravichandran, K.S. Clearing the dead: Apoptotic cell sensing, recognition, engulfment, and digestion. *Cold Spring Harb. Perspect. Biol.* **2013**, *5*, a008748. [CrossRef]
18. Wu, Y.; Tibrewal, N.; Birge, R.B. Phosphatidylserine recognition by phagocytes: A view to a kill. *Trends Cell Biol.* **2006**, *16*, 189–197. [CrossRef]
19. Muralidharan-Chari, V.; Clancy, J.W.; Sedgwick, A.; D'Souza-Schorey, C. Microvesicles: Mediators of extracellular communication during cancer progression. *J. Cell Sci.* **2010**, *123*, 1603–1611. [CrossRef]
20. Greening, D.W.; Gopal, S.K.; Xu, R.; Simpson, R.J.; Chen, W. Exosomes and their roles in immune regulation and cancer. *Semin. Cell Dev. Biol.* **2015**, *40*, 72–81. [CrossRef]
21. Colombo, M.; Raposo, G.; Théry, C. Biogenesis, Secretion, and Intercellular Interactions of Exosomes and Other Extracellular Vesicles. *Annu. Rev. Cell Dev. Biol.* **2014**, *30*, 255–289. [CrossRef] [PubMed]
22. Kowal, J.; Arras, G.; Colombo, M.; Jouve, M.; Morath, J.P.; Primdal-Bengtson, B.; Dingli, F.; Loew, D.; Tkach, M.; Théry, C. Proteomic comparison defines novel markers to characterize heterogeneous populations of extracellular vesicle subtypes. *Proc. Natl. Acad. Sci. USA* **2016**, *113*, e968–e977. [CrossRef] [PubMed]
23. Yáñez-Mó, M.; Siljander, P.R.M.; Andreu, Z.; Zavec, A.B.; Borràs, F.E.; Buzás, E.I.; Buzas, K.; Casal, E.; Cappello, F.; Carvalho, J.; et al. Biological properties of extracellular vesicles and their physiological functions. *J. Extracell. Vesicles* **2015**, *4*, 27066. [CrossRef] [PubMed]
24. Burns, G.W.; Brooks, K.E.; Spencer, T.E. Extracellular Vesicles Originate from the Conceptus and Uterus During Early Pregnancy in Sheep. *Biol. Reprod.* **2016**, *94*, 56. [CrossRef] [PubMed]
25. Bidarimath, M.; Khalaj, K.; Kridli, R.T.; Kan, F.W.K.; Koti, M.; Tayade, C. Extracellular vesicle mediated intercellular communication at the porcine maternal-fetal interface: A new paradigm for conceptus-endometrial cross-talk. *Sci. Rep.* **2017**, *7*, 40476. [CrossRef] [PubMed]
26. Salomon, C.; Yee, S.W.; Mitchell, M.D.; Rice, G.E. The possible role of extravillous trophoblast-derived exosomes on the uterine spiral arterial remodeling under both normal and pathological conditions. *Biomed. Res. Int.* **2014**, *2014*, 693157. [CrossRef]
27. Stefanski, A.L.; Martinez, N.; Peterson, L.K.; Callahan, T.J.; Treacy, E.; Luck, M.; Friend, S.F.; Hermesch, A.; Maltepe, E.; Phang, T.; et al. Murine trophoblast-derived and pregnancy-associated exosome-enriched extracellular vesicle microRNAs: Implications for placenta driven effects on maternal physiology. *PLoS ONE* **2019**, *14*, e0210675. [CrossRef]
28. Szatanek, R.; Baran, J.; Siedlar, M.; Baj-Krzyworzeka, M. Isolation of extracellular vesicles: Determining the correct approach. *Int. J. Mol. Med.* **2015**, *36*, 11–17. [CrossRef]

29. Marcilla, A.; Trelis, M.; Cortés, A.; Sotillo, J.; Cantalapiedra, F.; Minguez, M.T.; Valero, M.L.; Sánchez del Pino, M.M.; Muñoz-Antoli, C.; Toledo, R.; et al. Extracellular vesicles from parasitic helminths contain specific excretory/secretory proteins and are internalized in intestinal host cells. *PLoS ONE* **2012**, *7*, e45974. [CrossRef]
30. Gardiner, C.; Ferreira, Y.J.; Dragovic, R.A.; Redman, C.W.G.; Sargent, I.L. Extracellular vesicle sizing and enumeration by nanoparticle tracking analysis. *J. Extracell. Vesicles* **2013**, *2*. [CrossRef]
31. Li, H.; Durbin, R. Fast and accurate long-read alignment with Burrows-Wheeler transform. *Bioinformatics* **2010**, *26*, 589–595. [CrossRef] [PubMed]
32. Li, H. A statistical framework for SNP calling, mutation discovery, association mapping and population genetical parameter estimation from sequencing data. *Bioinformatics* **2011**, *27*, 2987–2993. [CrossRef] [PubMed]
33. Quinlan, A.R.; Hall, I.M. BEDTools: A flexible suite of utilities for comparing genomic features. *Bioinformatics* **2010**, *26*, 841–842. [CrossRef] [PubMed]
34. McCarthy, D.J.; Chen, Y.; Smyth, G.K. Differential expression analysis of multifactor RNA-Seq experiments with respect to biological variation. *Nucleic. Acids. Res.* **2012**, *40*, 4288–4297. [CrossRef]
35. Nikolayeva, O.; Robinson, M.D. edgeR for differential RNA-seq and ChIP-seq analysis: An application to stem cell biology. *Methods Mol. Biol.* **2014**, *1150*, 45–79. [CrossRef]
36. Robinson, M.D.; McCarthy, D.J.; Smyth, G.K. edgeR: A Bioconductor package for differential expression analysis of digital gene expression data. *Bioinformatics* **2010**, *26*, 139–140. [CrossRef]
37. Ghossoub, R.; Lembo, F.; Rubio, A.; Gaillard, C.B.; Bouchet, J.; Vitale, N.; Slavík, J.; Machala, M.; Zimmermann, P. Syntenin-ALIX Exosome Biogenesis and Budding Into Multivesicular Bodies Are Controlled by ARF6 and PLD2. *Nat. Commun.* **2014**, *5*, 3477. [CrossRef]
38. Muralidharan-Chari, V.; Clancy, J.; Plou, C.; Romao, M.; Chavrier, P.; Raposo, G.; D'Souza-Schorey, C. ARF6-regulated Shedding of Tumor Cell-Derived Plasma Membrane Microvesicles. *Curr. Biol.* **2009**, *19*, 1875–1885. [CrossRef]
39. Mellisho, E.A.; Velásquez, A.E.; Nuñez, M.J.; Cabezas, J.G.; Cueto, J.A.; Fader, C.; Castro, F.O.; Rodríguez-Álvarez, L. Identification and characteristics of extracellular vesicles from bovine blastocysts produced in vitro. *PLoS ONE* **2017**, *12*, e0178306. [CrossRef]
40. Saadeldin, I.M.; Kim, S.J.; Choi, Y.B.; Lee, B.C. Improvement of cloned embryos development by co-culturing with parthenotes: A possible role of exosomes/microvesicles for embryos paracrine communication. *Cell Reprogram.* **2014**, *16*, 223–234. [CrossRef]
41. Kim, J.; Lee, J.; Lee, T.B.; Jun, J.H. Embryotrophic effects of extracellular vesicles derived from outgrowth embryos in pre- and peri-implantation embryonic development in mice. *Mol. Reprod. Dev.* **2019**, *86*, 187–196. [CrossRef] [PubMed]
42. Giacomini, E.; Alleva, E.; Fornelli, G.; Quartucci, A.; Privitera, L.; Vanni, V.S.; Viganò, P. Embryonic extracellular vesicles as informers to the immune cells at the maternal-fetal interface. *Clin. Exp. Immunol.* **2019**, *80*, 1948. [CrossRef] [PubMed]
43. Capalbo, A.; Ubaldi, F.M.; Cimadomo, D.; Noli, L.; Khalaf, Y.; Farcomeni, A.; Ilic, D.; Rienzi, L. MicroRNAs in spent blastocyst culture medium are derived from trophectoderm cells and can be explored for human embryo reproductive competence assessment. *Fertil. Steril.* **2016**, *105*, 225–235. [CrossRef] [PubMed]
44. Théry, C.; Witwer, K.W.; Aikawa, E.; Alcaraz, M.J.; Anderson, J.D.; Andriantsitohaina, R. Minimal information for studies of extracellular vesicles 2018 (MISEV2018): A position statement of the International Society for Extracellular Vesicles and update of the MISEV2014 guidelines. *J. Extracell. Vesicles* **2018**, *23*, 1535750. [CrossRef] [PubMed]
45. Hammond, E.R.; McGillivray, B.C.; Wicker, S.M.; Peek, J.C.; Shelling, A.N.; Stone, P.; Chamley, L.W.; Cree, L.M. Characterizing nuclear and mitochondrial DNA in spent embryo culture media: Genetic contamination identified. *Fertil. Steril.* **2017**, *107*, 220–228. [CrossRef]
46. Shamonki, M.I.; Jin, H.; Haimowitz, Z.; Liu, L. Proof of concept: Preimplantation genetic screening without embryo biopsy through analysis of cell-free DNA in spent embryo culture media. *Fertil. Steril.* **2016**, *106*, 1312–1318. [CrossRef]
47. Xu, J.; Fang, R.; Chen, L.; Chen, D.; Xiao, J.-P.; Yang, W.; Wang, H.; Song, X.; Ma, T.; Bo, S.; et al. Noninvasive chromosome screening of human embryos by genome sequencing of embryo culture medium for in vitro fertilization. *Proc. Natl. Acad. Sci. USA* **2016**, *113*, 11907–11912. [CrossRef]

48. Vera-Rodriguez, M.; Diez-Juan, A.; Jimenez-Almazan, J.; Martinez, S.; Navarro, R.; Peinado, V.; Mercader, A.; Meseguer, M.; Blesa, D.; Moreno, I.; et al. Origin and composition of cell-free DNA in spent medium from human embryo culture during preimplantation development. *Hum. Reprod.* **2018**, *33*, 745–756. [CrossRef]
49. Ho, J.R.; Arrach, N.; Rhodes-Long, K.; Ahmady, A.; Ingles, S.; Chung, K.; Bendikson, K.A.; Paulson, R.J.; McGinnis, L.K. Pushing the limits of detection: Investigation of cell-free DNA for aneuploidy screening in embryos. *Fertil. Steril.* **2018**, *110*, 467–475. [CrossRef]
50. Wu, H.; Ding, C.; Shen, X.; Wang, J.; Li, R.; Cai, B.; Xu, Y.; Zhong, Y.; Zhou, C. Medium-based noninvasive preimplantation genetic diagnosis for human α-thalassemias-SEA. *Medicine (Baltimore)* **2015**, *94*, e669. [CrossRef]
51. Thakur, B.K.; Zhang, H.; Becker, A.; Matei, I.; Huang, Y.; Costa-Silva, B.; Zheng, Y.; Hoshino, A.; Brazier, H.; Xiang, J.; et al. Double-stranded DNA in exosomes: A novel biomarker in cancer detection. *Cell Res.* **2014**, *24*, 766–769. [CrossRef]
52. Guescini, M.; Genedani, S.; Stocchi, V.; Agnati, L.F. Astrocytes and Glioblastoma cells release exosomes carrying mtDNA. *J. Neural. Transm. (Vienna)* **2010**, *117*, 1–4. [CrossRef]
53. Waldenström, A.; Gennebäck, N.; Hellman, U.; Ronquist, G. Cardiomyocyte microvesicles contain DNA/RNA and convey biological messages to target cells. *PLoS ONE* **2012**, *7*, e34653. [CrossRef] [PubMed]
54. Cai, J.; Han, Y.; Ren, H.; Chen, C.; He, D.; Zhou, L.; Eisner, G.M.; Asico, L.D.; Jose, P.A.; Zeng, C. Extracellular vesicle-mediated transfer of donor genomic DNA to recipient cells is a novel mechanism for genetic influence between cells. *J. Mol. Cell Biol.* **2013**, *5*, 227–238. [CrossRef] [PubMed]
55. Pállinger, É.; Bognar, Z.; Bodis, J.; Csabai, T.; Farkas, N.; Godony, K.; Varnagy, A.; Buzas, E.; Szekeres-Bartho, J. A simple and rapid flow cytometry-based assay to identify a competent embryo prior to embryo transfer. *Sci. Rep.* **2017**, *7*, 39927. [CrossRef] [PubMed]
56. Kalluri, R.; LeBleu, V.S. Discovery of Double-Stranded Genomic DNA in Circulating Exosomes. *Cold Spring Harb. Symp. Q. Biol.* **2016**, *81*, 275–280. [CrossRef] [PubMed]
57. Mouse Genome Sequencing Consortium; Waterston, R.H.; Lindblad-Toh, K.; Birney, E.; Rogers, J.; Abril, J.F.; Agarwal, P.; Agarwala, R.; Ainscough, R.; Alexandersson, M.; et al. Initial sequencing and comparative analysis of the mouse genome. *Nature* **2002**, *420*, 520–562. [CrossRef]